Targeting Alternative Splicing as a Novel Approach to Chemotherapy Induced Peripheral Neuropathy

Matthew N. Swift BSc

A thesis submitted to the University of Nottingham for the degree of Doctor of Philosophy (PhD)

December 2020

Abstract:

Chemotherapy induced peripheral neuropathy (CIPN) is one of the most prevalent adverse effects of many chemotherapy drugs. It is estimated that up to 85% of patients suffer from CIPN during treatment and in many patients, painful neuropathy can continue beyond cessation of chemotherapy. Common symptoms of CIPN include, thermal and mechanical allodynia and painful sensations that are commonly described as burning and shooting pain. CIPN is often a dose limiting factor in the provision of chemotherapy. Currently, there are no effective treatments capable of preventing or treating CIPN. Consequently, CIPN is becoming an increasingly significant healthcare burden.

As a result of this burden, there is a pressing need to develop novel therapeutic approaches with which to prevent and treat CIPN. In addition to this, development of chemotherapy agents that are as effective as traditional compounds but lack the severe adverse effects is also desirable. Recently, the neuroprotective and anti-nociceptive properties of alternatively spliced VEGF-A isoforms were identified in the context of diabetic and platinum chemotherapy neuropathy. VEGF-A isoform expression is governed by the activity of splicing kinase SRPK1 which phosphorylates splicing factor SRSF1 and controls the expression of VEGF-A isoforms by selection of the proximal or distal splicing site of exon 8 of the *VEGFA* gene. Inhibition of SRPK1 leads to distal splice site selection and the expression of VEGF-A_{xxx}b isoforms which are neuroprotective and anti-nociceptive. Other splicing kinases with confirmed or putative roles in VEGF-A alternative splicing control include CLK1/CLK2 and DYRK1A. Therefore it has been proposed that novel compounds that inhibit these splicing kinases could have potential utility in preventing the onset of CIPN or be capable of reversing the neuropathy therapeutically via VEGF, or alternative splicing pathways.

This thesis investigated the anti-nociceptive and neuroprotective properties of 4 novel splicing kinase inhibitors in *in vitro* models of vincristine induced neuronal sensitisation and vincristine induced neurite dieback, using dissociated primary DRG neurons. Additionally, an early stage chemotherapy agent, jerantinine was used in the same models and was compared to the neurotoxic and sensitising effects of a traditional agent, vincristine. Alteration of splicing kinases SRPK1, CLK1, CLK2 and DYRK1A with the 4 compounds was able to significantly inhibit vincristine induced sensitisation, in addition to preventing neurite dieback in response to chemotherapy challenge whilst having little or no detrimental effect as independent treatments. Furthermore, jerantinine did not sensitise neurons to the same degree as vincristine and caused a milder degree of neurite dieback. Using a 3D tumour spheroid model, inhibition of all 4 kinases combined with vincristine treatment significantly reduced spheroid growth whilst inhibitors had no effect on spheroid growth in the absence of vincristine. These findings suggest that these compounds will not inhibit chemotherapy activity and appease concerns that they could drive tumour growth. These results demonstrate that control of alternative splicing via inhibition of multiple kinases could be a potentially beneficial in preventing or treating CIPN, and that the novel chemotherapy agent jerantinine is worth developing further due to its reduced adverse effects.

Publications, Abstracts and Awards

Publications:

Z.Blackley, H. Toop, N. Beazley-Long, C. Moss, R.P. Hulse, R. Babaei Jadidi, J. Batson, S.M. Bestall, **M.N. Swift,** J. Da Rocha, D.O. Bates, C. Vaughan, L.F. Donaldson and J.C Morris. *SRPINs: Development of novel inhibitors of splicing kinase SRPK1 as novel anti-inflammatory analgesics.* Manuscript in process.

Bestall SM, Hulse RP, Blackley Z, **Swift MN**, Ved N, Paton K, Beazley-Long N, Bates DO, Donaldson LF. Sensory neuronal sensitisation occurs through HMGB-1-RAGE and TRPV1 in high-glucose conditions. J Cell Sci. 2018 Jul 26;131(14):jcs215939. doi: 10.1242/jcs.215939. PMID: 29930087; PMCID: PMC6080605.

Durrant AM, **Swift MN**, Beazley-Long N. A role for pericytes in chronic pain? Curr Opin Support Palliat Care. 2018 Jun;12(2):154-161. doi: 10.1097/SPC.0000000000000342. PMID: 29553988; PMCID: PMC6027993.

Beazley-Long N, Durrant AM, **Swift MN** and Donaldson LF. The physiological functions of central nervous system pericytes and a potential role in pain [version 1; peer review: 2 approved]. *F1000Research* 2018, **7**(F1000 Faculty Rev):341 (https://doi.org/10.12688/f1000research.13548.1)

Abstracts :

18th World Congress on Pain (IASP 2020 postponed to 2021) - Poster Presentation: Inhibition of Serine-Arginine Rich Splicing Factor Kinase 1 Confers Neuroprotective

Benefits in *in vitro* Models of Vincristine Chemotherapy Induced Peripheral Neuropathy

BBSRC Spring School 2019 - Oral Presentation: Novel Approaches To Chemotherapy Induced Peripheral Neuropathy

6th UK RNA Splicing Workshop 2019 - Poster Presentation: Alternative Splicing Kinase Inhibition Inhibits Chemotherapy Induced Sensory Neuronal Sensitisation *in vitro*

BBSRC Spring School 2018 – Poster Presentation: Validation of a Novel Neuronal Cell Line For Use in High Throughput Drug Screening Assays.

Awards:

IASP Financial Award 2020

BBSRC Spring School 2019 - Best Oral Presentation (Neuroscience)

Acknowledgements:

The completion of this thesis would not have been possible without the support, advice and encouragement of so many fantastic people. Firstly thank you to Steph, my best friend and partner for everything you have put up with. The good days, the days where I wouldn’t shut up about concepts and days where I just didn’t know what the point was. You were always there to listen, make me laugh and pick me up and I couldn’t have done it without you. Thank you to Mum, Dad and Jess, you have always believed in me unfailingly and fostered my interests. You’ve always been there to help me, guide me, encourage me and ensured that I could always rely on you. This thesis is testament to the love and care I have received throughout my entire life and I can never repay that. I love you all.

To everyone who I have had the pleasure of working with in the past 4 years, I cannot thank you enough. To Nick Beazley-Long, thank you everything you have taught me and for our long, detailed discussions about the merits of xG and football statistics. You really made the transition from a naïve fresh faced graduate to a (somewhat) competent PhD student as easy as possible. I owe you a lot. Thank you to my lab group; Lexy, Zoe, Roaa, Dimi, Roheena and James. Your enthusiasm and support have made working in a lab a fantastic experience. You are all brilliant, fiercely intelligent individuals and to those still working towards this point, keep going and I look forward to helping you. Thank you to my friends in CBTRC, our lunches were often the only bright points in otherwise very difficult and frustrating days. Many thanks also go to Dr Beth Coyle for advice and willingness to help me complete a project spanning my interests. I wish you all the best. To everyone in TVBL, though I was only ever transient in the lab (mainly to hog the confocal) I always received help when I needed it and had some really good times. I will never forget any of it.

My final thanks are reserved from my supervisors, Professor Lucy Donaldson and Professor David Bates. Over the last 4 years, I have learnt so much from both of you. How to follow my data, how to ask what it actually means, how to piece it all together. When to pursue other things and when to persist and persist and persist despite how bleak and remote success may seem. I learnt something in every meeting with you and tried to then carry it into my work. You have both given me the confidence to overcome my rampant imposter syndrome and I cannot thank you enough.

Author's Declaration

I, Matthew Nicholas Swift, confirm that the work presented in this thesis was carried out in accordance with the requirements of the University's Regulations and Code of Practice for Research Degree Programs and that it has not been submitted for any other academic award. I confirm that the work and views demonstrated in this thesis are my own. Where information has been derived from other sources, I confirm this has been indicated in the thesis.

SIGNED: 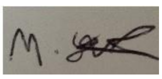 DATE: 16/12/20

Table of Contents:

LIST OF TABLES

LIST OF ABBRIEVIATIONS

AITC	Allyl Isothiocyanate
ANOVA	Analysis Of Variance
ATP	Adenosine Triphosphate
AUC	Area Under the Curve
BBB	Blood Brain Barrier
BDNF	Brain-Derived Neurotrophic Factor
BIN1	Bridging Integrator 1
Bp	Base Pairs
BSA	Bovine Serum Albumin
cDNA	Complementary DNA
CIPN	Chemotherapy Induced Peripheral Neuropathy
CLK	CDC2 Like Kinase
CNS	Central Nervous System
CNV	Choroidal Neovascularisation
COX-1/2	Cyclooxygenase 1/2

DMSO	Di-methyl Sulfoxide
DPN	Diabetic Peripheral Neuropathy
DRG	Dorsal Root Ganglia
DYRK1A	Dual Specificity Tyrosine Phosphorylation Regulated Kinase 1A
EC_{50}	Concentration Required for 50% Efficacy
eIF4E	Eukaryotic Initiation Factor 4E
FBS	Foetal Bovine Serum
FSK	Forskolin
HBSS	Hanks Balanced Salt Solution
HEK293	Human Embryonic Kidney
HIF-1	Hypoxia Inducible Factor 1
hnRNP	Heterologous Nuclear Ribonucleoprotein
hTERT	Human Telomere Reverse Transcriptase
IASP	International Association For The Study of Pain
IC_{50}	Concentration Required For 50% Inhibition
IgG	Immunoglobulin G
IP	Intraperitoneal
IS	Inflammatory Soup
Kb	Kilobase
MAPK	Mitogen Activated Protein Kinase
$MgCl_2$	Magnesium Chloride
MNK	MAP-Kinase Interacting Kinase
MKNK2	MAPK Interacting Serine/Threonine Kinase
mRNA	Messenger RNA
mTOR	Mammalian Target Of Rapamycin
NGF	Nerve Growth Factor
NMD	Nonsense Mediated Decay
NP-1	Neuropilin 1

NSAIDS	Non-Steroidal Anti-Inflammatory
PBS	Phosphate Buffered Saline
PCR	Polymerase Chain Reaction
PFA	Paraformaldehyde
PI3K	Phosphoinositide 3-Kinase
PKC	Protein Kinase C
PNS	Peripheral Nervous System
PSNI	Partial Saphenous Nerve Injury
pSR	Phosphorylated SR protein
RAGE	Receptor For Advanced Glycation End Products
RNA-SEQ	RNA Sequencing
RPE	Retinal Pigmented Epithelium
RPMI	Roswell Park Memorial Institute
RT-PCR	Reverse Transcription Polymerase Chain Reaction
SEM	Standard Error Of The Mean
snRNP	Small Nuclear Ribonucleoprotein
SRE	Splicing Regulatory Elements
SRPK	Serine/Arginine Protein Kinase
SRSF	Serine/Arginine Rich Splicing Factor 1
STZ	Streptozotocin
TGF-β	Transforming Growth Factor Beta
TNF-α	Tumour Necrosis Factor Alpha
TRP	Transient Receptor Potential
TRPA1	Transient Receptor Potential Ankyrin 1
TRPV1	Transient Receptor Potential Vanilloid 1
VEGF	Vascular Endothelial Growth Factor
VEGFR1	Vascular Endothelial Growth Factor Receptor 1
VEGFR2	Vascular Endothelial Growth Factor Receptor 2

1: Introduction

1.1.1 Nociceptive Pain

Pain as defined by the International Association for the Study of Pain (IASP) is "An unpleasant sensory and emotional experience associated with, or resembling that associated with actual or potential tissue damage". Pain is a mechanism that aims to protect the body following contact with a potentially damaging stimulus by triggering a behavioural response (Dubin and Patapoutian, 2010). In response to acute pain, this is usually a stimulation of a withdrawal reflex away from the stimulus to prevent progressive tissue damage from exposure (Woolf and Ma, 2007). Pain can also persist in the event of injury, with the injured area becoming inflamed. This pain is usually reversible, and exists to prevent further damage as the tissue is repaired. As such, pain is a vital survival protective mechanism (Amaya *et al.*, 2013). This canonical protective mechanism of pain is termed "nociceptive pain" and is a component of the somatosensory system.

The somatosensory system is fundamental to the detection of stimuli, be they noxious or benign and how these stimuli are processed and interpreted by the various components of the nervous system. The somatosensory system relies on peripheral first order neurons, so called "peripheral afferents" which detect the stimulus, generate action potentials and transmit this information to the spinal cord, where information is transferred across the first synapse in the central nervous system to dorsal horn neurons (Nelson 2001). Following first order neuron processing, second order neurons carry this nociceptive information to the thalamus before transmission to third order neurons in the cortex where perception occurs.

Information is also transmitted to areas such as the brainstem which integrates autonomic responses to stimuli. Involvement of the limbic system produces negative emotional responses that can exacerbate perceptions of pain. There is also input into the sensory cortex from the anterior cingulate, insular cortices, cerebellum and other sites in response to nociceptive stimulation, indicating involvement of multiple brain regions as shown by fMRI (Peirs and Seal, 2016). These regions cover both the sensory and emotional aspects of pain as referred to in the IASP definition. Despite the importance of these higher centres for pain processing, they rely on primary afferent nociceptors for first contact and it is crucial that these first order neurons can accurately transduce information about a stimulus be it thermal, mechanical or chemical so that the body can respond appropriately (Todd, 2002). To account for this, first order neurons can be stratified into a variety of classifications.

1.1.2: Nociceptor Classes

As mentioned, nociceptors are required to detect a variety of potentially damaging stimuli and then transfer this information to the CNS for processing. As such many nociceptors are described as possessing "polymodality" which essentially refers to the ability of chemical, mechanical and thermal stimuli to be detected and processed by a single receptor (Hoffmann *et al.*, 2008). First order neurons can be either myelinated or unmyelinated, which refers to the substance which acts as insulation on nerve cell axons and therefore serves to increase the speed at which action potentials can be transported along the nociceptive system (Williamson and Lyons, 2018). In the PNS, myelin is produced by Schwann cells, a sub-type of so called glial cells which are non-neuronal support cells of the nervous system (Salzer, 2015). In the CNS, myelin insulation is created by another type of glial cell, so called oligodendrocytes (Baumann and Pham-Dinh, 2001). CNS myelination is a key component of motor function as demonstrated by the debilitating effect of myelin disorders such as multiple sclerosis on these processes (Goldenberg, 2012). However in the PNS, unmyelinated sensory neurons play a key role in the detection of various stimuli. It is this myelination property that serves as a key distinguishing characteristic between classes of sensory neurons. Erlanger and Gasser classified unmyelinated neurons as possessing so called C-fibres that are small in diameter (Gasser and Erlanger, 1927). On average they are 0.2-1.5µm in diameter and have a slow conduction velocity due to the lack of myelin insulation of <1m/s. It is important to note that not all C-fibres are nociceptors, a proportion of these fibres are low threshold touch receptors, a population first identified by Nordin et al. and Vallbo et al. (Nordin, 1990; Vallbo *et al.*, 1993). This sub-population of C-fibres are generally associated with pleasant sensations relating to touch that is common across mammalian species. This slow conduction velocity contrasts with the 2 fibre types possessed by myelinated neurons. Myelinated neurons are split into two sub-classifications Aβ fibres and Aδ fibres. Aδ fibres are thinly myelinated but are larger diameter (1-5µm) than C-fibre counterparts. As a result of myelination, they also have faster conduction velocity of 2-10m/s (Lewin and McMahon, 1991). Aβ fibres are larger still in diameter (6-12µm), have even greater myelin insulation and as such even faster conduction velocity of >10m/s (Djouhri and Lawson, 2004). Though around 30% of Aβ fibres are associated with nociception, this fibre type is primarily involved with the detection of mechanical stimuli that is not harmful or noxious. A final fibre type Aα fibres are among the largest in diameter of sensory fibre types being up to 20µm. These fibres also possess very fast conduction velocities of more than 80m/s. However, these latter fibres are associated with muscle spindles and are associated with proprioception, or the sense of self movement and body position rather than nociception (Watson and Dyck, 2015).

Aδ fibres can be further sub-divided into Type I and Type II high threshold A-mechano-heat (AMH) nociceptor classifications (Treede *et al.*, 1995). Type I AMH are associated with high thermal thresholds of over 50°C but have important functions in detecting and processing ‘first pain’ information from noxious mechanical stimuli. Conversely, Type II AMH have a thermal activation threshold much lower than that observed in Type I, but higher mechanical thresholds. Type II AMH therefore are primarily involved in the detection and processing of ‘first pain’ noxious heat stimuli >50^{o}C probably transduced by TRPV2, a type of cation channel that is detailed in Section 1.1.3. Type I AMH can be sensitised under conditions of tissue damage, when their thermal thresholds for activation drop, resulting in increased signalling to thermal stimulation at temperature <50^{o}C (van den Broeke, Lenoir and Mouraux, 2016). C-fibres represent the largest population of nociceptors and due to their slow conduction velocity in the absence of myelination are responsible for dull, slow painful sensations that can be fairly wide-spread (Beissner *et al.*, 2010). This is in contrast to Aδ fibres which evoke short, sharp acute sensations of pain in response to stimuli (Ahlquist and Frmzta, 1994). The reason underpinning this difference can be partially explained by C-fibre populations converging inputs and creating larger receptive fields, resulting in a more general widespread sensation than that evoked by nociceptors with smaller discrete receptive fields (Hallin, Torebjork and Wiesenfeld, 1982). Therefore areas considered to be more sensitive often have clustered neurons in large numbers, but with small receptive fields. Less sensitive areas have fewer neurons across an area, but with much wider receptive fields. The majority of C-fibres are polymodal in nature and have the ability to detect thermal, mechanical and chemical stimuli, though single modality C-fibres also exist (Wooten *et al.*, 2014). There is also a subset of C-fibres that in normal nociceptive conditions are not activated by thermal or mechanical thresholds. However, in the event of tissue injury these “silent nociceptors” become sensitive to these two classes of stimuli, which is moderated by the release of inflammatory mediators (Prato *et al.*, 2017). This activation causes innervated tissue to become more sensitive and triggers nociception from otherwise non-noxious stimuli. Both Aδ fibres and C-fibres can be further sub-divided based on chemical properties. Both fibre types can be classed as peptidergic, associated with the expression and release of substance P and these account for ~40% of the nociceptor population (Lawson et al., 1997). These neurons are often identified through their expression of TrkA which is the binding receptor of Nerve Growth Factor (NGF). Peptidergic neurons are reliant on NGF to survive, meaning TrkA is also essential to transduce the effects of NGF. Non-peptidergic neurons are not dependent on NGF for survival, but rather glial derived neurotrophic growth factor (GDNF). The effects of this neurotrophin are mediated through the GFR-α and c-ret receptors. Non-peptidergic neurons are identified thorough expression of Isolectin B4; this is due to the fact that almost all neurons found expressing IB4 are also RET positive. Along with this, over 80% of IB4 positive neurons also express GFR-α. However, it is important to note that overlap exists within these populations and differences are present across species (Stucky and Lewin, 1999; Ernsberger, 2009).

Whilst the fibres of PNS neurons process out to the periphery via long projections, the cell bodies of these peripheral neurons are located in the dorsal root ganglia

(DRG). The DRG are located within the intervertebral foramina of the spinal column (Silav *et al.*, 2016). Primary afferent fibres of neurons projecting into these ganglia are so called pseudo-unipolar neurons. Unlike bi-polar neurons that have a sensory terminal connected a dendrite which projects action potentials to the cell body and then to upstream pathways via an axon, pseudo-unipolar neurons have only a single axon fibre (Takahashi and Ninomiya, 1987). This fibre splits into a peripheral projection where the sensory terminal responsible for stimuli is located and then into a central projection which transmit this information into the dorsal horn of the spinal cord and to second order neurons. The cell body contained in the DRG can serve as the interchange between the peripheral and central axonal projections though peripheral signals can often bypass it by transmitting directly straight through to the central projection (Liem *et al.*, 2016).

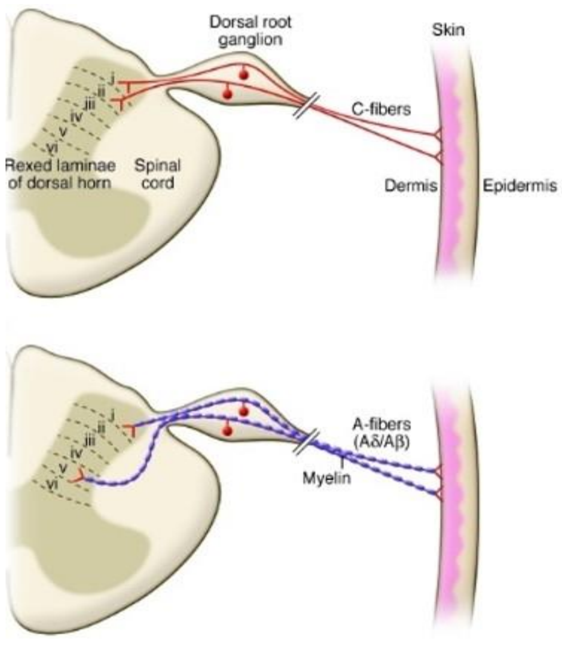

Figure 1.1: Schematic of primary afferent projections into the DRG and spinal cord

Representative schematic of primary afferent fibre projection from the peripheral epidermis to the dorsal root ganglia and then into the various laminae of the spinal cord. Dorsal root ganglia contain the cell bodies of peripheral afferents. In the top image, unmyelinated C-fibres (red) project into lamina I and II. In the bottom image, myelinated (blue) A-fibres project into lamina I and V. From Dubin and Patapoutian, 2010.

Different fibres also project to different areas of the dorsal horn of the spinal cord. These can be seen in Figure 1.1. Peptidergic C-fibres project into laminae I and outer laminae II, along with myelinated Aδ fibres which project into laminae I and laminae V. Non-peptidergic C-fibres also project into inner laminae II. Finally, the largely non-nociceptive Aβ fibres project into laminae III and IV (Naim *et al.*, 1997; D'Mello and Dickenson, 2008). Having reached these points, the release of neurotransmitters facilitates the activation of the aforementioned second order neurons which trigger the pain processing pathways of the brain described previously. It is important to mention that these pain processing centres of the spinal cord can be involved in ascending or descending pathways that can dampen or exacerbate pain processing and severity of pain sensation (Tesfaye et al., 2013).

1.1.3: Polymodality and Cation Channels

A fundamental property of primary afferents nociceptors, in particular C-fibres is their polymodality or ability to detect a variety of thermal, mechanical and chemical stimuli. Underpinning this property is neuronal expression of a variety of receptors which detect and transduce these stimuli into the flux of a variety of cations in response to the stimulus. This cation flux into the cell is the key mechanism underlying the receptor potential by which membrane depolarisation occurs and the action potential is generated initiating the processing of mechanical, thermal and chemical stimuli in the nervous system. A prime example of the channels by which this flux occurs is the transient receptor potential (TRP) cation channel family (Caterina *et al.*, 1997). Expression of these channels is not limited to the peripheral nervous system and there are 30 TRP channel proteins expressed in mammals across 6 sub-families. Nociceptors have been found to express at least 6 of these channels, including transient receptor potential vanilloid subtype 1 (TRPV1), transient receptor potential cation channel, subfamily A member 1 (TRPA1) and transient receptor potential cation channel subfamily M, member 8 (TRPM8) (Pedersen *et al*., 2005). These channels can be activated by a sliding scale of heat stimuli, and in response to various other stimuli. For instance, TRPV1 is activated at a threshold of around 43°C and by the potent chemical capsaicin, the active ingredient of chilli peppers (Touska *et al.*, 2011). TRPA1 has previously been associated with detection of colder temperatures and does have heat based activation threshold and activation by a variety of chemicals such as cinnamaldehyde and allyl isothiocyanate which is the active ingredient in pungent tasting foods such as wasabi, mustard and radishes (Boiko *et al.*, 2017). However, more commonly TRPA1 is regarded as a universal sensitiser that is activated by mediators of tissue damage (Karashima *et al.*, 2007; Fernandes *et al*., 2012). These two channels have particular importance in terms of nociception. TRVP1 causes rapid calcium influx and release from intracellular stores upon activation by capsaicin and heat. As TRPV1 is expressed predominantly in nociceptor populations of both C-fibres and Aδ fibres it is possible to use capsaicin to discern between nociceptive and non-nociceptive fibres, as only TRPV1 expressing fibres will respond. As there is considerable overlap between TRPV1 and TRPA1 expression in neurons, activation of TRPA1 with allyl isothiocyanate (AITC) would replicate this effect. This therefore allows for clear identification of nociceptors within a group of peripheral neurons (Ambrosino *et al.*, 2013). The importance of TRP channels in the detection of various stimuli has been examined in knock-out studies. Elimination of TRP channels in rodent models have revealed complete insensitivity to thermal (both noxious heat and cooling sensation) mechanical and chemical stimulants demonstrating the polymodal properties they retain and the mechanisms that underpin them in neurons (Kwan *et al.*, 2006; Hulse *et al.*, 2014).

Other channels that are fundamental to nociception and peripheral sensations are the voltage gated sodium channels such as $Na_V1.7$, $Na_V1.8$ and $Na_V1.9$. Though nine of these channels are expressed in primary afferents, these three channels are most heavily associated with nociception (Eijkelkamp et al., 2012). These channels are classified based on their sensitivity to tetrodotoxin (TTX), a sodium channel blocker and an inhibitor of action potential generation by blocking sodium cation influx. $Na_V1.8$ and $Na_V1.9$ are TTX resistant whereas $Na_V1.7$ is sensitive to TTX blockade (Fort *et al.*, 2009). All three channels are commonly expressed in small diameter neurons, though there is also expression in A-fibres. Na_V channels are associated with early responses to stimuli. For instance, $Na_V1.7$ is associated with minor changes to neuronal membrane voltage, so called “receptor potentials” which are first transduced by TRP channels in response to chemical or heat stimuli. As TRP channels open and cation flux occurs these potentials are then progressively amplified by $Na_V1.7$ which due to its slow inactivation properties allows small progressive depolarisations to build up into a so called “ramp current” (McDermott *et al.*, 2019). This effectively serves to prime $Na_V1.8$ channels which have a much higher depolarisation threshold, and serves as a main driver of sodium currents of the action potential. $Na_V1.8$ also has an extremely rapid recovery from activation allowing the neurons to fire repeatedly over a short period of time which is a key determinant of neuronal excitability (Hameed, 2019). The importance of these channels is again emphasised in knock out experiments and in patients suffering from neuropathy. Knockout of either or both channels reduced responses to thermal and mechanical stimuli and in the rare case of congenital loss of $Na_V1.7$ in humans, a total insensitivity to pain is present (Gingras *et al.*, 2014). Conversely, in neuropathy patients there is some evidence suggesting upregulation of both channels as a result of gain of function mutations (Dib-Hajj *et al.*, 1999; Tanaka *et al.*, 2017). These findings indicate that both TRP channels and Na_V channels are of great importance in determining neuronal excitability and function. Overviews of both TRP channels and Na_V channels can be seen in figures 1.2 and 1.3 respectively.

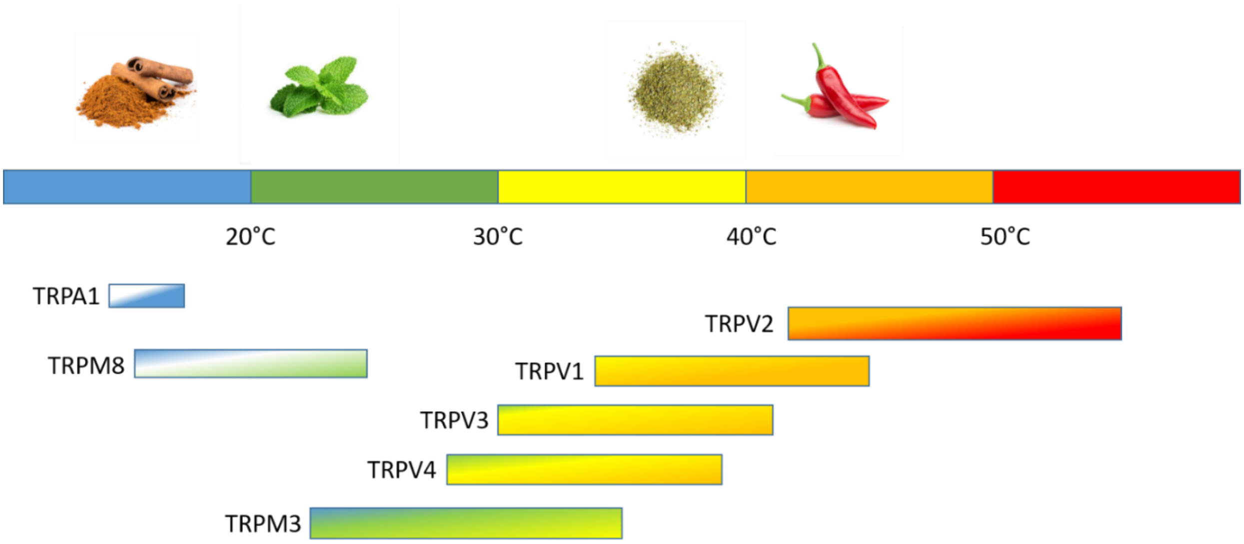

Figure 1.2: TRP Channel Summary

Diagram of TRP channels expressed in primary afferent fibres their thermal activation thresholds and chemical containing foods that lead to their activation. These are cinnamon, mint, oregano and chilli pepper respectively. Figure is adapted from Dhaka et al. 2006.

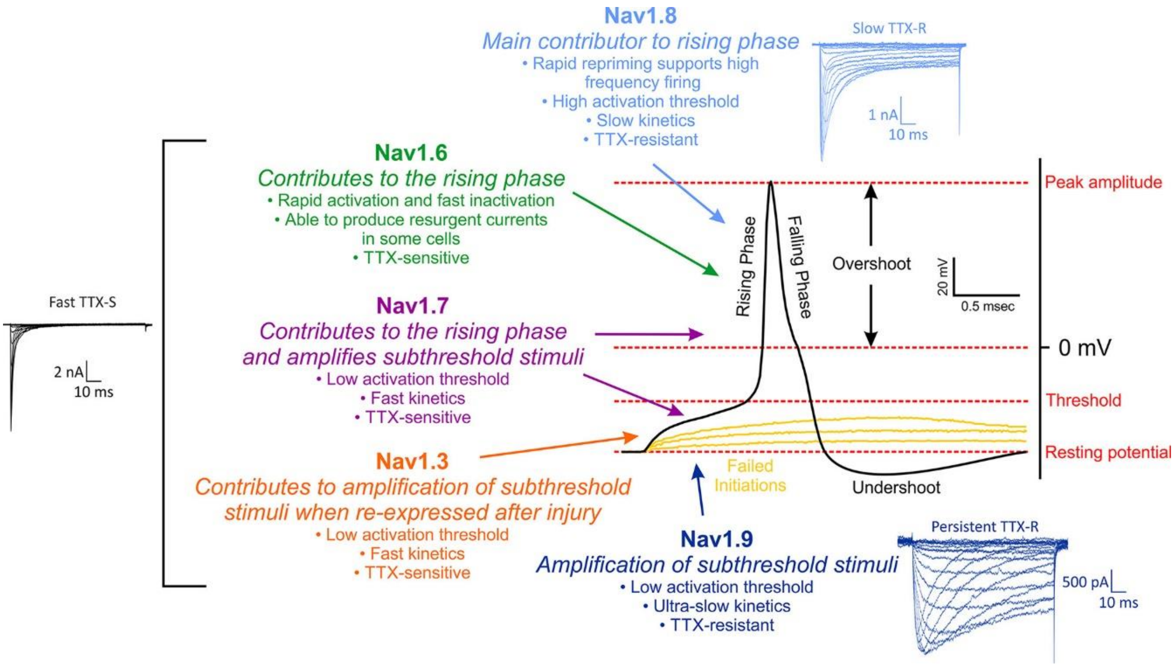

Figure 1.3: Na$_V$ Channel Summary

A summary of Na$_V$ channel contributions to the firing of an action potential. Na$_V$1.3/1.9 are associated with amplification of sub-threshold stimuli detected by a transducer (such as TRP channels) which is further amplified by Na$_V$1.6/1.7, leading to Na$_V$1.8 activation and action potential firing. Figure from Bennett *et al*. 2019.

1.1.4: Pathological Pain

Whilst nociceptive pain describes sensations that are components of essential evolutionary and protective mechanisms, pain that persists beyond the time taken for injury to heal can result in painful responses to what would normally be non-harmful stimuli. Such pain has no physiological function and is regarded as pathological in and of itself rather than a response to a potentially pathological factor. This type of pain is termed "neuropathic pain" and is defined by IASP as "pain caused by a lesion or disease within the somatosensory system" (Colloca *et al.*, 2017). This definition is broad and can refer to injury along any part of the sensory pathways described previously, both in the PNS and CNS. Neuropathic pain can also occur for prolonged periods, this is termed "chronic pain". IASP define chronic pain as any pain lasts or recurs for more than 3 months (Fayaz et al., 2016). Another closely linked form of pain that can lead to neuropathic pain but not inevitably is inflammatory pain. Inflammatory pain is initiated by the body’s response to damaged tissue in the event of injury. Though the aim of the response is tissue repair and protection, in many cases the inflammation becomes poorly regulated and impacts negatively on the surrounding nervous tissue often exacerbating the original injury or insult (Kidd and Urban, 2001). Whilst it is possible this dysregulation can result in neuropathic pain, a prominent example of non-neuropathic but chronic inflammatory pain is that often associated with rheumatoid arthritis (Gavrilă *et al.,* 2016).

1.1.4.1: Inflammatory Pain

Immune responses to damaged tissue are commonplace in nearly every system within the body (Cooke, 2019). Though usually promoting healing and protecting the body from further damage the potency of the various cytokines and immune cells released in response to said damage can often result in greater tissue pathology. The nervous system is no exception to this dysregulation. As the name suggests, the PNS is located at the outer extremities of the body, therefore these sites are also the most likely to subject damage from foreign bodies penetrating the dermal layers of skin and triggering the release of neutrophils and other components of the innate immune system to the site of injury (Ordovas-Montanes *et al.*, 2015). Therefore it is of no surprise that the cells in the periphery have the power to recruit such cells and to release cytokines, chemokines and interleukins in a co-ordinated attempt to repair and protect the body as part of a normal physiological response.

Neurons are no exception to this, with many peptidergic neurons capable of substance P release which is capable of upregulating myriad inflammatory factors and recruiting them to the site (Chen *et al.*, 2007). Accumulation of inflammatory mediators can lead to the creation of so called “inflammatory soup”. This inflammatory soup (IS) is a pivotal factor in the development of pain in response to direct tissue damage such as that acquired from a sprained ankle (Dubin and Patapoutian, 2010). It should be noted however that substance P release is only essential for this in neurogenic inflammation, in most cases the innate inflammatory response of surrounding tissue is responsible. Nociceptors also possess receptors for histamine and prostaglandins, the latter being essential inflammatory components that have been targeted for centuries via inhibition of the cyclooxygenases to prevent prostaglandin production in response to injury (Basbaum *et al.*, 2009). Use of willow bark, containing salicylates is a traditional example of an anti-inflammatory remedy and aspirin commonly used for pain and inflammation management is derived from the willow tree. In more recent years however, various investigations have revealed many more key components of the inflammatory soup. Tumour necrosis factor alpha (TNFα) is a cytokine contained within the IS and is capable of substance P like upregulation of numerous other inflammatory components. TNFα has a record of causing both mechanical and thermal hyperalgesia, when administered as a recombinant protein (Wang *et al.*, 2018). This has led to speculation that it may be a key factor in pain associated with diseases like arthritis, hence the creation of drugs such as etanercept which aim to neutralise its effects. As previously mentioned all of these factors are essential in resolving tissue damage effectively and safely, but it is also the case that a positive

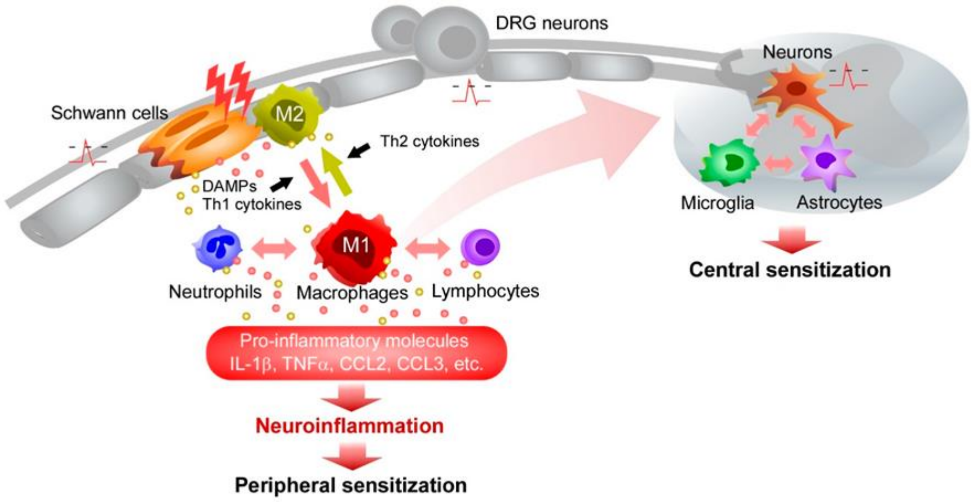

Figure 1.4: An overview of peripheral and central sensitisation mediated by inflammation.
Following direct damage to the neuron of sustained damage of local tissue resident produce factors which recruit immune cells to the point of injury. This triggers further release of inflammatory mediators and cytokines which causes ectopic peripheral neuronal activity resulting in peripheral sensitisation. This peripheral sensitisation then causes aberrant signalling to the spinal cord which results in pathological amplification of pain processing. Immune and support cells can then maintain this amplified pain signalling resulting in central sensitisation. From Kiguchi *et al.,* 2017.

feedback loop can emerge in response to damage, which in turn can lead to recruitment of noxious cytokines and mediators which in turn can damage neurons. This damage can in some cases eventually form a lesion and it is at this point where the neurons themselves become targets of injury or damage that neuropathic pain can occur (Langjahr *et al.*, 2018).

1.1.4.2: Neuropathic Pain

Neuropathic pain is caused by lesions to the somatosensory system (Woolf and Ma, 2007; Colloca *et al.*, 2017). Common symptoms in patients with neuropathic pain include but are not limited to numbness, tingling, burning, pruritus and fatigue. The range of potential causes for such lesions is extensive with chemical, physical, ischaemic, inflammatory, traumatic and cytotoxic agents all capable of invoking neuropathic pain in any component of the sensory system (Ellis and Bennett, 2013).

Neuropathic pain can also be caused by a number of iatrogenic causes such as surgery despite attempts to reduce the likelihood of and ameliorate such damage. Neuropathic pain affects large portions of society and can occur across all ages. It is estimated that over 10% of the population suffer from a degree of neuropathic pain deriving from a range of causes such as diabetes, spinal cord injury, post-stroke pain and chemotherapy induced neuropathy (Toth *et al.*, 2009; van Hecke *et al.*, 2014; Cruccu *et al.*, 2017). Neuropathic pain is caused by heightened activity of peripheral nociceptors and/or increased activity in central nervous system nociceptive processing; these two processes are called “peripheral sensitisation” and “central sensitisation” respectively.

Peripheral sensitisation (Fig 1.4) can be triggered by inflammatory factors or changes to nociceptor environments described above and is frequently mediated by changes in sensitivity and excitability in polymodal nociceptors and Type II AMH through modulation of TRP and VGNC channels (Shu and Mendell, 1999; Schaible, Ebersberger and Natura, 2011). For instance, the largely acidic environment that occurs as a result of inflammatory activation is capable of phosphorylating TRPV1 at its serine 800 residue. This increases the sensitivity of TRPV1 and thus lowers the threshold required for its activation and shift to an open channel conformation, resulting in easier generation of receptor potentials. This effect, combined with increased VGSC excitability due to prostaglandin modulation leads to erroneous firing of action potentials in response to non-harmful stimuli. These changes can also be mediated by release of neurotrophic factors in response to injury and can be amplified by surrounding neurons, glia and endothelial cells; as a result neuronal excitability increases, and increased peripheral input occurs into the spinal cord (Chen *et al.*, 2012; Hulse *et al.*, 2014).

This increased peripheral neuronal input and peripheral sensitisation can have profound effects on central nociceptive processing. In response to increased input from the periphery there is release of the neurotransmitter glutamate from peripheral afferents which then activate central NMDA receptors. NMDA activation then causes central spinal cord neurons to become more excitable in response to peripheral inputs which then drives further glutamate release and further excitability and results in central sensitisation (Latremoliere and Woolf, 2009). These changes can often be accompanied by alterations in spinal cord glia cells which can cause hyperexcitability in the dorsal horn. Recent evidence also points to the involvement of immune cell infiltration into the central nervous system, further exacerbating sensitisation and nociceptive processing in the CNS (Dalkara and Alarcon-Martinez, 2015).

The most common symptoms of neuropathic pain fall into two closely related but fundamentally different classes. Neuropathic pain causes both allodynia and hyperalgesia. The former describes a painful response to a non-harmful stimulus, such as very light touch generating an unpleasant sensation. Hyperalgesia describes an elevated painful sensation to a noxious stimulus (Sandkühler, 2009). An example of a hyperalgesic response would be a heightened response to a high temperature, which causes discomfort but in neuropathic pain triggers a much more unpleasant sensation. This heightened response to moderately harmful or totally unharmful stimuli can initially be a direct result of peripheral sensitisation but is likely maintained centrally when it becomes chronic (Lee, Nassikas and Clauw, 2011).

Despite the widespread prevalence of neuropathic pain, management options are severely limited (Katz, 2002). As a result of this lack of effective treatments, patients often suffer with depression and anxiety about their conditions which worsens mental health outcomes and has a detrimental effect on quality of life (McCarberg *et al.*, 2008; Ataoğlu *et al.*, 2013; Lin *et al.*, 2020). The most common first line therapeutic options for neuropathic pain irrespective of cause are anti-convulsants such as pregabalin and gabapentin and antidepressants such duloxetine and amitriptyline (Wiffen, 2013; Shahid *et al.*, 2019). These drugs are normally given in sequential processes with a transfer to another drug in these classes advised if the currently used drug begins to lose efficacy. It should be stated however, that the efficacy of these drugs is also questionable as a significant proportion of patients receive no pain relief from anticonvulsant/antidepressant therapy (Cavalli *et al.*, 2019). Other management options include the use of opioids, which target opioid receptors in the peripheral and central nervous system. Though they are extremely potent analgesic agents they also carry a high risk of addiction and abuse (Ling et al., 2011). The prevalence of chronic pain has led to their widespread use for pain management, however this usage has also been a key factor in the emergence of the so called "opioid epidemic", which is occurring worldwide but with the greatest degree of scrutiny in the United States of America (Bonnie, Ford and Phillips, 2017; Blanco *et al.*, 2020). The potency of opioids has also led to concerns about the risk of accumulation over time, with there being some evidence for pain actually worsening as a result of mass opioid use over a prolonged period. In both anti-convulsant and opioid based therapy side effects are common. Prolonged use of these management options can result in gastrointestinal defects such as diarrhoea, vomiting, dizziness, addiction as previously described, insomnia, severe sweating and weight loss (Fornasari, 2017; Onakpoya *et al.*, 2019).

As a result of the lack of efficacy and often profound side effects resulting from extensive usage of these drugs, there is an urgent need to develop novel therapeutic non-opioid analgesic options for neuropathic pain. An assumption that is often made regarding neuropathic pain is that treatment of the underlying pathology will result in resolution of pain. However, in many cases this is found not to be the case and pain can be persistent leading to the classification of chronic pain as a disease rather than simply a symptom (Cohen, Quintner and Buchanan, 2013). Of particular interest in this regard is an increasingly common trigger of neuropathic pain, that caused by a variety of chemotherapy agents which lead to the development of chemotherapy induced peripheral neuropathy (CIPN). Management of CIPN is notoriously difficult and the fact pain can continue beyond treatment itself is indicative of the progressive nature of the condition (Staff *et al.*, 2017). Therefore, appraisal of the mechanisms underlying its onset and the pathological means by which it persists and worsens is urgently required.

1.2.1: Chemotherapy and CIPN

The term “chemotherapy” refers to the use of a wide range of drugs used either independently or in combination with one another to prevent the growth, spread and survival of cancerous cells (Stone and DeAngelis, 2016). Cancer is one of the leading causes of worldwide mortality and is a major factor in healthcare burdens all over the world (Micheli *et al.*, 2002; Crocetti *et al.*, 2013; Nagai and Kim, 2017). The drugs used to treat cancer are usually very potent, target multiple areas of oncogenesis and are often used in co-ordinated approaches to treat various facets of specific cancer types (Huang *et al.*, 2017; Liston and Davis, 2017). However, a key limitation of nearly every class of chemotherapy drug is the prevalence of off-target effects which can have detrimental effects in myriad contexts and systems of the body. The nervous system is no exception to these off-target effects and chemotherapy induced peripheral neuropathy occurs in the majority of patients largely irrespective of drug class; with around 50-60% experiencing painful symptoms within a few weeks of treatment (Seretny *et al.*, 2014). Though nearly all chemotherapy agents have side effects that can affect the nervous system those most heavily linked to neuropathy and painful sensations fall under the vinca alkaloid, platinum and taxane classifications (Addington and Freimer, 2016). Despite this, these three drug classes are among the most commonly used chemotherapy agents to treat a multitude of tumours in both children and adults (André and Meille, 2006; Ruggiero *et al.*, 2013; Bjornard *et al.*, 2018). Refinement of their use over time has led to optimal outcomes in terms of survival however, the off-target effects of these drugs and the effects they have on people living beyond cancer have been neglected in terms of management and investigation (Arnold *et al.*, 2019). In the past this was largely due to the fact survival rates for cancer were low. Only as the burden of CIPN has increased due to increased survival have substantive efforts been made to ameliorate neuropathic effects of these compounds. As mentioned, neuropathic pain is progressive disease with multiple mechanisms, it would therefore be erroneous to ignore the fact that the differential mechanisms of action possessed by these three compound classes is likely responsible for triggering neuropathic pain in different ways. Indeed treating CIPN as a single, umbrella term likely obscures the various ways the condition could be managed effectively or even reversed (Flatters, Dougherty and Colvin, 2017). It is therefore useful to examine each of these classes separately and to assess their contribution to CIPN aetiology and sequelae before examining CIPN as a whole and elaborating where commonalities exist and how this could impact potential therapy development.

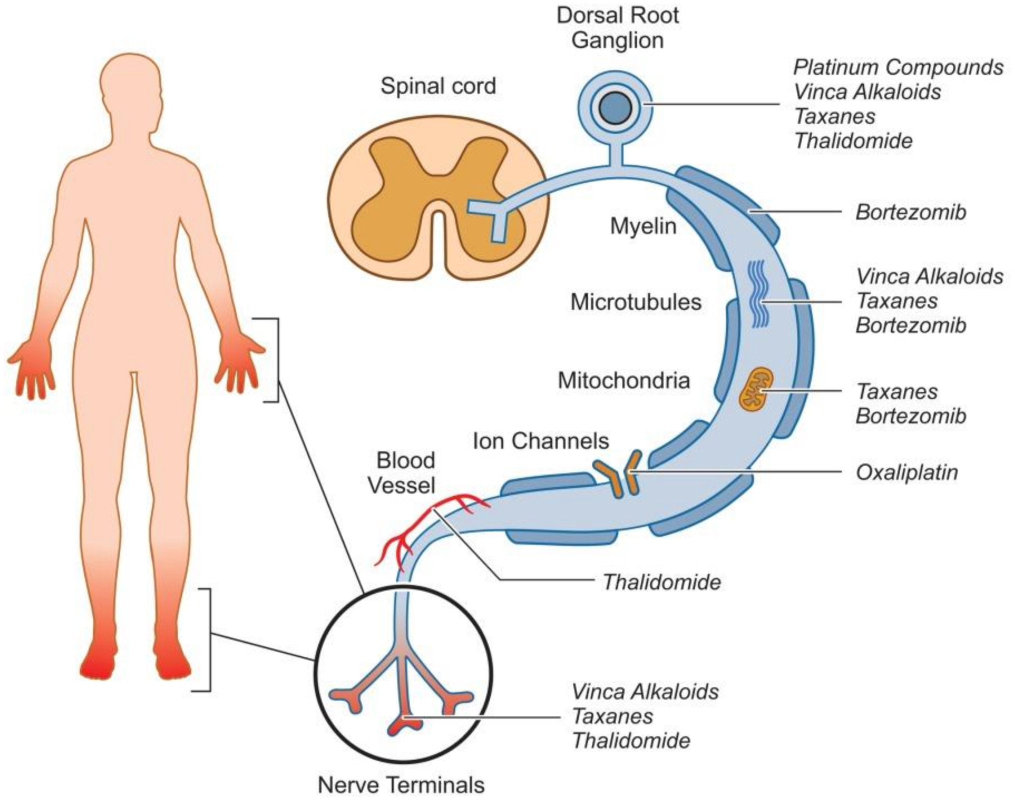

Figure 1.5: Putative sites where chemotherapy agents can cause damage to the peripheral nervous system.

Chemotherapy can affect multiple sites in the nervous system from the peripheral nerve terminals to the neuronal cell bodies located in the dorsal root ganglia. As nerve terminals are often affected first, this leads to early neuropathic symptoms developing in the extremities such as the hands and feet. However, as chemotherapy administration continues multiple sites including mitochondria, ion channels and axons can be damaged leading to more severe sequalae, with many chemotherapy classes capable of damaging multiple sites. From Park *et al*. 2013.

1.2.2.1: Vinca Alkaloids

The vinca alkaloids are a class of compounds derived from *Catharanthus roseus,* commonly referred to as the Madagascan Periwinkle. Common vinca alkaloids include vinblastine and vincristine which were isolated in 1958 and 1961 respectively (Moudi *et al.*, 2013). These compounds can be extracted naturally from the plant without the need for chemical synthesis though this was considered remarkably inefficient with nearly a tonne of periwinkle leaves required to make less than 30g of vincristine (Pennanen and Huhtikangas, 1990; Ishikawa *et al.*, 2009). As a result, semi-natural synthesis which uses precursors from the plant and combines them with chemical sidechains via synthetic reactions to produce vincristine was adopted (Verma *et al.*, 2007). This adopted approach also led to the discovery and production of the semi-synthetic chemical analogues vinorelbine, vinflunine and vindesine in the 1980s (Noble, 1990). In the past two decades however, various methods of total vincristine synthesis have been described (Keglevich *et al.*, 2012; Maqsood and Abdul, 2017). Whilst these newer compounds have limited licensed applications, vincristine is a widely used chemotherapy agent that forms part of combination therapies for non-small cell lung carcinoma, Hodgkin’s Lymphoma, leukaemia and nephroblastoma (Meerwaldt *et al.*, 1997; Douer, 2016; Daw *et al.*, 2020). However, one of vincristine’s most important uses is in the treatment of paediatric brain tumours such as medulloblastoma where it is a frontline therapeutic option (Sirachainan *et al.*, 2018).

All vinca alkaloids share a common mechanism of action, the prevention of microtubule polymerisation via binding to beta tubulin (Owellen *et al.*, 1976; Jordan, Thrower and Wilson, 1991). Microtubules are essential to maintenance of cell structure and transport but also essential in cell division and mitosis (Forth and Kapoor, 2017). Microtubules help form the mitotic spindles that form during cell division. Cell division is a process that relies heavily on the ability of the cell to readily polymerise and depolymerise the microtubule polymers in order to maintain proper microtubule dynamics. With this considered, it is obvious to see the mechanism by which vinca alkaloids operate as an antineoplastic drugs. By inhibiting microtubule function and preventing cell division by inhibiting mitotic spindles, vinca alkaloids prevent the rapid cell division of cancerous cells (Ferguson *et al.*, 1984; Jordan *et al.*, 1985). Microtubule function however is not limited to cell division in cancerous cells, and as a result vinca alkaloids can cause immense disruption to microtubules in healthy cells and other settings. A fundamental component of neurons is expression of β-III tubulin, an isoform of tubulin that is almost exclusively expressed in neurons (Menezes and Luskin, 1994; Katsetos *et al.*, 2002). Not only is β-III tubulin a component of neuron cell bodies, it is also a structural component of axonal processes and therefore essential in maintaining the functions and signals from primary afferents in the periphery (Kapitein and Hoogenraad, 2015). It is therefore unsurprising that all vinca alkaloids cause some degree of sensory neuropathy symptoms such as numbness and tingling; these symptoms are often dose dependent and worsen over time. This can be exacerbated by the eventual emergence of vinca alkaloid resistance in cancer cells, triggered by over activity of ABC transporters that cause drug efflux out of the cell, and require increased dosage in order to manage (Coyle *et al.*, 2015).

The most neurotoxic drug of the vinca alkaloids is vincristine, which has been shown to cause symptoms such as numbness and tingling which emerge quickly after early dosing in up to 90% of patients (Madsen *et al.*, 2019). It is believed the damaging effects of vincristine on axons, cell bodies and axonal transport can all be factors in the onset of neuropathic pain. Vinca alkaloids have poor penetration across the blood brain barrier meaning the majority of their effects are observed on peripheral nerves rather than the CNS, though as discussed neuropathic pain can often become centrally maintained when it persists. Furthermore, accidental administration of vincristine via the intrathecal route, or directly into the CNS is almost always fatal (Bain *et al.*, 1991).

1.2.2.2: Taxanes

Taxanes are a class of compounds derived from the *Taxus* genus, commonly referred to as yew trees (Elias and Korzhenevsky, 1992). Common taxanes include the foundation compound paclitaxel (commonly known as Taxol), docetaxel and cabazitaxel. Paclitaxel was first isolated in the 1970s and approved for usage in ovarian cancers, lung cancers and prostate cancer among others, whereas docetaxel was patented and approved for usage in the 1980s and is also used in a variety of tumours including those of the head and neck (Rowinsky, 1997). Taxanes were also subject the same manufacturing issues as vincristine, with early synthesis heavily limited by availability of the Yew tree, though these have been subsequently addressed (Heinig, Scholz and Jennewein, 2013). The mechanism of action possessed by all taxanes is analogous to that of the vinca alkaloids, they bind to the β tubulin monomer of the α/β tubulin heterodimer which form the sub-units that polymerise together to form functional microtubules (Derry *et al.*, 1997). However a key distinction exists between the two compound classes. Whereas vinca alkaloids bind to β-tubulin and prevent the polymerisation of the structural protein into microtubules that are essential for cancerous cell structure and support, taxanes bind to β-tubulin that is part of heterodimer with α-tubulin and stabilise them as microtubule subunits. This stabilisation prevents depolymerisation of the microtubules which is an essential step in normal microtubule dynamics (Jordan and Wilson, 2004). Throughout cell division for instance, the microtubules that form mitotic spindles are constantly remodelled, disaggregated and re-formed (Burbank and Mitchison, 2000). Stabilising the microtubules prevents this and leads to erroneous cell division, bundling of microtubule mass within the cell and eventually apoptosis and cell death. Again, as mitotic spindle formation is common in rapidly dividing cancer cells it is patently obvious as to why taxanes are extremely effective chemotherapy drugs and similar to vinca alkaloids have become an integral part of many chemotherapy regimens as independent treatments or as part of combination therapy. However as previously explained, microtubule function is not limited to cell division and inhibition of β-tubulin dynamics also affects the neuron specific β-III tubulin isoforms. Therefore it is again no surprise that taxanes are also heavily associated with off-target somatosensory effects (Cella *et al.*, 2003). All taxanes cause a degree of nervous system side effects, the most potent drug in this regard is the original taxane isolate paclitaxel. Paclitaxel causes CIPN in the vast majority of patients, and by some measures is estimated to occur in 87% of recipients (Garrison *et al.*, 2003). Taxanes can impact on fibres and neuronal cell bodies and can mediate the release of inflammatory cytokines following application by generating cancer cell debris or by directly stimulating macrophages (Cassidy *et al.*, 2002; Gartung *et al.*, 2019). As with vinca alkaloids, taxane adverse effects are commonly dose limiting factors in chemotherapy and similar symptoms as for vinca alkaloids commonly emerge in the form of numbness and tingling, commonly interpreted as an effect on large fibres in distal areas of the body (Bhatnagar *et al.*, 2014). Similar to vinca alkaloids, taxanes do not readily cross the blood brain barrier and therefore the effects on the CNS are limited but residual paclitaxel can remain in DRG cell bodies for prolonged periods of time (Wozniak *et al.*, 2016).

1.2.2.3: Platinum Based Chemotherapy

Unlike taxanes and vinca alkaloids, platinum based chemotherapies are not derived from naturally occurring plant sources. The first platinum containing compound, cisplatin was discovered in the 1800s but was not considered for use in chemotherapy until the 20th century and it was approved for use in cancer treatment in 1978 (Gómez-Ruiz *et al.*, 2012). Since then, various analogous compounds such as carboplatin, oxaliplatin and nedaplatin in have been discovered and patented, in chronological order (Piccart, Lamb and Vermorken, 2001). Platinum based compounds are widely used in the treatment of head and neck cancer, lung cancer, brain tumours, bladder cancer and in testicular cancer. In the latter case, platinum based chemotherapy has gained a reputation for being one of the most successful classes of chemotherapy (Hanna and Einhorn, 2014). Testicular cancer patients now have 5 year survival of 90% and it is very common for the young males most often diagnosed to live for several decades (Raghavan, 2003). Platinum based chemotherapies have a common mechanism of action, unlike the taxanes and the vinca alkaloids they do not target cellular machinery involved in cell division but instead target DNA replication at source. When entering a cell, platinum chemotherapy molecule is able to bind to the two purine bases of DNA, adenine and guanine. By crosslinking these bases, transcription of mRNA is disrupted and replication of DNA and downstream cell division is prevented. In addition to this, cisplatin can generate reactive oxygen species (ROS) which interfere with mitochondrial function and trigger apoptosis pathways (Dasari and Tchounwou, 2014; Johnstone, Park and Lippard, 2014). Platinum based chemotherapy can also trigger immune system activation and the release of inflammatory cytokines and disruption to calcium signalling (Leo *et al.*, 2017). Despite targeting alternative mechanisms to the vinca alkaloids and taxanes, platinum based compound are still associated with a high prevalence of CIPN. Some patients report sensory symptoms after the first dose, but over time as dosage begins to accumulate in DRG over 90% of patients report pain and neuropathy symptoms following treatment with cisplatin (Joseph and Levine, 2009). These symptoms present as for other chemotherapy classes as numbness, tingling followed by allodynia. Platinum based compounds readily accumulate in both peripheral ganglia, where it is believed the creation of ROS affects mitochondrial cell bodies and possibly sensitises various ion channels such as TRPA1 and TRPV1 (Dasari and Tchounwou, 2014). A feature very common to platinum based CIPN is the concept of “coasting” (Kanat, Ertas and Caner, 2017). This refers to the symptoms of chemotherapy actually worsening after treatment has stopped. Whilst these symptoms are still dose dependent the delayed onset of sensory sequelae can mean a damaging dose of chemotherapy is given to the patient that only becomes apparent after they treatment has stopped and by which time it is too late to lower the dose. Finally, platinum based chemotherapy can be associated with severe ototoxicity which significantly contributes to reduced quality of life in patients (Pearson *et al.*, 2019).

1.2.3: Jerantinine

The success of the above chemotherapy classes in increasing cancer survivorship in the clinic in spite of their clear and obvious side effects has created pressure around the development of new chemotherapy agents. Novel chemotherapy compounds must retain the efficacy of existing drugs in order to justify their use and as such all novel chemotherapy development focuses first and foremost on targeting cancer cells or the systems that support them such as mechanisms of angiogenesis. But this pursuit of improved efficacy at any costs means investigations into related side effects rarely occur (Berlin, Glasser and Ellenberg, 2008). Instead, research primarily focuses on alternative mechanisms of targeting cancer cells or improving on already proven concepts.

One compound at the earliest stages of development in this regard is the novel indole alkaloid, jerantinine. Jerantinine is derived from the *Tabernaemontana corymbosa* or “Sweet Love” plant endemic to South East Asia. Similar to vinca alkaloids and taxanes, jerantinine is a microtubule inhibitor and prevents the polymerisation of tubulin dimers into microtubule polymers. However, jerantinine causes this inhibition by binding to a different site, the so called colchicine binding site, named after the first compound found to bind to this area (Smedley *et al.*, 2018). Whilst taxanes and vinca alkaloids bind directly to β-tubulin, jerantinine binding at the colchicine site occurs at the interface between both tubulin heterodimers. The perceived advantage of this alternative binding site lies in the notion of cancer cell resistance to vinca alkaloid and taxane chemotherapy. Mutations of tubulin have been found to cause inadequate binding of vinca alkaloids and taxanes to the tubulin site, which prevents the drug from being fully able to inhibit microtubule function (Orr *et al.*, 2003; Ganguly and Cabral, 2011). The result of this is the creation of drug resistant sub-populations which present a threat to survival. By binding at the interface of the two monomers, jerantinine avoids any potential structural effects associated with mutation and thus can target these resistant cells. This has already been demonstrated in a number of different cancer cell lines and development of the compound continues (Raja *et al.*, 2014). However, this alternative binding site may also have promising effects in relation to off-target effects. Cytoskeletal disruption was only observed in a cancer cell lines and not neural stem cells which suggests the drug may be able to distinguish between different types of tubulin expressed in cancer cells and neurons which in turn may result in reduced side effects and CIPN symptoms (Roper *et al.*, 2018). However neural stem cells are significantly different from terminally differentiated neurons. Consequently, it will be useful to examine jerantinine in more specific adult neuronal models for off-target effects and to directly compare them to existing chemotherapy agents.

1.2.4: Common Features and Mechanisms of CIPN

As the above sections have demonstrated, there are multiple mechanisms by which CIPN and occur and be maintained. Though the 3 compound classes have different mechanisms of action they share remarkable similarity in how they can initiate pathological changes within the nervous system. The most obvious comparison to be drawn is between the taxanes and vinca alkaloids as both are microtubule inhibitors. The profound effects these compounds have on axons is cited within the literature as a major source of neuropathy (Sahenk *et al.*, 1994; Guo *et al.*, 2017). CIPN appears first in a “stocking and glove” pattern, with the toes, feet and hands affected, this is likely because longer axons tend to be affected first, therefore the effects of microtubule dysfunction on these fibres are logical (Starobova and Vetter, 2017). The involvement and activation of the inflammatory system is common across all 3 classes and increased expression of cytokines such as TNF-α are believed to contribute heavily to nervous tissue damage following therapeutic usage (Sprowl *et al.*, 2012; Wang *et al.*, 2018; Abdel-Wahab and Moussa, 2019). In addition to the potential damage, inflammatory cytokines can change the expression and excitability of peripheral neurons through modulation of sensory receptors such as TRP and ion channels. These changes could feasibly occur in the absence of overt damage as the inflammatory soup begins to accumulate and understanding whether pain and sensitisation can occur without overt neuronal damage, as examined via histology could be of major benefit when investigating the earliest stages of CIPN. Another reason as to why this could be important is in terms of diagnosis, commonly only larger fibres are examined for neuronal damage in the clinic, despite symptoms of small fibre neuropathy (tingling, burning) being common across all 3 classes (Sharma *et al.*, 2015). This is potentially a relatively unexplored avenue for investigation, as amelioration of small fibre neuropathy could in turn prevent progression to widescale CIPN that affects larger fibres. The high prevalence of CIPN and the potency of the compounds used, often invoking these effects at low or minimal doses demonstrates a clear need for proactive and prophylactic therapy when treating CIPN. Currently, all analgesics and anticonvulsants are used therapeutically despite evidence showing often irreversible damage has occurred by this stage. There is therefore a pressing need for novel approaches that can ameliorate the mechanisms noted above.

One such approach worthy of investigation is modulation of novel splicing kinases and alternative splicing. Use of differential VEGF isoforms and inhibition of the kinases responsible for this varying isoform expression has shown promising effects in cancer, ophthalmic and diabetic contexts, a component of the latter being amelioration of nervous system sequelae commonly seen in diabetic neuropathy (Ved *et al.*, 2018). Furthermore, chemotherapy can also have profound effects on alternative splicing itself which may contribute to these pathological neuronal changes (Shkreta *et al.*, 2008). Controlling alternative splicing in advance of chemotherapy via prophylaxis could be useful in CIPN prevention, and by modulating potential targets on the pathways listed or indeed putative neurotoxic alternative splicing events resulting from chemotherapy possibly aid in therapeutic recovery of damaged nervous tissue.

1.3.1: Alternative Splicing

Alternative pre-mRNA splicing (herein alternative splicing) describes the process by which multiple different mRNA transcripts can arise from the same gene, often leading to expression of functionally distinct but related protein isoform families (Wang *et al.*, 2015). As the name implies alternative splicing is distinct from constitutive splicing, the process by which non-protein coding introns are removed from nascent pre mRNA strands allowing all of the protein-coding exons in the primary transcript to be contained within the mature mRNA and translated sequentially (Fabrizio and Lührmann, 2012; Wickramasinghe *et al.*, 2015). Alternative splicing often results in exclusion of particular exons, or inclusion of intronic sequences leading to differential protein expression when translated. This serves to increase the of size the proteome relative to the human genome. Advances in genome sequencing revealed the size of the human genome to be approximately 20,000 to 25,000 genes, whereas analysis of the human proteome reveals upwards of 100,000 distinct proteins. This finding supplanted the “one gene = one protein” hypothesis that had predominated and vastly expanded investigations into control of gene expression in the body (Ponomarenko *et al.*, 2016). Other mechanisms such as single nucleotide polymorphisms enable a single gene to be able to produce potentially dozens of proteins from the same DNA template (Chiang, Wu and Chen, 2017). It is estimated that over 95% of human genes are alternatively spliced, the control of which can be initiated or blocked by multiple mechanisms such as developmental stage or tissue or tissue dependent factors (Chen and Manley, 2009). The different mechanisms of alternative splicing are shown in Figure 1.6. Briefly, alternative splicing can be mediated by the differential inclusion and exclusion of various exons from a primary transcript. Alternative splicing mechanisms include inclusion of introns, alternative 5’ and 3’ splice sites, use of alternative promoters and stop codons, and the existence of mutually exclusive exons. By these means, a single gene can give rise to numerous protein isoforms (Donaldson and Beazley-Long, 2016).

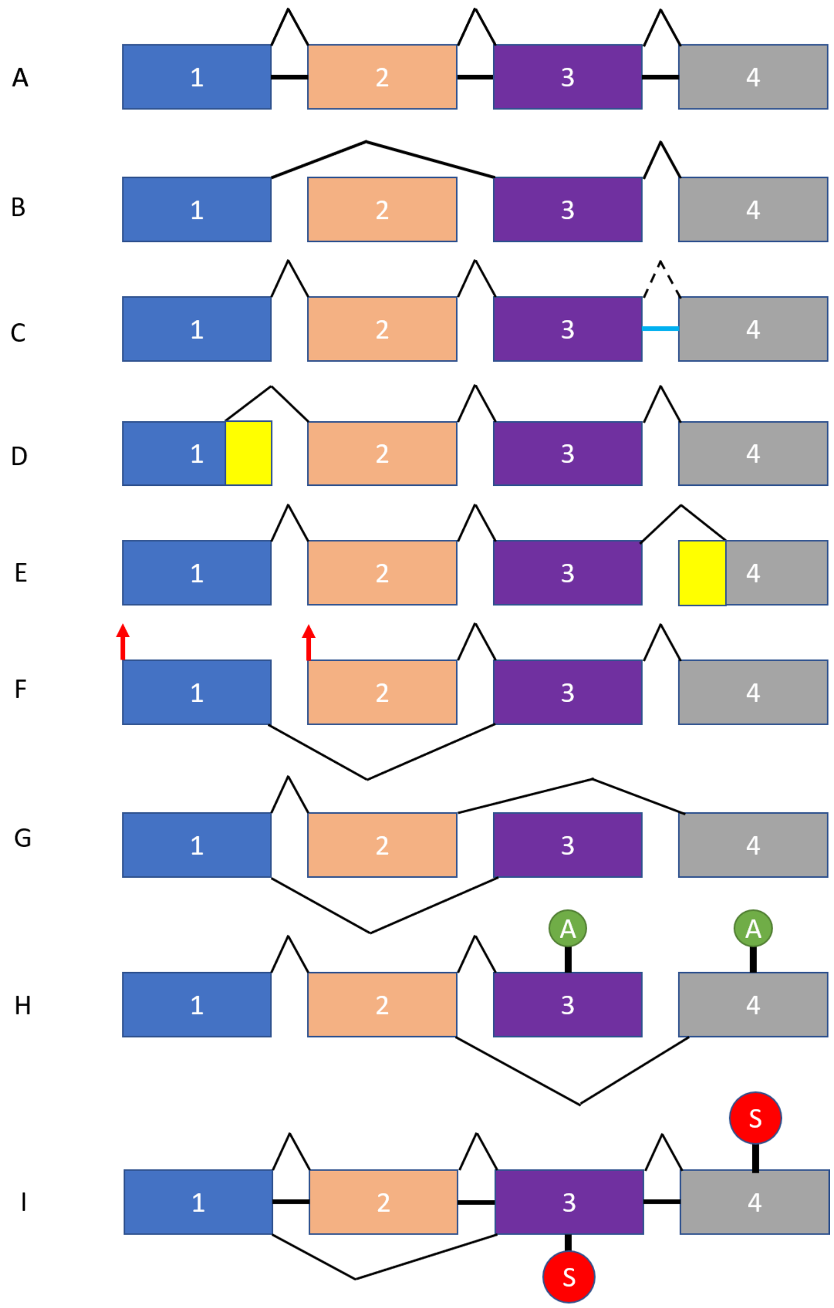

Figure 1.6: An Overview of Alternative Splicing Mechanisms:

A pre mRNA transcript that is constitutively spliced (A) can be alternatively spliced by the following mechanisms. Different colours denote different exons. (B) Exon skipping, exon 2 is omitted from mRNA transcript. (C) Intron retention, the intron between exon 3 and 4 is not spliced out. (D) Alternative 5' donor site, an alternative intra exonic splice site in exon 1 is used and gives an alternative 5' sequence. (E) Alternative 3' acceptor site, an intra exonic splice site in exon 4 is used and gives an alternative 3' sequence. (F) Alternative promoters, red arrow denote alternative promoters leading to multiple transcripts. (G) Mutually exclusive exons, exon 2 or exon 3 are differentially included or excluded. (H) Alternative polyadenylation states, creating truncated transcripts. (I) Alternative stop codons, constitutive splicing uses stop codon in exon 4, whilst exclusion of exon 2 leads to alternative stop codon in exon 3 and nonsense mediated decay.

Due to the profound effect that alternative splicing can have on protein function it is no surprise that dysregulation of alternative splicing can lead to a plethora of pathological conditions including but not limited to cancer, dementia and peripheral arterial disease (Ward and Cooper, 2010). Aberrant splicing can lead to the production of isoforms that are non-functional, or over-active. For example, in various cancers, alternatively splicing defects lead to the expression of genes associated with drug efflux such as *ABCB1* and *MRP* pumps, contributing to tumour resistance (He *et al.*, 2004; Eblen, 2012). These changes often occur due to mutations of components responsible for regulation of alternative splicing causing dysregulation. These other targets can aid the cell in evading apoptosis or aid the tumour in developing a blood supply via angiogenesis. Therefore control of alternative splicing is pivotal to normal physiology and this is reflected in the complex mechanisms by which alternative splicing is regulated and carried out.

1.3.2: Regulation of Alternative Splicing

The mediator of RNA splicing within mammals is the spliceosome. The spliceosome consists of a number of small nuclear ribonucleoproteins (snRNPs) that form a complex. In total the spliceosome consists of around 100 associated proteins, and the SNPs themselves are associated with a complimentary small nuclear RNAs (snRNA) that aid with regulation of pre-mRNA and transcription factors. The main constituents of the spliceosome are the 5 snRNPs U1, U2, U4, U5 and U6 (Wilkinson, Charenton and Nagai, 2020). Canonically, the spliceosome recognises an intron via its 5’ splicing site and U1 and U2 form the so called “A complex”. This complex then conjugates with the tri snRNP B complex which consists of the remaining snRNPs and the pre-mRNA. From this point U4 detaches and unwinds U6snRNA and forms the active site of the "B_{act} complex" which is the first catalytic state of the complex. From this point, the B_{act} complex is further remodelled into the C complex to enable further catalysis and initiate exon ligation, that is to say the process by which two constitutively expressed exons are joined into mature mRNA. From here the ligated exons are released and the so called lariat introns, that is the introns removed during the process of splicing, are decayed as the spliceosome deconstructs and the components are recycled for further use in future splicing events (Lee and Rio, 2015). It should also be said at this point, the process described here is the activity of the major spliceosome, which is responsible for around 99% of splicing events within the body. The remaining 1% is carried out by the minor spliceosome which utilises the U11 and U12 snRNPs among others (Turunen *et al.*, 2013; Verma *et al.*, 2018).

This intrinsically complex process describes constitutive splicing performed as one may expect to see according to the "one gene = one protein" hypothesis. However, the spliceosome can be moderated and adapted to result in alternative splicing mechanisms (Figure 1.5) by a range of different promotional and inhibitory factors. These can include the presence differential motifs on pre-mRNA that may enhance or inhibit splicing by the spliceosome. The most commonly observed intron-exon boundary motifs that determine a splicing site are GU at 5' and AG at 3' sites respectively. However, the nucleotide sequence downstream and upstream of these motifs determines whether a splicing site is "strong" or "weak". Strong splicing sites are much more likely to result in regulation of constitutive splicing. However "weaker" splice sites are much more likely to lead to alternative splicing as the spliceosome does not catalyse the pre-mRNA at this point, leading to ligation of the intron and the exon together (Dvinge, 2018). It is also the case that weak splice sites may contain multiple alternative splice sites that can be recognised and may therefore compete with each other and the original “authentic” splice site.

Another route of alternative splicing regulation is based on tissue specificity (Rodriguez *et al.*, 2020). Whilst mechanisms of splicing are becoming increasingly well defined in general contexts there is comparatively less literature on how alternative splicing of mRNAs within certain tissues or at discrete developmental stages actually occurs (Ke and Chasin, 2011). There are however a few well documented exceptions to this that have been extensively investigated. Namely in neurons the splicing factor NOVA is responsible for the differential expression of voltage gated calcium channels and the development expression of various synaptic proteins. Tissue specific splicing factors can act as enhancers or promoters of splicing or can work in concert with each other to regulate it. Such is the importance of tissue specific splicing that NOVA-2 knockout mice die soon after birth, with deficits associated with disrupted synaptic function such as tremor (Allen, Darnell and Lipscombe, 2010; Racca *et al.*, 2010).

The promoting or suppressive activity of tissue specific splicing factors is similar to another key regulator that can control alternative splicing, the so called RNA Binding Proteins (RBPs). RBPs serve to either suppress or enhance alternative splicing and are often termed splicing factors (Singh, 2002). Though several families of RBPs exist, two of the most prominent are the heterogeneous nuclear ribonucleoproteins (hnRNPs) and the serine/arginine rich splicing proteins (SR Proteins). As their name implies these RBPs can bind directly to immature pre-mRNA transcripts and from this point they can have profound effects on splicing and hence the nature of the functional protein that is expressed as a result of their activation (Zhou and Fu, 2013). SR proteins are generally viewed as factors that enhance splicing facilitated by the presence of repeated Arg-Ser amino acids on the C-terminus, a region appropriately termed the RS domain. At the N-terminus there exists the RNA Recognition Motif (RRM) domain (Shen and Green, 2006; Ghosh and Adams, 2011). The RRM is responsible for the recognition of small, distinct RNA sequences or so called Splicing Regulatory Elements (SREs). These sequences can either be exonic splice enhancers or suppressors (ESEs or ESSs) or intronic splice enhancers or suppressors (ISEs or ISSs) (Wang and Burge, 2008).

As mentioned, SR proteins are associated with enhanced alternative splicing and therefore the SRE they most commonly associated with are the ESEs. SR proteins can be present both inside and outside of the nucleus and this can often dictate the activity of the protein as to how it influences alternative splicing (Ghosh and Adams, 2011).

Conversely, the hnRNPs are largely viewed as splicing suppressors, they most commonly bind to ISS SREs, However, the two families can often compete with each other and regulate the activity of the other family. A prominent example of this is the interaction between SRSF1, a SR protein that can be trafficked to the nucleus under certain conditions and the hnRNPA1 protein. In this example it is the balance of these two families that controls the process of alternative splicing. If the hnRNPA1 protein is present in greater quantity than SRSF1 it antagonises the effects of SRSF1 and leads to the selection of distal splicing sites, whereas if SRSF1 predominates the opposite occurs and more proximal splice sites are selected by the spliceosome. It is the complex nature of these interactions and the balance between them that dictates the level and nature of alternative splicing within the body (Ladomery, Harper and Bates, 2007; Golan-Gerstl *et al.*, 2011; Gonçalves *et al.*, 2014).

1.3.3: Regulation of SR Proteins

As aberrant alternative splicing can result in an array of diseases such as cancer, tight control of splicing is essential to maintaining healthy function within the body. As such, components of the splicing pathway that can enhance splicing activity such as SR proteins are tightly regulated. Some SR proteins are themselves alternatively spliced with only 1 transcript coding for a protein with functionality (Ladomery, 2013). The remaining splice variants result in frameshifts or incorporation of premature stop codons to generate SR protein that is then removed via nonsense mediated decay. This reduces alternative splicing activity by SR proteins and downregulates functional SR. Perhaps more interestingly, SR protein activity is often influenced by the activity of upstream mediators. For example, SRSF1 will only translocate to the nucleus following phosphorylation by Serine/Arginine Protein Kinase 1 (SRPK1). This phosphorylation occurs in the RS domain and causes the SRSF1 protein to be translocated to the nucleus. Even after this, SRSF1 will then only interact with the spliceosome when released from so called nuclear speckles or ‘splicing factor compartments’ which contain the protein (Spector and Lamond, 2011). To be released from speckles SRSF1 is further phosphorylated by cdc-2 like kinase 1 (CLK1) (Aubol *et al.*, 2016).

The full mechanism behind this regulation is yet to be fully elucidated but the most current model indicates that SRPK1 and CLK1 are capable of forming a complex that works to release “primed” SRSF1 protein from nuclear speckles. This model has largely supplanted a previous, more straightforward model that suggested SRPK1 would prime SRSF1 protein and then CLK1 would effectively carry this forward. The presence of SRPK1 within the nucleus however precipitated further investigation that revealed a much more complex mechanism. Briefly, the SRPK1/CLK1 complex can release SRSF1 in 2 distinct ways; firstly SRPK1 cannot phosphorylate Ser-Pro residues of the SRSF1 RS domain and is reliant on CLK1 to phosphorylate these residues; CLK1 as an independent kinase however is a very slowly acting kinase but when joined to the SRPK1 complex it overcomes its slow turnover number (the maximum chemical conversions of a given enzyme at a given concentration) to rapidly hit Ser-Pro residues and release SRSF1 to interact with the spliceosome (Nowak *et al.*, 2008; Aubol *et al.*, 2016). Secondly, slowly acting, non-complex bound CLK1 binds to SRSF1 by its inherently disordered N-terminus which phosphorylates the RS domain stochastically (Aubol *et al.*, 2013). SRPK1 can remove the CLK1 N-terminus bound to the SRSF1 RS domain and release the phosphorylated protein by effectively preventing CLK1 from stabilising it. The released SRSF1 is then present in an activated state and can readily interact with the spliceosome. This brief explanation provides an insight into the potential complexity of alternative splicing regulation. It also emphasises the number of steps involved in these processes that gives rise to a multitude of targets that could be available to potential control. It is clear from the explanation above that inhibiting both CLK1 and SRPK1 would have profound effects on SRSF1 alternative splicing targets. One such downstream target is Vascular Endothelial Growth Factor A (VEGF-A), a growth factor primarily linked to angiogenesis but one that has been shown in the literature to have effects on pain. Control of VEGF-A function by alternative splicing control therefore could be a novel therapeutic target for analgesia (Hulse *et al.*, 2014; Donaldson and Beazley-Long, 2016)

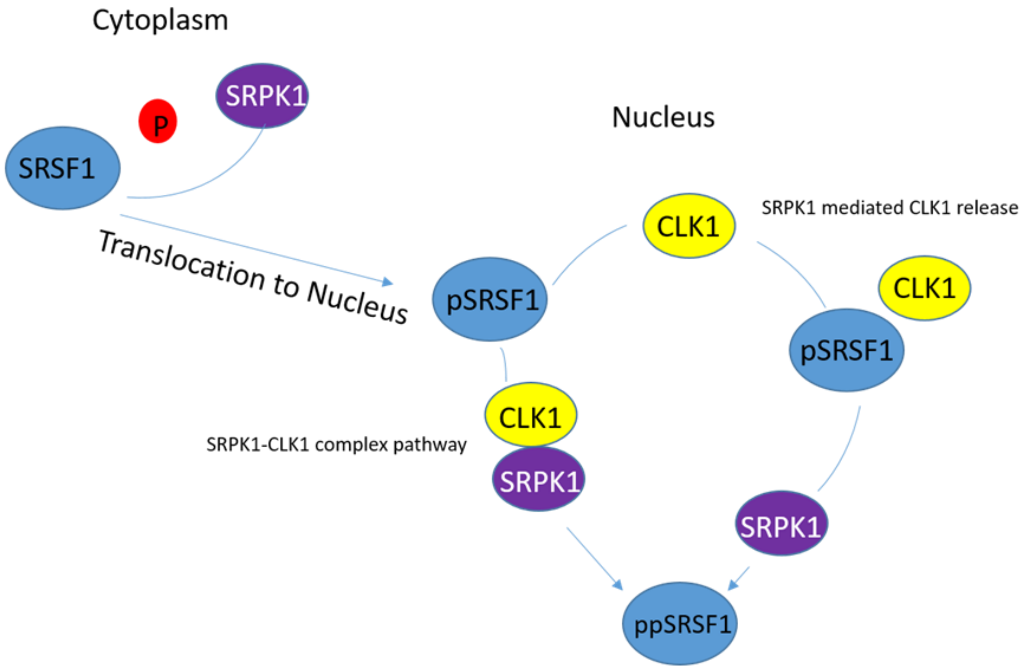

Figure 1.7: Overview of SRPK1/CLK1 mediated phosphorylation and activation of SRSF1 protein. Adapted from Aubol et al. 2020.

Cytoplasmic SRPK1 phosphorylates inactive SRSF1 which then translocates to the nuclear speckles. From here phosphorylated SRSF1 (pSRSF1) can be further activated in 2 pathways. Firstly, by slow phosphorylation by CLK1 and subsequent SRPK1 mediated CLK1-SRSF1 separation. Secondly by the formation of the SRPK1-CLK1 complex which rapidly phosphorylated RS domain SRSF1 residues. Both pathways culminate in hyper-phosphorylated SRSF1 (ppSRSF1) that can exert effects in the spliceosome. Adapted from Aubol *et al.* 2020.

1.3.4.1: Alternative Splicing of VEGF-A

Vascular endothelial growth factor A is a growth factor that is most commonly associated with major physiological functions in angiogenesis, maintenance of endothelial cells and vascular permeability control. VEGF-A is the prototypical member of the VEGF family which also contains VEGF-B, VEGF-C, VEGF-D VEGF-E and VEGF-F. VEGF-B-D are found endogenously in the body and have roles in cardiovascular development and lymphangiogensis respectively (Shibuya, 2011). VEGF-E is encoded in multiple viruses and can lead to the development of pustular skin lesions. Finally VEGF-F is found within snake venom (Yamazaki *et al.*, 2009). VEGF-A was first identified and termed “Vascular Permeability Factor” by Senger et al. due its profound effects on interstitial fluid accumulation before later work by Ferrara and Henzel found the protein had profound mitotic influence on cultured endothelial cells leading to a change in nomenclature (Senger *et al.*, 1983; Ferrara and Henzel, 1989). Since then the importance of VEGF-A in normal physiological processes has been studied in depth. VEGF-A is essential in embryonic development of blood vessels, with knockout models demonstrating lethality (Hiratsuka *et al.*, 2005). VEGF-A exerts vascular effects via two main receptors; VEGFR1 and VEGFR2. Knockout of these receptors at embryonic stages is again lethal and in adult animal models causes severe endothelial cell dysregulation (Ferrara, Gerber and LeCouter, 2003). Since its discovery in vascular contexts several roles have been found for VEGF-A including important functions in both nociception and the wider nervous system (Hulse *et al.*, 2014). VEGF-A and its functions are dependent on the way it is alternatively spliced.

VEGF-A has two families of splice variants of varying length and potentially opposing functions, these two families are termed VEGF-A_{xxx}a and VEGF-A_{xxx}b (xxx denotes amino acid length of protein.). In the majority of tissues VEGF-A_{xxx}b isoforms predominate and are associated with maintenance of tissue integrity and function in non-angiogenic tissues such as DRG, skin and colon (Pritchard-Jones *et al.*, 2007; Varey *et al.*, 2008; Hulse *et al.*, 2014). VEGF-A_{xxx}a isoforms play important roles in the prototypical function of the protein, contributing to angiogenesis in developing tissues and in the placenta and as such expression of VEGF-A_{xxx}a isoforms is physiological feature (Ortega *et al.*, 2019). The potency of alternative splicing leading to different functional proteins is apparent by the fact that the physiological function of these two families is dictated by just six amino acids on the C-terminus of the protein. In the case of the VEGF-A_{xxx}a isoforms the final six amino acids are cysteine, aspartate, lysine, proline and two arginine repeats (CDKPRR), whereas the terminal six amino acids of the VEGF-A_{xxx}b isoforms are serine, leucine, threonine, arginine, lysine and aspartate (SLTRKD) (Bates *et al.*, 2002). This sequence is determined by the selection of alternative 3' splice sites in Exon 8 of the *VEGFA* gene. This selection is in turn decided by the actions of SRSF1 and upstream SRPK1 and CLK1 activity. An overview of VEGF alternative splicing can be seen in Figure 1.8.

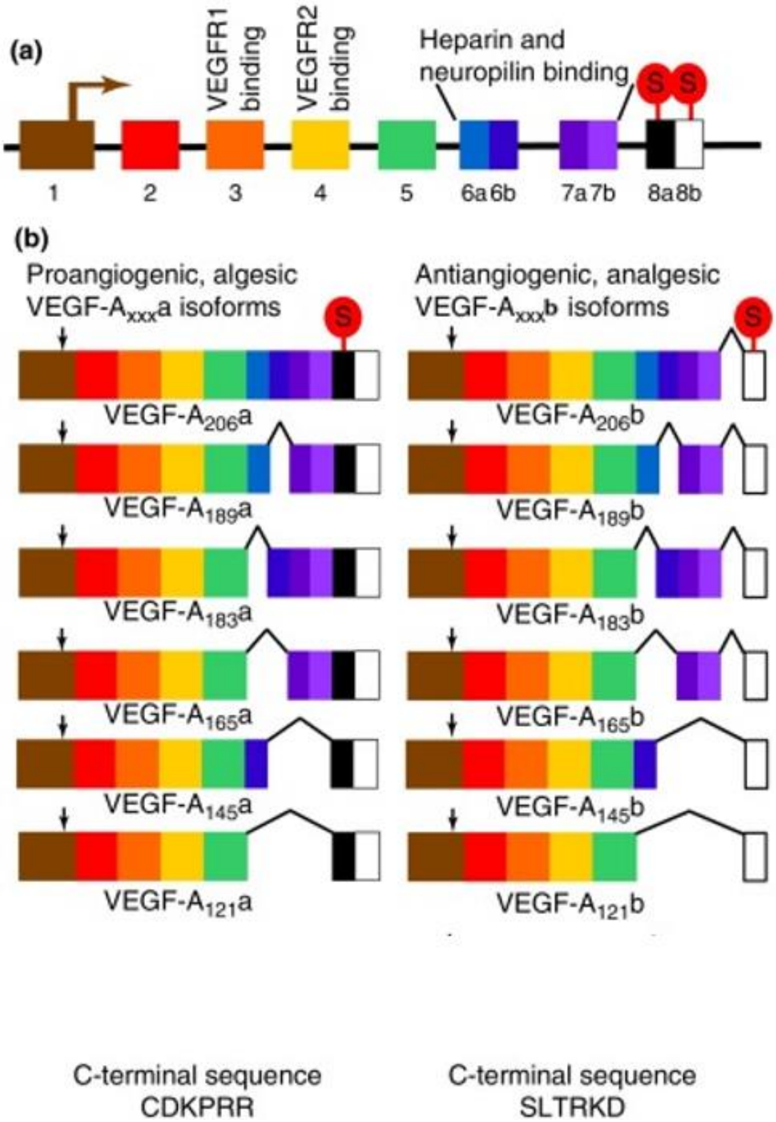

Figure 1.8: VEGF Isoforms Summary

(A) Structure of the *VEGFA* gene showing translational start (Exon 1 Arrow), VEGFR binding sites, neuropilin binding sites and heparin binding sites. (B) The VEGF splice variant family, the angiogenic, algesic VEGF-A_{xxx}a family are displayed on the left and the non-angiogenic VEGF-A_{xxx}b isoforms are displayed on the right. Splice site selection on Exon 8 determines the isoform expressed. Selection of the proximal splicing site results in the inclusion of exons 8a and 8b. Selection of the distal splice site on exon 8 only results in inclusion of Exon 8b. The C-terminal sequences are displayed at the bottom of the figure. From Donaldson, 2016.

Selection of the proximal splice site in exon 8a occurs when SRSF1 is phosphorylated by SRPK1/CLK1 and released from nuclear speckles to interact with the spliceosome (Nowak *et al.*, 2008, 2010). This leads to the expression of the most commonly recognised VEGF-A_{xxx}a isoforms. Conversely, if SRPK1 phosphorylation does not occur SRSF1 does not translocate to the nucleus and the distal splice site on Exon 8b occurs leading to expression of the alternatively spliced VEGF-A_{xxx}b isoforms. Splice isoforms of varying length between 121 and 206 amino acids exist in humans and mouse and in most conditions in which VEGF-A plays a role the two most abundantly expressed and studied isoforms are VEGF-A_{165}a and VEGF-A_{165}b. These two isoforms have directly contradictory functions in multiple contexts (Beazley-Long *et al.*, 2013; Gammons *et al.*, 2014; Mavrou *et al.*, 2015; Hulse *et al.*, 2016). Other splice variants include VEGF-A_{183} and VEGF-A_{206} which have strong heparin binding properties and are largely sequestered to the cell surface and extra-cellular matrix. Conversely, VEGF-A_{121} lacks heparin binding capabilities. VEGF-A_{165} isoforms can bind heparin, but not as strongly as VEGF-$A_{183/201}$ and is therefore also found in circulation and can be secreted, a property also possessed by VEGF-A_{121} and VEGF-A_{145}. Some isoforms are also to be tissue specific, as VEGF-A_{145} and VEGF-A_{206} are seemingly restricted to the placenta (Azimi-Nezhad, 2014; Peach *et al.*, 2018).

1.3.4.2: Functions of VEGF-A_{165} Isoforms acting at VEGFR1/2

Although the VEGF-A_{xxx}a and VEGF-A_{xxx}b isoforms may have opposing functions both isoforms exert their effects primarily through binding to the tyrosine kinase receptor/ vascular endothelial growth factor receptor 2 (VEGFR2, also known as Flk1) (Ferrara, Gerber and LeCouter, 2003). Upon binding to VEGFR2, VEGF-A_{165}a isoforms trigger conformational changes to the receptor and its various domains resulting in receptor dimerization and binding of neuropilin 1 (NP-1), a membrane bound co-receptor to VEGFR2. These changes are followed by phosphorylation, predominantly of key tyrosine residues such as Y1175 which is key for full activation of receptor signalling (Hulse *et al.*, 2016; Peach, Kilpatrick, *et al.*, 2018; Peach *et al.*, 2018). Complete VEGFR2 phosphorylation activates a number of downstream pathways (Figure 1.9) which result in the canonical functions of VEGF-A_{165}a such as increased vascular permeability, cellular proliferation, transformation of cells into migrating phenotypes from previous quiescent states and angiogenesis when binding occurs in endothelial cells (Benton and Whittemore, 2003; Harper and Bates, 2009). Because of these effects on VEGFR2 phosphorylation, dimerization and NRP binding VEGF-A_{165}a is regarded as a full agonist of VEGFR2. In contrast, VEGF-A_{165}b does not induce these effects. Previous theories included reduced affinity for VEGFR2, however studies have shown VEGF isoforms have remarkably similar affinities for the receptor (Peach, Kilpatrick, *et al.*, 2018). It has been observed that whilst VEGF-A_{165}b has equal affinity for VEGFR2 the effects it has in terms of inducing conformational changes or causing phosphorylation of tyrosine residues are different. For example, Y1175 is not fully phosphorylated by VEGF-A_{165}b binding to VEGFR2 and there is a weaker NRP interaction and little to no PiP2 hydrolysis and PKC activation (Ballmer-Hofer *et al.*, 2011; Kisko *et al.*, 2011). As a result, fewer or different intra-cellular pathways to those associated with canonical VEGF function are activated. VEGF-A_{165}b is also recognised as being anti-angiogenic, though whether this is caused by actual blockade or competition for VEGFR2 is still somewhat debated. Though recent evidence does demonstrate that VEGF-A_{165}b isoforms are clearly functional at VEGFR2, even if the downstream signalling pathway is yet to be fully defined.

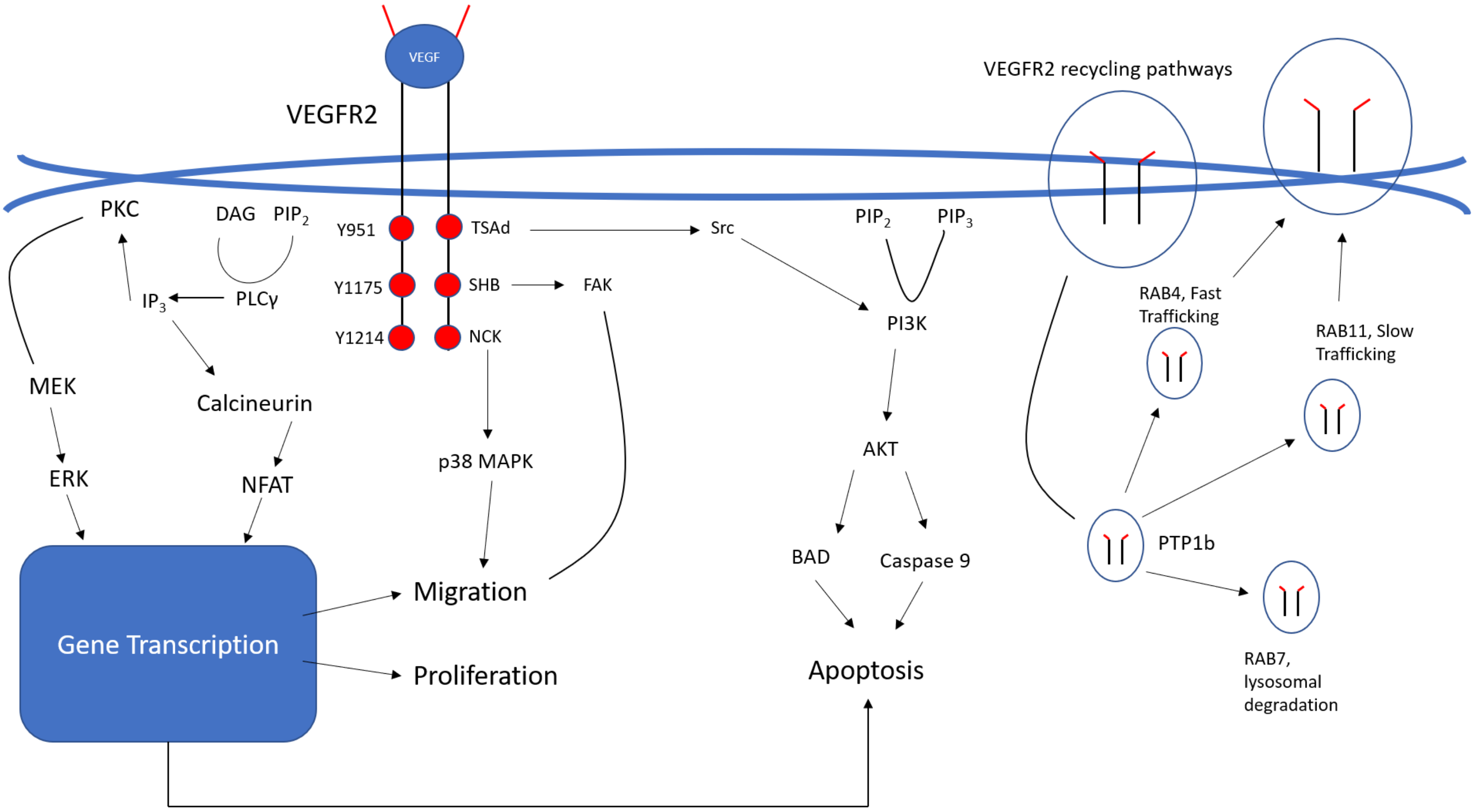

Figure 1.9: VEGF Signalling at VEGFR2

Following binding of VEGF-A ligands to the VEGFR2 receptor, the transmembrane helices rotate causing conformational changes in the VEGFR2 receptor and phosphorylation of various tyrosine residues (represented by Yxxx). This phosphorylation causes the creation of binding sites for downstream cytoplasmic proteins which in turn initiate cell signalling via pathways such as MAPK, ERK1/2, AKT signalling, FAK and PLCγ. This in turn triggers differential cellular mechanisms such as migration, proliferation, apoptosis, changes to vascular permeability and reorganisation of the cytoskeleton. VEGFR2 is internalised and can be recycled or degraded via lysosomes. It should also be noted this diagram assesses pathways in endothelial cells. Assessment of VEGF signalling in neurons has revealed an absence of MAPK signalling and PLC/PKC related calcium signalling. Adapted From Peach *et al.* 2018.

VEGF-A_{165}a is vital for vascular development important during development as mentioned previously with regard to lethality in knockout models. VEGF-A_{165}a is also important in physiological regulation and pathological conditions such as hypoxia, inflammation and tumorigenesis and is often upregulated in these conditions (Ferrara and Davis-Smyth, 1997; Mavrou *et al.*, 2015). The VEGF-A_{165}a isoform is also upregulated by the release of damage-related cytokines such as TNF-alpha to levels that may result in increased circulating levels of VEGF-A_{165}a in some patients groups (Gavrilă *et al.*, 2016; Beazley-Long *et al.*, 2018). The two isoforms can be co-expressed in tissues, can bind to VEGFR2 with similar affinities and act as competitors for the VEGFR2 site. It is therefore hypothesised that that it is the ratio of these isoforms present in tissue and therefore the control of alternative splicing that determines the eventual VEGF-A-mediated effects at a specific site (Oltean *et al.*, 2012). Because of VEGF-A_{165}b's partial agonism of VEGFR2 it has been demonstrated that occupancy of VEGFR2 over the more potent isoform serves as a form of antagonism, whilst not actually being classified as a VEGFR2 antagonism in of itself (Peach *et al.*, 2018). It is therefore evident that controlling isoform expression via alternative splicing is pivotal in determining the functional effects of VEGF and in recent years control of this process has been linked with profound ramifications in terms of nociception.

1.3.4.3: VEGF, Nociception and Neuropathic Pain

Despite being discovered some 30 years ago it is only in recent years that a role for VEGF in the nervous system and in nociception has emerged. VEGF-A has been found to promote neurite outgrowth, neuron growth and have trophic effects on neuronal companion cells such as glia in both the PNS and CNS (Muratori *et al.*, 2018; Sondell, Sundler and Kanje, 2000; Beazley-Long *et al.*, 2013; Calvo, Pastor and de la Cruz, 2018). Anti-VEGF therapy such as bevacizumab is often used alongside other chemotherapy agents and the anti-angiogenic effects of vinca alkaloids, taxanes and platinum based chemotherapy have been associated with painful symptoms in patients (Burger *et al.*, 2007; Cohen *et al.*, 2007). As these agents can downregulate both isoform families it suggests a neuroprotective role for both isoforms. However, promoting VEGF-A_{165}a expression for purely neuroprotective purposes would not be advisable because of the profound effects the isoform can have on pathological angiogenesis and aberrant vascular permeability (Hulse *et al.*, 2014). Furthermore, despite being neuroprotective there is increasing evidence demonstrating that the angiogenic isoform is pro-nociceptive. As mentioned in inflammatory conditions or tissue damage scenarios, VEGF-A_{165}a isoforms are likely to predominate over their counterparts. Hulse et al. demonstrated that when applied as recombinant protein in mouse models VEGF-A_{165}a protein induced mechanical sensitisation whereas a larger dose of VEGF-A_{165}b protein had no effect on sensitivity. Furthermore in response to partial saphenous nerve injury (PSNI), VEGF-A_{165}a expression increased 10 fold, which was associated with SRSF1 nuclear localisation suggesting injury or chemical insult may activate SRPK1 and induce changes in alternative splicing (Hulse *et al.*, 2014, 2016). This was also associated with VEGFR2 phosphorylation in DRG neurons showing that VEGF may directly initiate these effects through signal transduction of neuron bound receptors. These changes were reversed by application of SRPIN340, an SRPK1 inhibitor which was administered to the injured rats therapeutically. Furthermore in rodent models of diabetic neuropathy Bestall et al. demonstrated the benefits of VEGF-A_{165}b recombinant protein in reducing dissociated neuronal sensitivity to TRPV1 stimulation following application of capsaicin, in addition to finding VEGF-A_{165}b expression was decreased in STZ induced diabetic rats which was then associated with neuropathic pain in these animals (Bestall, 2017). This is also important as TRPV1 knockout mice do not experience sensitisation when subjected to VEGF-A_{165}a, suggesting TRPV1 may be pivotal in causing VEGF related sensitisation. Bestall also demonstrated diabetic related pain could be prevented by prophylactic dosing of VEGF. More relevant to CIPN, Vencappa et al. showed that cisplatin induced neuropathy could be attenuated by both isoforms of VEGF. Administration of cisplatin resulted in upregulation of stress factors such as cleaved caspase 3, which were reversed with recombinant application of VEGF, however this study did not examine nociception in these animals leaving the role of VEGF in ameliorating chemotherapy induced pain as to yet unanswered (Vencappa, Donaldson and Hulse, 2015).

It should be noted however that there is some conflict within the literature with regard to the roles of VEGF isoforms in nociception. Some studies have demonstrated that VEGF-A_{165}b to be nociceptive in chemotherapy related pain (Di Cesare Mannelli *et al.*, 2018). Interestingly, the same study found this effect to be ameliorated by co-treatment with the VEGF neutralising antibody bevacizumab, which as noted above have been associated with painful symptoms in patients. In spite of this, the majority of the literature does suggest an anti-nociceptive role of VEGF-A_{165}b in a variety of painful conditions but it is worth considering that control of alternative splicing and modulation of splicing kinases would not affect just one protein family and that other mechanisms may also underpin any observed anti-nociceptive effects.

Though the mechanisms behind VEGF-A_{165}a related sensitisation remain to be fully explored, it is clear the protein has profound effects in a variety of painful conditions including diabetic neuropathy, a close analogue of CIPN and in cisplatin induced neuropathy (Bestall *et al.*, 2018). It is likely that activation of splicing kinases such as SRPK1 is responsible for these changes. Though most of these studies used recombinant protein to demonstrate promising effects, recombinant proteins are limited in clinical usage by short half-lives, side-effects, limited systemic distribution and specificity (Hutt *et al.*, 2012). Therefore it is more practical to prevent pathological changes occurring upstream of splicing by inhibiting novel splicing kinases such as SRPK1 and CLK1. As these kinases are activated in neuropathic pain states they are responsible for a number of downstream splicing events not limited to VEGF, it is important to consider other mechanisms of splicing and alternatively spliced proteins that could invoke neuropathic symptoms. Nonetheless the creation of novel compounds capable of inhibiting these kinases could have seismic effects on how neuropathic pain is treated. One such set of compounds are the recently developed SPHINX and Griffin compounds developed by Professor Jonathan Morris and his group at the University of New South Wales.

1.4.1: Novel Splicing Kinase Inhibitors

The concept of splicing kinase inhibition is not necessarily new, multiple efforts have been made to develop SRPK1/2 inhibitors as potential antivirals for use in both Human Immunodeficiency Virus (HIV) and Hepatitis B virus (HBV) infections where the viruses can hijack alternative splicing kinase activity to force viral replication (Zheng, Fu and Ou, 2005; Fukuhara *et al.*, 2006). However, compounds such as TG003 and various quinoxaline derivatives lack kinase selectivity/specificity which would likely result in various off-target effects in a number of alternatively spliced pathways or a lack of potency against key targets (Batson *et al.*, 2017). If alternative splicing kinase inhibition is to be viable as a potential adjunct therapy to chemotherapy the inhibitors used must demonstrate potency and selectivity in order to be effective at the pre-clinical stage. These pre-clinical properties help to ensure that selection and development of lead compounds is likely to result in efficacious outcomes when it reaches the clinic, though this process is complicated by the need to develop appropriate delivery formulations, enhancing of solubility and the need to acquire to “drug-like” properties such as those denoted in the Lipinski rules (Benet *et al.*, 2016). Another obstacle to overcome is the fact that many splicing inhibitor compounds are often reliant on targeting of the ATP binding site of the kinase which means innovative approaches must be taken to ensure potency and specificity parameters can be met (Gammons *et al.*, 2014; Batson *et al.*, 2017). This thesis examines 4 novel potent and selective compounds splicing kinase inhibitors; SPHINX31, Griffin 6, Griffin 23 and Hippogriff 1, developed by the Morris group at UNSW as potential adjuncts to vincristine in the context of chemotherapy induced peripheral neuropathy. In the case of the Griffins and Hippogriff this is the first time they have been assessed in any *in vitro* physiological model following initial validation of their inhibitory characteristics in kinase assays. These compounds target SRPK1, CLK1, CLK2 and DYRK1A in various combinations. SPHINX31 is a well-characterised compound with demonstrable efficacy in studies aimed at controlling the alternative splicing mechanisms downstream of the kinase particularly those with respect to the control of VEGF-A alternative splicing (Batson *et al.*, 2017; Tzelepis *et al.*, 2018).

The selectivity and IC_{50}s of splicing kinase inhibitors are determined using *in vitro* kinase radioactive filter binding assays (MRC PPU International Centre for Kinase Profiling) against a panel of 140 kinases. Whilst older compounds such as SRPIN340 and the quinoxaline derivatives have IC_{50}s approaching 1µM for SRPK1 inhibition, SPHINX31 has an IC_{50} for SRPK1 of just 6nM. Furthermore, while quinoxalines demonstrated inhibitory activity on a number of different kinases in screens SPHINX31 was highly selective for only SRPK1. Showing no significant inhibition of other kinases in a screen of 140 kinases including the closely related kinases SRPK2, CLKs and Dyrks. The reason for the potency and specificity of these agents is due to innovative approaches to their synthesis which result binding to a site adjacent to the ATP site rather than competing for the ATP site, as is the case for other compounds (Batson *et al.*, 2017).

1.4.2.1: SPHINX31

SPHINX31 is the most established of the compounds used in this thesis and has already been trialled in a number of pre-clinical models with success. SPHINX31 has been shown to prevent TNF-α mediated activation of SRPK1 and reduce phosphorylation of SRSF1 in PC-3 cells in a concentration dependent manner with an IC_{50} of 320nM (Mavrou *et al.*, 2015). Whilst this IC_{50} is much higher than the 6nM quoted above, it is important to consider the assay used. The kinase screening assay uses a purified, isolated kinase and therefore in the latter assay performed in cells SPHINX31 must be able to get across the membrane and avoid efflux in order to exert its effects. Therefore it is logical that inhibitor IC_{50} values are higher in a cell system than those observed when the inhibitors are used against isolated kinases.

Gammons et al. and Batson et al. both demonstrated the ability of SPHINX31 to effect changes to VEGF-A splicing in retinal pigmented epithelial cells which was associated with reduced choroidal re-vascularisation following retinal lesioning in a model of wet Age-related Macular Degeneration (Gammons *et al.*, 2013; Batson *et al.*, 2017). Wet AMD is a VEGF-A-dependent condition which causes progressive blindness. SPHINX31 can induce functional changes to neuronal sensitivity where neurons treated with SPHINX31 showed reduced capsaicin-induced TRPV1 activation (Blackley, 2019). These inhibitory effects on neuronal activation were also shown to be VEGF-A dependent using a VEGF-A_{165}b neutralising antibody. This latter experiment is the only investigation of SPHINX31 effects on neurons to date, but given the promising potential of SPHINX31 demonstrated in other fields, use of SPHINX31 to reduce CIPN related sensory neuronal sensitivity via control of alternative splicing warranted investigation.

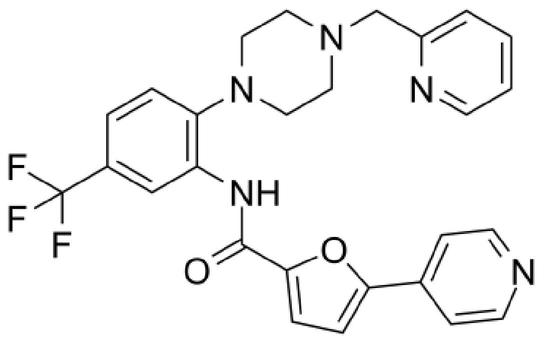

Figure 1.10: Structure of SPHINX31, Batson et al 2017

SPHINX31 skeletal compound structure. The Trifluoromethyl group (CF_3) is responsible for binding the hydrophobic pocket in the SRPK1 adjacent to the hinge region. The pyridine group in the uppermost sidechain is responsible for tight contacts with the binding region.

A key asset of SPHINX31 over other earlier SRPK1 inhibitor compounds is found within its structural chemistry. SPHINX31 does not directly target the ATP binding site of SRPK1 but rather an associated site close to it. SRPK1 possesses a so-called "hinge" region which is strongly hydrophobic. The trifluoromethyl found on SPHINX31 (Figure 1.10) is capable of being directed to this region where it forms a strong interaction between the kinase and the inhibitor. Once bound, the attachment of a pyridine group to the SPHINX31 sidechains allows more stable binding to the hydrophobic pocket which increases the potency of the compound. When this occurs the hinge regions flips and prevents binding of ATP which then prevents the kinase activity of SRPK1. Therefore, SPHINX31 is a highly selective and potent inhibitor with already proven efficacy in controlling SRPK1-dependent alternative splicing. As such it is a very useful tool compound for investigations into alternative splicing as a therapeutic strategy for CIPN (Batson *et al.*, 2017).

1.4.2.2: Griffin Compounds

Whereas SPHINX31 has been tested in a variety of *in vitro* and *in vivo* pre-clinical models in multiple contexts, the other compounds examined in this thesis namely Griffin 6, Griffin 23 and Hippogriff 1 had not previously been examined in cell-based models. Unlike SPHINX31 that is a highly selective SRPK1 inhibitor, Griffin 6 is a selective inhibitor of CLK1 and CLK2. As described above, CLK1 interacts with SRPK1 in the control of SRSF1 phosphorylation and activation and has been implicated in multiple splicing events in oncogenesis and neurodegeneration (Lee *et al.*, 2019a). Investigations into the functions of CLK2 are limited. There is some evidence to suggest CLK2 plays a role in neural development, where it was found to induce expression of key neuronal markers in octopus models. However, more substantive studies have found implications for CLK2 activity in the liver, particularly in gluconeogenesis which describes the creation of glucose from non-carbohydrate sources (Tabata *et al.*, 2014). Activation of CLK2 downstream of insulin in hepatocytes by Akt signalling triggers CLK2 phosphorylation activity, which supresses PGC-1A, a master regulator of transcription factors that trigger the gluconeogenesis metabolic response (Fernandez-Marcos and Auwerx, 2011). Investigations into the role of CLK2 in pain or the nervous system are scarce, although the Wnt inhibitor Loricivivint which also inhibits CLK2 and DYRK1A, inhibits inflammation, pain behaviour and cartilage damage in osteoarthritis models (Deshmuhk et al 2019).

Whereas SPHINX31 and Griffin 6 inhibit a single kinase or a single family of kinases, Griffin 23 and Hippogriff were synthesised as dual kinase inhibitors. In the case of Griffin 23 the inhibitor has similar selectivity for SRPK1 and CLK1/CLK2, which have been considered in depth in previous sections as key modulators of alternative splicing of growth factors such as VEGF-A. Use of more non-selective inhibitors may allow for direct comparisons between agents that inhibit a single kinase such as SRPK1, which is valuable for more rapid evaluation of the kinases that may be more important in neuronal tissue and in CIPN related neuronal changes. Additionally designing highly selective kinase inhibitors is notoriously difficult, so use of less selective compounds can both inform development and move understanding forwards. Hippogriff 1 also has dual selectivity as it is capable of inhibiting CLK1/CLK2 and DYRK1A. DYRK1A is a splicing kinase that has been implicated in the development of multiple disorders related to central nervous development primarily in the brain and in inflammatory processes. Aberrant expression and activity of the kinase is suggested to be a potential cause of learning deficits in Down syndrome and is also associated with Autism Spectrum disorders (Tahtouh *et al.*, 2012; Jarhad *et al.*, 2018). Investigations into the role of DYRK1a and pain are limited although as mentioned above Lorecivivint, a CLK/DYRK1A inhibitor decreased expression of inflammatory cytokines and pain behaviour in experimental arthritis. These findings suggest a roles for both kinases in pain and disease modulation through mechanisms other than VEGF-A splicing and provides an encouraging rationale for examination of these two kinases in alternative models of pain such as CIPN.

1.5: Aims and Hypotheses

Overall Hypothesis: Control of alternative splicing via inhibition of splicing kinases will ameliorate the sensitising and neurotoxic effects of vincristine chemotherapy in *in vitro* models. Furthermore, these novel inhibitors will not cause a reduction in the efficacy of vincristine to treat cancer cells.

Aims:

- Develop a model of neuronal activation and sensitisation using immortalised or primary sensory neurons. (Chapters 3 & 4)

- Develop a model of vincristine neurotoxicity using immortalised or primary sensory neurons. (Chapter 5).

- Use these models to screen novel splicing kinase inhibitors for effects that ameliorate observed vincristine toxicity. In addition, screen a novel chemotherapy agent, jerantinine for comparative neurotoxicity (Chapters 4 & 5)

- Assess the effects of novel splicing kinase inhibitors and vincristine on cancer cells to ensure they do not compromise the properties of vincristine to reduce cancer cell proliferation. (Chapter 6).

2: General Methodology

2.1 General Cell Culture Methods

For investigations into neuronal activation prior to the use of primary adult rat DRG neurons, 2 immortalised cell lines were used, 50B11s and MED17.11s. Both of these cell lines required specific differentiation protocols that are detailed in section 3.2.1 and 3.2.2 respectively. In addition to these neuronal lines, for cancer spheroid growth assays ONS76 cells, a sonic hedgehog sub-type medulloblastoma cell line were used. Specific information on spheroid formation and analysis can be found in section 6.2. For MYC expression analysis the immortalised prostate cancer cell line PC3 was used. All cell lines were grown in T25 flasks (Corning) following initial thawing and then subsequently passaged in T75 flasks (Corning) following expansion. All cells were incubated at 37°C at 5% CO_2 unless otherwise stated.

2.1.1 50B11 Culture Conditions & Passaging

Immortalised 50B11 cells were a kind gift from Dr Ahmet Hoke and were cultured and expanded in Neurobasal (Gibco 21103049) containing 10% foetal bovine serum (FBS, Sigma F2442-500mL), 1x B-27 supplement (Thermo-Fisher 17504044), 0.5mM L-Glutamine (Sigma G7513-100mL) and 0.2% glucose (Sigma G7021). Cells were allowed to grow to a maximum of 80% confluence before being passaged. During passaging, culture media was aspirated and cells washed using phosphate buffered saline (PBS, D8537-500mL). PBS was then removed and replaced by 1mL of 1x trypsin-EDTA (trypsin = 0.05% w/v, EDTA = 0.5mM) (T4049-100mL) in a T25 flask or 2mL of 1x trypsin-EDTA in a T75 flask. Cells were then incubated with 1x trypsin-EDTA at 37°C at 5% CO_2 internal incubator conditions for no longer than 5 minutes and subsequently split at a 1:5 ratio following centrifugation at x150G for 5 minutes.

2.1.2 MED17.11 Culture Conditions & Passaging

Immortalised MED17.11 cells were a kind gift from Dr Mohammed Nassar (University of Sheffield) and were cultured in DMEM/F12 with GlutaMAX (Gibco 10565018), 10% FBS, 1% Penicillin/Streptomycin (Merck P4333), 5ng/mL IFN-γ (R&D Systems 485-MI) and 0.5% chicken embryonic extract (CEE, Sera Lab CE-650J). Depending on differentiation protocol, some MED17.11 cells were cultured in the absence of CEE during the proliferation phase of experiments. Cells were passaged as described in section 2.1.1 but split at a 1:10 ratio due to the fact the line is rapidly proliferating by nature. Additionally, due to the immortalisation process the cells MED17.11s were incubated for proliferation at 33°C to prevent premature inactivation of the SV40 large T-antigen responsible for the immortalisation of the cell line and thus premature differentiation into sensory neuronal phenotypes.

2.1.3 ONS76 Culture Conditions & Passaging

ONS76 medulloblastoma cells were a kind gift from Dr Beth Coyle and were cultured in RPMI 1640 medium (Sigma R8758) supplemented with 10% FBS. ONS76 cells were split at 70% confluence. During passaging ONS76 cells were first washed with Hanks Buffered Salt solution (HBSS, Gibco 14170) instead of PBS before being passaged as described in section 2.1.1. ONS76 cells were also split at a 1:10 ratio due to the rapidly expanding nature of the cell line.

2.1.4 PC3 Culture Conditions & Passaging

PC3 cells were purchased from ATCC (CRL-1435) and were cultured in DMEM (Sigma D6546-500mL) supplemented with 10% FBS, 1% penicillin/streptomycin and 0.5mM L-glutamine. PC3 cells were passaged as described in section 2.1.1 and split at a ratio of 1:10 due to rapidly growing nature of the cell line. Specific information on PC3 cell seeding for MYC expression experiments can be found in section 6.2.

2.1.5 Preparation and Raising of Cell Stocks

To prepare stocks of cell lines all cells were detached from flasks using 1x trypsin-EDTA and centrifuged (Eppendorf 5810) at 150g for 5 minutes. Cells were then re-suspended in bespoke freezing medium consisting of basal growth medium dependent on cell line, supplemented with 20% FBS and 10% dimethyl-sulphoxide as cryo-protectant (DMSO, Thermo-Fisher 20688) at a cellular density of $1x10^6$/mL. Cells were then aliquoted into an appropriate number of 1mL cryo-vials (Nunc, V7384) and placed in an isopropanol chamber (Mr Frosty, Sigma C1562) and incubated at -80°C for 24 hours. Following this, vials were then moved directly to liquid nitrogen for long term storage. To thaw cell stocks vials were removed from liquid nitrogen and thawed as quickly as possible in a water bath or incubator set at 37ºC and the 1mL cryovial contents added to 4mL of preheated growth medium. Cells were then centrifuged at 150g for 5 minutes to remove DMSO content, before cells were re-suspended in 8mL of appropriate medium and placed in a T25 flask for normal growth and passaging procedures.

2.2 Primary Adult Rat Dorsal Root Ganglia Culture

The majority of experiments contained within this thesis were conducted using adult rat dorsal root ganglia (DRG) sensory neurons following dissection and dissociation into single cell cultures. All rats used in these experiments were male Wistar strain and were purchased from Charles River UK and were at least 200g at the time of termination and no rat used exceeded 300g. Based on these weights rats were considered to be "young adults" according to growth curve studies (McCutcheon and Marinelli, 2009). One rat was used to produce one neuronal culture at a time, there was no pooling of tissues derived from each rat. Experimental units were assay specific and are laid out in Chapters 3,4 and 5. Rats were terminated according to Schedule 1 of the Animals in Scientific Procedures Act (ASPA) by terminal anaesthesia via intra-peritoneal injection of 0.5mL of 200mg/mL sodium pentobarbital (Sigma P3761) by a competent handler. Confirmation of death was performed via cervical dislocation again by a competent handler designated competent in Schedule 1 termination and on the S1 register of the University of Nottingham's Bio-Support Unit (BSU).

2.2.1 96 Well Plate Coating

Prior to dissection a black sided 96 well plate (Corning) was coated in 0.01% Poly-L-Lysine solution (Sigma A-005-C) in sufficient volume to cover the bottom of the plate. Plates were then incubated overnight at 37°C. Coating solution was removed the following morning and plates were washed with 50µL PBS and then allowed to dry in the incubator.

2.2.2 Preparation of DRG Medium

Cell culture medium for primary DRG cultures consisted of Ham’s F12 medium (Gibco, 31765035) supplemented with 1x N2 supplement to support growth of post-mitotic primary neurons, (Gibco 17502048), 2% Penicillin/streptomycin to prevent contamination from dissection and 3% Bovine Serum Albumin as a source of cell nutrients (BSA, A5976-50mL). 50mL of this medium was prepared fresh prior to dissection protocols. Media was stored in the fridge for no longer than 7 days to ensure standardisation of media preparation protocols.

2.2.3 Rat Dissection & Laminectomy

Following terminal anaesthesia and cervical dislocation of the rat, the cadaver was moved to the dissection rig which had been sterilised with 70% Industrial Methylated Spirit (IMS). Using tools also sterilised in IMS, an incision was made along midline from head to tail and the revealing the underlying musculature covering the spine. Excess skin and muscle was cut away until discrete vertebrae of the spine were visible. The head was then removed to expose the spinal cord and cervical vertebrae. Using rongeurs, a laminectomy was performed along the full spine of the animal by removal of the vertebral spinous processes and posterior vertebral arch thus exposing the underlying cord and nerve roots. Using fine forceps and micro-scissors the cord was lifted and the DRG exposed either side of the intervertebral foramen, at which point the DRG were isolated via cutting of the connection to the peripheral nerve root. DRG were then immediately placed within cold, basal Ham’s 12 medium until the dissection was finished. Once DRG from every level of the spinal cord had been removed the isolated DRG were then at least partially de-sheathed using a dissection microscope and had the remaining nerve roots from initial dissection cut away and removed. DRG were then returned to a fresh aliquot of cold, basal Ham’s F12 medium. All dissections had a maximum time limit of 120 minutes post cervical dislocation with which to gather tissue, this was to standardise the protocol and to ensure tissue taken was as viable as possible ahead of culture.

2.2.4 Dissociation of DRG and Culturing Protocol

Following the conclusion of the dissection, DRG were placed Ham’s F12 medium containing 0.0125% collagenase type IV (Sigma C5138) and were incubated at 37°C for 2 hours. During this time, 96 well plates were removed and coated with 0.1µg/mL laminin (Sigma, L2020) for at least 1 hour. Using 3 15mL Falcon tubes, 3 15% BSA cushions were made using 1mL of 30% BSA solution and 1mL of basal Ham’s F12. Any bubbles arising from the mixing of these two solutions were pipetted off. Following incubation, and using a cut P1000 pipette tip, the DRG were carefully lifted from the collagenase solution into 5mL of warm Ham’s 12 medium to inactivate and dilute any remaining collagenase. Ham’s F12 medium was then aspirated and replaced by 500µL of aforementioned DRG medium (section 2.2.2) which had been warmed prior to use. Using a cut P1000 pipette tip and with the pipette set at 250µL DRG were mechanically triturated and dispersed into dissociated cells. A cut pipette tip was used to prevent fatty debris from blocking the tip by ensuring a wide bore size. This process was repeated with smaller pipette bore size (the pipette tip was cut lower down) at least 3 times until the mixture could be readily pipetted with an uncut tip with fatty debris fully broken up. The DRG medium containing the dissociated cells was then topped up to 3mL and 1mL added per cushion to 15% BSA cushions which consisted of 1mL F12 medium and 1mL 30% BSA. This created a sharp interface and clearly visible phases in the mixture, with the cell suspension resting on top of the BSA/F12 mix. Cushions were then centrifuged at 150xG for 8 minutes with no brake applied. Following centrifugation, the supernatant was removed and cells re-suspended in 200µL of DRG medium and moved to a new Falcon tube. Dissociated primary neuronal cells were then counted using a Neubauer Haemocytometer and suspended in an appropriate volume. Cells were then plated at a maximum of $2x10^3$ cells per well in 100µL of DRG medium. Plates were incubated overnight at 37°C and the following morning media was aspirated and replaced by 100µL of DRG medium supplemented with 30µg/mL 5-fluoro-2' deoxyuridine (FdU) to inhibit the mitosis of non DRG cells within the culture, such as glial cells. The neuronal cultures ~~cells~~ were then ready to use in a variety of experiments.

2.3 Total Ribonucleic Acid Extraction

For investigations into molecular expression of cell characterisation markers such as TRPV1 and $Na_V1.7$, total ribonucleic acid was extracted from cultured cells. The following protocol was adhered to as a standardised procedure, any alterations to this procedure are denoted within accompanying results chapters. Firstly, cell culture media was aspirated and frozen for use in downstream analyses, the cells were then washed twice with ice cold PBS. Cells cultured in a 6 well plate were immediately washed with 1mL of Tri-Reagent (Thermo-Fisher, AM9738) per well. To ensure even distribution of the Tri-Reagent over the cell monolayer cells were scraped repeatedly until the mixture became homogenised and absent from any visible cellular clumps or debris. Following homogenisation, 1mL cell lysates were moved into 1.5mL Eppendorf tubes and incubated for 5 minutes at room temperature to facilitate the breakdown of nucleoproteins, ensuring the release of free RNA molecules. After this incubation, 200µL of chloroform (Sigma, C2432) was added to each Eppendorf tube.

Tubes were then inverted multiple times and incubated at room temperature for 15 minutes. Following this, tubes were centrifuged at 12,000g for 15 minutes at 4°C at which point the lysate separated into 3 distinct phases. A clear, aqueous solution at the top contained RNA, a milky white interface contained DNA and the lower pink phase contained proteins. Approximately 500µL of the upper phase was transferred into fresh Eppendorf tubes and the lower phases were disposed of. In order to precipitate the RNA within the aqueous phase, 500µL of isopropanol (Thermo Fisher, 9500-1) was added to the tubes. Tubes were inverted several times and incubated at room temperature for 10 minutes before being centrifuged at 12,000g for 10 minutes at 4°C. After centrifugation, visible RNA pellets appeared in the tubes and supernatants were discarded. The pellets were then washed using 1mL of 75% Ethanol to wash away excess salts from the pellet (Sigma, 459836-1L) and vortexed for up to 30 seconds to ensure a full wash. Tubes were then centrifuged for a final time at 10,000g for 5 minutes at 4°C and the supernatant removed. Pellets were dried for 5-10 minutes depending on size and subsequently dissolved in 20µL DEPC treated water (Invitrogen, 10289104). RNA was immediately quantified and tested for purity using a Nanodrop 2000 spectrophotometer (Thermo-Fisher). To quantify, 1µL of RNA was added to the Nanodrop pedestal and absorbance ratios at 260/320 and 260/280nm were calculated to assess RNA quality and the Nanodrop also quantified RNA in ng/mL.

2.4 cDNA Synthesis

In order to synthesise complementary DNA (cDNA) for use in downstream PCR applications, 1µg of RNA solutions previously described was made up to 8µL in nuclease free water in a 0.2mL PCR tube (Starlab, I1402-8100). For experiments using RNA derived from dissociated primary DRG where RNA yield was usually significantly lower than from cell lines, the total RNA isolated was dictated by the sample with the lowest yield. Other samples with higher yield were diluted in nuclease free water to give the same input RNA in each sample. In order to reduce any potential genomic DNA contamination within the samples, 1µL of RQ1 DNAse (DNAse enzyme in 10mM HEPES, 50% v/v glycerol, 10mM $CaCl_2$ and 10mM $MgCl_2$.) and 1µL of RQ1 DNAse buffer (400mM Tris-HCl, 100mM $MgSO_4$ and 10mM $CaCl_2$) were added for a total reaction mixture of 10µl. Tubes were then incubated at 37°C for 30 minutes in a PTC-200 Thermocycler. The reaction was then stopped after this period via the addition of 1µL of DNAse stop solution (20mM EGTA) and incubation of the samples at 65°C for 10 minutes. To initiate reverse transcription, 0.5µg of Oligo-dT (Promega C110A) to hybridise to mRNA poly-A tails and 250ng of random hexamers to bind randomly to the template were added to the samples and incubated at 70°C for 10 minutes before samples were removed and placed in ice water to prevent RNA from entering secondary conformation structures. Subsequently, 0.5mM dNTPs (deoxyribonucleotide tri-phosphate) 4µL of 5x MMLV-Reverse Transcriptase buffer (250mM Tris-HCl, 375mM KCl, 15mM $MgCl_2$ and 50mM DTT) and 1.5µL of nuclease free water were added to the samples for a total reaction mixture of 19µL. Finally 1µL of MMLV-RT enzyme was added to all samples for a final reaction mixture of 20µL. The Moloney Murine Leukaemia Virus Reverse Transcriptase is an RNA dependent DNA polymerase capable of generating cDNA templates of 5kb and has lower RNAse H activity than other reverse transcriptases ensuring fidelity of RNA template. All experiments involving cDNA synthesis also included a –RT control which contained a final addition of nuclease free water to the sample instead of reverse transcriptase. Samples were then incubated at 37°C for 60 minutes, 42°C for 30 minutes and 70°C for 10 minutes. Following this samples were then kept at -20°C until further use. All products used in this protocol were from the Promega Reverse Transcription System. (Promega A3500)

2.5 Polymerase Chain Reaction Primers

Investigations into cell characterisation via detection of molecular markers required design and production of numerous primers for use in reverse transcription polymerase chain reaction (RT-PCR). The following primers denoted in Table 2.1 were designed using NCBI Primer Blast and cross referenced using Ensembl to identify exon-exon junctions. All primers designed had a mandatory requirement to span an exon-exon junction to demonstrate any amplification a result of mRNA reverse transcription to cDNA rather than potential contamination with genomic DNA. Multiple primers were designed for individual targets, with their usage described in greater detail in their respective chapters. All primers were manufactured by Sigma in lyophilised form before reconstitution in DEPC treated water to form 100µM stocks. The full list of primers used can be found in Table 2.1 below. All primers are listed in 5' to 3' format. Primers derived from previously described literature are referenced within accompanying results chapters. Information on cross-specificity of primers used to validate cDNA across different species is also in specific results sections.

Primer Target	Forward Primer	Reverse Primer	Product Size (bp)
1. Rat/Mouse TRPV1	AGCGAGTTCAAAGACCCAGA	TTCTCCACCAAGAGGGTCAC	233
2. Mouse TRPA1	CCCCACTACATTGGGCTGCA	CCGCTGTCCAGGCACATCTT	487
1. Mouse Only $Na_V1.7$	AGCAGGAAGAAGCCGAGGTAGTAT	AATGCTGAGTGGTGACTGGTTGG	350
1. Mouse/Rat $Na_V1.7$	GATGCTCTACTCTGCGGCTT	TCATACGCCATGGCTACCAC	287
1. Rat Only $Na_V1.7$	*TTCGGCTCATTCTTCACGTT*	*CACTCCCCAGTGAACAGGAT*	359
GAPDH	CAACTACATGGTTTACATGTTC	GCCAGTGGACTCCACGAC	201
c-MYC	TGAGGAGACACCGCCCAC	CAACATCGATTTCTTCCTCATCTTC	71

Table 2.1: Primers and accompanying product sizes

2.6.1 Reverse Transcription Polymerase Chain Reaction (RT-PCR)

The following protocol denotes the standardised components of the experiment, for specific information on reaction cycles and primer annealing temperatures please consult individual chapters. Following reverse transcription and synthesis of cDNA, 50ng (1µL in standard reaction) of cDNA samples were added to a 0.2mL PCR tube. Forward and reverse primers were then mixed together to a final concentration of 10µM, 1µL of this primer mix was then added to the PCR tube for a final primer concentration of 0.5µM per primer. 10µL of PCR Master Mix (Promega) and 8µL of water were then added to the samples for a final reaction volume of 20µL. To test for generic PCR contamination, a water control was prepared alongside samples, containing the same components other than the addition of 1µL water instead of cDNA sample. –RT samples were prepared as for cDNA samples. Samples were then placed in a PTC-200 thermocycler to carry out the reaction. Samples in all experiments were then initially denatured at 95°C for 5 minutes, before being cooled to an annealing temperature dependent on the primer set used. These annealing temperatures and further information on number of cycles for each experiment can be found in the methods section of their respective results chapter. All reactions concluded with a 10 minute final extension at 72°C. Samples were then kept overnight a 4°C or immediately taken for analysis via agarose gel electrophoresis.

2.6.2 Agarose Gel Electrophoresis

1.5% agarose gels were made by dissolving 3g of agarose powder (Sigma, A9535) in 200mL of 1x TAE Buffer (40mM Tris base, 1mM EDTA, 0.1042% v/v glacial acetic acid). Agarose powder was melted by heating in a microwave at high power for repeated 30s intervals until fully dissolved. The solution was then allowed to cool slightly before the addition of 5µL ethidium bromide (Sigma, E1510) per 100mL of solution to allow visualisation of cDNA in GelDoc. The agarose solution was then poured into the gel mould and a comb added to create wells within the gel. Once solidified, the comb was removed and the gel placed within a BioRad gel tank. Fresh 1x TAE buffer was then added to fully submerge the gel. Samples were added to 4µL of 6x loading buffer (Thermo, R061 0.03% Orange G Dye + 0.03% Xylene cyanol FF in 60% Glycerol) for a total sample volume of 24µL. A maximum of 18µL of sample was then loaded into the gel, with 5µL of Bio-Line 50BP Hyperladder (Bio-

Line loaded in one lane for amplicon size comparison. The gel tank was then attached to a power pack and the samples allowed to run for approximately 90 minutes at 90v. Gels were visualised on GelDoc software using a UV visualisation plate (BioRad), images were then exported in TIFF format for analysis.

2.7 Neurite Outgrowth Assay

For investigations into chemotherapy induced neurite dieback, primary DRG neurons cultured as described in section 2.2 were treated with 10nM of the vinca alkaloid chemotherapy agent vincristine or co-treated with a combination of vincristine and a novel splicing kinase inhibitor to ameliorate the effects on neurite dieback exerted by vincristine. Specific information regarding drug concentrations can be found within Chapter 5. Due to the use of dispersed cultures rather than organotypic cultures, traditional Scholl analysis using concentric rings from the user defined soma definition was not possible as many individual neurons were usually present in a single field of view. Consequently, a new method of quantifying neurites within a field of view was developed using Image J software with the Simple Neurite Tracer plugin. The following protocols denote the overarching methodologies used across all experiments.

2.7.1 Neurite Outgrowth Workflow

Following dissection and culture of neurons into 96 well plates as described previously neurons were left overnight to stick down to coated laminin. The following morning 30µg/mL of FdU was added to the cultures to prevent glial proliferation and takeover of the culture. To encourage neurite outgrowth, 8ng/mL of Nerve Growth Factor (NGF) (R&D Systems, 556-NG) was also added to the cultures. Neurons were then incubated for a total of 72 hours to allow neurites to grow. Optimisation methods and results to establish this time window can be found in Chapter 5. After this period neurons were then treated with an experimentally dependent concentration of vincristine. Neurons were then left for a further 72 hours, to allow for the effects of vincristine to be exerted. After this period cells were then prepared for immunocytochemistry protocols.

2.7.2 Immunocytochemistry

Following conclusion of the above workflow neurons were immediately fixed using 4% (w/v) paraformaldehyde (PFA, Sigma P6148) for 10 minutes at room temperature. PFA was then aspirated and neurons washed 1x using PBS. Neurons were then permeabilised and blocked using a PBS solution containing 0.2% Triton X-100 (Sigma 11332481001) and 1% of normal horse serum incubated at room temperature for 30 minutes. Blocking solution was then removed and a 1% Serum/PBS solution containing primary mouse anti-beta III tubulin (R&D Systems, MAB1195) was added to the cells. This was then incubated overnight in a humid box at 4°C. The following morning, antibody solution was removed and plates were washed with 0.5mL/L Tween 20 PBS solution (PBS-T) 3 times, with an incubation of 5 minutes between washes. After washing, a 1% BSA PBS solution containing 1:1000 dilution of Hoechst 33258 and 1:1000 dilution of donkey anti-mouse Alexa Fluor 488 secondary antibody (Thermo, R37114) was added to the cells and incubated for at least 30 minutes in darkness. Secondary antibody solution was then aspirated and plates washed again using PBS-T at least 3 times to reduce non-specific binding of antibodies. Plates were sealed with clingfilm and covered with foil and incubated at 4°C until imaging.

2.7.3 Confocal Imaging

Plates were imaged using Leica DMIL 521665 Confocal Microscope. To eliminate biased selection of potential neurite hotspots, fields of view were selected using only the Hoechst filter. Furthermore, to standardise imaging in each well, 3 fields of view were selected and each counted as an internal repeat to account for plating density variance. The fields were selected in approximately the top, middle and bottom third of the well. Images were taken at 20x and 40x magnification, and Z-stacks containing 15 images per field of view were created with a Z-step size of 10µm per step. Using Leica Confocal Software, these stacks were condensed into one image using maximum projection function and this image was then taken for downstream analysis. Laser was set at 50% and gain set at 900 units. Images taken were exported as TIFFs. Each plate treatment group therefore had a maximum of 18 internal repeats and each plate was counted as a single N value.

2.7.4 Image J & Simple Neurite Tracer Analysis

Images exported as TIFFs were processed using free open access Image J (FIJI) software downloaded online. Firstly, images were blinded using the “File Randomizer” macro available off the Image J website. This created anonymised copies of all files prior to analysis. Blinded images were then opened using Simple Neurite Tracer and neurite outgrowth measured in a semi-automated fashion. The user input was to select the proximal and distal extremities of the neurite with the neuron cell body as the point of reference. Where this could not be achieved due to the neurite reaching the edge of the field of view, the neurite length was terminated at this point. For neurites emerging from other neurites, the distal end and proximal sprouting point was selected. The simple neurite tracer software would then automatically trace the path between the two selected points and record the distance according to the set image scale. Once all neurites in the field were recorded in this manner, the “Render Skeleton” function was selected, leaving only the selected neurite paths present within the image (Figure 2.1).

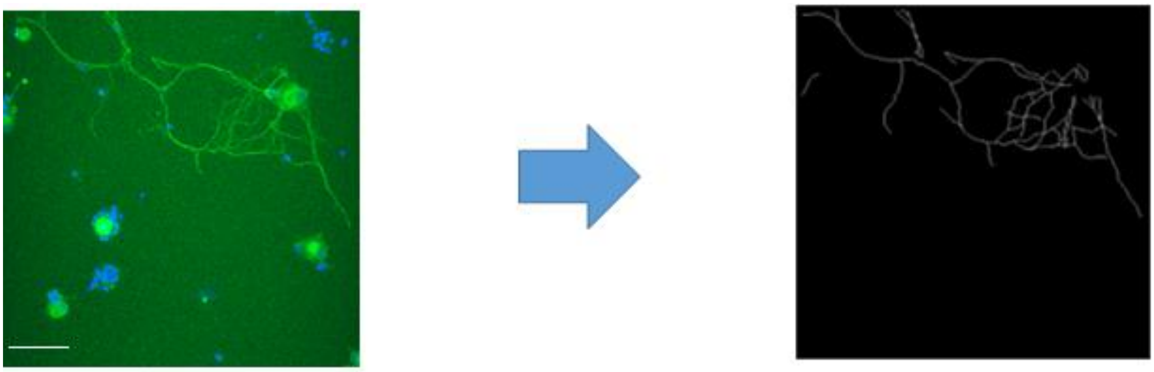

Figure 2.1: Neurite Skeleton Render

An example of a neurite skeleton created using simple neurite tracer. All neurites are lifted from background image and are individually assigned an ID with associated length in µm. Green stain = Beta-III tubulin. Blue stain = Hoechst. Scale bar = 100µm.

As cell density within cultures was not necessarily even across all plates, this could potentially have skewed results erroneously, to account for this total neurite lengths from the recorded skeleton were normalised to the number of neurons which were manually counted within the field of view of the original image. This therefore created a measurement output of neurite outgrowth per neuron. For instance, a field of view containing 500µm of total neurite outgrowth with 1 neuron was considered equivalent to 1000µm of total neurite outgrowth with 2 neurons present in the field of view. Data from a maximum of 18 images per treatment were then collated together on Graphpad Prism version 7 or 8. These 18 images were collected from 6 wells per treatment with an image being taken from the top third, middle third and bottom third of the well to account for plating density variation. Measuring plates in this manner accounted for fairly high intra-plate variability and resulted in low inter-plate variability. Blinding was only removed once all images had been quantified. Specific information on downstream statistical analyses can be found in the methods section of Chapter 5. Images taken at 20x magnification were chosen for analysis. Some images had brightness adjusted via modulation of the “minimum” parameter to no less than 70 arbitrary units on the Image J command panel. This was done to ensure smaller neurites that were could be weakly stained were not excluded from the analyses.

2.8 Neuronal Activation/Sensitisation Assay

For investigations into effects of interventions on chemotherapy induced neuronal activation/sensitisation *in vitro* a high throughput assay was designed to assess the effect of novel compounds on TRPV1 channels via capsaicin stimulation. Use of veratridine stimulation for effects on $Na_V1.7$ was optimised for assessment of effects on these channels. The following sections detail the generic workflow of the neuronal activation/sensitisation assay, for specific information on the drug regimens used in optimisation and final experiments please refer to Chapter 4. All findings used in this high-throughput assay have been previously validated at the single cell level using patch clamp techniques (Hulse *et al.*, 2014; Bestall *et al.*, 2018).

2.8.1 Preparation of Fluo-4 Calcium Direct Assay Dye

Within this assay the read out for neuronal sensitisation was defined as the level of calcium ion influx into neurons following stimulation with either capsaicin or veratridine, assessed using the Fluo-4 Direct Calcium Assay (Thermo F10471). The assay makes use of a dye that fluoresces strongly upon binding of calcium whilst also being able to load more efficiently into cells than traditional calcium dyes. As a result background fluorescence is reduced and observed signal is much more specific to cell based calcium influx rather than detection of calcium in complete media solutions. This property also removes the need for several washing steps and complete removal of cell culture medium prior to use, which could potentially influence the normal activity of cultured neurons. The Fluo-4 direct dye in the following assays were prepared according to the manufacturer's instructions minus the addition of the calcium extrusion inhibitor probenecid. Exclusion of probenecid was an experimental decision made to ensure calcium influx could peak and then reduce overtime in a more physiologically relevant process and represents the net release and influx into and extruded out of the cell rather than simply enhance the combination of release and influx within the assay.

2.8.2 Neuronal Sensitisation Workflow

Following dissection and overnight culture in of adult rat sensory DRG neurons in 96 well plates (section 2.2.4), culture media was discarded and replaced by media containing relevant treatments as described in Chapter 4. In all experiments, glial proliferation was inhibited via the addition of 30µg/mL FdU to the treatment media. Plates were then incubated for 24 hours in standard cell culture conditions at 37ºC and 5% CO_2. Following this, 50µL of the 100µL total culture medium was removed and replaced by 50µL of 2x Fluo-4 Direct calcium assay dye. Plates were then incubated for at least 1 hour in standard cell culture conditions in darkness. During this incubation period, a relevant concentration of capsaicin or veratridine agonist was prepared at 6x working concentration. For specific stimulant concentrations please see Chapter 4. Agonists were added to a dummy plate and placed on a heating block set to 37°C. To standardise conditions at the time of measurements, the Perkin Elmer Victor 4 and Fluo-Star Omega plate readers used in these assays were set to 37°C during this incubation period. After at least 1 hour incubation, plates were loaded into the reader and background (dye minus cells) and baseline (dye plus cells) fluorescence measured at 488nm. Using a multichannel pipette, 6 x 20µL of the 6x concentrated agonist solution was then added to wells containing 100µL of media/dye for a final 1x working concentration on a row by row basis. Fluorescence was then measured at a least 10 intervals across a 120 second window creating a time course of fluorescent change. Fluorescent values were then exported to excel and background fluorescence deducted from measurements. At this point, fluorescent measurements were divided over the baselines taken before stimulation providing a ratio of change in fluorescence from baseline over time. From this, Area Under the Curve (AUC) values were derived across the time course via analysis in Graphpad Prism versions 7 or 8. AUC values were then used in various downstream analyses as described.

2.8.3 Conversion of AUC Values to Percentage Reduction in Sensitisation

Due to the high level of variability observed in the assay due to various factors such as even plating density, quality of dissection, quality of culture, and the consequent effects on the viability of neuronal cells significant differences across treatments were potentially masked. To account for this AUC data from novel compound experiments were transformed to percentage decrease from the maximum mean response of the positive control. In all experiments involving the use of novel splicing kinase inhibitors this positive control was neurons treated with vincristine chemotherapy alone. The process by which this was achieved is outlined in the steps below using a basic example showing a sensitisation experiment involving Vincristine treatment + Capsaicin, DMSO vehicle control + Capsaicin and DMSO vehicle + HBSS capsaicin vehicle control:

B	C	D	E	F	G	H	I	J	K
									Mean
DMSO AUCs	138.4	134.7	150.1	116	129.6	132.4	141.2		134.629
Vinc AUCs	173.8	210.1	160.1	198.2	145.4	178	177.6		177.6
HBSS AUCs	108.8	108.5	101.5	114.1	101.3	104.6	105.7		106.357

1. AUC values per treatment were averaged to produce a mean response per treatment.

2. Using the highest mean AUC value as the comparator, percentage change from this value was then calculated for each individual AUC repeat using the following formula:

Highest Mean = Vinc: 177.6			=(n-177.6)/177.6*100				
DMSO AUCs	-22.0721	-24.1554	-15.4842	-34.6847	-27.027	-25.4505	-20.4955
Vinc AUCs	-2.13964	18.29955	-9.8536	11.5991	-18.1306	0.225225	0.00000
HBSS AUCs	-38.7387	-38.9077	-42.8491	-35.7545	-42.9617	-41.1036	-40.4842

(AUC value – Highest Mean AUC Value) ÷ Highest Mean AUC × 100

3. As vincristine in this case had the highest AUC mean, the mean percentage change value is 0%, but with variation around this value now observable and reflective of the variable responses within the assay. These values are then imported into GraphPad Prism.

4. Once in Graphpad Prism the data is normalised with the vincristine percentage change (0% change) as 100% response and HBSS percentage change (40.11% decrease) as 0% response. The normalised data is then used in non-linear regression analyses using GraphPad Prism.

2.9 Statistical Analyses

All data was statistically analysed using Graphpad Prism software (GraphPad Prism version 7.0.0 or 8.0.0 for Windows, GraphPad Software, San Diego, California USA, www.graphpad.com). For specific information on the statistical tests used in each experiment, please consult the relevant results chapters and their accompanying figures. All statistical tests used a P value of less than 0.05 as a threshold for rejecting the null hypothesis. All figures display mean ± standard error of the mean unless otherwise stated. N numbers for each experiment are available within figure legends and accompanying explanation in relevant methods sections.

3: Assessment of Immortalised Neuronal Cell Lines as potential drug screening models

3.1.1: Introduction

The development of reliable, well characterised and phenotypically reflective immortalised sensory neuronal cell lines has been a major obstacle in the development of therapeutic compounds for a variety of sensory neuropathies including CIPN and diabetic neuropathy (Datta, 2013). Unlike cells used in studies in other fields, adult neuronal populations are unable to proliferate. Therefore many high throughput methods used for drug screening are unavailable because of the time constraints, limited tissue yield, financial costs and the labour intensive nature of deriving sensory neuronal tissue from primary sources such as rodents and in recent times, human samples (Kaur and Dufour, 2012).

Since the discovery of TRPV1 as the active receptor for capsaicin in 1997 (Caterina *et al.*, 1997), there has been a concerted effort to develop immortalised cell lines expressing this receptor for use in high throughput assays and for drug screening. This includes cell lines both neuronal and non-neuronal in nature. Indeed the cell line used to identify TRPV1, human embryonic kidneys cells (HEK293) were transfected with plasmid cDNA for a range of putative neuronal receptors derived from pooled rat and mouse dorsal root ganglia tissue causing heterologous expression of TRPV1 within the HEK cells. Stimulation with capsaicin then yielded a calcium influx along which was later corroborated following stimulation of the cells with heat in a noxious range. Despite these landmark findings and the identification of one of key mediators of neuronal sensitisation in a number of sensory neuropathies, several limitations still remain around the use of non-primary neuronal/non neuronal cell lines for investigations into sensitisation. For example, non-neuronal cell lines expressing ion channels such as TRPV1 and TRPA1 may help elucidate responses to certain agonists and the effects of therapeutic antagonists of these receptors in a functional context, however they could lack key elements of the intracellular signalling pathways required to further probe the mechanisms as to how painful neuropathies manifest. This therefore limits the efficacy of non-neuronal cell lines as a tool for diagnostic screening of novel compounds (Yin *et al.*, 2016). Alternatives to non-neuronal cell lines such as HEK293s include cell lines derived from nervous tissue malignancies such as SH-SY5Y and N2A cells which were isolated from human and murine neuroblastoma respectively. Both cells express immature neuronal markers which can be further matured following differentiation induced by a range of agents including retinoic acid and phorbol esters. However even after differentiation these cells lines do not express markers of nociceptive neurons such as functional TRP channels. N2A cells have been used for heterologous expression of TRP channels, however similar caveats therefore exist for these cells as for non-neuronal lines such as HEK293s.

To circumvent these limitations many groups have attempted to develop cell lines from isolated primary sensory neuronal tissue which are subsequently immortalised. Putatively providing a tool for investigations using phenotypically sensory neuronal tissue albeit without the associated costs and time commitments concomitant with traditional primary neuronal cultures. Examples of these cell lines, primarily derived from neonatal or embryonic rodent dorsal root ganglia include 50B11, F11, MED17.11 and ND7/23 cells (Dunn *et al.*, 1991; Fan *et al.*, 1992). In theory, these sensory neuronal cell lines should express key nociceptive markers such as TRP receptors and VGSCs that are functional and also by virtue of their origin retain their key intracellular signalling pathways that are integral to investigations of mechanisms underlying a number of neuropathies. It is therefore a key requirement of any sensory neuronal cell line used for screening to emulate primary DRG responses to agonists of these key mediators such as capsaicin for TRPV1 and the steroidal alkaloid veratridine for NaV1.7. The former of these compounds was fundamental in the discovery of TRPV1 and has since been used regularly in investigations into DRG sensitisation. The latter compound is regularly used as an agonist of sodium channels in screens of potential VGSC blocking agents. The robust effect of both agents on DRG neurons is well established and therefore provides reliable controls with which to assess the utility of immortalised cell lines in replicating nociceptive neuronal mechanisms (Ambrosino *et al.*, 2013; Chernov-Rogan *et al.*, 2018).

Early cell lines developed using these methods such as F11 and ND7/23 cells principally used somatic fusion of sensory rat DRG cells with a cancer cell line such as N18TG2, a murine neuroblastoma line. These hybrid lines therefore contain transcripts from both mouse and rat, which limits the utility of these cell lines in genomic and proteomic studies. Furthermore, F11 cells have been shown to lose chromosomes between passages. This was associated with loss of opioid receptor expression when differentiated after just 10 passages of proliferation (Cruciani *et al*., 1994). Nonetheless, both cell lines have been used extensively in the literature. F11 cells demonstrate neurite outgrowth and contain a heterogenous population of cells with varied morphology and response profiles to stimulants such as NGF and retinoic acid. More recently established immortalised lines have predominantly made use of Large T antigen derived from Simian Virus 40 (SV40) to induce oncogenic like proliferation of cells without the need for somatic fusion with another cell line. Another key component of contemporary immortalisation is the Human Telomerase Reverse Transcription Subunit (hTERT). This catalytic subunit allows a telomerase repeating unit to be added to telomeres in target cells which are usually senescent or have reached the so called Hayflick Limit. The Hayflick limit refers to the point at which mammalian cells will be unable to divide due to a critical shortening of telomere length (Lee, Choi and Ouellette, 2004). The result of hTERT insertion into cells is therefore a lengthening of otherwise truncated telomeres, a resumption of cell division and immortalisation of the cells in question. Immortalisation of cells is usually accomplished via incorporation of SV40 or hTERT into plasmid vectors and cells are then transfected via electroporation. Alternatively, the immortalising agents are incorporated into lentivirus vectors and cells passively transduced in culture. The main advantage of these methods over fusion with a tumour cell lines from another species is the prevention of potential genetic contamination from the hybrid cell line and the stability of the SV40 antigen in maintaining proliferation properties. Clones are normally identified through expression of a antibiotic resistance gene tagged to the genetic insert and clones are then screened across several divisions to determine the colony demonstrating the most robust proliferation whilst still maintaining fidelity of functional characteristics and markers when differentiated (Wang *et al.*, 2019).

Despite these advances in immortalisation procedure, cell lines can still have many limitations. For example the 50B11 immortalised cell line contains only a single neuronal cell type ostensibly small diameter neurons and thus is not representative of the diversity of sub-populations normally found in a primary sensory DRG neuronal culture (Raymon *et al.*, 1999; W. Chen *et al.*, 2007) This often limits immortalised cell line utility as drug screening tools as the absence of specific receptors and ion channels within the immortalised population can render the entire cell line obsolete if they do not recapitulate normal channel/receptor activation when stimulated. Therefore, when selecting an immortalised neuronal cell line, it is of pivotal importance to select lines expressing receptors of interest and regularly confirm continued expression of these receptors at both the molecular and functional level between passages. Another limitation is that despite the immortalisation process, some cell lines lose their potential for differentiation following continued division and thus expressed characteristics of said differentiation are reduced or totally absent when shifting from a proliferative to a differentiated state (Mummery, 2016). Differentiation of cells and their maintenance can also be difficult and expensive to sustain just to reliance on costly reagents to maintain cultures.

Recent work identifying the potential utility of differentiating Human Pluripotent Stem Cells (hPSCs) into nociceptor populations took as long as 7 weeks to yield a result, with often painstaking monitoring and maintenance of the cell lines required to ensure viability (Chambers *et al.*, 2012). For non-stem cell laboratories, this is not a practical alternative due to the level of expertise required for said maintenance and differentiation. Many differentiation protocols for immortalised lines require numerous small molecule inhibitors or growth factors to induce differentiation which may not be viable for long term studies or projects with financial constraints. However, despite these limitations immortalised cell lines can provide a suitable alternative to primary neuronal tissue where access to rodents for primary tissue is limited due to administrative or financial constraints. Additionally many studies, such as those by Vetter et al. have now been carried out on more established lines, characterising their responses and molecular expression of key receptors and ion channels such as TRPV1 and various sodium channels (Vetter and Lewis, 2010). Additionally, this allows for selection of cell lines relevant to a specific set of hypotheses on discrete receptors or pharmacological targets. Another advantage of immortalised cell lines is that they are far more readily available for molecular investigations into protein and gene expression than primary neuronal tissue. Immortalised cells can rapidly be expanded to levels enough for cell lysis and western blotting whereas primary tissue must often be pooled across samples in order to satisfy the requirements of protein investigations (Bestall, 2017). The presence of non-neuronal cells such as astrocytes and glia in primary neuronal cultures can also compromise proteomic and genomic studies acting as confounders however, single cell approaches can help to address this issue (Timmerman, Burm and Bajramovic, 2018). Many immortalised cell lines derived from embryonic DRG also display robust neurite outgrowth following differentiation, providing scope for multi-parametric drug screening investigations into both anti-nociceptive and neuroprotective properties of novel compounds. Therefore, when considering immortalised cell lines as alternatives to primary neuronal cultures it is practical to balance the benefits and limitations of immortalised cells and whether the sacrifice of some physiological fidelity is valid when comparing to the difficulties associated with primary neuronal cultures such as cost, intensity of training and animal handling (Haberberger *et al.*, 2020). As previous work in the group has demonstrated immortalised cell lines such as 50B11 cells can be an effective tools in high-throughput investigations such as neuronal sensitisation and outgrowth. Therefore, this chapter will present experiments attempting to characterise the functional and molecular characteristics of two immortalised cell lines, the novel murine MED17.11 cell line and the established 50B11 cell line. As the latter had previously been used within the group, it was possible to compare newly generated data with that gathered previously on the same Perkin Elmer plate reader which accounted for potential differences in different cell lines across laboratories.

3.1.2: Immortalised 50B11 Cell Line

The 50B11 neuronal cell line was developed by Chen et al. in 2007 and was derived from DRG taken from day 14.5 embryonic rats (Chen *et al.*, 2007). The DRG were then dissociated and electroporated with plasmids containing SV40 Large T antigen and hTERT constructs. One transfected clone colony (50B11) retained proliferative properties throughout several passages. The 50B11 cells were then differentiated into a more neuronal phenotype via the addition of forskolin which raises levels of intracellular cyclic AMP (cAMP). Elevation of cAMP levels within DRG neurons has been found to increase neuritogenic capacity and axonal elongation in embryonic neurons. After just 24 hours in the presence of forskolin, the authors observed 90% of the neurons ceasing cell division and extending processes resembling neurites. These neurites were later probed for and had confirmed expression of key neuronal markers such as neurofilament and β-III tubulin. Additionally, the authors probed the molecular expression of key nociceptive neuronal markers such as TRPV1, NaV1.7 and NaV1.4. Function of the former was confirmed via stimulation with capsaicin. The 50B11 line is therefore a robustly characterised cell line with extensive expression of neuronal molecular markers and demonstrable functionality of neuronal and key nociceptive receptors. Despite this, when Vetter et al. probed the responses of various immortalised neuronal cell lines and their receptors to stimulation, they found expression of TRPV1 but no functional capsaicin induced calcium influx (Vetter and Lewis, 2010). Probing this disparity between the two studies is essential for the assessment of 50B11 cells as a valid immortalised sensory neuronal model. Therefore, I decided to assess whether 50B11 cells could be used as a viable alternative to primary neuronal tissue derived from rodents in a sensitisation assay.

3.1.3: Immortalised MED17.11 Cells

The murine DRG cell line MED17.11 was first established by Doran et al. in 2015 and was the first immortalised murine DRG cell line to be described (Doran *et al.*, 2015). Unlike the electroporation methods used in the creation of the 50B11 cell line, the MED17.11 cells were instead derived from DRG neurons taken from day 12.5 embryos of the Immortomouse. The Immortomouse is a transgenic mouse stably expressing SV40 large T antigen controlled by the MHC H-2K promoter. The authors dissociated the DRG taken from embryos and maintained them in media containing interferon gamma to augment SV40 expression driving a proliferative phenotype. As the antigen is thermolabile and inactivated at 39°C, cells were maintained at 33°C to maintain proliferation. To differentiate the MED17.11 cells into nociceptive phenotypes, the cells were cultured without interferon and in a medium containing forskolin and FGF to elongate neurite processes, NGF and GDNF to promote nociceptor survival and rock inhibitor Y-27632 to induce neural crest cell differentiation. Additionally when inducing differentiation, the authors incubated the cells at 37°C to passively inactivate the SV40 antigen gradually to reduce proliferation and enhance retention of differentiated nociceptive phenotype.

The differentiated MED17.11 cells express functional markers of nociceptive neuronal phenotype, including NaV1.7 and TRPV1, and structural proteins such as neuron specific β-III tubulin found in rapid onset neurite outgrowth following differentiation. In summary, the MED17.11 cells appear to be a robust alternative to primary neuronal cultures capable of recapitulated expression and functionality of many sensory neuron specific receptors and ion channels. Furthermore, the incubation times of 6 days for differentiation and expression of said markers is much more manageable than timescales described for other cell lines in development such as manipulation of human pluripotent stem cells. However, despite these positive developments, the MED17.11 cell line is yet to be assessed outside of the initial paper describing its establishment. In addition, following consultation with the authors, I was informed the differentiation protocol for MED17.11 cells is not universally optimised for use in a range of assays and thus it is important to optimise culturing and differentiation conditions on a lab by lab basis with consideration for their intended use in specific assays. For example, the time taken for the expression of key channels and receptors (6 days in differentiation medium) is markedly longer than that for required for rapid and robust neurite outgrowth (3 days) and therefore these parameters would need further optimisation. Nonetheless, the potential benefits of a cell line capable of extensive expression of neuronal markers, that can be differentiated in an expedient fashion would be a powerful tool for high-throughput drug screening assays capable of assessing the potential of novel therapeutics such a novel splicing kinase inhibitors. Therefore, I decided to assess the MED17.11 cell line in this context and make direct comparisons to the performance 50B11 cells and primary sensory neuronal cell cultures in sensitisation assays.

3.1.4 Hypothesis & Aims

Hypotheses

- Primary dorsal root ganglia neuron stimulation with capsaicin and veratridine will induce Ca^{2+} influx that is significantly higher than vehicle control.
- The MED17.11 and 50B11 cell lines will express functional TRPV1 and NaV1.7 sensory neuronal markers
- Stimulation of the immortalised neuronal cell lines 50B11 and MED17.11 will produce comparable stimulation and calcium influx to primary DRG neurons that is significantly higher than vehicle control.

Aims

- Establish basal responses of DRG neurons to TRV1 and NaV1.7 stimulation.
- Assess whether the immortalised cell lines are viable alternatives to DRG neurons within the Fluo-4 direct sensitisation assay.

3.2 Methods

3.2.1: 50B11 Culturing and Differentiation

50B11 cells were a kind gift from Dr Ahmet Hoke (John Hopkins University) and were cultured prior to differentiation as described in section 2.1.1. No experiments with 50B11 cells were performed beyond passage 30. Therefore, all experiments were conducted well within the range of that deemed acceptable by Chen et al. To differentiate 50B11 cells for use in sensitisation assays, 50B11 cells were trypsinised and removed from flask as per normal passaging conditions. Subsequently, 50B11 cells were seeded at a density of 5,000 or 10,000 cells per well in a black sided 96 well plate. Cells were allowed to attach in proliferation medium described in section 2.1.1 for approximately 2 hours. Following attachment proliferation medium was removed and replaced by media supplemented with 75µM of the cAMP activator forskolin (Sigma F3917). Cells were then incubated at 37°C for 24 or 48 hours to allow for differentiation of 50B11 cells to occur dependent on experiment.

3.2.2: MED17.11 Culturing and Differentiation

MED17.11 cells were a kind gift from Dr Mohammed Nassar (University of Sheffield) and were cultured for proliferation at 33°C as described in section 2.1.2. For some differentiation experiments cells were cultured in proliferating conditions in the absence of chicken embryonic extract as part of cell line optimisation investigations. This was based on advice from the authors who used the extract in initial description of the cell line but were concerned it resulted in reduced expression of mature neuronal markers. Differentiation was considered to successful when cells stopped proliferating and demonstrated neurite outgrowth alongside morphological shift to a bi-polar morphology. No experiments with MED17.11 cells were conducted beyond passage 20, therefore all experiments were conducted well within the 100 passage limit denoted by Doran et al.

As MED17.11 cells are not an established neuronal cell line, several differentiation protocols were carried out. In all differentiation protocols MED17.11 cells were trypsinised as for normal passaging. Cells were then seeded at 1000, 2000, 3000, or 5000 cells per well of a black sided 96 well cell culture plate in proliferation medium and incubated at 37°C. Cells were allowed to attach to the plate for at least 2 hours before proliferation medium was removed and replaced with differentiation medium. Differentiation medium consisted of basal DMEM/F12 + 10% FBS, 1% penicillin and streptomycin supplemented with 25µM forskolin (Sigma F3917), 0.5mM di-butyrlcAMP (D0627) , 10ng/mL GDNF (R&D Systems 512-GF), 100ng/mL NGF (R&D Systems 1156-NG), 10ng/mL FGF (R&D Systems 3139-FB-025) and 5µg/mL Y-27632 rock inhibitor (Chemdea CD0141). Differentiation medium was prepared in bulk, distributed into single aliquots and stored at -20°C.

MED17.11 cells were then incubated in this differentiation medium for 96-144 hours in order to optimise conditions that resulted in maximal differentiation and functionality of the cell line. These timings were selected based upon author's advice that differentiation may not take a full 144 hour window to result in expression of nociceptive markers, but expression of markers was variable prior to 96 hour incubation in differentiating conditions. Differentiating MED17.11 cells were incubated at 37°C as per the author's instructions so as to inactivate the SV40 Large T antigen. A full summary of the various differentiation conditions trialled is shown in Table 3.1.

MED17.11 Cells Per Well	Chicken Embryonic Extract	Incubation time in differentiating conditions
1000	+	96 Hours
1000	+	144 Hours
2000	+	96 Hours
2000	+	144 Hours
2000	-	144 Hours
3000	+	96 Hours
3000	+	144 Hours
3000	-	144 Hours
5000	+	144 Hours
5000	-	144 Hours

Table 3.1: Variations in differentiation protocol used for MED17.11 cells.

3.2.3: Primary Neuronal Tissue

To evaluate the robustness of the immortalised line performance in the chosen Fluo-4 sensitisation assay it was necessary to isolate and culture sensory neurons from adult rat primary DRG to allow for direct comparisons using the same assay. Adult Wistar rats were terminally anaesthetised using an intra-peritoneal injection of 50mg/mL sodium pentobarbital and death was confirmed via cervical dislocation. DRG neurons were then collected, dissociated and cultured as extensively described in section 2.2.

3.2.4 TRPV1/NaV1.7 Sensitisation Assay & Drug Treatments

To assess the sensory functionality of the immortalised cell lines compared to traditional *ex-vivo* primary sensory DRG neurons, the Fluo-4 Direct Calcium assay was used. The general workflow of the assay and conversion of outputs to graphed values are detailed in section 2.8. In these experiments cellular responses to TRPV1 and NaV1.7 were measured following stimulation of the cells using capsaicin and veratridine respectively. In brief, 50µL of the total 100µL of media was removed from wells containing differentiated 50B11 cells, MED17.11 cells or primary DRG neurons. This was replaced by 50µL of 2X Fluo-4 Direct Calcium Dye after which cells were then incubated with the dye for at least 60 minutes. During this time, drugs for stimulation of TRPV1 or veratridine were made up to 6x the final working concentration and distributed into a dummy 96 well plate allowing addition of the drugs to be simultaneous via use of a multi-channel pipette. During the incubation with the dye, the Perkin-Elmer Victor 4 plate reader was set to 37°C at least 15 minutes prior to the end of dye incubation.

Following dye incubation cells were placed in the reader, prior to agonist stimulation. For experiments assessing functional NaV1.7 expression in immortalised cell lines, cells were treated with veratridine (Tocris Bioscience Cat-2918). 50B11 cells were treated with 1µM-30µM, MED17.11 cells with 10µM-100µM and primary DRG sensory neurons with 30-100µM. The difference between these concentrations reflect the different stages of assay optimisation at which these cell lines were used. However, all concentrations were concomitant with previous studies investigating activation of NaV1.7 in sensory neurons. No concentrations above 100µM were used as high concentrations of veratridine have been linked to off target activation of potassium ion channels (Mohammed *et al.*, 2017) . For studies investigating capsaicin stimulation of the TRPV1 receptor all cell cultures were treated with 1µM-5µM with capsaicin (Huls*e et al*., 2014) (Sigma M2028). This concentration range was derived from previous optimisation data of DRG responses to capsaicin within the group using the same assay. Above 5µM capsaicin has been found to cause variable desensitisation of TRPV1, reducing calcium influx and narrowing the experimental window. To verify the dependence of calcium influx on TRPV1 stimulation in primary sensory neuronal cells the TRPV1 inhibitor capsazepine was added to cells at least 20 minutes prior to stimulation in the sensitisation assay. Though capsaicin is widely recognised as a specific TRPV1 agonist at low concentrations it can have off-target effects on VGSCs, calcium and potassium channels at higher concentrations (Kuenzi and Dale, 1996). Stimulation of all cell types with 45mM KCl (Sigma 137009100) was used a positive control for depolarisation and calcium influx. Sensitisation was recorded over a 120 second time scale at regular intervals and was exported to excel and processed as described in section 2.8.

3.2.5: Assessment of TRPV1/NaV1.7 mRNA expression

To assess expression of the key receptor TRPV1 and the NaV1.7 ion channel following differentiation of immortalised cell lines, RNA was extracted from differentiated cells as described in section 2.3. Generation of cDNA was as described in section 2.4. Rat cDNA from primary sensory DRG served as a positive expression control in these experiments and was a kind gift of Dr Andrew Bennett (University of Nottingham). The primer sequences used for all targets are shown in Table 2.1 (section 2.5), which also gives expected amplicon sizes. Rat NaV1.7 primer pair 1 (Table 2.1) was used for 50B11 cDNA with an expected product size of 359bp. Primary rat positive control cDNA and 50B11 cDNA were denatured for 5 minutes at 95°C followed 34 cycles of: 60s annealing at 59°C; 60s extension at

72°C, and 60s denaturation at 95°C for a further minute. 60s annealing at 59°C; final extension at 72°C for 10 minutes, denaturation and storage at 4°C.

For investigations into murine MED17.11 *NaV1.7* expression a cross-hybridising primer was needed to detect the primary cDNA derived from rat. Therefore, the mouse/rat *NaV1.7* primer described in Table 2.1, section 2.5 was used with an expected product size of 287bp. This primer was originally designed using NCBI Primer Blast and Ensembl using murine sequences but has high homology with the analogous gene in rats. Primary rat positive control cDNA and MED17.11 cDNA was denatured for 5 minutes at 95°C. To encourage a cross reaction across species a lower annealing temperature of 52°C was used for 45 seconds. This was followed by an extension phase at 72°C for 45 seconds and a denaturation at 95°C for 45 seconds. This was repeated 35 times for a total number of 36 cycles, the PCR was concluded by a final 10 minute extension phase at 72°C.

For investigations into TRPV1, a cross reacting primer was used for all cell types. Though designed against rat transcripts using NCBI primer blast and Ensembl, the rat/mouse *TRPV1* primer possessed identical homology in the primer design spanning across exons 3-5 of the *TRPV1* gene in rats and mice. The primer set had an expected amplicon size of 233bp. Initially, cDNA from all cell types was denatured for 5 minutes at 95°C. This was followed by primer annealing at 50°C for 30 seconds followed by a 60 second extension at 72°C and a further denaturation for 60 seconds at 95°C. This was repeated a further 39 times for a final total of 40 cycles.

All PCR amplicons were visualised following 2% agarose gel electrophoresis as described in section 2.6.2 and imaged on a BioRad Gel Doc set to automatic exposure detection time.

3.3: Results

3.3.1.1: Capsaicin stimulates primary DRG neurons, which is reversible with administration of capsazepine

Following dissection, dissociation and incubation for 24 hours in basal F12 medium (Section 2.2.) primary DRG neurons were incubated with the Fluo-4 Direct Calcium Assay dye and subsequently treated with a final concentration of 1µM of the TRPV1 agonist capsaicin, vehicle or 1µM capsaicin and 10-20µM of the capsaicin inhibitor capsazepine (CPZ) which was applied 20 minutes prior to capsaicin stimulation. Calcium influx was then measured across a 120 second interval. Stimulation with capsaicin resulted in a significant increase in calcium influx compared to HBSS vehicle control resulting in an increase in F/F ratio (1µM Capsaicin: 42.4 ± 1.31 AU SEM). This stimulation was subsequently reversed in DRG neurons co-treated with the capsaicin inhibitor capsazepine at both 10µM and 20µM (10µM CPZ: 30.5 ± 1.76 AU SEM, 20µM CPZ: 20.7 ± 1.2 AU SEM). Despite this significant inhibition of capsaicin induced sensitisation, neurons stimulated with capsaicin but also treated with CPZ still had significantly higher levels of calcium influx compared to HBSS control. These results can be seen in Figure 3.1.

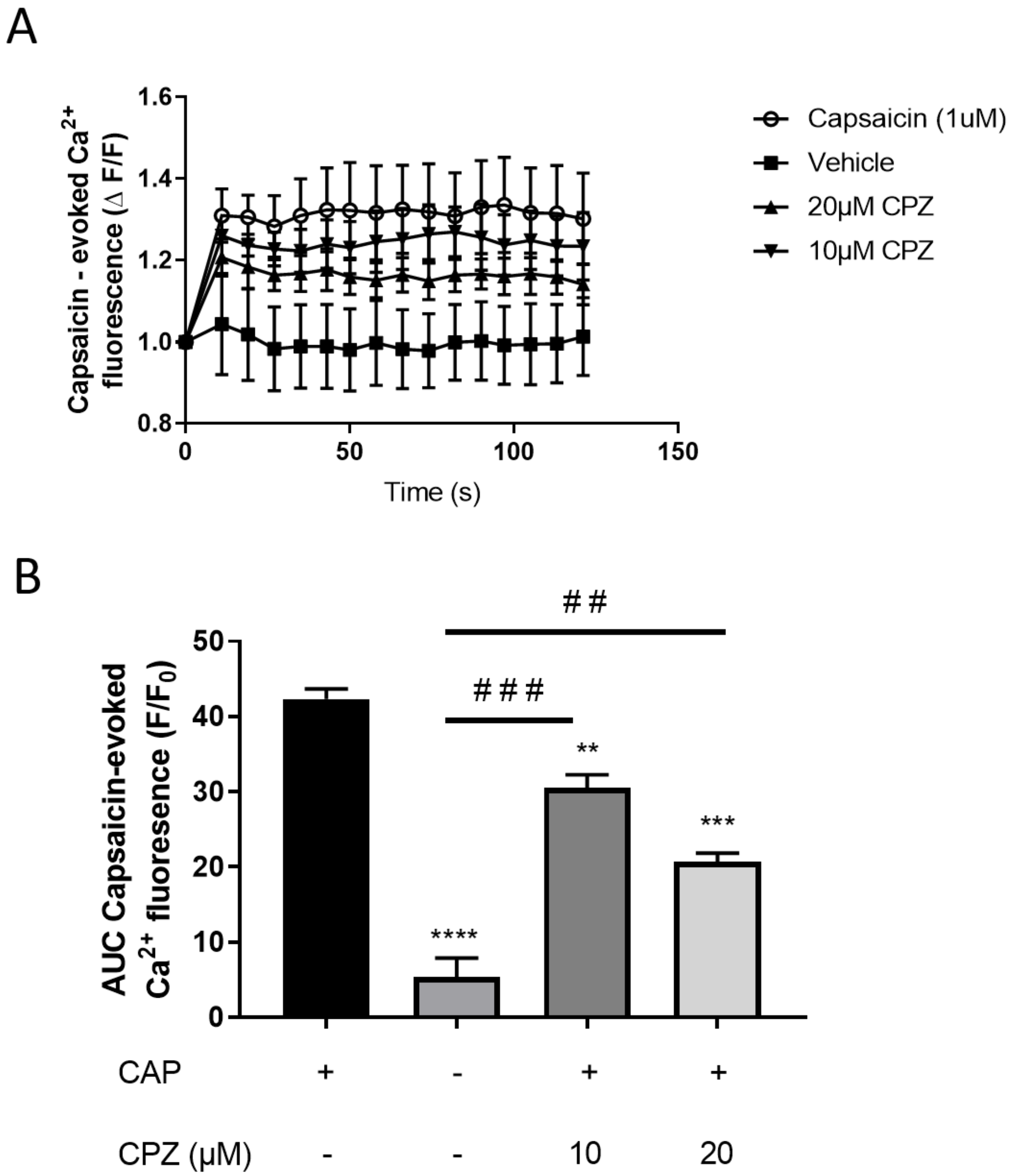

Figure 3.1: The effect of capsaicin and its inhibitor capsazepine on primary DRG neurons

Baseline fluorescence was read prior to application of 1µM capsaicin, vehicle or 1µM capsaicin + capsazepine and stimulation recorded over 120 seconds, each well was normalised to its baseline value (A). (B) AUC values for change in fluorescence over the 120 second period. N=3 rats with at least 3 internal replicates per plate. One Way ANOVA with Tukey's multiple comparisons. **** p = <0.00001, *** p= <0.0002, ** p= <0.002, ## p = < 0.003, ### p = <0.0004. Star significance = compared to CAP, Hash = compared to non-capsaicin vehicle.

3.3.1.2 Veratridine stimulates primary DRG neurons at high concentrations

Stimulation of primary DRG with 30µM-100µM of the $Na_V1.7$ agonist veratridine resulted in a concentration-dependent increase in intracellular calcium, but only stimulation with the maximal 100µM produced a significant increase in F/F ratio (100µM VTD: 19.89 ± 2.616 AU SEM) compared to HBSS vehicle control (HBSS: 3.9 ± 1.7 AU SEM). Whilst stimulation with 30µM and 50µM did produce modest increases in calcium influx neither of these were significantly above that of vehicle. The results of DRG neurons stimulation with veratridine can be seen in figure 3.2.

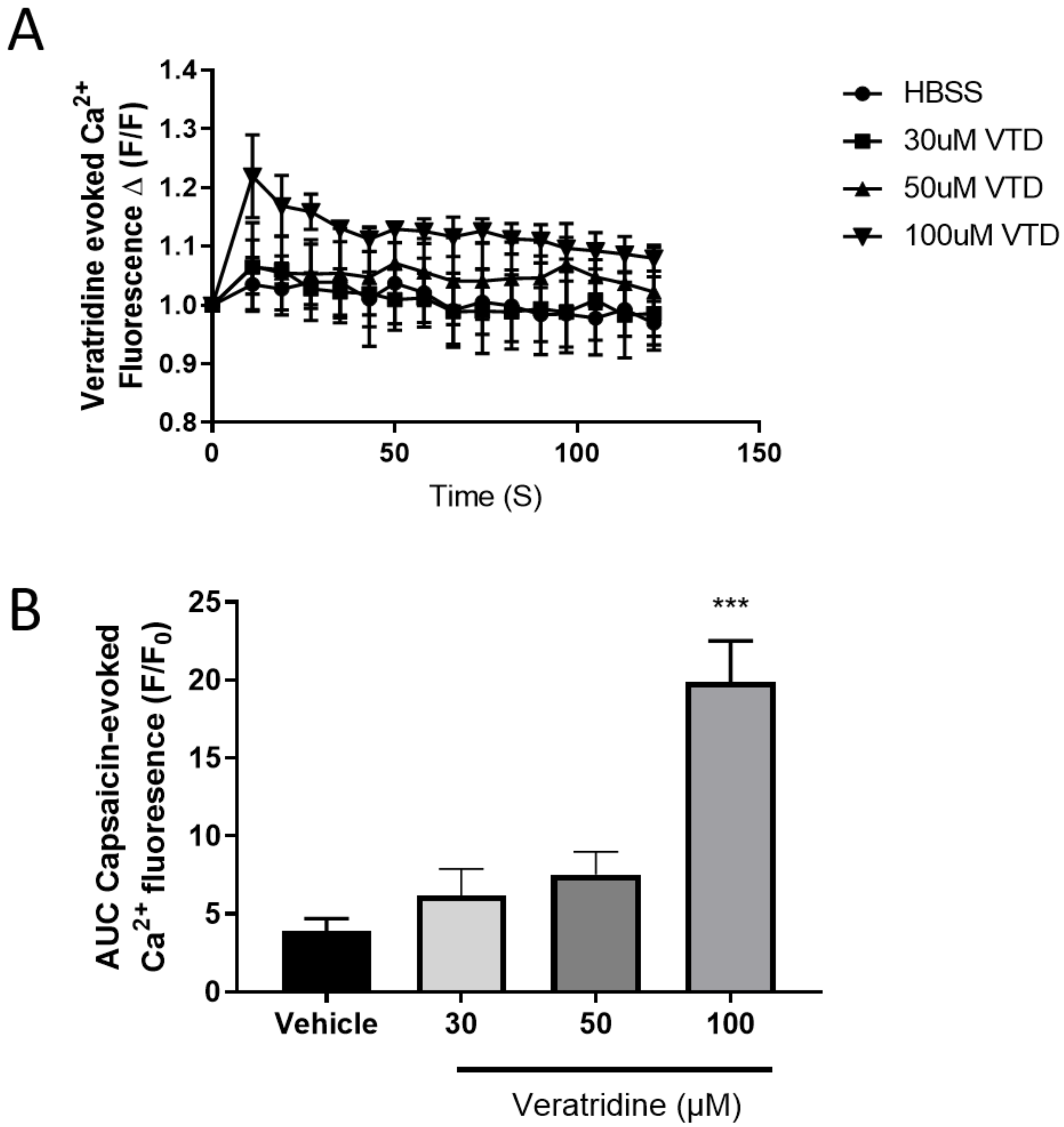

Figure 3.2: The effect of veratridine on primary DRG neurons

Baseline fluorescence measured using the Fluo-4 Direct Calcium Assay Dye was read prior to application of 30µ-100µM veratridine and stimulation recorded over a 120 second period, each well was normalised to its baseline value (A). (B) Area under the curve (AUC) values of the changes in fluorescence across the 120 second period. N=3 rats with at least 3 internal repeats on each plate. One Way ANOVA with Dunnett's multiple comparisons to vehicle. *** p = 0.0006. All data shown are mean ± SEM.

3.3.2.1: MED17.11 cells display robust neurite outgrowth when cultured in differentiation medium

Irrespective of the differentiation conditions denoted in table 3.1, MED17.11 cells displayed robust morphological differentiation and neurite outgrowth when incubated in a variation of differentiation media. MED17.11 cells adopted a bi-polar morphology and developed extensive processes resembling neurites. Many of these neurites formed connections with neurites originating from other MED17.11 cells in the culture. Neurites were of varying length with some neurites extending beyond 100µm. Emergence of these properties was recorded within 72 hours of differentiation, though some cells retained the flattened fibroblastic morphology up to this time point.

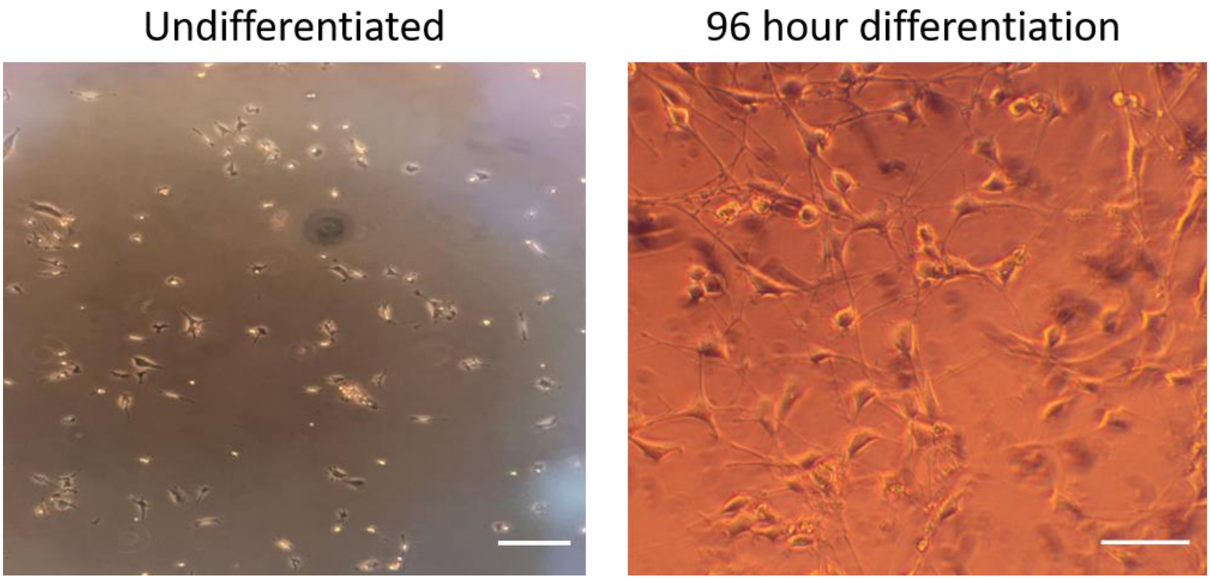

Figure 3.3: MED17.11 Neurite outgrowth following differentiation

Representative images of MED17.11 cells prior to incubation in differentiation medium (undifferentiated) and after 96 hours following incubation in differentiating conditions. Neurite outgrowth is clearly visible in differentiating MED17.11 cells which is absent in undifferentiated cells. Scale bar for undifferentiated image = 100µm. Scale bar for 96 hour differentiation image = 50µm.

3.3.2.2: No significant NaV1.7 responses were detected in MED17.11 cells that had been proliferated in CEE and differentiated for 96 or 144 hours.

The first report on MED17.11 cells showed expression of functional $Na_V1.7$ post differentiation (Dora*n et al*., 2015) after proliferation in the presence of chicken embryonic extract. Despite alteration to seeding density and length of incubation in differentiation conditions I could not demonstrate functional NaV1.7 responses in MED17.11 cells as previously reported. No significant differences in calcium influx were observed following stimulation of MED17.11 cells following veratridine stimulation compared to HBSS vehicle irrespective of MED17.11 seeding density. The absence of veratridine induced NaV1.7 stimulation and lack of responses can be seen in figure 3.4.

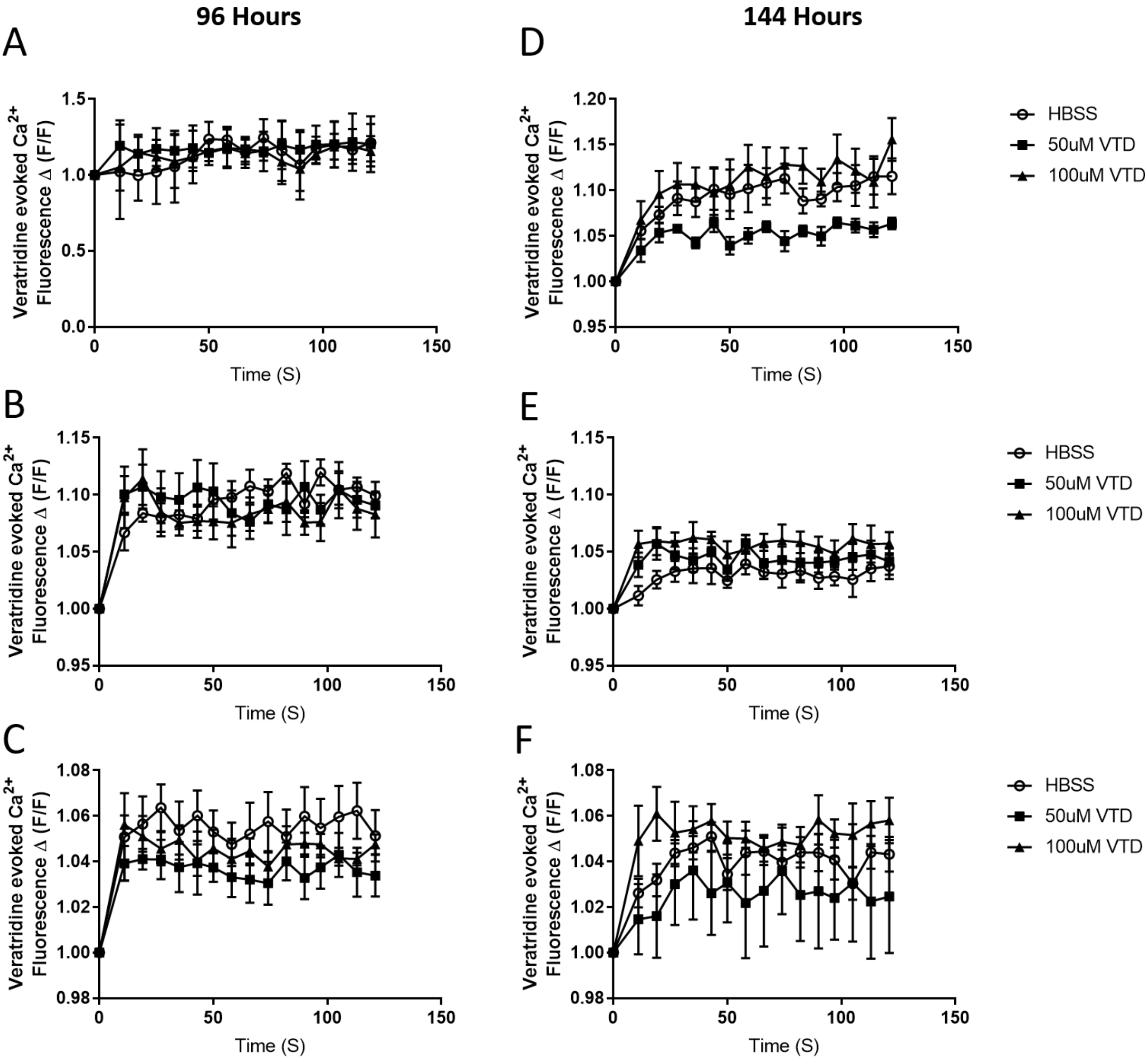

Figure 3.4: Effects of seeding density and 96/144 hours differentiation on MED17.11 NaV1.7 responses

MED17.11 cells seeded at 1000 (A), 2000 (B) and 3000 (C) per well and incubated for 96 hours in differentiating conditions display no significant NaV1.7 stimulation compared with control, following treatment with 50μM-100μM of veratridine. MED17.11 cells seeded at 1000 (D), 2000 (E) and 3000 (F) cells per well and incubated for 144 hours in differentiating conditions display no significant NaV1.7 stimulation and associated calcium influx following treatment with 50μM-100μM of veratridine. N=3 plate repeats with 6 internal repeats on each plate. Data shown are mean ± SEM. No significant differences detected, One Way ANOVA with Dunnett's multiple comparisons to HBSS vehicle control.

3.3.2.3: No significant NaV1.7 responses, nor NaV1.7 mRNA was detected in MED17.11 cells proliferated without chicken embryonic extract

Following correspondence with the authors of the original MED17.11 paper following the lack of responses shown in figure 3.4, I was advised to remove the 0.5% chicken embryonic extract from the MED17.11 culture medium. Chicken embryonic extract is believed to allow cells to retain proliferative and primitive phenotypes. However, in discussions with the original authors they expressed concern that CEE may reduce the efficacy and efficiency of differentiation. I therefore cultured MED17.11 cells in the absence of CEE and differentiated at a seeding density of 5000 cells per well. All other differentiation conditions remained constant. These changes to protocols had no effect on Na_V1.7 mediated calcium influx following stimulation with 10µM-100µM of veratridine compared to HBSS vehicle control. Furthermore, there was no detectable expression of NaV1.7 mRNA in MED17.11 cells proliferated without CEE and maintained in differentiating conditions for 144 hours. NaV1.7 mRNA expression was detected in primary rat cDNA using the murine based cross hybridising primer.

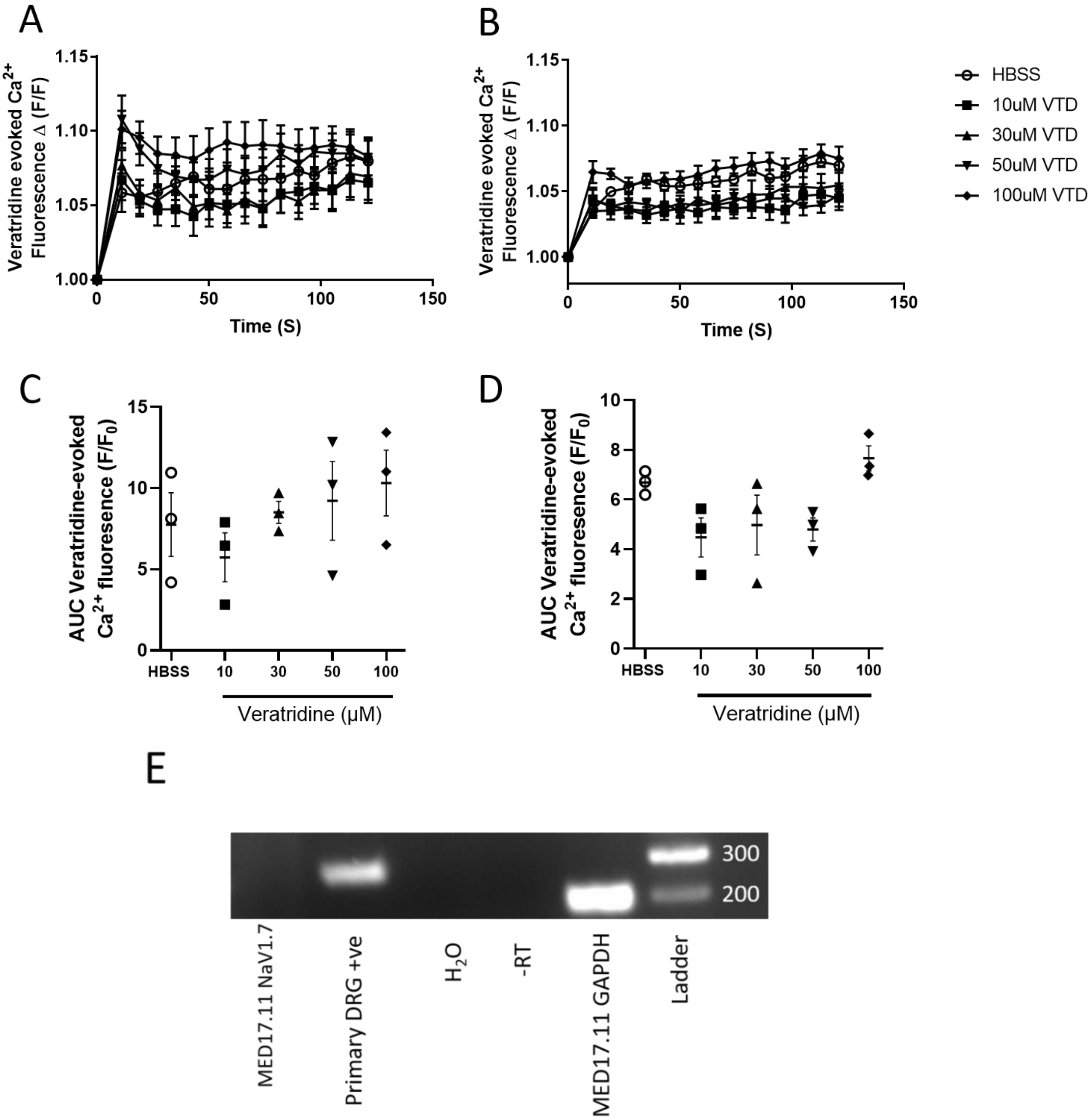

Figure 3.5: MED17.11 NaV1.7 responses from cells not exposed to chicken embryonic extract.

MED17.11 cells proliferated without CEE and incubated in differentiating conditions for 96 (A) or 144 (B) hours display no significant veratridine induced NaV1.7 responses and associated calcium influx when differentiated compared to HBSS vehicle control at any concentration of veratridine stimulation. (C) Area under the curve values for NaV1.7 responses following 96 hours of differentiation. (D) Area under the curve values for NaV1.7 responses following 144 hours of differentiation. N=3 plate repeats with 6 internal replicates per treatment. Data shown are mean ± SEM. No significant differences detected, One Way Anova with Dunnett's multiple comparisons to HBSS vehicle control. (E) No NaV1.7 mRNA (product size = 287) was detected in MED17.11 cells proliferated without CEE and incubated for 144 hours in differentiating conditions. N=3 separate RNA extractions from MED17.11 cells cultured in above conditions at passages 9,10 and 11.

3.3.2.4: MED17.11 cells do not show functional TRPV1 responses after a 144 hour differentiation protocol, nor do MED17.11 cells express TRPV1 mRNA.

The first report on MED17.11 cells also showed expression of functional TRPV1 (Dora*n et al*., 2015), but as with $Na_V1.7$ I was also unable to reproduce these responses in these cells. MED17.11 cells differentiated for 144 hours and seeded at various densities per well also failed to respond to capsaicin induced stimulation at either 1µM or 5µM (Fig 3.6) These concentrations had previously invoked responses in MED17.11 cells and in primary DRG sensory neurons as shown in section 3.3.1.2 (Doran *et al.*, 2015). Furthermore, there was no expression of TRPV1 in the MED17.11 cells seeded at 3000 cells per well and differentiated for 144 hours despite detection in rat primary DRG positive control with a cross hybridising primer.

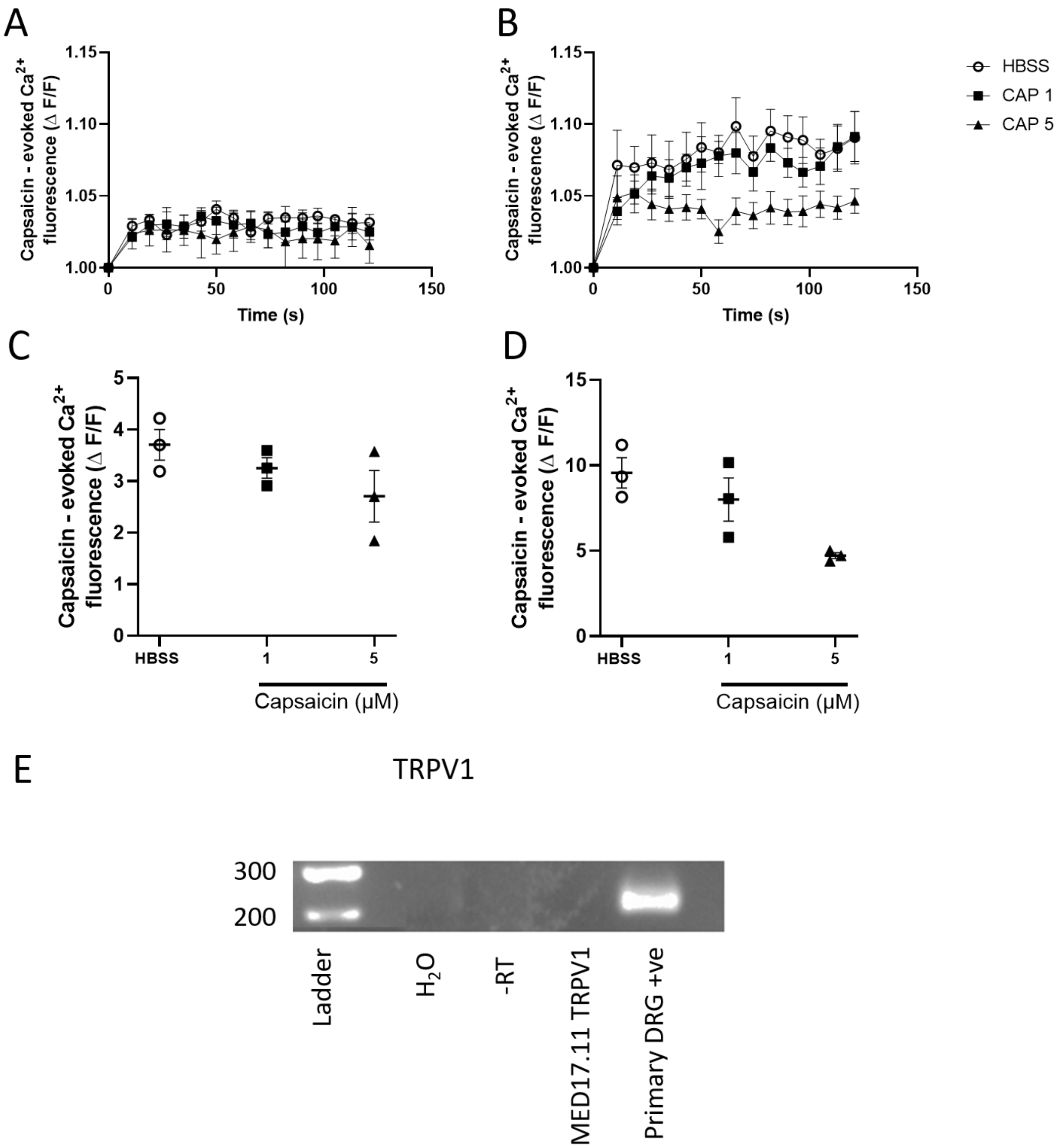

3.6: Effects of seeding density on MED17.11 responses to capsaicin stimulation

MED17.11 cells proliferated without CEE and incubated in differentiating conditions for 96 (A) or 144 (B) hours display no significant capsaicin induced TRPV1 responses and associated calcium influx when differentiated compared to HBSS vehicle control at either capsaicin concentration. (C) Area under the curve values for TRPV1 responses following 96 hours of differentiation. (D) Area under the curve values for TRPV1 responses following 144 hours of differentiation. N=3 plate repeats with 6 internal replicates per treatment. Data shown are mean ± SEM. No significant differences detected, One Way ANOVA with Dunnett's multiple comparisons to HBSS vehicle control. (E) No TRPV1 mRNA (product size = 233) was detected in MED17.11 cells proliferated without CEE, seeded at 5000 cells per well and incubated for 144 hours in differentiating conditions. N=3 separate RNA extractions from MED17.11 cells cultured in above conditions at passages 10,11 and 12.

3.3.3.1: 50B11 cells do not demonstrate NaV1.7 mediated calcium influx when stimulated by veratridine following a 24 hour differentiation, nor was NaV1.7 expression detected via RT-PCR

Previous results in our group and within the wider literature have shown robust functional responses in differentiated 50B11 cells, plated at seeding densities of 5000-10000 cells per well (96 well plate) similar to those in nociceptive DRG neurons (Bestall, 2017). However, I was not able to replicate these findings. When stimulated with veratridine 50B11 cells did not respond to stimulation at any concentration and irrespective of cell density per well. Furthermore, I was unable to detect expression of NaV1.7 cDNA in differentiated 50B11 cells seeded at 10000 cells per well despite positive amplification of 50B11 GAPDH cDNA and positive detection of TRPV1 expression in rat primary DRG cDNA at 359bp. I therefore concluded that 50B11 cells did not exhibit functional NaV1.7 expression after differentiation.

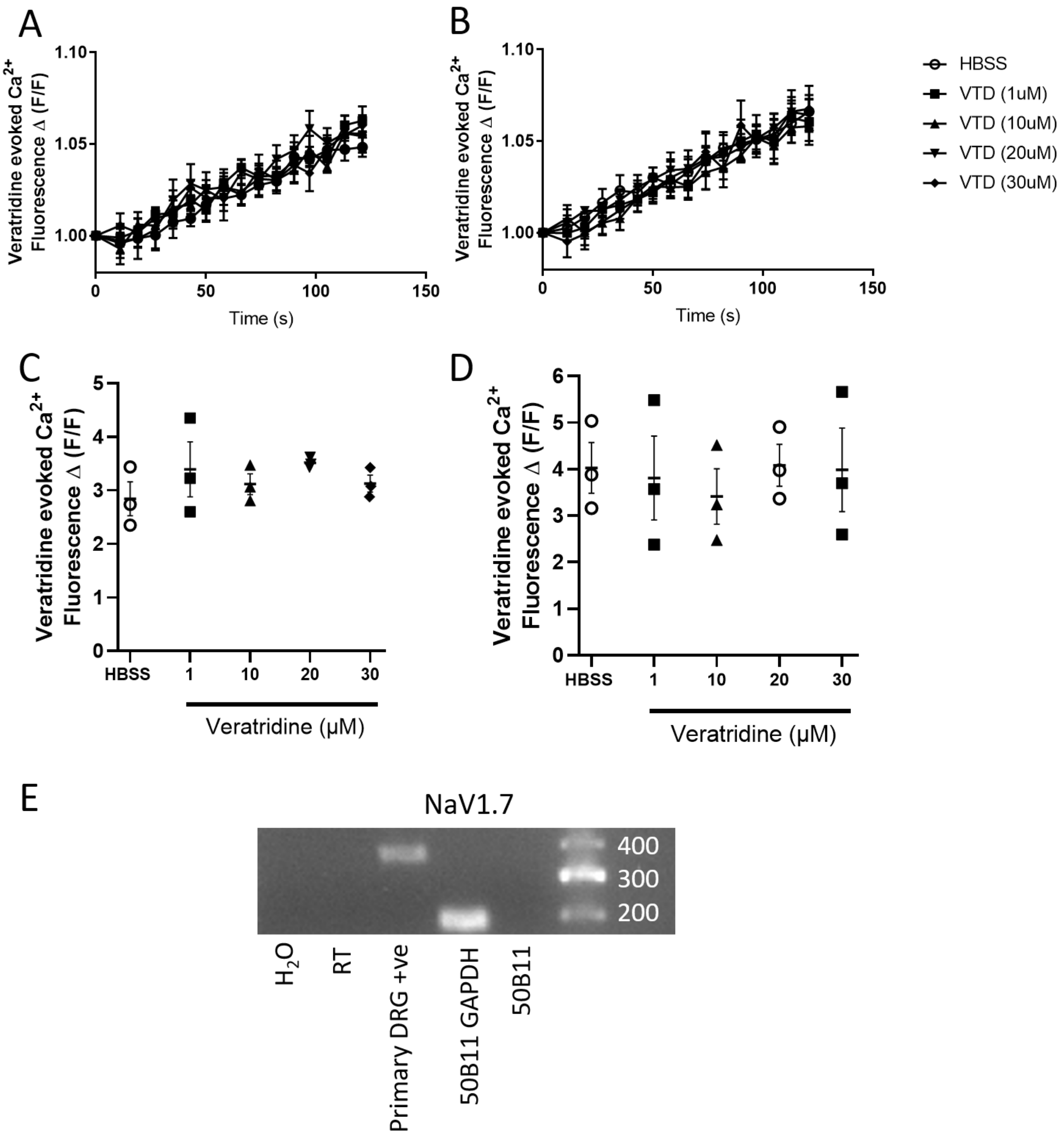

Figure 3.7: Effects of veratridine stimulation on NaV1.7 mediated calcium influx in 50B11 cells at different seeding densities and NaV1.7 expression.

50B11 cells seeded at 5000 (A) and 10000 (B) cells per well and differentiated for 24 hours in the presence of 75µM forskolin did not display significant increases in calcium influx following 1µM-30µM veratridine stimulation compared to HBSS vehicle control across the 120 second measuring period. (C) Area under the curve values at 5000 cells per well. (D) Area under the curve values at 10000 cells per well. N=3 plate repeats with 6 internal replicates per plate. Data shown are mean ± SEM. No significant differences detected, One Way ANOVA with Dunnett's multiple comparison to HBSS vehicle control. (E) No NaV1.7 mRNA (product size = 357bp) was detected in 50B11 cells seeded at 10000 cells per well and incubated for 24 hours in differentiating conditions. N=3 separate RNA extractions from 50B11 cells cultured in above conditions at passages 20,21 and 22.

3.3.3.2: 50B11 cells do not show functional TRPV1 responses following stimulation with capsaicin, nor was TRPV1 expression detected via RT-PCR

Despite using concentrations of capsaicin previously shown to activate 50B11 cells in our lab (Hulse *et al.*, 2014, 2015), there were no detectable responses in 50B11 cells compared to HBSS vehicle control, irrespective of seeding density. Furthermore, despite validation of successful synthesis of cDNA from 50B11 exemplified by successful detection of GAPDH at expected amplicon product size, there was no detectable expression of TRPV1 cDNA in the same samples. There was detection of TRPV1 cDNA in the rat primary DRG positive control sample at the expected product size of 233bp. I therefore determined that 50B11 cells did not exhibit functional TRPV1 expression following differentiation.

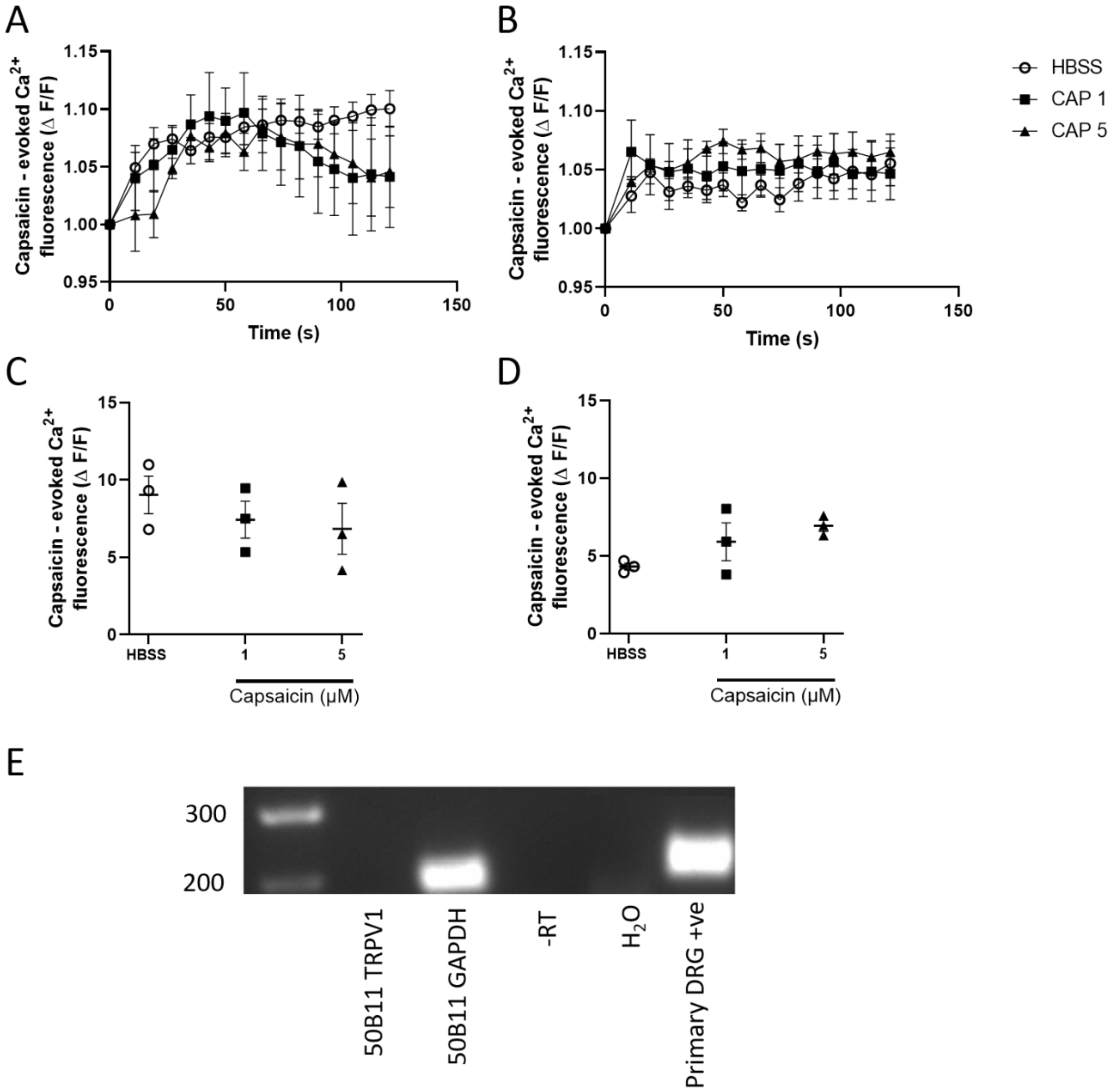

Figure 3.8: Effects of capsaicin stimulation on TRPV1 mediated calcium influx in 50B11 cells at different seeding densities and TRPV1 expression.

50B11 cells seeded at 5000 (A) and 10000 (B) cells per well and differentiated for 24 hours in the presence of 75µM forskolin did not display significant increases in calcium influx following 1µM-5µM capsaicin stimulation compared to HBSS vehicle control across the 120 second measuring period. (C) Area under the curve values at 5000 cells per well. (D) Area under the curve values at 10000 cells per well. N=3 plate repeats with 6 internal replicates per plate. Data shown are mean ± SEM. No significant differences detected, One Way ANOVA with Dunnett's multiple comparison to HBSS vehicle control. (E) No TRPV1 cDNA (product size = 233bp) was detected in 50B11 cells seeded at 10000 cells per well and incubated for 24 hours in differentiating conditions. N=3 separate RNA extractions from 50B11 cells cultured in above conditions at passages 24,25 and 27.

.

3.4 Discussion

The potential for immortalised neuronal cell lines as a supplementary tool or even as an eventual replacement for primary tissue is vast and is subject to widespread discussion and development within scientific literature. By circumventing various administrative limitations and financial burdens that are concomitant with animal housing and handling, immortalised lines could enable large numbers of research groups to engage with investigations into various neuropathies including CIPN (Obinata, 2007). However, despite their immense potential and concerted efforts to develop cell lines with key neuronal characteristics that are maintained with high fidelity over dozens of passages, there are still many limitations in most neuronal cell lines that necessitate careful consideration when utilising them as a preference over *ex vivo* primary neuronal tissue. These limitations include: the speed at which immortalised lines may lose their ability to differentiate into neuronal phenotypes due to extensive passaging (Bucchia *et al.*, 2018), the population of neurons from which the cell line is derived, the age of the animal from which they are obtained, and how this affects the expression of key markers and receptors; the costs associated with differentiation, as many immortalised cell lines make use of expensive reagents in media that are quickly exhausted during extensive use of the cell line and finally and perhaps most importantly, how immortalised lines perform in functional assays compared to primary tissue such as neurite outgrowth and sensitisation.

As both MED17.11 and 50B11 cell lines have been shown to demonstrate some functional properties of nociceptive sensory neurons, I aimed to validate these cell lines for functional responses using TRPV1 and NaV1.7 agonists as these are two key nociceptive channels (W. Chen *et al.*, 2007; Doran *et al.*, 2015). This would help to determine whether responses were comparable to those of primary sensory neurons. (Malin, Davis and Molliver, 2007). Despite variations in time based differentiation protocols and seeding density both cell lines failed to recapitulate either the relatively small veratridine induced Na$_V$1.7 or the larger response capsaicin-induced TRPV1 response in primary neurons. Subsequent investigations showed an absence of target cDNA for both targets in these lines. Determining why these functional assays failed to recapitulate primary DRG neurons is of essential importance for the development of immortalised lines as an alternative to primary tissue and such concerns must be considered before any immortalised line is used.

3.4.1: Primary DRG neurons respond to stimulation with capsaicin and veratridine

Before assessing the validity of immortalised cell lines it was necessary to characterise the responses of sensory neurons derived from adult rat primary tissue to capsaicin and veratridine. Primary DRG sensory neurons demonstrated significant responses to both compounds representing activity of TRPV1 and NaV1.7 respectively. The former of these responses was significantly but not fully reversed by the application of 10µM-20µM of the capsaicin inhibitor capsazepine, providing evidence the observed calcium influx was largely capsaicin and TRPV1 dependent (Nguyen *et al.*, 2010) (Yang *et al.*, 2019). Interestingly, 10µM capsazepine has previously been shown to abolish TRPV1 mediated DRG responses to 500nM capsaicin stimulation *in vitro*. Therefore, the presence of residual response following 1µM stimulation with capsaicin potentially suggests a non-TRPV1 dependent route of calcium flux at higher capsaicin concentrations. However, there is considerable evidence in the literature to suggest 1µM capsaicin stimulation is within the range of

TRPV1 specificity rendering this suggestion unlikely. As I opted to not use probenecid in these experiments, extrusion of calcium from the cells was not inhibited therefore it is possible that the observed flux that was not inhibited by capsazepine was due to release from intracellular calcium stores or indeed influx from other sites.

Furthermore, stimulation with a moderate concentration of capsaicin facilitated a larger response than stimulation with a high concentration of veratridine. Significant stimulation of NaV1.7 only occurred at a concentration at the threshold of inducing non-specific inhibition of voltage gated potassium channels and sustained depolarisation. A possible reason for this is the heterogeneity of NaV1.7 and TRPV1 expression of the various neuronal populations found in a primary DRG cell culture and how isolation and dissection protocols could potentially alter the distribution of this expression. For example, various studies have found that following culturing procedures, the expression of TRPV1 has increased markedly compared to neurons isolated in the same manner, but immediately subjected to RNA extraction procedures (Mohammed *et al*., 2017) (Ren *et al.*, 2014). In future work it would therefore be of use to greater characterise the components of the dissociated DRG cell culture in greater detail and how this could potentially affect the relevance of the model. Previous studies involving dissociated adult murine cultures and their responses to veratridine identified that 66% of the cellular composition in a DRG culture consists of nociceptors responsive to stimulation of either TRPA1 with AITC, TRPV1 with capsaicin of ATP with α-β methylene observed via calcium imaging. (Mohammed, Kaloyanova and Nassar, 2020) Of these, 64% responded to stimulation with veratridine and of those that did respond there was variety of response profiles including some with large periods of latency to stimulation of up to two minutes. Therefore it is possible that the reduced response to VTD in comparison to capsaicin stimulation observed in the above experiments could be mediated by these factors. Additionally, in these experiments I assessed calcium influx as an output of VGSC activity which is a common method used within the literature. However, using a sodium based dye such as ANG-2 may help to improve the signal of veratridine stimulation by directly measuring influx of sodium ions across the cell membrane (Iamshanova *et al.*, 2016). However, high throughput sodium dye assays often require a wash step to quench background fluorescence, which can cause cell detachment even on poly-lysine coated surfaces creating a source of inter-well variation. The Fluo-4 direct calcium assay used avoids the requirement for a wash-step through its formulation with a suppression dye which limits extracellular calcium sources of background fluorescence. Recently, a range of similar dyes were suggested for use in sodium indicator assays which may make this approach more viable in the future (Tay *et al.*, 2019). DRG responses to capsaicin were comparable to previous sensitisation experiments and the significant effect of the capsaicin inhibitor capsazepine in reducing calcium influx at both concentrations used provided evidence that TRPV1 specific responses within this model can be accurately probed and defined as mainly TRPV1 dependent rather than being predominantly mediated by any potential off-target effects of capsaicin stimulation on dissociated DRG cultures. (Hulse *et al.*, 2015; Bestall *et al.*, 2018)

3.4.2: MED17.11 cells are not robust alternatives to primary DRG neurons in plate based calcium influx assays

The murine MED17.11 cell line was subject to extensive differentiation and optimisation protocols in the experiments listed within this chapter. Despite this, they did not demonstrate any functional utility within the neuronal activation assay following stimulation with capsaicin or veratridine and following RT-PCR investigations were found to be lacking mRNA expression of both targets. As previously mentioned, the MED17.11 cells are a newly developed immortalised neuronal cell line and therefore there is a lack of confirmation of the initial findings on these cells. Indeed, at the time of writing the only paper describing their use and functionality successfully is the paper establishing the creation of the cell line (Doran *et al.*, 2015). However, there are myriad reasons as to why the results in this chapter fail to reflect those observed by Doran et al. When I received the cell line as a kind gift I was advised that this cell line was still in the preliminary stages of its characterisation both functionally and in terms of expression of molecular markers. The MED17.11 cells used within this study were expanded from passage 2 and no experiments using the cell line were conducted beyond passage 20. Therefore it is unlikely that extensive passaging and subsequent phenotypic drift were responsible for the absence of responses and expression of key neuronal targets, however to definitively prove this it would be necessary to characterise cells repeatedly between passages.

Furthermore, the differentiation protocols described in section 3.2.2 were developed in constant correspondence with the authors of the initial characterisation. Multiple variations of the differentiation protocol were used prior to activation experiments, which were extensive both in terms of incubation time, consideration of seeding density and determining the effect of certain elements of proliferation media such as chicken embryonic extract would have on any effective differentiation process. Therefore it is again unlikely that the protocols used were responsible for the absence of functional response and molecular expression given these protocols had previously resulted in successful expression of functional TRPV1 and NaV1.7. Further modification and adjustments to the concentration of the various growth factors and inhibitors used within these experiments would further corroborate this assertion but as this was not the primary aim of this project these further experiments were not carried out due to time constraints and the robust responses demonstrated by primary DRG neurons. A final possible explanation for the lack of observed TRPV1/NaV1.7 expression and responses in MED17.11 could be batch-specific effects between different vials of immortalised cells and laboratory reagents. The vial I received as a gift had not been expanded and used in previous experiments by Doran et al. and therefore may have different properties than those originally described. Furthermore, though media and growth reagents were obtained from the same suppliers, the constitution of reagents such FBS and Chicken Embryonic extract are often heterogeneous between batches and therefore may have contained components such as growth factors that limited the ability of the cell line to differentiate appropriately and express functional receptors. The effects of serum variation and the variability between different vials of the identical cell lines are well documented in the literature. For example, SH-SY5Y cells have been documented to proliferate and differentiate with varying efficiency across serum batches (Xicoy, Wieringa and Martens, 2017). Vetter et al. also demonstrated variance of expression of histamine receptor expression between two batches of SH-SY5Y cells from separate vials, despite culturing in the same batch of serum (Buttiglione *et al.*, 2007; Vetter and Lewis, 2010; Xicoy, Wieringa and Martens, 2017).

3.4.3: 50B11 cells above passage 20 are not robust alternatives to primary DRG neurons for plate based calcium influx assays.

As for MED17.11 cells, the immortalised rat embryonic 50B11 cell line was subject to investigations into TRPV1 and NaV1.7 expression following putative differentiation. The 50B11 cell line lacked functionality in the neuronal activation assay and expression of key molecular markers following a 24 hour differentiation period with the cAMP synthesis inducer, forskolin. There was no detectable expression of TRPV1 or Na$_V$1.7 in the cells using RT-PCR, despite previous reports of expression albeit in earlier passages (Haberberger, Barry and Matusica, 2020). However, unlike MED17.11 cells, there have been several studies utilising the 50B11 cells characterising their properties (Vetter and Lewis, 2010; Van Opdenbosch *et al*., 2012; Bhattacherjee, Liao and Smith, 2014; Gnavi *et al.*, 2015; Mohiuddin *et al*., 2019). These studies include characterisation of calcium responses following stimulation by a number of different agonists such as capsaicin, bradykinin, histamine and ATP, all of which activate nociceptive sensory neurons. As a result it is useful to consider the results observed within this chapter in comparison with these other studies. For example, the paper establishing 50B11 cells showed that the cell line displayed neuronal characteristics such as expression of TrkA and could still be differentiated beyond 100 cellular passages, this being sustained to an upper limit of 400 passages. In contrast, Vetter et al. observed that 50B11 cells when cultured and differentiated as described by Chen et al. remained sensitive to differentiation only up to a limit of 20 passages. This is significant and potentially indicative of batch specific differences between cell lineages during sub-cloning procedures. I used 50B11 cells between passages 20-30 as they were not available at earlier passage number, it is possible that these cells had lost the ability to fully differentiate. Earlier passages in the lab had demonstrated TRPV1 evoked responses (Hulse *et al.*, 2015; Blackley, 2019). It should also be noted that Vetter and colleagues only investigated functionality in calcium response assays and expression of these channels. Nonetheless, 50B11 cells have demonstrated a heterogeneous capacity for differentiation between batches, between our group Vetter's, and the authors who developed the cell line. Vetter at al. also found 50B11 cells differentiated at passages numbers below 20 and thus hypothetically sensitive to forskolin induced differentiation protocols, did not display any TRPV1 mediated responses to capsaicin despite responses to other stimulants such ATP being associated with a transient increase in calcium influx (Vetter and Lewis, 2010). Previous work within the group has identified TRPV1 expression within 50B11 cells and functional responses to AITC (TRPA1 agonist), capsaicin, and VEGF isoforms in *in vitro* diabetic neuropathy models, therefore this largely accounts for potential variations in equipment and laboratory conditions and further suggests the lack of consistency observed in the 50B11 cell line is likely to be due to genetic variation in batches caused by the cloning procedures used to establish the line. (Hulse *et al.*, 2015; Bestall *et al.*, 2018)

3.4.4: MED17.11 cells and 50B11 cells display robust neurite outgrowth following differentiation

Whilst differentiation of neither cell line resulted in detectable expression of the target neuronal markers in these experiments nor demonstrated any response to stimulation in functional assays, both cell lines did undergo noticeable morphological changes and exhibited robust neurite outgrowth. In the MED17.11 cells, robust morphological changes occurred within just 72 hours of the full 144 hour differentiation protocol and occurred across increasing numbers of cells in the period when images were taken. Neurites were observed in MED17.11 cells irrespective of CEE treatment. This robust outgrowth was also seen in the initial publication (Doran et al. 2015), with visible neurite outgrowth with strong expression of TUJ1/β-III tubulin detected within hours of incubation under differentiating conditions. This suggests that culturing in differentiation conditions promotes some neuronal features in MED17.11 cells even in the absence of expression of functional TRPV1 and $Na_V1.7$ and that the cell line may have utility beyond that of these functional responses.

In a similar fashion, 50B11 cells also demonstrated neuronal morphological changes after undergoing forskolin induced differentiation, showing neurite outgrowth in the majority of cells within 24 hours (Chen et al. 2007). TUJ1/β-III tubulin positive neurite outgrowth is evident in 50B11 cells after just 4 hours in differentiating conditions (Chen et al. 2007). This cell line has been used to investigate the effects of trophic and hormonal factors such as NGF and GDNF on neurite outgrowth by Bhattacherjee et al. (Bhattacherjee, Liao and Smith, 2014).

Previous work in the group also used 50B11 cells as a tool in assessing neurite outgrowth in the context of a diabetic model. 50B11 cells were exposed to various glucose concentrations in culture and then imaged via light microscopy and manual quantification. High glucose conditions visibly reduced observed neurite outgrowth that was ameliorated by supplementation with the neuroprotective VEGF isoform, VEGF-A_{165}b. The versatility of the cells within this study was visibly on display as 50B11 cells responded readily to glucose challenge and stimulation with a number of trophic factors such as NGF and VEGF-A_{165}a, corroborating the findings of Bhattacherjee et al. It should be noted however that these studies did not probe expression of key neuronal markers within these neurites and therefore this should also be taken into consideration when assessing 50B11 cells as an alternative to primary neuronal cultures as they make have lacked markers crucial to neuronal characterisations. I did not investigate the characteristics of the MED17.11 or 50B11 neurites further due to time constraints and the prioritisation of refining the sensitisation assay in DRG for screening of splicing kinase inhibitors.

3.4.5: Concluding Remark

Immortalised neuronal cell lines can have immense potential as cost and time effective alternatives to primary neuronal culture derived from rodents. However, due to the methods often employed in immortalisation to establish the cell lines, experimental conditions and various batch specific effects it is of paramount importance to fully characterise neuronal cell lines prior to use in order to ensure experimental consistency. This includes assessment of expression of key markers and the performance of the cells within functional assays. In this chapter, I assessed the validity of two immortalised neuronal cell lines, the 50B11 immortalised rat line and the novel murine MED17.11 cell line for use in high throughput neuronal activation assays. Despite use of previously published differentiation protocols neither cell line responded in a high-throughput calcium influx based sensitisation assay to either capsaicin or veratridine. Additionally, differentiated cells did not express the key nociceptive markers NaV1.7 and TRPV1. However, both cell lines did show morphological changes in response to differentiation with robust neurite outgrowth following attempted differentiation protocols. Therefore, whilst immortalised cell lines represent an attractive option for replacement of primary neurons due to lack of responses observed using these lines, I concluded that it was most suitable to continue investigations into amelioration of CIPN using primary neuronal cultures.

4: An *in vitro* model of vincristine induced neuropathy as a screening tool for novel therapeutics

4.1.1: Introduction

Painful neuropathies are among the commonest adverse effects of sustained use of chemotherapy agents (Han and Smith, 2013). Neuropathy is a consistent phenomenon that occurs across multiple classes of chemotherapy, including the vinca alkaloids, the taxanes and platinum based chemotherapy drugs such as cisplatin (Ta *et al.*, 2006; Grisold, Cavaletti and Windebank, 2012; Mora *et al.*, 2016). Crucially, the onset of this pain is a dose limiting factor in the provision of chemotherapy to patients with the onset of pain often used as the benchmark for the cessation of a chemotherapy cycle. However, prior loss of fine motor control and tactile sensation is not uncommon (Sabarre, Rassekh and Zwicker, 2014). Furthermore, the earliest symptoms reported by patients with CIPN most commonly present primarily in the distal portions of the body such as the toes, feet and hands. Whilst pain during chemotherapy regimens is common, it can also be prevalent many months or even years following the termination of a successful treatment and in many cases is irreversible (Silva *et al.*, 2006). In some cases, patients have refused treatments due to painful contraindications which presents an additional challenge to survival (Mora *et al.*, 2016). In spite of this and considering the increased survivorship in people living with and beyond cancer due to refinement of chemotherapy and radiotherapy, there is a lack of clinical treatments available to ameliorate the symptoms of severe and often long term chemotherapy induced peripheral neuropathy. Consequently, there has been a profound increase in pre-clinical investigations probing potential mechanisms by which painful chemotherapy neuropathies emerge and as a result of this a number of potential candidates for treatment have emerged.

However, there are certain obstacles preventing rapid development of novel approaches. Foremost among these is the fact that as previously mentioned, despite the high prevalence of CIPN among patients there is little consistency in how the neuropathy is assessed (Flatters, Dougherty and Colvin, 2017). There is often a lack of standardised diagnostic tests used to monitor the severity and sequelae of the neuropathy. In some cases patients are asked only to self-report symptoms, leading to poor characterisation of symptom development and resolution across different healthcare groups. A further potential consequence of this inter-observer variability is a disparity between clinical findings which may unveil more severe levels of pathology and CIPN progression, offset by patient reports which regularly underreport symptoms due to difficulties in articulating early onset symptoms such as numbness and tingling (Kelley and Fehrenbacher, 2017). Consequently, in the past it has been difficult to outline groups of patients who are potentially at greater risk of developing CIPN when treated with a certain class of chemotherapy. However, contemporary systematic reviews have been carried out to address this issue and identified a number of risk factors such as age, and a patient history of neuropathy with or without a diagnosis of diabetes (Seretny *et al.*, 2014; Molassiotis *et al.*, 2019). Patients in insurance provider based healthcare systems can also be reticent about fully disclosing sensory symptoms due to concerns over how this will affect their standing or access to medication or even concerns about full cessation of treatment (Center for Drug Evaluation and Research (CDER) and U.S. Food and Drug Administration (FDA), 2017). Similarly clinicians can often be unwilling to investigate symptoms fully due to the lack of available preventative or therapeutic options (Knoerl *et al.*, 2019). This in turn fosters the creation of a vicious cycle that minimises the observed severity neuropathy and potentially masks information on patient symptoms that could help focus pre-clinical mechanistic investigations. Another obstacle to investigations into the mechanisms of CIPN manifestation is the lack of biopsies taken from patients during their chemotherapy or on follow up. There are several reasons for this including the aforementioned reluctance to fully investigate CIPN, but also that due to the fact that routine skin biopsy to assess neurite dieback, axonal degeneration and sensory receptor expression of intra-epidermal nerve fibres (IENFs) are not recommended under current NHS guidelines due to patient welfare concerns (West London Cancer Alliance, 2019). As a result, the biopsies that are taken are often analysed in chemotherapy follow up appointments and therefore when long term damage to nerves is likely to have occurred. This prevents analysis of the putative acute mechanisms behind CIPN related pain during the earlier stages of a chemotherapy regimen in the vast majority of patients suffering from CIPN.

In response to the growing difficulties experienced by cancer survivors with regard to reduced quality of life and the rising incidence of CIPN there is an urgent need to develop physiologically relevant *in vivo, ex vivo* and *in vitro* models to mirror chemotherapy related neuropathies and the sensitisation that is associated with them. Limitations on these approaches include those discussed in depth in Chapter 3, the lack of well-established immortalised neuronal cell lines, the expense in both time and finance of long term animal studies and the technical expertise required for the maintenance of *ex vivo* cultures. There are also limitations surrounding the translatability of neuronal culture models of CIPN and their relationship to the neuropathy in a clinical setting (Gadgil *et al.*, 2019). Nonetheless, in spite of these limitations there has been significant progress in recent years in elucidating the various aetiologies of acute CIPN caused by different chemotherapy agents, neuronal sensitisation and how these factors eventually progress into the sustained neuronal damage associated with chemotherapy neuropathy. One of the principle receptors identified as a potential driver of acute sensitisation in CIPN is the aforementioned TRPV1 and pathways related to its activation. TRPV1 is described in depth in Chapter 1 and explored in the context of a neuronal activation model in Chapter 3.

Screening of novel compounds such as novel splicing kinase inhibitors relies on development of high fidelity, high throughput screening *in vitro* models for key outcomes prior to use in pre-clinical *in vivo* studies. Use of traditional techniques such as patch clamping are expensive, time consuming and require high levels of technical expertise (Zhao *et al.*, 2016). However, as described in Chapter 3, immortalised cell lines lack consistency in both functional assays and genetic expression of key targets including the putative CIPN mediator TRPV1. Therefore it is important to reach a compromise between the two approaches when developing novel neuronal drug screening methods. In Chapter 3, I described a nociceptive neuronal activation assay which focused on stimulation of TRPV1 and NaV1.7 with various agonists and subsequent recordings of calcium dye influx in response to said stimulation. Calcium dyes and capsaicin application to activate nociceptors *in vitro* presents an opportunity to assess whether novel compounds can alter nociceptive responses prior to *in vivo* studies.

Therefore, I decided to develop the activation model further, whilst basal responses of dissociated DRG neurons to capsaicin and veratridine stimulation were recorded in Chapter 3, the versatility of the cultured neurons and the ease of using a plate reader to record their responses within the assay following stimulation allows for more complex investigations. For example, previous work in the group has used a variation of the DRG Fluo 4 assay to record the sensitised responses of dissociated neurons that were maintained in high glucose conditions prior to stimulation (Bestall *et al.*, 2018). This mirrors the hyperglycaemic conditions often observed in cases of diabetic neuropathy. TRPV1 stimulation of neurons cultured in high glucose conditions resulted in greater responses seen in untreated neurons and this enabled the assay to be used to identify potential compounds that reduced neuronal responses to those cultured in basal glucose conditions. Developing such a screening tool would be of immense utility as it would inform any future *in vivo* experiments assessing behavioural thresholds and bolster the pre-clinical portfolio of any therapeutic candidate. Additionally, an in vitro model of sensory neuronal sensitisation could be used to assess the properties of novel chemotherapy agents and probe the potential mechanisms responsible for sensitisation and pain.

Previous work within the group has demonstrated *in vitro* sensitisation assays can achieve these aims. By modelling diabetic hyperglycaemia, Bestall et al. found enhanced nociceptive responses to capsaicin could be reversed with co-application of alternatively spliced VEGF-A isoforms. Furthermore using this diabetic sensitisation model TRPV1 was found to be one of the principle components of an axis of sensitisation driven by glucose induced upregulation of the Receptor for Advanced Glycation Endproducts (RAGE) protein which in turn is driven by high glucose induced upregulations of High Mobility Group Protein B1 (HMGB1) and protein kinase C (PKC). Actions of both these molecules were inhibited by recombinant VEGF-A_{165}b isoform application, clearly demonstrating a role for VEGF-A in nociceptive neuronal sensitisation which was also demonstrated by Hulse et al. *in vivo* (Hulse *et al.*, 2014). Therefore, modulating the activation assay to model the acute effects of chemotherapy on neurons would provide a tool with which to investigate the potential of novel compounds developed to ameliorate sensitisation and with consideration of their targets allow for investigations into the potential mechanisms behind the sensitisation and any demonstrated inhibition.

As previously described TRPV1, the functional receptor for capsaicin is crucial in the detection and regulation of bodily responses to thermal stimuli and is primarily expressed in C-fibre nociceptive afferents. TRPV1, along with other TRP channels such as TRPA1, TRPV3, TRPV4 and TRPM8 is implicated as a potential means of sensory neuronal activation and sensitisation. Long term dysregulation of TRPV1 has previously been linked to a number of painful neuropathies including diabetic neuropathy (Hulse *et al.*, 2015). Indeed, both diabetic neuropathy and CIPN share components of early sensory sequelae originating in distal portions of the body, fingers and toes (Tesfaye, Boulton and Dickenson, 2013). In most cases, symptoms in these areas of the body manifest as thermal allodynia and noxious responses to otherwise non-harmful stimuli which is underscored by sensitisation of peripheral neurons and aberrant activation of the TRPV1 receptor nociceptive signalling pathway. As chemotherapy treatment continues the progression of these neuropathies proceeds proximally from the extremities, also involving damage to larger fibres which results in paraesthesia and reductions in nerve conduction velocities as larger, myelinated fibres begin to degenerate. This culminates in severe ataxia, loss of reflexes and decreased proprioception and in many cases pain as the degeneration of large fibres alters the properties of adjacent intact C- and A-nociceptors (Djouhri *et al.*, 2012). However, as initial symptoms are linked to erroneous thermal signalling in the periphery investigations into the mechanisms underlying this phenomenon have been carried out in recent years, centred on TRP channel modulation of this nociceptive signalling.

PKC/TRPV1 dependent neuropathy has been identified in rodent models of CIPN for vinca alkaloid, taxane and protease inhibitor chemotherapy agents (Tsubaki *et al.*, 2018). Tamoxifen, a known inhibitor of PKC and thus a key part of the TRPV1 sensitisation axis was able to abolish vincristine and paclitaxel induced thermal allodynia in mice behavioural experiments. Furthermore, there is evidence to suggest treatment with chemotherapy results in increased expression of TRPV1 within small diameter and medium diameter neurons in DRG cultures and whole DRG following *in vivo* application of paclitaxel and vincristine, indicating potentially pathologic changes in subsets of DRG neurons that based on size, are likely to be predominantly nociceptive populations. This is supported by behavioural experiments demonstrating that application of the TRPV1 inhibitor capsazepine, supplied to mice just 30 minutes prior to testing following a 14 day treatment with vincristine significantly reduced paw withdrawal frequency in von Frey behavioural testing (Chiba *et al.*, 2017). This clearly demonstrates a rapid and comprehensive reversal and blockade of a mechanism of sensitisation in rodents that cannot be attributed to neuronal cell death and long term damage. TRPV1 knockout studies have also revealed a critical role for the receptor in driving and maintaining pathological sensitisation in various neuropathies (Premkumar and Sikand, 2008)

Despite the clear importance of TRP channels such as TRPV1 in sensitisation pathways, targeting the receptors themselves has proved difficult beyond the pre-clinical stage. Inhibitors of TRPV1 and TRPM8 have both been withdrawn from Phase 1 clinical trials due to severe adverse effects, predominantly hyperthermia (Trevisani and Gatti, 2013). This is largely due to the fact both channels are key regulators of body temperature homeostasis and direct inhibition leads to disruption of these crucial functions. Therefore it is more pragmatic to target upstream mediators of sensitisation, rather than these receptors themselves to avoid these effects. Furthermore, targeting upstream signalling may have effects across a variety of TRP channels, rather than a solitary target. The experiments by Hulse, Beazley-Long and Bestall demonstrated for the first time the differential effects of VEGF isoforms on nociceptor sensitivity. Furthermore, Blackley demonstrated that in dissociated DRG neurons, pre-treatment with an anti- VEGF-A_{165}b antibody increased the calcium influx in response to capsaicin stimulation, suggesting that endogenous VEGF-A_{165}b inhibited TRPV1-mediated responses (Blackley, 2019). Compounds that can alter VEGF-A splicing in favour of VEGF-A_{165}b may therefore be capable of reversing neuronal sensitisation. Evidence for this was also provided by Blackley, as the SRPK1 inhibitor SPHINX31 reduced TRPV1-mediated calcium influx in otherwise untreated neurons and this was reversed by the anti-VEGF-A_{165}b antibody suggesting the SPHINX31 inhibitory effect is mediated by production of VEGF-A_{165}b. It remains to be seen whether the effect of SRPK1-mediated alternative splicing can be replicated in neurons that are sensitised by chemotherapy or hyperglycaemia. Therefore, there is a clear rationale for testing inhibitors of SRPK1 or the interacting CLK1 kinase for effects on nociceptor sensitisation via these VEGF mediated mechanisms. These experiments would also provide valuable insight into alternative splicing within neurons and the association with nociception, a fairly neglected area of the literature relative to investigations into the role of alternative splicing in oncological contexts.

A final use for a chemotherapy sensitisation assay would be to screen new chemotherapy agents for off-target neuronal effects. Despite the increasing burden of CIPN, new chemotherapies are rarely if ever tested for these effects. A versatile and relatively straightforward pre-clinical first pass experiment such as the Fluo-4 direct assay could provide valuable insight into how likely it is a compound will produce neuropathic symptoms or how severe these are compared to a currently used drug such as vincristine. Therefore I decided to examine the sensitising effects of the novel indole alkaloid jerantinine in a direct comparison with vincristine. Though previous work has identified jerantinine to be less damaging than other related compounds towards non-cancerous cells, this is the first time it has been applied to neurons. Effectively identifying any differences between the neurotoxic and sensitising capacity of the compound could then be used as a basis for more thorough *in* vivo investigations.

4.1.2: Hypotheses and Aims

1. Treatment of dissociated primary DRG neurons with vincristine will result in acute neuronal sensitisation.

2. DRG neurons treated with the novel indole alkaloid jerantinine, will exhibit reduced sensitisation compared to that induced by vincristine.

3. SRPK1 inhibition will reduce DRG neuronal sensitisation induced by vincristine based on prior data demonstrating the anti-nociceptive effects on VEGF isoform expression.

4. CLK inhibition will reduce DRG neuronal sensitisation induced by vincristine based on interactions with SRPK1.

5. DYRK1A inhibition will reduce DRG neuronal sensitisation induced by vincristine.

Experimental Aims:

1. Determine whether primary DRG neurons can be acutely sensitised by vincristine.

2. Optimise a neuronal sensitisation model based upon the neuronal activation model described in Chapter 3.

3. Use the sensitisation model to screen a novel chemotherapy agent and determine the level of sensitisation it induces in primary DRG neurons to assess transferability.

4. Validate the sensitisation model by using it screen novel splicing kinase inhibitors as putative desensitising compounds.

4.2 Methods

4.2.1: Isolation and culturing of dissociated primary DRG neurons

Dorsal root ganglia were isolated from adult male Wistar rats as described in section 2.2.3. Briefly, terminally anaesthetised rats humanely sacrificed in accordance with Schedule 1 of the Animals in Scientific Procedures Act 1986 (ASPA) were subject to a laminectomy, exposing the spinal cord. DRG were then removed from all levels of the spine using fine forceps and micro-scissors. DRG were then placed in cold, basal Ham's F12 media until the conclusion of the dissection. After this, removed DRG were carefully desheathed using the same instruments and had any remaining nerve roots removed. Desheathed DRG were then placed in a fresh aliquot of Ham's F12 and incubated for 2 hours at 37°C in a 0.0125% Collagenase Type IV solution. DRG were then mechanically triturated to create single cell suspensions and seeded at

2,000 cells per well of a black sided 96 well plate in coated with poly-L-lysine solution and 0.1µM/mL laminin in 100µL of DRG medium described in section 2.2.4. Plates were then left overnight to allow neurons to adhere to plates. The following morning, specific treatments detailed throughout this chapter were added and neurons were incubated for a further 24 hours. All treatment media also contained 30µg/mL of FdU to prevent glial cell proliferation.

4.2.2: TRPV1 Sensitisation Assay

All experiments in this chapter were carried out using the Fluo-4 Direct Calcium assay described in detail in section 2.8. In brief, 50µL of DRG medium with treatments or vehicle was removed and replaced by 50µL of 2x Fluo-4 Direct Calcium Assay Dye, diluting the dye 1:2. Plates were then incubated with the dye for at least 60 minutes. Following this incubation period, plates were placed in a Perkin Elmer Victor 4 plate reader set to 37°C. Background and baseline fluorescence were recorded as previously described. Cells were then stimulated with 1µM of TRPV1 agonist capsaicin. The concentration of capsaicin used was optimised in section 4.3.1, in these experiments capsaicin was used between 0.1µM and 5µM. Calcium influx and observed fluorescence were then recorded over a 120 second period. Measurements were then exported for downstream analysis such as calculation of area under the curve values and normalisation as described in section 2.8.3.

4.2.3 Optimisation & Drug Treatments

4.2.3.1: Optimisation of capsaicin concentration

In order to establish an experimental window with which to detect any vincristine induced neuronal sensitisation above that neurons exhibited by cells treated with vehicle controls it was essential to optimise the concentration of the TRPV1 agonist capsaicin. To accomplish this, neurons were treated for 24 hours with 1nM of vincristine or DMSO vehicle control (0.1%). Vincristine concentration was set at 1nM for these experiments as this closely matches the circulating levels of vincristine found in patients following a cycle of chemotherapy (D. V. J. Jackson *et al.*, 1981) . Following 24 hour incubation, neurons were loaded with the Fluo-4 Calcium dye for 1 hour and processed according to the sensitisation assay workflow before being stimulated with either 0.1µM, 0.5µM, 1µM or 5µM of capsaicin in Hanks Buffered Salt Solution (HBSS, NaCl 8g, KCl 0.4g, $CaCL_2$ 0.14g, $MgSO_4{\bullet}7H_2O$ 0.1g, $MgCL_2 \bullet 6H_2O$ 0.1g, KH_2PO_4 0.06g). HBSS alone was used as a negative control for stimulation. The capsaicin concentrations used were selected due to their response profiles in previous experiments on DRG neurons in a similar assay, modelling diabetic neuropathy. Responses were recorded immediately following the addition of capsaicin and for a 120 second period.

4.2.3.2: Assessment of Vincristine and Jerantinine induced nociceptive neuronal sensitisation

Isolated neurons were treated with DMSO vehicle control (0.1%), 0.1nM, 1nM or 10nM of vincristine for 24 hours. These concentrations were chosen based upon a range of recorded values for circulating vincristine doses in patients following a chemotherapy cycle (D. V. Jackson *et al*., 1981). Jackson et al. demonstrated that vincristine had a prolonged half-life within the blood of up to 37 hours. Therefore, this dose of vincristine circulating for this length of time and in such strength would likely result in nervous tissue being subject to sustained vincristine exposure. After 24 hours, neurons were loaded with Fluo-4 direct calcium assay dye and stimulated with 1µM of capsaicin prior to recording of evoked fluorescence.

Following determination of the acute effects of vincristine on neuronal responses by vincristine, additional isolated neurons were treated with 125nM, 250nM or 500nM of synthetic Jerantinine acetate A for 24 hours. As Jerantinine has not been used in humans or animal models, the concentrations selected were based on IC_{50} data from the Coyle Laboratory on the ability of jerantinine to prevent medulloblastoma colony formation. The concentrations in those assays were as effective as the concentrations of vincristine above at targeting colonies and therefore represent the concentrations that might be required for effective cancer treatment, however this remains to be established in anything other than an *in vitro* pre-clinical model. Responses to 1 µM of capsaicin were recorded after 24 hours as above.

4.2.3.3: Assessment of the effect of Novel Splicing Kinase Inhibitors on nociceptive neuronal sensitisation.

The novel splicing kinase inhibitors used for investigations into potential amelioration of acute chemotherapy induced neuronal sensitisation are listed in Table 4.1. These compounds were selected based on the rationale that their targets of inhibition may be key modulators of various components of the acute sensitisation mechanisms that activate following chemotherapy provision. For example, the aforementioned SPHINX31 is a potent and highly selective inhibitor of SRPK1 which is a major mediator of *VEGFA* alternative splicing. Control over VEGF splicing has been postulated to be anti-nociceptive due to the effects of alternatively spliced VEGF isoforms in the context of diabetic neuropathy. The Griffin compounds preferentially inhibit the CLK kinases that have been found to operate in a close relationship with SRPK1. The DYRK1A kinase has been implicated in many neuronal development studies, with over-activity of the kinase linked to cytokine driven neuroinflammation observed in Alzheimer's Disease. However its role and function within the PNS remains unexplored. Additionally, CLK and DYRK1A inhibiting compounds within the literature are being developed as potential cancer treatments, therefore any interactions between the novel compounds and a widely used chemotherapy agent are useful to establish. Of the 4 compounds used Griffin 6, Griffin 23 and Hippogriff 1 were kind gifts, synthesised and received from Professor Jonathan Morris of the University of New South Wales. SPHINX31 was a gift from Exonate Ltd.

Compound	IC50 SRPK1 (nM)	IC50 CLK1 (nM)	IC50 CLK2 (nM)	IC50 DYRK1A (nM)
SPHINX31	5.9	282	623	>1000
Griffin 6	199 ± 36	5.6 ± 1.1	3.9 ± 0.6	1400 ± 283
Griffin 23	34 ± 7	10.4 ± 1.0	5.6	161.7 ± 24.6
Hippogriff 1	386.2 ± 83.4	7.4 ± 1.2	<0.5	13.5 ± 0.8

Table 4.1: Outline of Novel Splicing Kinase Inhibitor Used & IC50s.

To assess the therapeutic potential of the novel splicing kinase inhibitors DRG were isolated, dissociated and cultured as described previously. Following overnight incubation, neurons were treated with DMSO vehicle control (0.1%), 1nM of vincristine or a co-treatment of 1nM vincristine and one of the four splicing inhibitors listed. All splicing inhibitors were used at 1µM, 3µM, 5µM and 10µM. The IC_{50} values displayed in table 4.1 were derived from assays where only the test kinase and a substrate are present along with ATP and the inhibitor compound. Therefore these IC_{50}s do not take into account several factors that may affect the ability of the compound to inhibit the kinase within cells, such as active transport and permeability of the cell membrane. Therefore, to address this reduction in potency, concentrations were selected based on previous use of SPHINX31 in cell based assays and *in vivo* mouse models (Batson *et al.*, 2017). Additionally, due to improvements in dissection and culturing technique, experiments using Griffin 6 and Hippogriff 1 included additional concentrations of 0.1µM and 0.5µM due to increased neuronal yield. Neurons were incubated with treatments for 24 hours before being loaded with the Fluo-4 Direct Calcium Assay Dye and incubated for 60 minutes. Following incubation, the plates were placed in the plate reader and then stimulated with 1µM of capsaicin as previously described. Evoked fluorescence was then measured over a 120 second period.

4.2.4: Data Processing & Statistical Analyses

The primary output for the assays contained in this chapter was the measurement of evoked fluorescence following neuronal stimulation by capsaicin. As described, background and baseline fluorescence were recorded prior to stimulation and the F/F ratio was then calculated using post stimulation values divided by unstimulated baseline value. The workflow of how these ratios were processed and statistically analysed is described in detail in section 2.8.3. In brief, as the effects of stimulation were measured at 15 discrete timepoints across a 120 second period it was possible to convert the F/F ratios into a total area under the curve (AUC) value (Graphpad Prism version 7+8 for Windows, GraphPad Software, San Diego, California USA, www.graphpad.com). AUC values for each internal replicate were then exported to Microsoft Excel and the means for each treatment group were calculated. Percentage change from the maximal mean response was then calculated for each internal replicate. In novel splicing kinase inhibitor and jerantinine experiments, the

1nM vincristine only control was the maximal mean response used to calculate percentage change. In the capsaicin optimisation experiment, the mean value used was that of 1nM vincristine treated neurons stimulated with 1µM of capsaicin. These values therefore appear as 100% mean response on associated graphs. However, due to each individual AUC value being normalised to the mean response, SEM error bars are also displayed denoting variability in response between cultures and internal replicates. The HBSS vehicle control was used as the normalising value for 0% response in all experiments. Graphpad Prism was used for all statistical tests shown in figure legends. N numbers and information on internal replicates can be found in figure legends. All data are mean ± SEM unless otherwise stated.

4.3: Results

4.3.1: Vincristine treated neurons demonstrated significantly higher sensitisation in neurons than vehicle treated neurons

In order to optimise and create a robust model of chemotherapy induced neuronal sensitisation, it was first necessary to discern the experimental window where vincristine treatment would evoke the maximal sensitisation, compared to vehicle treated neurons given the same concentration of capsaicin stimulation.

Primary adult rat DRG neurons showed an increase in calcium response by the first reading at ~30s, which was maintained over the entire period of recording, irrespective of treatment (Fig. 4A). Responses to capsaicin in vehicle treated DRG neurons were significantly higher than the HBSS stimulation negative control responses, though no significant dose dependent increase in calcium influx was present across the 0.1µM-5µM capsaicin concentration range.

However, DRG neurons treated with 1nM vincristine for 24 hours showed a dose-dependent calcium response to the TRPV1 agonist capsaicin. Stimulation of vincristine treated neurons with 1μM capsaicin (41±4 ΔF/F•s) demonstrated significantly increased calcium influx compared to vincristine treated neurons stimulated with 0.1μM (20.5 ±6 ΔF/F•s) and 0.5μM (21 ± 4 ΔF/F•s) respectively (Fig 4B). Furthermore, vincristine-treated neurons stimulated with 1μM capsaicin showed a significantly larger calcium response than vehicle treated neurons subject to equal stimulation (41 ± 4 ∆F/F•s vincristine compared to 17 ± 3 ∆F/F• s vehicle treated neurons, Figure 4.1A&B). This represented the peak sensitisation in vincristine treated neurons as stimulation with 5μM of capsaicin resulted in a lower calcium influx and change in capsaicin evoked fluorescence, with a mean AUC value of 26 ± 5 ∆F/F•s (Fig 4B). This value was not significantly different from the evoked change in fluorescence and total response following 5μM capsaicin stimulation of untreated neurons (25 ± 3 ∆F/F•s). Similarly there was no significant difference in evoked fluorescence in vincristine treated and untreated neurons when stimulated with capsaicin below 1μM. These results therefore demonstrate that a 24 hour treatment with 1nM vincristine acutely sensitises neurons to stimulation with the TRPV1 agonist capsaicin, compared to untreated neurons and to vincristine treated neurons stimulated with capsaicin concentrations lower than 1μM.

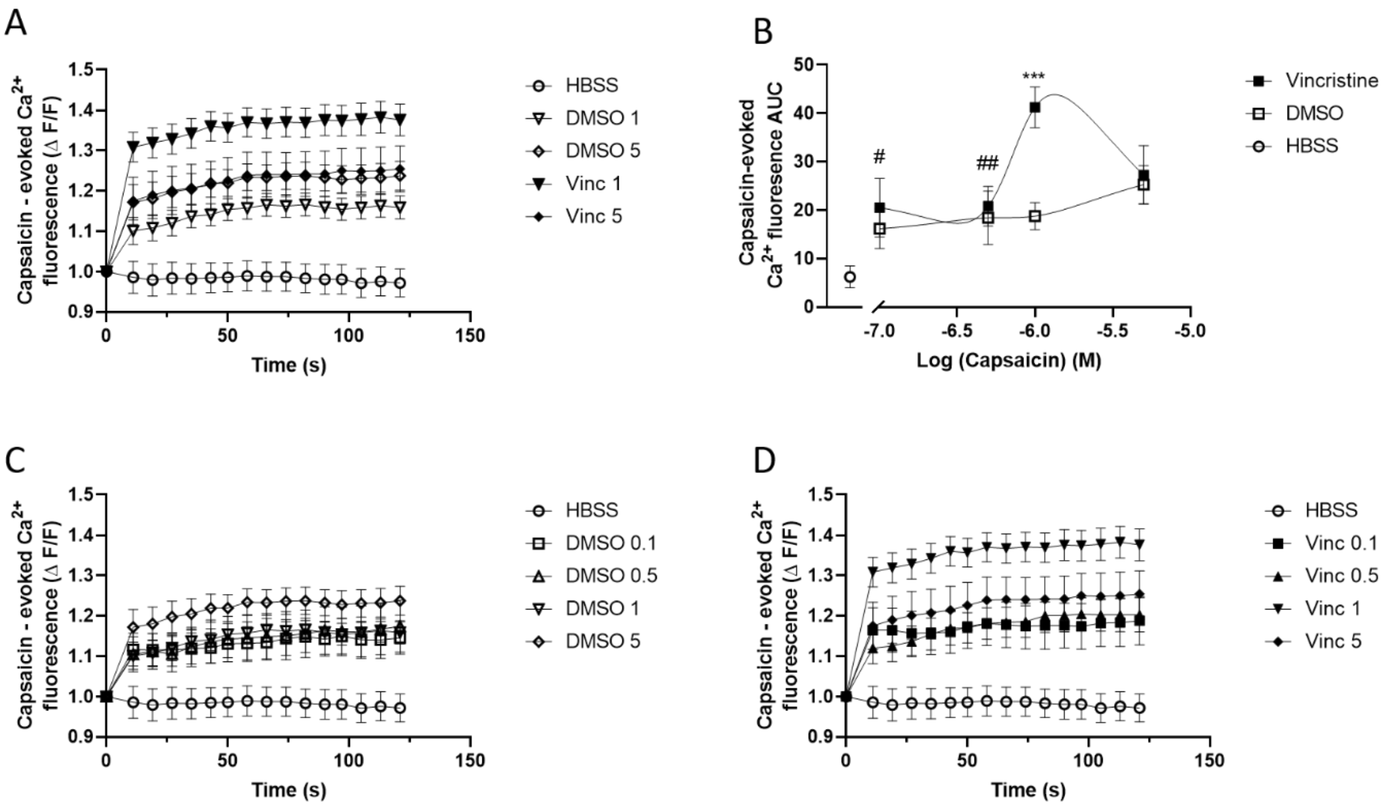

Figure 4.1: Capsaicin evoked fluorescence in vincristine treated and untreated DRG neurons

(A) Primary rat DRG neurons treated with vincristine or vehicle were stimulated with 0.1-5µM of the TRPV1 agonist capsaicin. Evoked calcium fluorescence was recorded over 120 seconds and divided over baseline fluorescence taken prior to stimulation to calculate F/F fold change with each well normalised to its baseline. Traces for 0.1-0.5µM are omitted for clarity. (B) Total response induced by capsaicin stimulation calculated from the F/F ratio denoting changes in calcium influx caused by differential concentrations of capsaicin. (C) Whole concentration range for vehicle treated neurons stimulated with 0.1-5µM capsaicin. (D) Whole concentration range for vincristine treated neurons stimulated with 0.1-5µM capsaicin. Data presented is from 3 rats with at least 3 internal replicates per plate, normalisation of data to individual baselines allowed pooling of data resulting in n=9-24 replicates per treatment. *** p= 0.0001, One Way ANOVA with Sidak's Multiple comparisons (Vinc 1µM Cap v DMSO 1µM Cap). # p = <0.02, ## p = 0.01 One Way ANOVA with Sidak's Multiple comparisons (Vinc 1µM v Vinc 0.1µM/Vinc 0.5µM).

4.3.2: Jerantinine did not sensitise neurons to the same extent as vincristine

To investigate the hypothesis that the novel indole alkaloid jerantinine would be less sensitising compared to vincristine, I treated neurons with both compounds independently for 24 hours and assessed them in the same assay. Neurons treated with 1nM vincristine (Figure 4.2a) exhibited the maximal response to capsaicin (1nM Vinc AUC 32.9 $\Delta F/F \cdot s$ ± 4.63 SEM). As noted in section 4.2.4, this value was then normalised as 100% response (± 12% SEM) and the value against which other values were compared against to calculate percentage change. Treatment with 0.1nM vincristine and 10nM vincristine resulted in a reduced level of sensitisation compared to 1nM vincristine treatment (0.1nM: 74% ± 16 SEM, 10nM: 65% ± 6 SEM). The response profile of jerantinine treated neurons (Figure 4.2b) differed from those treated with vincristine. Neurons treated with jerantinine did not exhibit the observed peak and subsequent desensitisation found in vincristine treated neurons across the concentration range used, indeed sensitisation in jerantinine treated neurons (125nM: 54% ± 10 SEM, 250nM: 58% ± 8 SEM, 500nM: 60 ± 7) was comparable with DMSO control (52% ± 8 SEM). There was a significantly lower in jerantinine induced sensitisation at all concentrations used compared to neurons treated with 1nM vincristine, however this effect was not observed when jerantinine treatments were compared to vincristine treatments at 0.1nM and 10nM.

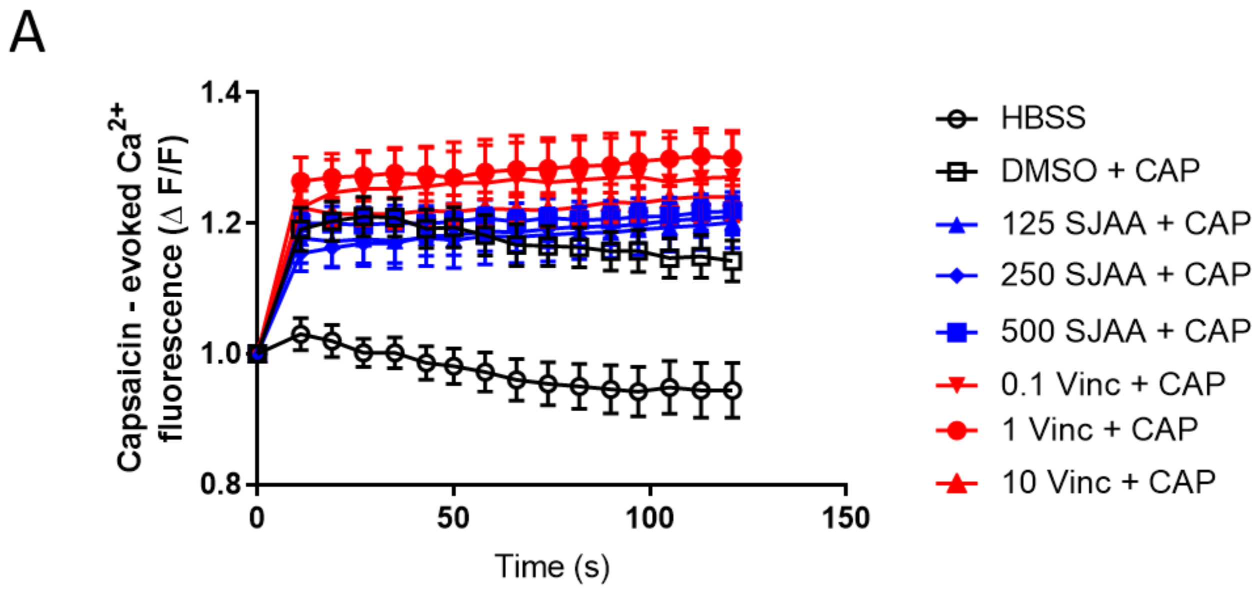

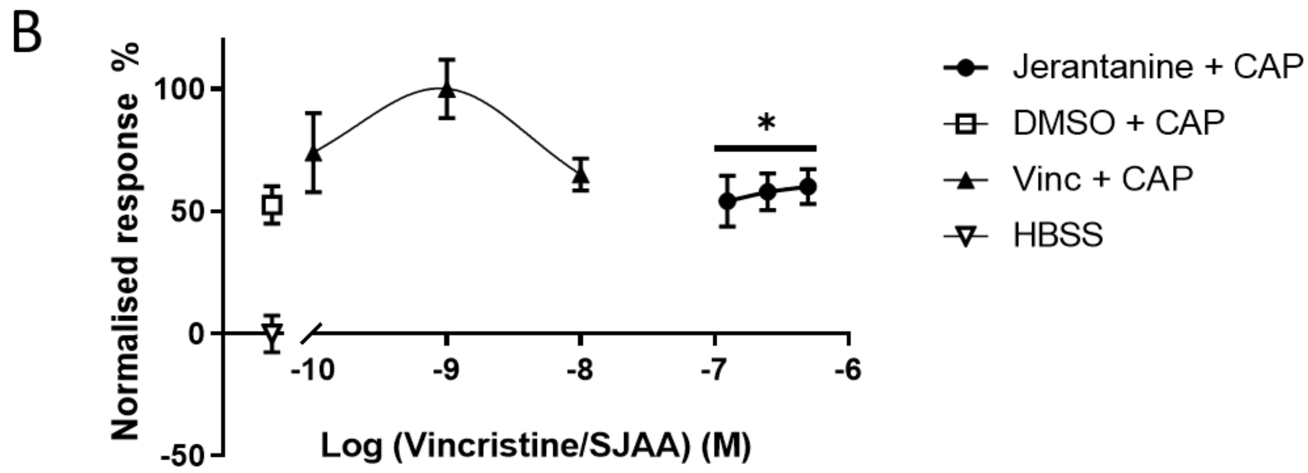

Figure 4.2: The effects of vincristine and jerantinine treatment on neuronal sensitisation

(A) Primary rat DRG neurons treated with vehicle, 0.1-10nM vincristine or 125-500nM jerantinine for 24 hours were stimulated with 1µM capsaicin. Evoked fluorescence was recorded over 120 seconds and divided over baselines fluorescence calculated prior to stimulation to calculate F/F ratio. (B) Total responses evoked by capsaicin calculated from F/F ratios were then used to calculate percentage change from the maximal response which was then normalised using HBSS response as 0% and maximal vincristine response as 100%. Data presented is from 4 rats with at least 4 internal replicates per plate. Normalisation of data allowed pooling of these replicates resulting in n=12-24 replicates per treatment. * p= <0.04 One Way ANOVA with Tukey's Multiple Comparisons (Vinc 1nM v Jerantinine 125-500nM) Data shown are mean ± SEM.

4.3.3.1: Co-treatment of vincristine treated neurons with the specific SRPK1 inhibitor SPHINX31 significantly reduces sensitisation

I next examined the potential of SPHINX31, a SPRK1 specific inhibitor to interrogate the hypothesis that inhibition of splicing kinases could be a novel therapeutic option for CIPN. Maximal sensitisation occurred as expected in the neurons treated with vincristine alone (Figure 4.3a). However this sensitisation was much reduced compared to previous experiments where 1nM vincristine was used both in optimisation protocols and in experiments probing jerantinine. Nonetheless, SPHINX31 co-treatment did significantly reduce sensitisation (Figure 4.3b) in a concentration dependent manner with an IC_{50} of 3.6µM. Maximal inhibition was achieved at the 5µM SPHINX31 concentration (5µM S31 2% of maximal response ± 17). Non-significant inhibition was also observed at 3µM SPHINX31 (55% of maximal response ± 16) and 1µM SPHINX 31 (77% of maximal response ± 14). Following maximal reduction in activity at 5µM there was then a moderate increase in sensitisation at the highest concentration used though this was not significantly different than any other SPHINX31 concentration being used. These results demonstrate that SPHINX31 has the potential to ameliorate vincristine induced sensitisation in a concentration dependent manner.

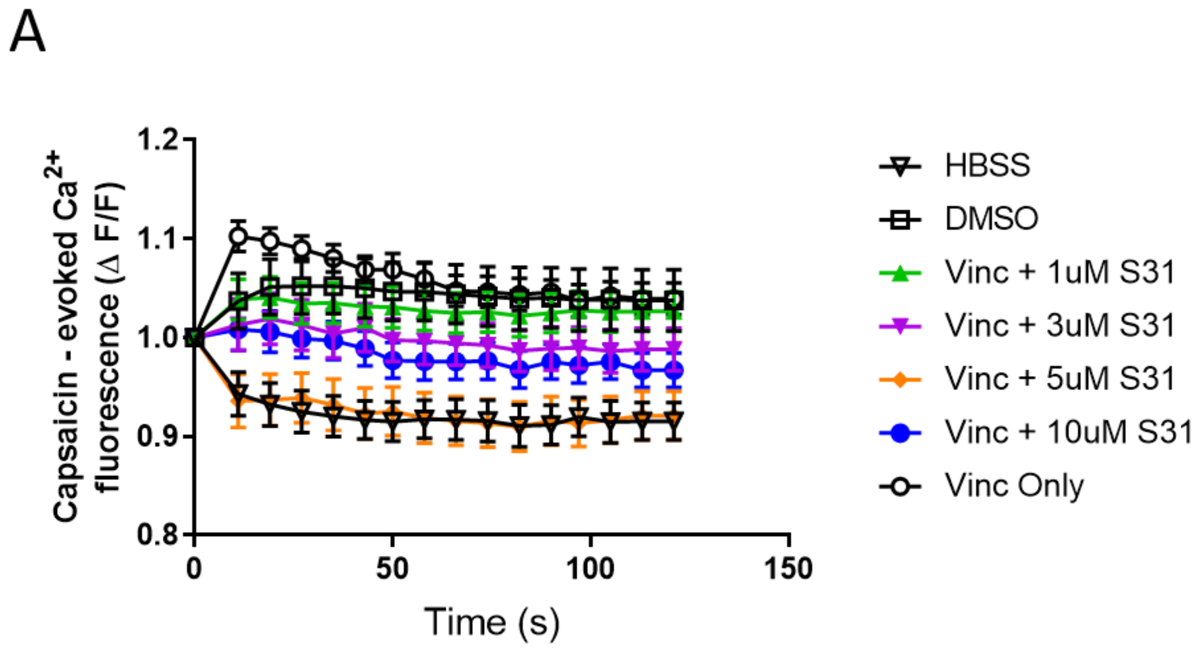

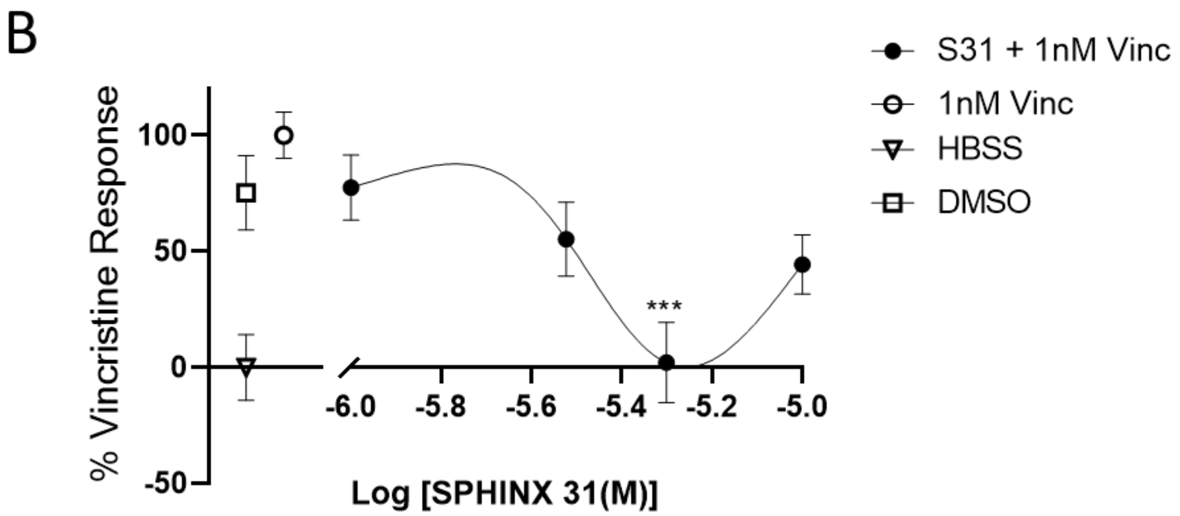

Figure 4.3: The inhibitory effects of SPHINX31 adjunct treatment on vincristine sensitised neurons

(A) Primary adult rat neurons treated with vehicle, 1nM vincristine alone or 1nM vincristine and 1-10µM of the SRPK1 specific inhibitor SPHINX31 for 24 hours were stimulated with 1µM capsaicin. Evoked fluorescence was then recorded over a 120 second period and divided by baseline fluorescence recorded prior to stimulation in order to calculate F/F ratio. (B) Total responses evoked by capsaicin were calculated from the F/F ratio and used to calculate percentage change from response in the vincristine only treatment group. This was normalised as 100% with HBSS capsaicin negative control normalised as 0% response. Data presented is from 4 rats with at least 4 internal replicates per plate resulting in n=16-17 per treatment when pooled following normalisation. *** p= 0.0004, One Way ANOVA with Dunnett's multiple comparisons to vincristine only response.

4.3.3.2: Co-treatment of vincristine treated neurons with the CLK1/SRPK1 inhibitor Griffin 23 significantly reduces neuronal sensitisation

The next compound tested was the dual CLK1/2 and SRPK1 inhibitor Griffin 23 which is more selective for CLK1 over SRPK1 and 16 fold more selective for CLKs than DYRK1A (Table 4.1). As previously, primary adult rat DRG neurons were dissociated and cultured and treated for 24 hours with 1nM vincristine alone or as a co-treatment with 1-10µM of Griffin 23, reflecting the potential use of the novel compound as an adjunct treatment to chemotherapy. As previously observed, maximal sensitisation occurred in neurons treated with vincristine alone (AUC 30.17 ΔF/F•s ± 7.495, Fig 4.4a) which was subsequently normalised to 100% response (± 23%). The response in co-treated neurons was variable (Fig 4.4b) with the lowest and highest concentrations of Griffin 23 culminating in significant inhibition of vincristine induced sensitisation compared to vincristine treatment alone (1µM G23: 62% ± 8, 10µM G23: 33.0 ± 9). The IC_{50} for Griffin 6 was 6.2µM. These values were comparable with the sensitisation observed in neurons treated with DMSO vehicle alone (DMSO: 46% ± 5.00). Indeed, in neurons treated with 10µM G23, sensitisation was below that observed in neurons treated with vehicle. At the intermediate 3µM and 5µM G23 concentrations, sensitisation was not reduced in a significant manner from the sensitisation of neurons treated with 1nM vincristine alone. Despite the heterogeneity of response observed in neurons treated with G23, these results demonstrate clearly that the compound does have the capacity to ameliorate chemotherapy induced sensitisation at 1µM before abolishing this sensitisation strongly at 10µM.

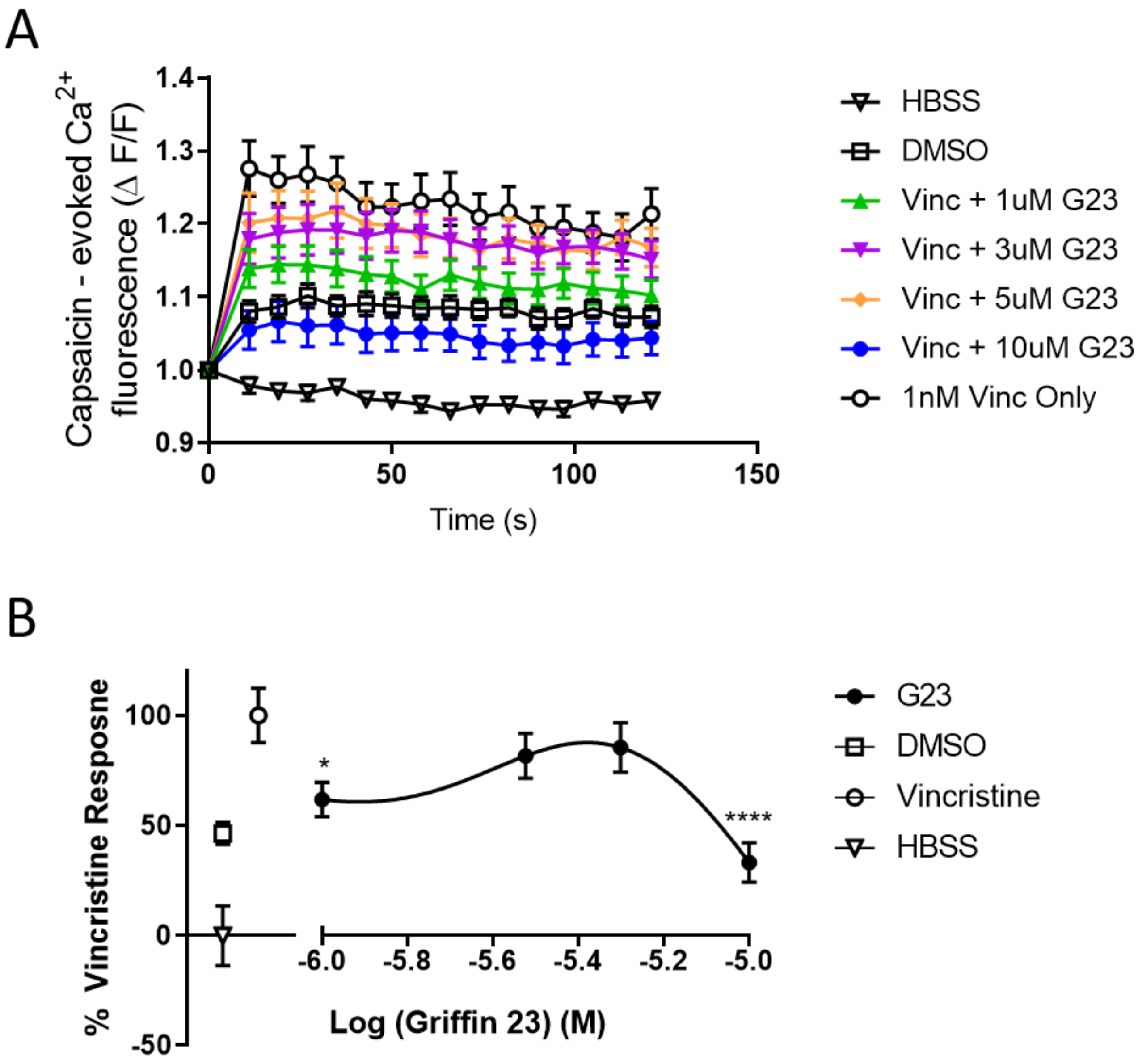

Figure 4.4: The inhibitory effects of Griffin 23 adjunct treatment on vincristine sensitised neurons.

(A) Primary adult rat DRG neurons treated with vehicle, 1nM vincristine alone or 1nM vincristine and 1-10µM of the CLK1/2/SRPK1 inhibitor Griffin 23 for 24 hours were stimulated by 1µM capsaicin. Evoked fluorescence was then recorded over a 120 second period and divided over baseline fluorescence recorded prior to capsaicin stimulation to calculate F/F ratio. (B) Total responses induced by capsaicin were calculated from the F/F ratio and used to calculate percentage change from the vincristine only response. This was then normalised as the 100% response and HBSS vehicle as 0% response. Data presented is from 5 rats with at least 3 internal replicates per plate resulting in n= 15-24 when pooled after normalisation. * p = < 0.03, **** p = <0.0001, One Way ANOVA with Dunnett's multiple comparisons to vincristine only response.

4.3.3.3: Co-treatment of vincristine treated neurons with the dual CLK1/CLK2 inhibitor Griffin 6 significantly reduces neuronal sensitisation

Following validation of Griffin 23 and SPHINX31 *in vitro* the next compound screened for anti-nociceptive properties driven by splicing kinase inhibition was the CLK family specific inhibitor Griffin 6. Griffin 6 has closely similar IC_{50}s for CLK1 and CLK2 as shown in table 4.1 and is significantly more selective for CLKs over SRPK1 and DYRK1A than Griffin 23. As previously observed, maximal sensitisation was observed in the vincristine only treatment group (1nM vincristine AUC 21.97 ΔF/F●S ± 4.85, Figure 4.5a) which was then defined as the 100% normalised response. In contrast to Griffin 23, the effect of Griffin 6 showed a bell-shaped response (Figure 4.5b) with the lowest (0.1µM) and the highest concentrations (5µM and 10µM) having a significant inhibitory effect on vincristine induced sensitisation. (0.1µM 28% of maximal response ± 7, 5µM 22% of maximal response ± 11, 10µM 39% of maximal response ± 14). Intermediate concentrations from 0.5µM-3µM had minimal effects on vincristine induced sensitisation with up to 85% of maximal response observed in neurons co-treated with 3µM. These results suggest that Griffin 6 does have potential to ameliorate chemotherapy induced sensitisation depending on concentration.

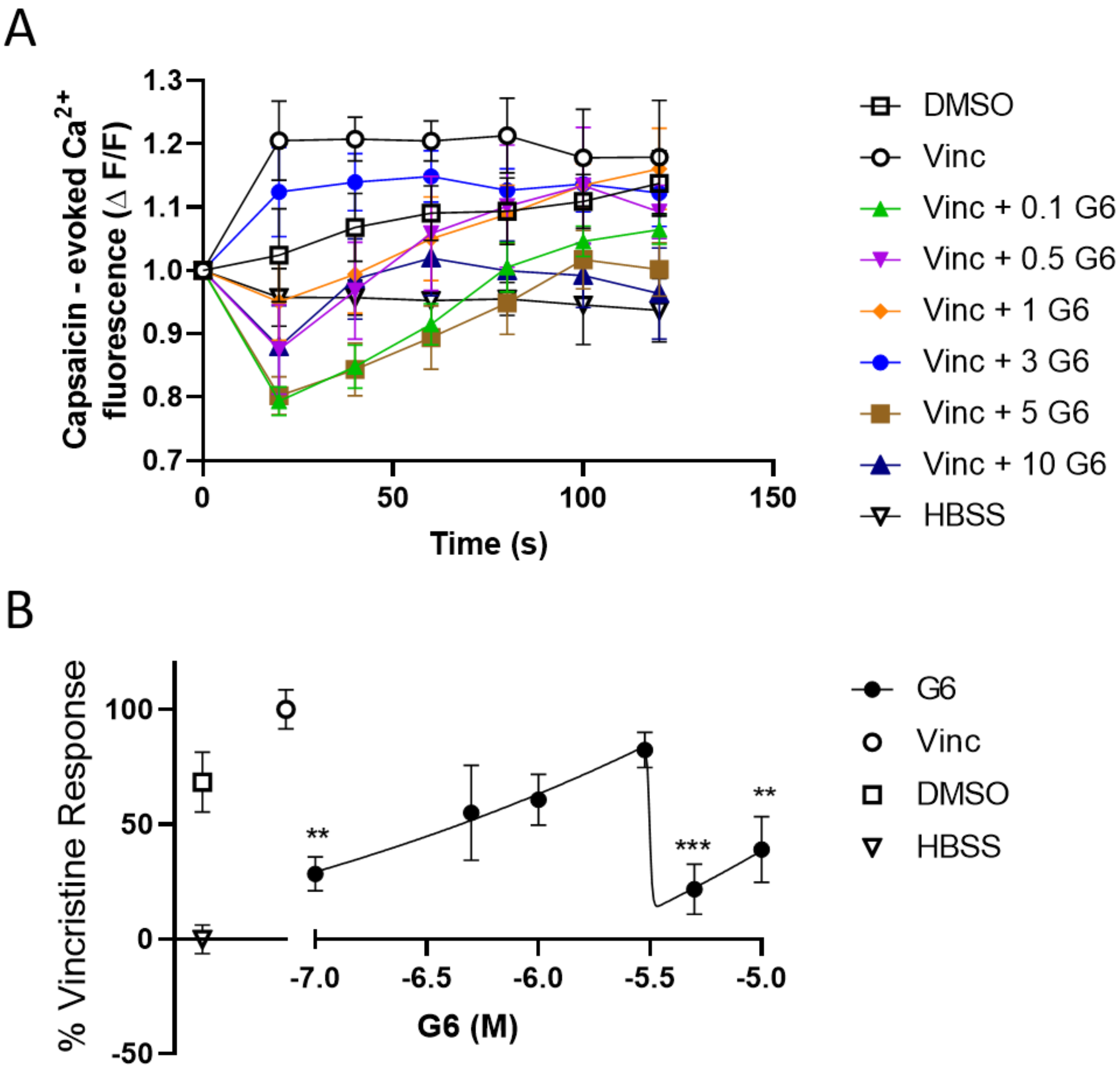

Figure 4.5: The inhibitory effects of Griffin 6 adjunct treatment on vincristine sensitised neurons.

A) Primary adult rat DRG neurons were treated with vehicle, 1nM vincristine alone or 1nM vincristine and 0.1µM-10µM of the CLK1/CLK2 inhibitor Griffin 6 for 24 hours and stimulated with 1µM capsaicin. Evoked fluorescence was then recorded over a 120 second period and divided by baseline fluorescence recorded prior to stimulation in order to calculated F/F ratio. (B) Total responses induced by capsaicin were calculated from F/F ratio and used to calculate percentage change from the response in the vincristine only treatment group which was normalised as 100% response, with HBSS negative control being normalised as 0% response. Data presented is from 3 rats with 3 internal replicates per plate resulting in n=9 when pooled following normalisation. ** p = <0.001, *** p = 0.0004. One Way ANOVA with Dunnett's multiple comparison to vincristine control response.

4.3.3.4: Co-treatment of vincristine treated neurons with the dual CLK1/DYRK1A inhibitor Hippogriff 1 significantly reduces neuronal sensitisation

The final compound assessed in the sensitisation assay was the dual kinase family inhibitor Hippogriff 1. Hippogriff1 is slightly more selective for CLK1 over DYRK1A, but is significantly more selective for these kinases than SRPK1. Neurons treated and sensitised with vincristine alone exhibited the largest capsaicin evoked response (Figure 4.6a), though this response (AUC 18.1 ΔF/F●s ± 5.5) was only marginally higher than the evoked response in neurons that were treated with DMSO vehicle only (AUC 14.1 ΔF/F ●s ± 4.6). The vincristine only response was normalised to 100% and the responses of vincristine and Hippogriff 1 co-treated neurons were then compared against this. The response profile of Hippogriff 1 co-treated neurons (Figure 4.6b) was similar to that observed in neurons co-treated with Griffin 6 with a bell shaped concentration response relationship. At the lowest concentration (0.1µM) and highest (5µM) concentrations Hippogriff 1 significantly inhibited vincristine induced sensitisation (0.1µM 34% ± 8 SEM; 5µM 27% ± 12 SEM). Intermediate concentrations and the highest concentration (10µM) had no significant effects (Figure 4.6B). It should be noted that due to time constraints and disruption caused by the COVID19 pandemic, data shown for Hippogriff 1 was pooled from fewer samples than those used to assess SPHINX31, Griffin 6 and Griffin 23, specific information on samples and replicates can be found in the appropriate figure legends.

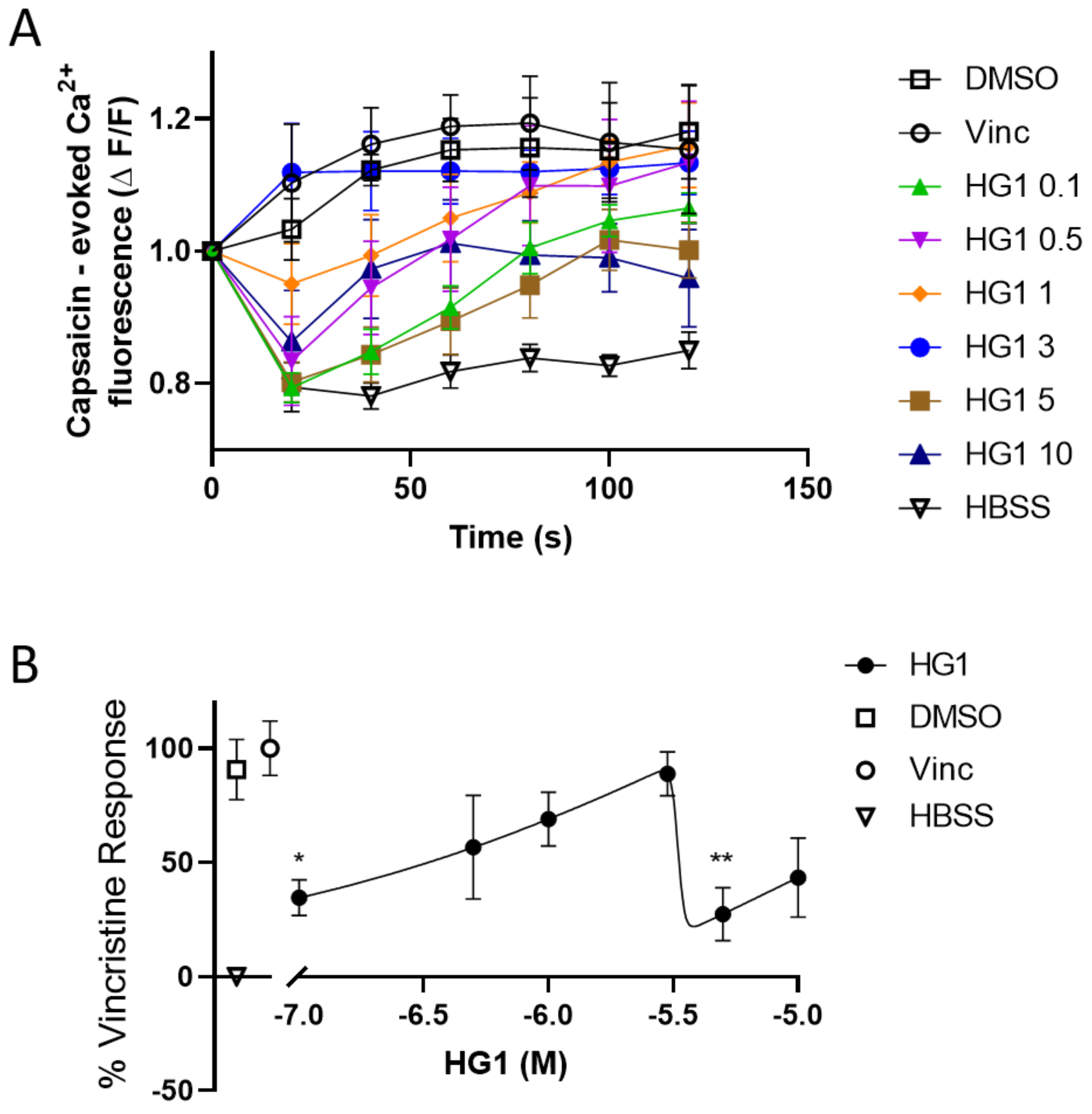

Figure 4.6: The inhibitory effects of Hippogriff 1 adjunct treatment on vincristine sensitised neurons.

A) Primary adult rat DRG neurons were treated with vehicle, 1nM vincristine alone or 1nM vincristine and 0.1µM-10µM of the CLK1/DYRK1A inhibitor Hippogriff 1 for 24 hours and stimulated with 1µM capsaicin. Evoked fluorescence was then recorded over a 120 second period and divided by baseline fluorescence recorded prior to stimulation in order to calculated F/F ratio. (B) Total responses induced by capsaicin were calculated from F/F ratio and used to calculate percentage change from the response in the vincristine only treatment group which was normalised as 100% response, with HBSS negative control being normalised as 0% response. Data presented is from 2 rats with 3 internal replicates per plate resulting in n=6 when pooled following normalisation. ** p = <0.007, * p = 0.02. One Way ANOVA with Dunnett's multiple comparison to vincristine control response.

4.3.4: Novel Splicing Kinase inhibitors reduce vincristine induced neuronal sensitisation, but effects vary depending on the compound used.

Of the 4 novel splicing kinase inhibitors used, only the SRPK1 specific inhibitor SPHINX31 reduced sensitisation in a concentration dependent manner up to 5µM (Fig 4.7A). The remaining compounds significantly reduced sensitisation at the lowest and highest concentrations used. Griffin 6 and Hippogriff 1 which both inhibit CLK1 and CLK2, but with the latter additionally inhibiting DYRK1A produced remarkably similar curves despite the inhibition of an extra kinase in the case of Hippogriff 1. A similarity between all compounds is the observation that intermediate concentrations did not produce significant reductions in neuronal sensitisation though it should be noted that 1µM of Griffin 23 (Fig 4.7b) was effective in significantly reducing sensitisation whereas this effect was lost at the same concentration in the two other CLK inhibiting compounds Griffin 6 (Fig 4.7c) and Hippogriff 1 (Fig 4.7c) which displayed significant inhibition below 1µM. Finally, Griffin 23 at the highest concentration used is the only compound that demonstrates a reduction in sensitisation compared to the second highest concentration used. For SPHINX31 and Hippogriff1 the significant reduction in sensitisation was lost at the highest concentration and whilst the effect of the highest concentration in Griffin 6 experiments was still significantly reduced compared to vincristine only treatments, there is still a mild increase in sensitisation in the highest concentration compared to the second highest concentration used.

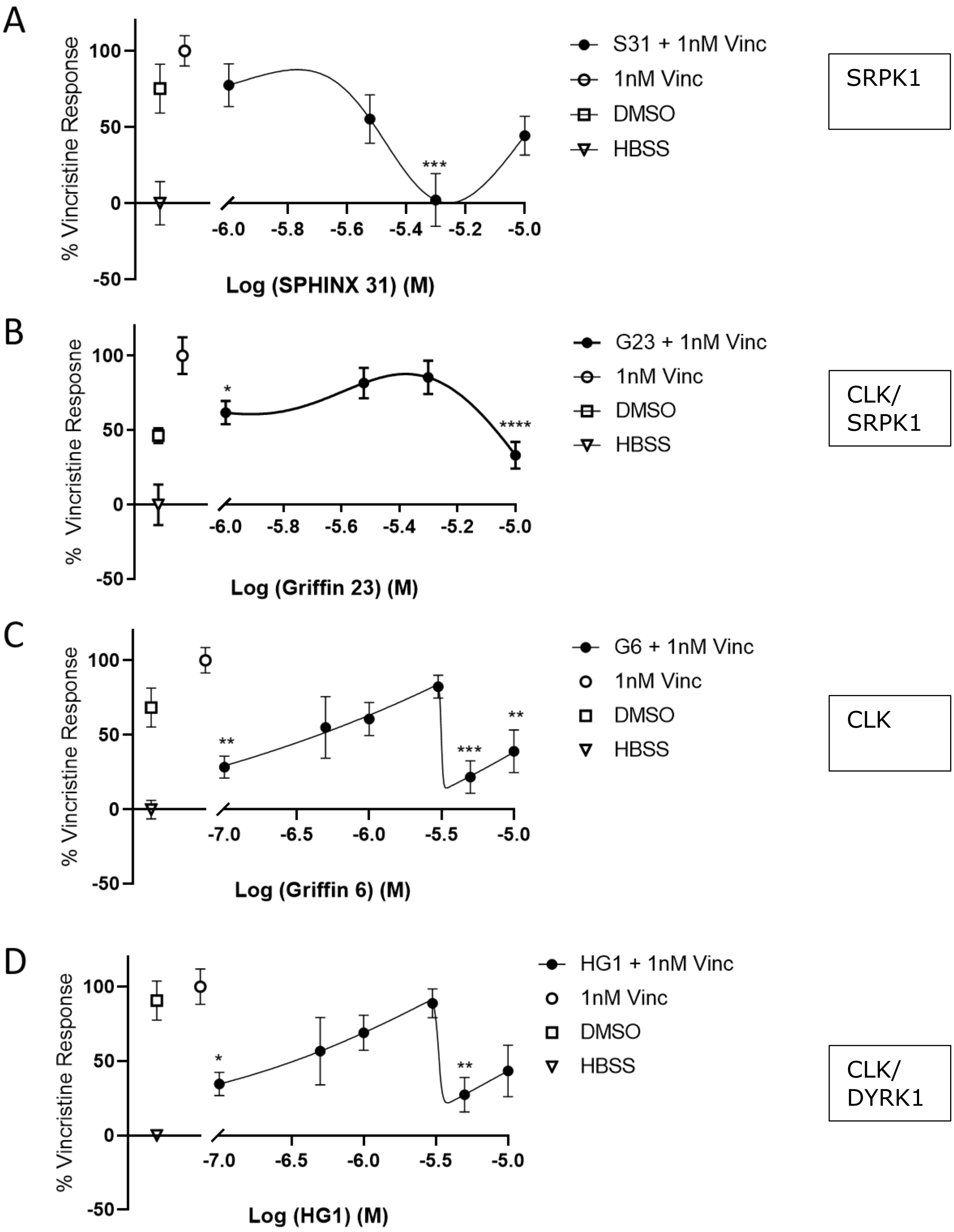

Figure 4.7: Novel Splicing Inhibitor effects on vincristine induced sensitisation

An overview of neuronal responses following treatment of primary neurons with vincristine alone or a co-treatment of vincristine and SPHINX31 (A), Griffin 23 (B) Griffin 6 (C) and Hippogriff (D) and subsequent stimulation with 1µM of capsaicin. All data shown are mean ± SEM. Individual statistical tests used and significance values are present in the figure legends in sections 4.3.3.1-4.3.3.4. n= 6-24 pooled replicates from at least 2 separate rat primary tissue preparations. Details for each compound are provided in relevant figure legends above.

4.4: Discussion

Firstly, I have demonstrated that the Fluo-4 direct calcium assay is a robust, sensitive and relatively high throughput tool with which to screen novel compounds and their potential to ameliorate chemotherapy induced sensitisation. Crucially, the results above have demonstrated that a common chemotherapy agent such as vincristine can have profound effects on neuronal sensitisation after relatively short term treatments. This provides evidence that pain mechanisms in CIPN may not be limited to the effects of long term exposure and neuronal damage often associated with sustained chemotherapy but can be triggered by acute treatment. This effect in vincristine has been further validated by comparative experiments with a proposed novel chemotherapy agent, the indole alkaloid jerantinine which demonstrated reduced sensitising capacity compared to vincristine. Finally, I used the sensitisation assay to screen 4 novel splicing kinase inhibitor compounds to assess their potential to block the observed sensitising effect vincristine had on primary neurons. In the case of all 4 compounds there was a significant reduction in observed sensitisation in neurons at some concentrations. Interestingly, the response pattern observed across these concentration ranges was often heterogeneous, with inhibition at the lowest or maximal concentrations used but no effect at intermediate concentrations indicating that patterns of inhibition may be related to the splicing kinase targeted and compound affinities for these kinase targets.

4.4.1: The ex-vivo nociceptor assay provides a robust tool with which to probe neuronal sensitisation

A principle aim and key hypothesis of the investigations within this chapter was the creation of a robust assay with which to investigate the hypothesis that vincristine could induce sensitisation in neurons acutely and in the absence of long term neuronal damage. I hypothesised that a relatively short term exposure of neurons to a relevant concentration of the vinca alkaloid vincristine would result in greater sensitisation of these neurons, manifested by elevated TRPV1 dependent calcium increases following stimulation with capsaicin. This hypothesis was made in consideration of previous data showing hyperglycaemia, another cause of TRPV1 sensitisation could induce acute sensitisation in dissociated neurons without associated long term damage (Bestall *et al.*, 2018). The results in section 4.3.1 demonstrate that neurons treated with 1nM vincristine exhibited significantly elevated responses compared to untreated neurons stimulated with the same capsaicin concentration. This indicates nociceptor sensitisation, thus providing a clear example of chemotherapy induced sensitisation that is independent of sustained exposure and long term neuronal damage as a result of long term chemotherapy treatment. This suggests that the onset of chemotherapy-induced enhanced nociception may occur before any neuronal damage by direct effects on neurons, and that by management of the mechanisms behind this sensitisation there is scope to alleviate earlier symptoms of the neuropathy.

However, the importance of optimising the concentration of the capsaicin stimulation used was also demonstrated. Stimulation above or below the 1µM capsaicin used to exhibit the sensitising effects of vincristine culminated in desensitisation of vincristine treated neurons in the former case and an inability to stimulate neurons adequately in the latter case. High concentrations of capsaicin, or more potent effects of capsaicin resulting from vincristine effects on TRPV1 function can lead to desensitisation of the TRPV1 receptor at lower capsaicin concentrations than under control conditions, which could potentially mask the full sensitising effects of chemotherapy on neuronal sensitisation (Smutzer and Devassy, 2016). Therefore optimisation must be carried out prior to using the Fluo-4 sensitisation model. TRPV1 desensitisation in response to strong acute stimulation (high concentration) or repeated stimulation at lower concentrations, so called tachyphylaxis. Tachyphylaxis is regularly cited within the literature as the mechanism by which capsaicin can invoke TRPV1 desensitisation (Tian *et al.*, 2019). Though not fully elaborated, acute TRPV1 desensitisation is mediated by post-translational changes to TRPV1 channels following acute stimulation that take place as a possible feedback mechanism to protect the nociceptive neuron via prevention a potentially toxic overload of calcium ions (Touska *et al.*, 2011). These changes are believed to be dependent on enzymes such calmodulin dependent serine-phosphatase which reverses the TRPV1 sensitising phosphorylation at serine 800 which is driven by PKC activation. Within the nociceptor assay, as capsaicin is only applied at a single point, the desensitisation of TRPV1 observed at 10µM capsaicin stimulation is likely to be driven by these mechanisms, which can decrease responses of TRPV1 within seconds of application. This dampened response is likely in response to the sensitisation of TRPV1 induced by the vincristine treatment and either direct or indirect activation of PKC leading to TRPV1 sensitivity. Previous work in the lab using the Fluo-4 sensitisation assay has shown similar TRPV1 desensitisation to higher capsaicin concentrations (Bestall, 2017). In that prior research, neurons maintained in high glucose conditions modelling diabetic neuropathy exhibited higher calcium influx than neurons maintained in basal conditions. This influx then reduced when neurons were stimulated with higher capsaicin concentrations. This is encouraging as it reinforces a growing body of evidence demonstrating similarities in the mechanisms by which both conditions result in acute pain and sensitisation other than that mainly driven by long term neuronal damage. Most importantly however, these results clearly demonstrate the Fluo-4 sensitisation assay is sensitive enough to detect changes in neuronal sensitisation caused by vincristine. This therefore provides a clear experimental window with which to probe the efficacy of novel compounds in dampening this proposed mechanism of acute pain in CIPN, therefore satisfying the aim of creating a robust assay as laid out in section 4.1.2.

4.4.2: Sensitisation induced by jerantinine was not as severe as that evoked by vincristine

Determining the extent and severity of any neuronal sensitisation or neurotoxic effects induced by novel chemotherapies such as the novel indole alkaloid jerantinine should be of paramount importance when developing novel chemotherapy agents. Off target toxicity and neuropathy are associated with reduced quality of life and poorer mental health outcomes (Ewertz, Qvortrup and Eckhoff, 2015). However, both historically and in contemporary drug development this screening does not occur or has been deemed an acceptable risk to increase chances of patient survival. Whilst refinement of drug provision has been in progress since the discovery of vincristine the compound is still intrinsically neurotoxic and associated with high incidence of CIPN. Therefore, moving forward novel drugs must at least match or retain the efficacy of traditional agents whilst aiming to reduce off-target effects such as neuronal sensitisation. Screening candidates in sensitisation screens such as the Fluo-4 direct assay could be of benefit to this end. Jerantinine has been shown to be effective against vincristine-resistant cancer cells at sub micro molar concentrations in colony formation assays and did not cause cytoskeletal changes in off-target neural stem cells, which occurred with vincristine treatment (Roper, 2019). I therefore hypothesised that jerantinine would not induce sensitisation in primary DRG neurons as severely as that induced by vincristine treatment when using jerantinine at concentrations derived from the aforementioned colony formation experiments.

At the concentrations used jerantinine induced less sensitisation than that induced by the 1nM vincristine treatment at least partially validating the hypothesis. However, there are several caveats to this finding. Firstly, vincristine treatment did not induce significant sensitisation at the 0.1nM or 10nM concentration with sensitisation comparable to both the DMSO vehicle control and the 125-500nM concentration range used for jerantinine. It is possible that 10nM vincristine treatment combined with 1µM stimulation with capsaicin recapitulated the TRPV1 desensitisation described in section 4.4.1. As demonstrated in that section, there is a bell shaped response to increasing capsaicin stimulation in neurons treated with 1nM vincristine. In combination with this, vincristine has been shown to directly sensitise TRPV1 *in vivo* via upregulation of TNF-α which then drives activation of PKC resulting in phosphorylation of TRPV1 at the serine 800 residue, thus sensitising the receptor (Wang *et al.*, 2018). Within the literature, this relationship between PKC activation and vincristine has been explored by use of tamoxifen as a PKC inhibitor. Tamoxifen was able to reverse vincristine induced peripheral neuropathy when applied with vincristine, possibly by reducing vincristine induced PKC activation and TRPV1 sensitivity (Tsubaki *et al.*, 2018). It is possible that treatment of neurons with 10nM vincristine caused a left-wards shift of this bell shaped response and that peak evoked activity in neurons treated with 10nM vincristine would be recorded at capsaicin concentrations below 1µM. S800 phosphorylation by PKC has been shown to increase TRPV1 sensitivity and lower response thresholds to both capsaicin and heat stimuli, underpinning this hypothesis (Por *et al.*, 2013).

Conversely, the 0.1nM vincristine concentration was likely not sufficient to sensitise TRPV1 to the same degree. The lower vincristine concentration in these experiments approximately 10 times more dilute than the average circulating dose recorded in patients following chemotherapy. Therefore this concentration may lack some physiological relevance to the patient context in which chemotherapy accumulates but does have utility both in establishing the bell shaped distribution of the vincristine sensitisation in addition to simulating the effects of lower circulating doses on neurons after a cycle. However, it important to therefore consider this bell shaped response in relation to any jerantinine induced sensitisation and the concentrations the novel compound was trialled at. As vincristine has been fully tested, validated and approved for human use for more than half a century, vincristine can be analysed for its sensitising properties at clinically relevant concentrations within *in vitro* assays both in terms of the dose at which it is deemed efficacious in treating patient tumours and the rate at which is clears from the body and how this effects the circulating concentration of vincristine that is responsible for inducing off-target effects. Equivalent clinical data for jerantinine does not exist, nor pre-clinical *in* vivo data. Therefore as mentioned concentrations were derived from the limited pre-clinical *in vitro* data generated by the Coyle Laboratory. Therefore, whilst it was encouraging that jerantinine did not appear to sensitise primary DRG neurons in a manner similar to 1nM vincristine treatment, it is possible the concentrations used are in reality at the lower end of the range for jerantinine usage and therefore it would be valuable to consider this experiment as more informative following the generation of *in vivo* data regarding the anti-tumour properties of jerantinine. It would also be immensely useful in future work to compare rodent nociceptive behaviour following treatment with both compounds. However, as the compound is not commercially available and synthesis reported as complex it would be difficult to produce sufficient jerantinine for *in vivo* studies in the immediate future. As an alternative, establishing the properties of jerantinine in terms of neuronal toxicity and neuronal damage markers such as neurite outgrowth would be much more feasible and would provide a useful comparison to a notoriously neurotoxic agent in the form of vincristine.

As previously described, whilst jerantinine is a microtubule inhibitor it binds primarily to the colchicine binding site on the microtubule as opposed to the vinca binding site occupied by vincristine (Smedley *et al.*, 2018). There is increasing evidence in the literature suggesting this alternative binding site promotes the ability of colchicine site binding drugs to overcome paclitaxel and vincristine-resistant sub-populations through common resistance pathways such as tubulin mutations and overexpression. Though jerantinine itself has not reached anything other than pre-clinical *in vitro* screens, several other drugs which share the colchicine binding site to microtubules are currently undergoing assessment as potential alternatives to traditional chemotherapy agents (Lu *et al.*, 2012). Among these drugs, there is a range of adverse effects relating to the nervous system, for example the estrogen metabolite 2-Methoxyestradiol (2-ME) induced neuropathy symptoms in 50% of patients examined, though whether this neuropathy manifested as pain or numbness was not defined (Matei *et al.*, 2009). Conversely indibulin, another colchicine binding site molecule had no observable neurotoxic effects in rodent models measuring nerve conduction velocity and rotor rod performance. However, these tests which are measures of co-ordination and neuronal damage do not take into account that sensitisation can occur independently of neuronal damage as demonstrated by the acute effect of vincristine. This provides a clear example of off target effects in chemotherapy development not being fully investigated (Kapoor, Srivastava and Panda, 2018). Despite this, Indibulin has been found to capable of discriminating between neuronal tubulin and nonneuronal tubulin due to post-translational modifications to neuronal tubulin. These modifications render the indibulin binding motif unable to access the colchicine binding site on the neuronal microtubule, depriving the ability of the molecule to depolymerise and disrupt neuronal microtubule dynamics.. This was shown to occur in tubulin polymerisation assays on SH-5YSY and PC12 cells with a disparity in tubulin inhibition shown pre and post differentiation of the cell line (Sawaguchi *et al.*, 2015; Kapoor, Srivastava and Panda, 2018). Whereas vincristine and paclitaxel had consistently inhibitory effects on neuronal tubulin polymerisation and depolymerisation respectively regardless of differentiation state. This is potentially a route of sensitisation and for the development of pain following use of these compounds. Evidence has shown blocking of microtubule dynamics and inhibition of axonal transport via vinca alkaloid application can result in c-fibre sensitivity without concomitant degeneration of the axon, or damage to the neuronal cell body (Dilley and Bove, 2008). Conversely indibulin was unable to inhibit differentiated SH-5YSY tubulin, resulting in no disruption to the microtubule dynamics of these cells. Therefore, to further corroborate the observed absence of significant sensitisation in jerantinine treated neurons, it would also be of great benefit to assess whether jerantinine can indeed target neuronal tubulin or whether post-translational modifications to neuronal tubulin would prevent its access to the colchicine binding site as observed in indibulin treatments. Investigations into the effects of jerantinine and neurite outgrowth, a readout for microtubule inhibition can be found in Chapter 5.

4.4.3.1: Novel compound inhibition of the SRPK1 and CLK splicing kinases prevents vincristine induced neuronal sensitisation

As hypothesised, I observed significant reduction in neuronal sensitisation induced by vincristine following SRPK1 inhibition with SPHINX31. In addition hypothesised inhibition of CLK1 and CLK2 with (Griffin 23) and without (Griffin 6) SRPK1 inhibition also reduced vincristine induced neuronal sensitisation. The SRPK1 splicing kinase, which as previously mentioned is responsible for the phosphorylation of SRSF1, drives nuclear localisation of the SR protein. When this process is inhibited, SRSF1 nuclear localisation does not occur (Harper and Bates, 2009). However, it has been shown that SRSF1 protein phosphorylated by SRPK1 can remain contained in so called “nuclear speckles”. It was originally thought that CLK1 would then additionally phosphorylate basally phosphorylated SRSF1 protein and release it from the speckles allowing full access to splicing machinery. However, Aubol et al. demonstrated that rather than act in discrete manner, with CLK1 activity directly dependent on SRPK1’s upstream actions on SRSF1 protein, it is actually the case that SRPK1 forms a complex with CLK1 that works synergistically within the nucleus to release “hypophosphorylated” SRSF1 and invoke alternative splicing events (Aubol *et al.*, 2016). It has also been shown that CLK1 is a much less efficient kinase than SRPK1 at inducing phosphorylation of SRSF1 protein when the kinases act independently and SRPK1 is the predominantly active kinase when the two form a complex. An overview of SRPK1/CLK1 interaction is shown in figure 4.8.Therefore, inhibition of one or both of these kinases at varying affinities is likely to have profound effects on downstream splicing events, such as those that govern the splicing of the VEGF isoform family.

SPHINX31 along with another SRPK1 inhibitor, SRPIN340 have previously been found to induce major changes to VEGF splicing in *in vivo* models of age related neovascular eye disease at micromolar concentrations preventing choroidal neovascularisation (CNV) (Gammons *et al.*, 2013; Batson *et al.*, 2017). CNV is a hallmark of age related “wet” macular degeneration (AMD). Furthermore, in neurons Hulse et al. demonstrated that alternatively spliced isoforms of VEGF had differential effects on sensitisation when administered as recombinant protein. VEGF-A_{165}a isoforms acutely sensitised neurons within 60 minutes of application and were responsible for generating ongoing activity in mechanosensitive nociceptors, co-application of recombinant VEGF-A_{165}b isoforms blocked this effect (Hulse *et al.*, 2014). Nerve injury is also associated with upregulation of VEGFR2 and expression of VEGF-A_{165}a in DRG neurons which lowered mechanical withdrawal thresholds. These changes were abolished in injured neurons by application of SRPIN340, demonstrating clear modulation of neuronal sensitisation post injury via a SRPK1-SRSF1-VEGF dependent mechanism. In section 4.3.3.1 I demonstrated that

SPHINX31 significantly reduced vincristine induced sensitivity to capsaicin in a concentration dependent manner. This effect was significant at a 5µM concentration, similar to that used in experiments by Blackley demonstrating VEGF-A_{165}b alternative splicing as a key component of SPHINX31's mechanism of action.

It is reasonable to hypothesise therefore that this influence on VEGF splicing is likely to be the principle mechanism behind SPHINX31 ameliorating the effects of vincristine treatment, given the use of an identical compound on the DRG neurons and stimulation of the same receptor, TRPV1 via application of capsaicin. TRPV1 is sensitised by PKC mediated phosphorylation following activation of the kinase. This activation of PKC can be triggered by multiple routes in neurons including as previously discussed by vincristine itself, either directly or by upregulation of mediators of inflammation such as TNF (Wang *et al.*, 2018). TNF has previously been shown to induce acute sensitisation in DRG neurons to capsaicin (Constantin *et al.*, 2008). Activation of PKC is also associated with activation of SRPK1 and downstream VEGF-A_{165}a expression (Harper and Bates, 2009; Hulse *et al.*, 2014). SPHINX31 may therefore be harnessing alternative VEGF splicing to target these mechanisms. For example VEGF-A_{165}b isoforms have been shown to significantly reduce TRPV1 phosphorylation at the serine 800 site in reducing sensitisation of TRPV1 (Bestall, 2017). This may be caused by VEGF-A_{165}b isoforms not activating PKC downstream of VEGFR2 binding as has previously been demonstrated in endothelial cells which contrasts with the canonical effects of the VEGF-A_{165}a isoform upon VEGFR2 binding following PKC activation of SRPK1. Therefore increasing the ratio of VEGF-A_{165}b isoforms via SPHINX31 treatment would reduce VEGFR2 mediated PKC activation and downstream TRPV1 sensitisation.

Alternatively, it is possible that SPHINX31's control of VEGF splicing ameliorated sensitisation via upstream targets of PKC activation. VEGF-A_{165}b has been previously blocked TNF driven expression of ICAM in retinal pigmented epithelium cells, ameliorating a pathway of inflammation within the eye (Thichanpiang *et al.*, 2014). A similar effect in neurons could diminish TNF mediated activation of PKC.

Nishida et al. demonstrated in an *in vivo* model of vincristine CIPN the release of the receptor for advanced glycation endproduct (RAGE) agonist High Mobility Group Protein B1 (HMGB1) into extracellular space following chemotherapy insult (Feldman *et al.*, 2012; Nishida *et al.*, 2016). Prophylactic dosing with a HMGB1 neutralising antibody prevented the onset of mechanical allodynia whereas therapeutic dosing was found to reverse observed neuropathy. There is also evidence demonstrating HMGB1 application to dissociated neurons similar to those used in above experiments results in sensitisation. VEGF-A_{165}b isoforms have been shown to prevent this HMGB1 induced sensitisation, this effect could be mediated by VEGF-A_{165}b isoform preventing HMGB1 binding to RAGE or by inhibition of downstream RAGE signalling (Bestall *et al.*, 2018). Interestingly, HMGB1 mRNA in neurons has been found to localise within axons rather than neuronal cell bodies and that after paclitaxel treatment this disparity in expression between the two sites widened further. It is speculated that axonal HMGB1 may be secreted in response to axonal insult and that this secreted HMGB1 may be acting in a paracrine manner on neurons as discussed above (Merianda *et al.*, 2015). Therefore, it is feasible that vincristine as an agent that targets axonal microtubules and can effect changes in axonal transport without associated long term damage, could in turn drive this secretion leading to acute neuronal sensitisation and that SPHINX31 blocks the effects of this secretion by preventing paracrine signalling.

In these experiments I also screened Griffin 23, a dual SRPK1 and CLK1/2 inhibitor and Griffin 6, which inhibits CLK1 and CLK2 only. As for SPHINX31, I hypothesised that adjunct treatment of vincristine treated neurons with Griffin 23 and Griffin 6 would attenuate the increased neuronal sensitisation exhibited by these cells. Following assessment in the Fluo-4 sensitisation assay I observed a heterogeneous concentration response following treatment with both compounds (Figure 4.7). Unlike SPHINX31 treatment, treatment with both Griffin compounds resulted in both the lowest and maximal concentration producing a significant reduction of vincristine induced neuronal sensitisation compared to vehicle. The uneven response across the concentration range provokes the need for further interrogation of the potential mechanism behind CLK1+CLK2/SRPK1 inhibition and reducing acute TRPV1 sensitisation. Information on the role of CLK kinases in the context of neuronal sensitisation is limited within the literature, however through exploration of the interactions between the SRPK1 and CLK kinases it is possible to examine the possible mechanisms underpinning the effects of the inhibitors. It is reasonable to suggest that Griffin 23 as an inhibitor of both SRPK1 and CLKs would have profound effects on this splicing complex that may manifest at differentially when used at lower and higher concentrations. Griffin 23 is preferentially selective for CLK1 and CLK2 over SRPK1 (Table 4.1). Therefore at lower concentrations Griffin 23 mediated inhibition of these kinases would likely manifest in the CLKs rather than SRPK1. In terms of the SRPK1/CLK complex, such inhibition would prevent the ability of CLK1 to release “hypophosphorylated” SRSF1 protein from nuclear speckles, preventing access to cellular splicing machinery and leading to downstream splicing events such as the expression of VEGF-A_{165}b and mediation of sensitisation via the putative VEGF mechanisms described. At the highest Griffin 23 concentration used, inhibition of both kinase classes will be less selective for the CLKs and there will not only sizeable inhibition of the CLK activity releasing primed SRSF1 protein from the speckles and reduced complex activity but also a reduction in cytoplasmic SRPK1 phosphorylation of SRSF1 leading to a reduced “priming” of SRSF1 protein that translocates into the nuclear speckles. Downstream of this, there will be subsequent reduction in CLK1-SRPK1 complex activity on sequestered SRSF1 protein and interaction with the spliceosome. This would further dampen the expression via alternative splicing of potentially nociceptive growth factors and proteins possibly including VEGF and culminate in reduced sensitisation of neurons.

Griffin 6 and Hippogriff 1 display similar properties to Griffin 23, although significant inhibition occurred following use of 0.1µM of both compounds compared to 1µM used in Griffin 23 experiments. Griffin 6 has two fold greater potency for CLK1 inhibition compared to Griffin 23. Similarly, Hippogriff 1 is 1.5x more potent for CLK1 than Griffin 23, therefore it was not surprising to see effects with these compounds at lower concentrations. Though it would be useful in future experiments to expand the range of Griffin 23 concentrations used to allow for comparisons at sub-micromolar concentrations, this was prevented by Griffin 23 experiments being conducted earlier and lower neuronal yield being acquired from dissection. Usage of both Griffin compounds and Hippogriff 1 did not replicate the concentration dependent inhibition of vincristine sensitisation observed following SPHINX31 treatment. Instead, intermediate concentrations were accompanied by increased responses to capsaicin stimulation compared to the lowest concentrations used. This was consistent across all 3 CLK inhibiting compounds (Figure 4.7b,c,d) irrespective of the secondary SRPK1 and DYRK1A targets of Griffin 23 and Hippogriff 1, which suggests this effect may be more likely due to CLK inhibition. CLK1 is known to be a key mediator in the aforementioned TGF-β signalling pathway where it phosphorylates SRSF6, an SR protein responsible for distal splice site selection of exon 8 of the *VEGFA* gene (Nowak *et al.*, 2008). This leads to expression of VEGF-A_{165}b and runs in parallel to the SRPK1-CLK- SRSF1 splicing axis. The overall balance of activity in these pathways is ultimately a key factor in VEGF splicing and isoform expression. If inhibition mediated by the novel compounds manifests through the SRPK1-CLK1 complex at low concentrations and then at intermediate concentration suppression the TGF-β pathway occurs this could potentially underpin the reduced efficacy of the compound inhibition of sensitisation as the VEGF-A_{165}b pathway is suppressed. With regard to Hippogriff 1 and the possible effects of DYK1A inhibition there is limited information in the literature regarding DRYK1a activity in neurons and possible influences of the kinase in the context of pain. The neuronal response to Hippogriff 1 treatment was very similar to that in Griffin 6 treated neurons. Hippogriff 1 inhibits CLKs with a similar potency to that of Griffin 6 so potential effects at low concentrations will be recapitulated in Hippogriff 1 treated neurons. Without a DYRK1A specific inhibitor, effectively the equivalent of SPHINX31 for SRPK1 it is difficult to identify the effects of DYRK1A inhibition would be on neuronal sensitisation. The stark similarity in response between Hippogriff 1 and Griffin 6 may suggest a possible redundancy of the DYRK1A kinase in ameliorating acute neuronal sensitisation. Nonetheless, there is some evidence of DYRK1A having a mediating role in the onset and maintenance pain. In a murine model of inflammatory arthritis, the DYKR1a/CLK2 inhibitor lorecivivint was found to reduce expression of inflammatory cytokines such as TNFα via inhibition of components of the WNT pathway such as SIRT1 (Deshmukh *et al.*, 2019). If DYRK1A inhibition could reduce potential inflammation induced by vincristine treatment this may provide a potential pathway which could reduce acute sensitisation, though further research and use of a DYRK1A specific inhibitor is needed to investigate this possibility further.

In addition to the mechanisms discussed above, it is also important to consider that the activity of these kinases is not limited to the splicing of VEGF. Even though the compounds used are highly specific inhibitors, the various substrates of the respective kinases will also be effected by their inhibition. For instance, other targets of SRSF1 include MYC and BIM, both proto-oncogenes, the tumour suppressors BIN1 and MKNK2 and other angiogenic actors such as TEAD1 and RON (Oltean *et al.*, 2012; Rowlinson *et al.*, 2015; Tzelepis *et al.*, 2018). Z Blackley demonstrated SPHINX31 mediated SRPK1-SRSF1 inhibition significantly reduced expression of MYC in 50B11 cells and similar effects have been shown in THP-1 leukaemia cell line. Though associated traditionally with pro-proliferative properties, in injured DRG neurons, MYC expression has been found to be enriched and associated with programmed neuronal cell death (Qin *et al.*, 2018). Though other studies have found MYC to be involved in the regeneration of axotomised sensory neurons which is more aligned with the traditional properties of the gene though how these factors would influence pain is unclear (Belin *et al.*, 2015). Other mediators of axonal regeneration, such as VEGF can be directly involved in nociception despite regenerative properties. *MKNK2*, a gene which encodes MNK2 a kinase responsible for the phosphorylation of eukaryotic initiation factor 4E (eIF4E) a translation activating factor. eIF4E when phosphorylated by MNK2 has been implicated in the control of DRG neuronal excitability and onset of CIPN. When SRSF1 is overexpressed and phosphorylated by SRPK1 it drives expression of the phosphorylative MNK2b isoform which in turn would exacerbate eIF4E activity (Amin *et al.*, 2011). SPHINX31 in theory therefore should be able to reverse this MNK expression to a MNK2a an isoform associated with a MAPK binding domain which is associated with regulated and reduced eIF4E phosphorylation. However, when examined in rat 50B11 neurons alternative splicing of MNK2 was not detected, preventing examination of this hypothesis (Blackley, 2019). This is believed to be caused by MNK2 not being alternatively spliced in rodents which differs from findings in humans, highlighting the need for tissue/species specific experiments where possible. To conclude, this list of alternative targets is not exhaustive, but the myriad targets of SRPK1, CLKs and DYK1a emphasises the need for thorough RNA Seq investigations into downstream targets effected by novel splicing kinase inhibitor treatment. These investigations would give a much wider indication of the full range of downstream splicing targets for the compounds and would enable better understanding of the proposed mechanisms involving VEGF or putative supplementary components of acute chemotherapy induced sensitisation.

4.4.4: Concluding Remark

I have developed and optimised an *in vitro* model to show that vincristine treatment with a physiologically relevant concentration of the compound acutely sensitises neurons within a 24 hour time period which is demonstrated by sensitisation of the TRPV1 receptor and increased calcium ion influx following capsaicin stimulation.

This may be due to the involvement of the activation of the PKC-TRPV1 pathway as previously observed in diabetic rats nociceptive behaviour and more recent *in vivo* studies demonstrating PKC dependency for pain onset. Furthermore I have shown this sensitisation can be ameliorated via adjunct application of novel splicing kinase inhibitors, which may be attenuating sensitisation by alteration of the isoform expression of genes concomitant with nociception such as VEGF. I have also compared for the first time, the neuronal effects of the novel indole alkaloid synthetic jerantinine to a traditional chemotherapy agent, vincristine. Jerantinine did not sensitise neurons as severely vincristine did at its peak activity, though sensitisation was similar below this level. Further pre-clinical *in vitro* and *in vivo* data is essential for the development of understanding this reduction in sensitisation following jerantinine treatment in addition to information on neuronal toxicity and damage. Further exploration into the neuroprotective properties of Griffin 6 and SPHINX31 in reversing the effects of vincristine can be found in Chapter 5.

5: Investigation into the Neuroprotective Properties of Novel Splicing Kinase Inhibitors

5.1.1 Neurite Dieback within CIPN

Chemotherapy Induced Peripheral Neuropathy (CIPN) is a complex pathology with myriad clinical and physiological manifestations (Wolf *et al.*, 2008). As one of the principle aims of chemotherapy is the sustained targeting and inhibition of rapidly dividing cells many agents are principally designed to inhibit the formation and activity of mitotic spindles during metaphase and thus inhibit the ability of a cancer cell to replicate (Jordan and Wilson, 2004). However, due to the non-specific nature of the effects chemotherapy exerts on cells, this also regularly results in the apoptosis of or critical damage to a variety of non-cancerous cells such as the various cell types of the immune system leading to detrimental effects such as severe immunosuppression in patients (Morrison, 2014).

Crucially, the principle target of many chemotherapy classes such as taxanes and vinca alkaloids is the structural protein beta-tubulin (Naaz *et al.*, 2019). Canonically, the two drug classes have subtly different mechanisms of action; taxanes primarily inhibit cell division by preventing the depolymerisation of microtubules. Microtubules are a key structural component of mitotic spindles which form during cell division (Meunier and Vernos, 2012). Taxanes bind to beta-tubulin sub-units and stabilise them within the microtubule and prevent their depolymerisation. This results in over-accumulation of microtubule mass during cell division at the metaphase/anaphase boundary and thus an interruption to regular microtubule dynamics during chromosome separation. As a result, dividing cells remain in G2/M cell cycle arrest and undergo apoptosis due to aberrant division (Bates and Eastman, 2017).

Conversely, vinca alkaloids prevent the formation of microtubule dimers, formed of alpha and beta subunit tubulin molecules via inhibition of the polymerisation of beta tubulin monomers. This decreases the available microtubule polymer mass and again results in erroneous microtubule dynamics, culminating in apoptosis of the dividing cell due to cell cycle arrest (Kerckhove *et al.*, 2017). An overview of how microtubule inhibitors operate within the cell cycle and mitosis can be seen in figure 5.1.

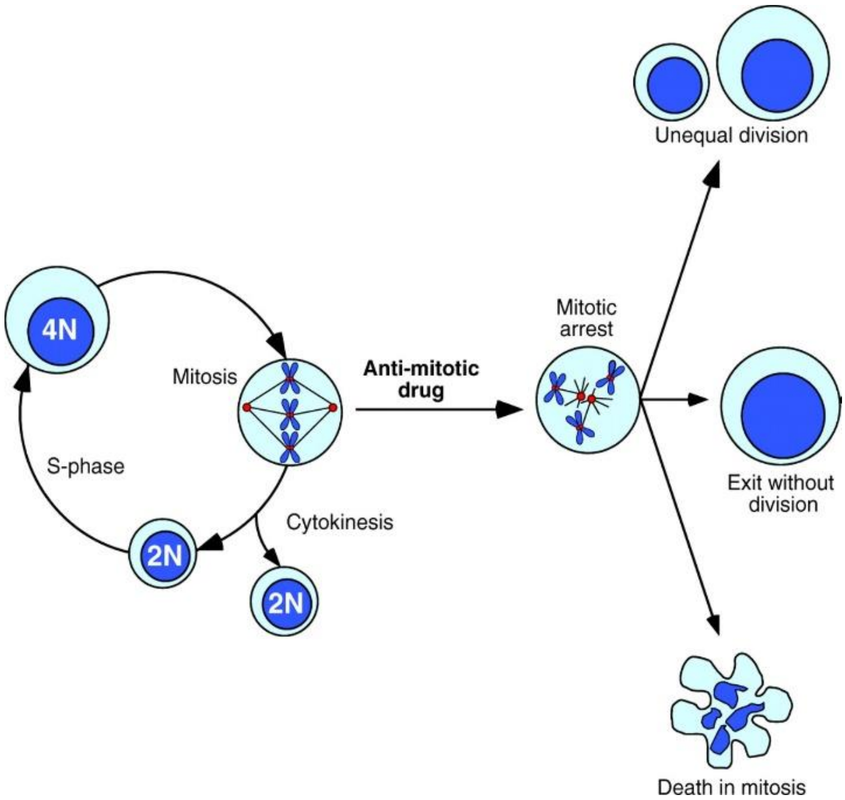

Figure 5.1: Schematic of vinca alkaloid and taxane microtubule inhibition induced cell death

Following transition from interphase, the microtubule network becomes activated during the metaphase of mitosis. In normal conditions, microtubules form mitotic spindles to separate chromosomes. Application of vinca alkaloids prevent formation of this assembly via depolymerisation of tubulin monomers whereas taxanes stabilise microtubule polymers preventing separation, leading to mitotic arrest. Mitotic arrest following inhibition of microtubules and alterations to microtubule dynamics results in apoptotic cell death within mitosis or erroneous division which is subsequently detected at the G1 cell cycle checkpoint. (Gascoigne and Taylor, 2009)

However, as previously mentioned these effects are not specific and systemic application of these compounds during chemotherapy treatment risks the burden of these effects being placed on non-target cells which include those undergoing normal cell division but also cells where tubulin is essential for structure and function. This includes the largely non-dividing cells of the peripheral and central nervous system (Zajaczkowską *et al.*, 2019). Within the PNS and the CNS neuronal tubulin exists in the form of the β-III tubulin isotype, one of 7 such isotypes known to be expressed within the human genome. Though also present within testis, β-III tubulin is widely considered to be a neuronal marker and is often used to distinguish between neurons and support cells such as glia in nervous tissue samples, such is specificity of the isotype (Guo, Walss-Bass and Ludueña, 2010). In addition to providing structural support via formation of a heterodimer with α-tubulin and assortment into cytoskeletal microtubules, β-III tubulin is a critical component of axonal growth, development and transport. The microtubule inhibiting properties of chemotherapeutic drugs can have profound effects on essential neuronal activity. Among these, chemotherapy induced-neurite dieback and axonal degeneration are among the most common pathological events observed in *in vitro* preclinical studies and this is subsequently reflected in patient nerve conduction velocity examinations indicative of longer term damage to myelin and the Schwann cells responsible for its production (Gordon-Weeks, 2004; Argyriou *et al.*, 2008; Ewertz, Qvortrup and Eckhoff, 2015). Interestingly, taxanes and vinca alkaloids appear to induce dedifferentiation of Schwann cells rather than outright cell death when used at clinically relevant concentrations in a pre-clinical rodent co-culture model with DRG neurons, though viability was decreased at higher concentrations. This contrasts with platinum-based compounds which failed to induce any changes to Schwann cell maturity, suggesting a heterogeneity of mechanism between microtubule inhibitors and drugs preventing DNA replication (Imai *et al.*, 2017). Both mechanisms have been shown to reduce myelin formation in these models detected by Quantitative sensory testing (QST), mirroring evidence of longer term fibre damage in patients. Via these methods, Dougherty et al. demonstrated that chronic vinca alkaloid pain in patients incorporated a sequential involvement of thickly myelinated Aβ fibres, followed by thinly myelinated Aδ fibres and eventually unmyelinated C-fibres. A similar study on chronic pain in taxane treated patients revealed similar findings in terms of A fibres, but an absence of C-fibre related pain (Dougherty *et al.*, 2007). However, neurological symptoms such as paraesthesia and tingling can occur following the first provision of chemotherapy therefore whilst these clinical techniques help to elucidate potential causes of long-term pain they do not explain why pain can occur in the absence of long-term damage following acute treatment.

In healthy neurite outgrowth and axonal development, microtubules provide the neurite with adequate scaffolding with which to develop in a proximal to distal fashion relative to the soma (Kapitein and Hoogenraad, 2015; Nirschl *et al.*, 2017). This ensures both anterograde and retrograde axonal transport is maintained allowing the movement of lipids, proteins and mitochondria to occur. However, this process is dynamic, with depolymerisation and polymerisation occurring in equilibrium to provide optimal structural support. Disruption of this process by reduction of microtubule mass or organisation by vinca alkaloids or by so called “bundling” induced by taxanes and over stabilisation has been purported to be a potential cause of neurite dieback and axonal degeneration in many *in vitro* and *in vivo* studies of chemotherapy induced peripheral neuropathy (Jordan and Wilson, 2004). Additionally, degeneration of neurites projecting from DRG neurons predominantly occurs in a distal to proximal pattern, with neurites retreating towards their cell bodies following application of chemotherapy (Fukuda et al., 2017). This strongly resembles “Wallerian Degeneration” (WD) observed in physical axon injury models. One of the key mediators of WD is SARM1 (sterile-alpha and toll interleukin-receptor [TIR] motif-containing protein 1) a highly conserved, pro-degenerative enzyme that has been described as the “central executioner” of the axonal degeneration process observed following injury and chemical insult (Gerdts *et al.*, 2016). Investigations into SARM1 loss of function or knockout have resulted in the rescuing of axons post crush injury and prevention of vincristine mediated degeneration *in vivo* (Geisler *et al.*, 2016; Tian *et al.*, 2020). Conversely, gain of function experiments have resulted in axonal degeneration of otherwise healthy neurons in the absence of physical or chemical insult (Loring and Thompson, 2020). Schwann cells are also targeted by SARM1 and the interaction between these cells is likely also to be a contributing factor towards longer term chemotherapy damage. However, in the short term the onset of pain is likely to be caused by a combination of factors. In terms of vincristine, *in vitro* application in compartmentalised chambers revealed axonal dieback only in the treated chamber that did not cross into the chamber containing the cell body nor the chamber containing the sister axon (Geisler *et al.*, 2019). If axonal transport deficit was the sole event in early dieback then these effects would have to be observed across the whole neuron. It is therefore more likely that damage to the most distal axon is likely the trigger for a cascade involving hypothesised pathways in Chapter 4, immune activation, inflammatory responses and changes to ion channel sensitivity that culminate in acute pain. Nonetheless, preventing damage to neurites either from long term application and eventual degeneration via Wallerian like mechanisms or preventing damage and activation of various sensitising pathways in the short term represents an attractive target for novel therapeutics.

Consequently, the fact that most established microtubule inhibitors are largely unable to distinguish between tubulin isotypes presents a fundamental challenge regarding their use as chemotherapeutic agents. However, since the discovery and synthesis of vincristine the 1960s, several semi-synthetic derivatives from the *Catharanthus roseus* have since been identified including vinorelbine which has demonstrable selectivity for mitotic tubulin over neuronal isotypes reducing the prevalence and severity of CIPN observed in patients (Stone and DeAngelis, 2016; Zhang, Yang and Guo, 2017). Unfortunately, vinorelbine is only approved for use in a limited set of cancer types compared to other members of the vinca alkaloid family and CIPN though less common does still occur, potentially via the mechanisms discussed in Chapter 4. Therefore, there is a pressing need to develop novel chemotherapy compounds that are as potent as older vincas, whilst retaining the specificity of microtubule inhibition demonstrated by vinorelbine. Jerantinine , the indole alkaloid tested in Chapter 4 has also demonstrated putative selectivity for mitotic tubulin with cytoskeletal damage to neural stem cells not observed at effective concentrations for treating cancer cells *in vitro* (Roper *et al.*, 2018). The compound has shown *in vitro* pre-clinical efficacy against lung, colon and breast cancer cells suggesting possible use against a wider spectrum of targets compared to vinorelbine (Raja *et al.*, 2014). Therefore, assessing the effects of Jerantinine on neurite outgrowth compared to vincristine *in vitro* would further bolster the encouraging results seen in Chapter 4 regarding its reduced sensitisation of neurons compared to vincristine and generate important pre-clinical data with regard to potential neurotoxicity.

In previous studies by Beazley-Long et al. application of alternatively spliced VEGF-A_{165} isoforms was found to be neuroprotective in hippocampal neurons following application of toxic concentrations of glutamate (Beazley-Long *et al.*, 2013). Furthermore, recombinant VEGF-A_{165}b application was found to reduce expression of the apoptosis marker caspase in DRG neurons isolated from rat and treated with oxaliplatin. Additionally, application of the isoform increased neurite outgrowth of these peripheral neurons suggesting both a neuroprotective and neurotrophic role for the isoform *in vitro* (Beazley-Long *et al.*, 2013). However, administration of recombinant proteins as therapeutics is limited by the need for routine administration, short plasma half-lives and antibody degradation (AlQahtani *et al.*, 2019). Therefore, use of the novel splicing kinase inhibitors could potentially be used to modulate splicing of these kinases such as SRPK1, CLK1/2 and DYRK1A in patients, recapitulating the observed *in vitro* neuroprotective effects. However, as many of the downstream mechanistic effects of splicing kinase inhibition remain unclear, it is essential to screen any novel compound capable of mediating alternative splicing in a physiologically relevant *in vitro* screen.

An obstacle to elucidating both the short-term effects of chemotherapy and the impact of longer term damage is the rarity of which biopsies are taken from patients with CIPN. Much of the aforementioned understanding has been ascertained via *in vivo* models using rodents and from a variety of *in vitro* screens using DRG explants, dissociated *ex vivo* neuronal cultures or from immortalised cell lines such as N2A or SH-SY5Y cells (Flatters *et al.,* 2017). These cells are derived from mouse and human neuroblastoma respectively and grow quickly, with large volumes of neuritic processes when differentiated (Haberberger *et al.,* 2020). In the case of both of these lines, the use of a single neuronal cell type is not reflective of the diverse nature of neuronal populations within the DRG and does not take into account the potential role of supportive cells such as glia in mediating the damaging effects of chemotherapy. Additionally, many DRG explant or single cell models utilise neonatal cultures due to the comparative ease of preparation and culture. Therefore effects of chemotherapy observed in treatment of these developing neurons may not be as physiologically relevant compared to an adult culture where neurons are terminally differentiated. It should also be noted that a lack of regenerative capacity in terminally differentiated neurons post axonal degeneration following the conclusion of treatment is proposed as a deleterious mechanism by which CIPN persists as exemplified Sahenk et al. in a study of taxol neuropathy, further exemplifying the advantage of using an adult rodent neurite outgrowth model (Sahenk *et al.*, 1994).

Thus, given the putative importance of neurite dieback and degeneration in CIPN, a physiologically relevant model with which to assess any novel therapeutic compounds is absolutely essential. Consequently, I have developed an adult rat DRG model of neurite dieback which is fully described in section 2.7 and the below sections including optimisation steps. With this model, I was able to investigate the potential neuroprotective benefits of novel splicing kinase inhibitors as an adjunct to chemotherapy treatment in addition to screening the novel chemotherapy agent jerantinine for the first time in a peripheral neuron model. Establishing this model via rigorous assessment of experimental parameters such as concentration of chemotherapeutic drug used, length of neurite regeneration period following dissection and length of chemotherapy treatment before imaging was fundamental in being able to thoroughly interrogate the below hypotheses.

5.1.2: Hypotheses & Aims

Hypotheses:

- SPHINX31 mediated SRPK1 inhibition protects against vincristine induced neurite dieback, but has no effect on neurite outgrowth as an independent treatment.
- Griffin 6 mediated CLK1 and CLK2 inhibition protects against vincristine induced neurite dieback but has no effect on neurite outgrowth as an independent treatment
- Hippogriff 1 mediated DYRK1A has no effect on neurite outgrowth as an independent treatment.
- Jerantinine will cause reduced neurite dieback compared to the traditional chemotherapy agent vincristine.

Aims:

- Establish an in vitro model of neurite outgrowth
- Demonstrate vincristine causes profound neurite dieback within the model
- Use the model to screen novel splicing kinase inhibitors and a novel chemotherapy agent for neuroprotection and reduced toxicity respectively.

5.2 Methods

5.2.1 Establishing a Neurite Outgrowth and Dieback Model

Primary adult rat DRG neurons were acquired following humane killing and DRG dissection under Schedule 1 of ASPA. Neurons were processed as described in section 2.2 and cultured. The first stage of optimisation was to determine an adequate length of time for neurites to regenerate and whether this would provide a viable experimental window. To do this, following overnight incubation neurons were cultured in DRG media (see section 2.2.2) containing 8ng/mL NGF to encourage outgrowth and 30µg/mL FdU to prevent glial mitosis and then incubated for 72, 96 or 120 hours before fixation and imaging. For these experiments, the rat was the experimental unit with the dissected neurons split evenly across the different incubation periods, 3 rats were used in total and each treatment had 6 well replicates. To account for variability in plating density each well was imaged in 3 different fields creating 18 internal replicates per treatment in the final analysis.

To mirror sensitisation experiments, vincristine was selected as the chemotherapy in the neurite outgrowth model. It was essential to optimise the concentration and duration of vincristine treatment within the assay. To test this, following 72 hours of incubation neurons were treated with DMSO vehicle control or 0.1, 1, 5, 10nM of vincristine for 72 hours to match time allowed for neurite outgrowth. The results of these optimisations resulted in the final experimental model described in section 2.7.

5.2.2 Drug Treatments to Ameliorate Neurite Dieback

After the establishment of a viable and versatile *in vitro* neurite outgrowth model, the potential of novel splicing kinase inhibitors in ameliorating chemotherapy induced neurite dieback could be assessed. In addition to assessing the reduced impact of the vincristine analogue, jerantinine on neurite dieback. The 3 novel splicing kinase inhibitors selected were SPHINX31, Griffin 6 and Hippogriff 1. These compounds target kinases that have been implicated in previous studies as potentially neuroprotective in studies of various physical and chemical insult. For information as to the targets for these novel compounds please consult Table 4.1 and their detailed description in section 1.4. Following standard neuron isolation and culturing procedures, neurons were incubated with 8ng/mL NGF and incubated for 72 hours in standard cell culture conditions. To test the effects of the novel splicing kinase inhibitors on neurite outgrowth and dieback independent of chemotherapy, neurons were treated with DMSO vehicle or 0.1-10µM of the novel splicing kinase inhibitors. To assess the efficacy of novel splicing kinase inhibitors in ameliorating chemotherapy induced dieback, neurons were treated with DMSO vehicle, 1nM vincristine or 0.1-10µM novel splicing kinase inhibitors in the presence of 1nM vincristine. Neurons with treatments were then incubated for 72 hours prior to fixation and immunocytochemistry protocols as described in section 2.7.2. Downstream analyses calculating mean neurite length per neuron were carried out following staining and imaging as described in sections 2.7.3 and 2.7.4 respectively.

For investigations into the comparative effects of the novel indole alkaloid jerantinine and vincristine on neurite dieback, neurons were isolated and cultured as previously described with NGF and mitotic inhibitors for 72 hours. Neurons were then treated with vehicle control, 0.1-10nM of vincristine or 125-500nM of synthetic jerantinine acetate-A (SJAA). The concentrations used for jerantinine treatments were taken from IC_{50} values derived from jerantinine use in various metabolic assays to determine the effects of the novel compound on cancer cells. Neurons with treatments were then incubated for 72 hours before fixation, staining, imaging and analysis.

5.2.3 Statistical Analyses

Following the image processing and mean neurite length per neuron calculations as described in section 2.7.4 all statistical analyses were carried out using GraphPad Prism V8. Specific statistical tests are denoted within figure legends, all error bars displayed are mean ± SEM unless otherwise stated. Relative size of scale bars are denoted within figure legends.

Drug	Target	Vehicle	Source
Vincristine	β Tubulin	DMSO	Sigma V8388
Jerantinine	β Tubulin	DMSO	UoN School of Pharmacy
SPHINX31	SRPK1	DMSO	Morris Lab, UNSW
Griffin 6	CLK1/CLK2	DMSO	Morris Lab, UNSW
Hippogriff 1	CLK1/CLK2/DYRK1	DMSO	Morris Lab, UNSW

Table 5.1: Drugs used in neurite outgrowth models

5.3 Results

5.3.1 Neurons Incubated for at least 72 Hours Exhibit Robust Neurite Outgrowth Post Isolation

Establishment of a versatile and viable experimental neurite outgrowth model was fundamental to assessing the potential of novel compounds in ameliorating chemotherapy induced neurite dieback. Following dissection and isolation, DRG neurons plated at a density of approximately 2,000 cells per well were incubated across 72, 96 and 120 hour intervals to determine optimal timescale for regrowth of neurites following axotomy. No significant difference was found in neurite outgrowth between neurons incubated for 72 hours and those incubated for longer periods (figure 5.3.1). As such, 72 hours incubation was deemed appropriate for use in the neurite outgrowth model to expedite workflow.

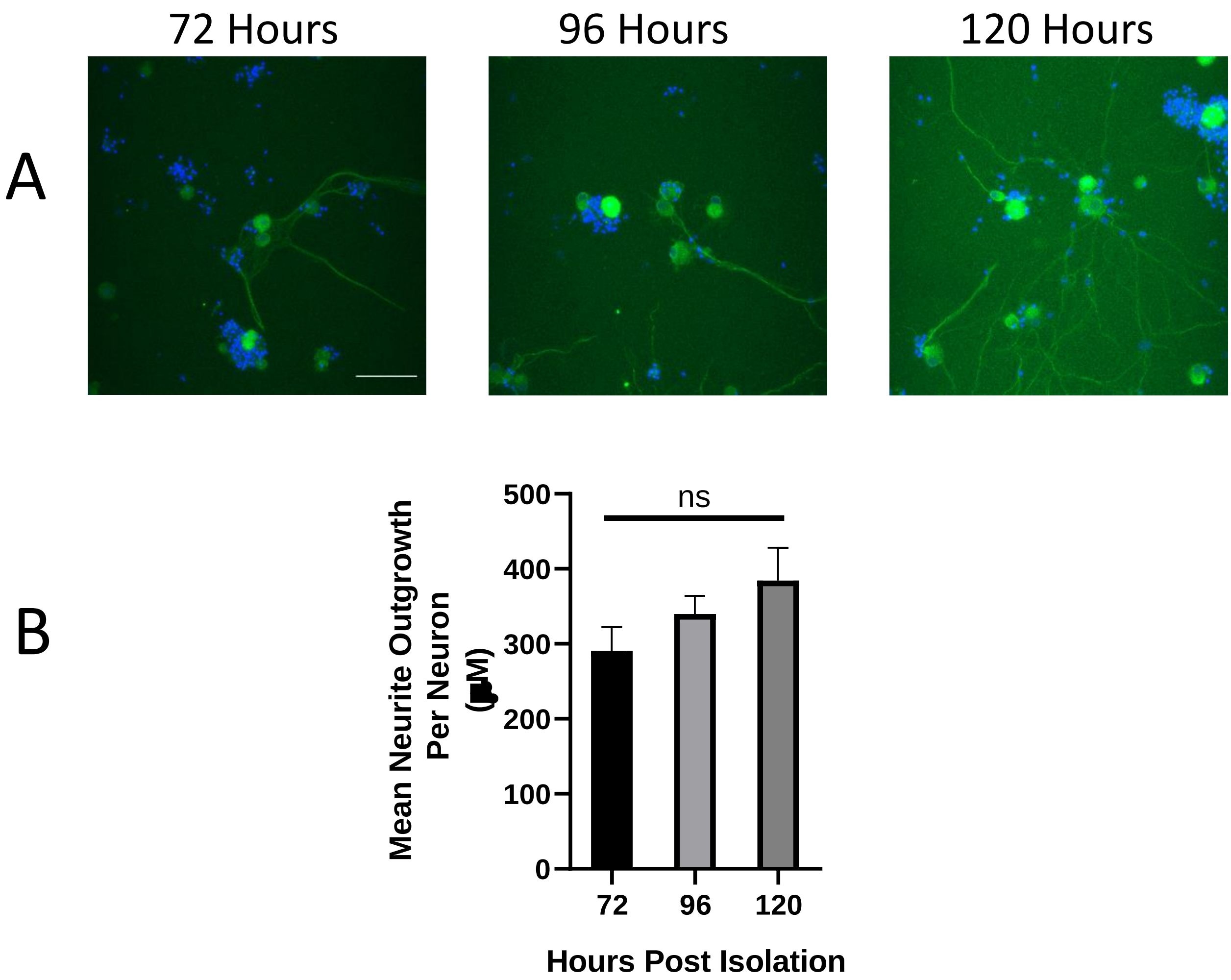

Figure 5.3.1 Primary DRG Neurite outgrowth post isolation

Representative images (A) of DRG neurons exhibiting robust neurite outgrowth 72-120 hours post incubation with NGF and FdU mitotic inhibitor. Neurons are stained with mouse anti β-III tubulin and Hoechst. Scale bar = 100µm. (B) When neurite outgrowth is normalised to the neurons count within a field of view, there was no significant difference in neurite outgrowth across all incubation periods. Data shown are mean ± SEM, n=3. Statistical test used: One Way ANOVA with Tukey's multiple comparisons test, p = > 0.05 for all comparisons and thus no statistical significance detected, 72 v 96, 72 v 120, 96 v 120.

5.3.2 Vincristine induces neurite dieback in a concentration dependent manner

To establish the optimal concentration of chemotherapy to be used in the neurite dieback models, neurons were isolated, cultured and incubated for 72 hours to establish neurite outgrowth as denoted in section 5.3.1. Neurons were then treated with 0.1-10nM of the vinca alkaloid vincristine and incubated for a further 72 hours. At all concentrations, vincristine induced significant neurite dieback compared to DMSO control. This effect was also exhibited in a concentration dependent manner. Outgrowth was reduced from a mean of 294.6µm ±51.4µm per neuron in DMSO controls to a mean of 144.5µm ±30.54µm when treated with the minimal concentration of vincristine. This dieback was exacerbated further at the maximal concentration with neurons treated with 10nM vincristine exhibiting a mean neurite outgrowth of just 80.4µm per neuron as seen in figure 5.3.2.

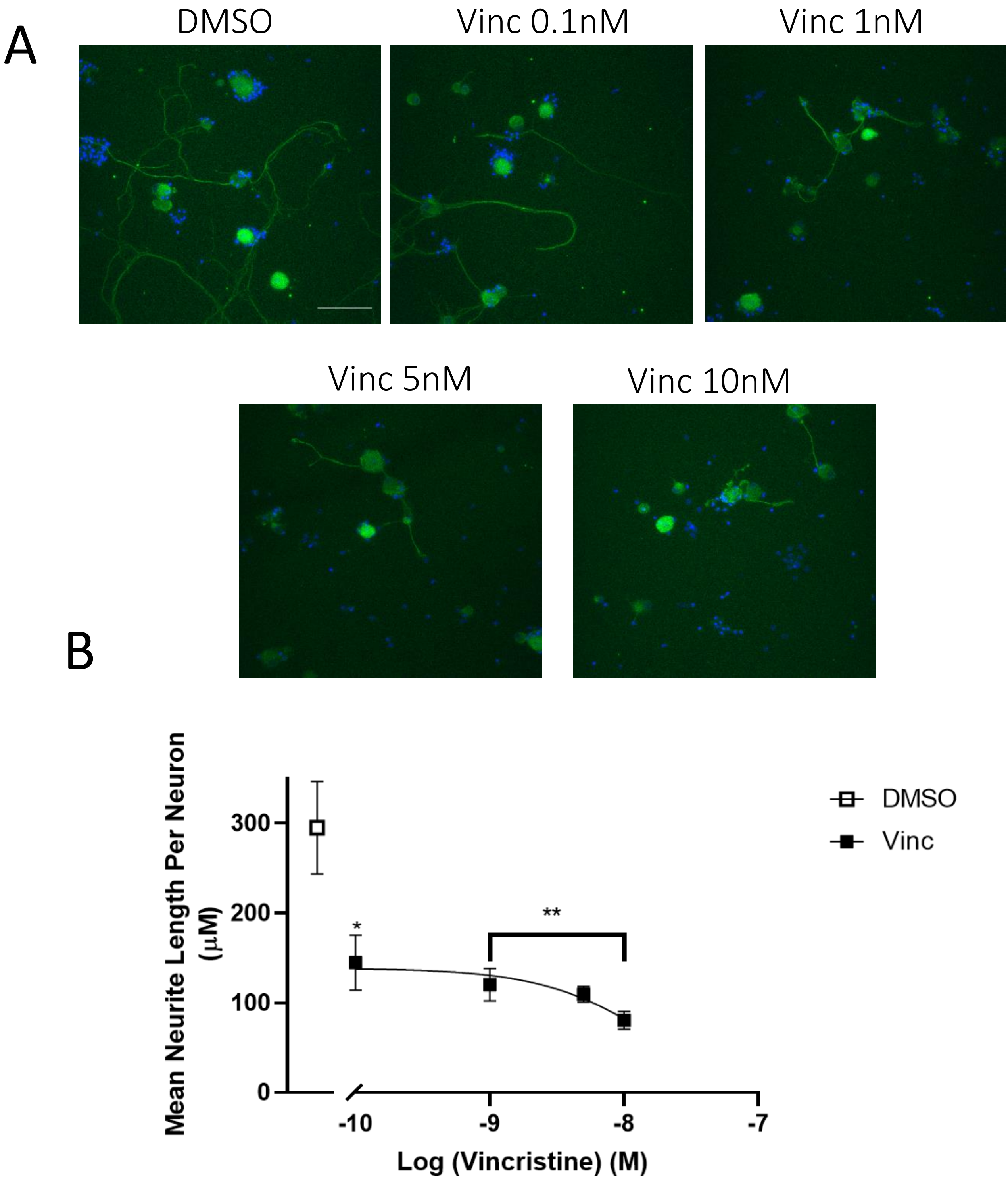

Figure 5.3.2 The noxious effects of vincristine on DRG neurite outgrowth

Representative images (A) of primary adult rat DRG neurons following treatment with 0.1-10nM of the vinca alkaloid vincristine for 72 hours. Neurons are stained with mouse anti-β-III tubulin and Hoechst. Scale bar = 100µm. (B) Vincristine treatment for 72 hours significantly reduces mean neurite outgrowth at all concentrations (IC50 = 1.75nM) in a concentration dependent manner compared to vehicle. Data shown are mean ± SEM. N=3 biological repeats per treatment group. Statistical test used: One Way ANOVA with Dunnett's multiple comparison to vehicle control. * p= <0.05, ** p= <0.01.

5.3.3.1 SPHINX31 has no effect on neurite outgrowth independent of chemotherapy

To test whether SPHINX31 would induce changes in neurite outgrowth independent of chemotherapy, primary DRG neurons incubated for 72 hours post isolation were treated with 0.1-20µM of SPHINX31 and incubated for a further 72 hours with the novel compound. SPHINX31 neither significantly reduced nor increased mean neurite outgrowth per neurons compared to DMSO vehicle at any concentration. (Fig 5.3.3.1) Outgrowth was consistent across all concentrations other than 20µM which exhibited a reduced outgrowth comparative to other concentrations though this difference was non-significant. These data confirm that treatment of isolated DRG neurons with SPHINX31 independent of chemotherapy induces no significant changes in neurite outgrowth and thus any dieback observed in neurite outgrowth in chemotherapy co-treatments are not induced by novel compounds in a synergistic fashion.

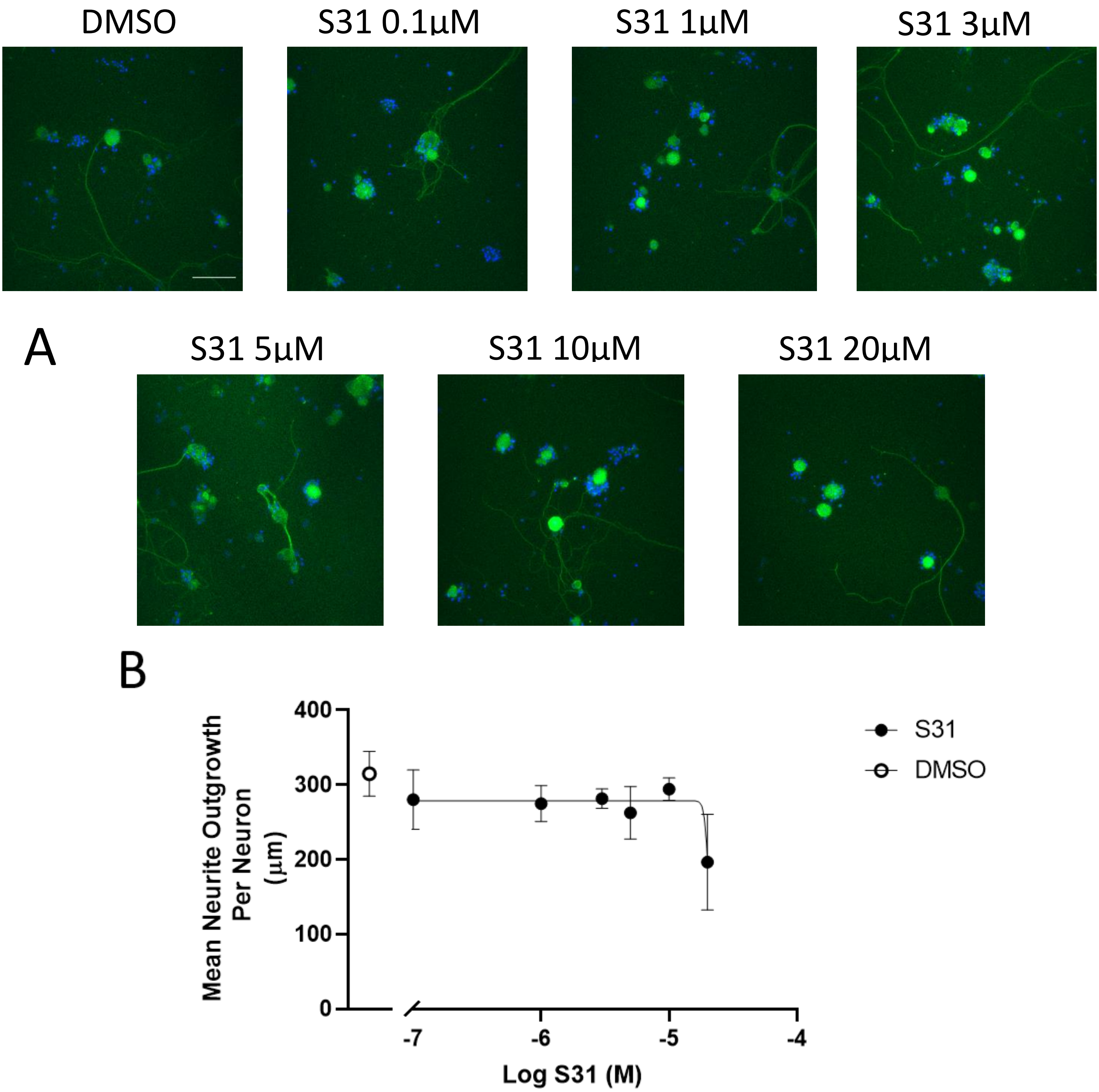

Figure 5.3.3.1 DRG Neurons Display Robust Neurite Outgrowth Following SPHINX31 Treatment

Representative images (A) of rat primary DRG neurons treated SPHINX31 for 72 hours. All treatment groups display robust neurite outgrowth that is comparative to that of vehicle. Neurons are stained with mouse antiβ-III tubulin and Hoechst. Scale bar = 100µm. (B) Concentration response curve for SPHINX31 treatment, no statistical difference was detected between treatment groups and vehicle control. N=3, statistical test used One Way ANOVA with Dunnett's Multiple comparisons.

5.3.3.2 SPHINX31 Significantly Ameliorated Vincristine Induced Neurite Dieback in a 72 hour co-treatment

To assess the potential of SPHINX31 as an adjunct therapeutic to ameliorate the deleterious adverse effects of vincristine, primary rat DRG neurons were co-treated with 10nM vincristine and a range of SPHINX31 concentrations. Following treatment with 10nM vincristine all groups exhibited significant neurite dieback compared to vehicle control which exhibited a mean neurite outgrowth per neuron of 546.5µm ± 88.9µm. Treatment with vincristine alone resulted in mean neurite outgrowth per neuron of 75.79µm, a reduction of approximately of 87% from vehicle. However, despite significant neurite dieback and reduction in neurite outgrowth compared to vehicle, SPHINX31 co-treatment with vincristine resulted in higher neurite outgrowth compared to vincristine treatment alone at all concentrations of SPHINX31. These increases were significant in the 0.1µM and 0.5µM SPHINX31 co-treatment groups which had mean neurite outgrowth per neuron of 178.4µm ± 22.11 and 184.4µm ± 20.22 respectively representing a 20% increase in neurite outgrowth as a percentage of vehicle compared to vincristine alone. These data demonstrate that SPHINX31 confers a degree of neuroprotection at low concentrations when used as an adjunct to vincristine (Figure 5.3.3.2).

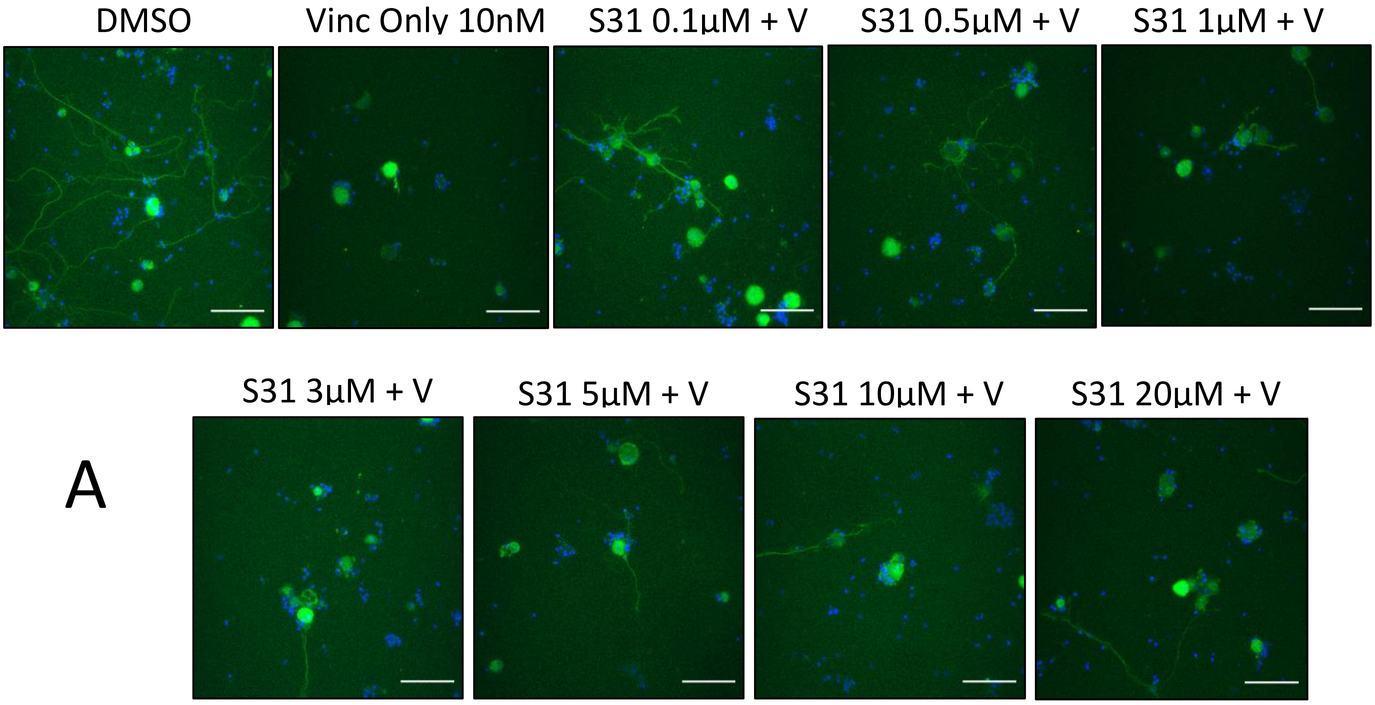

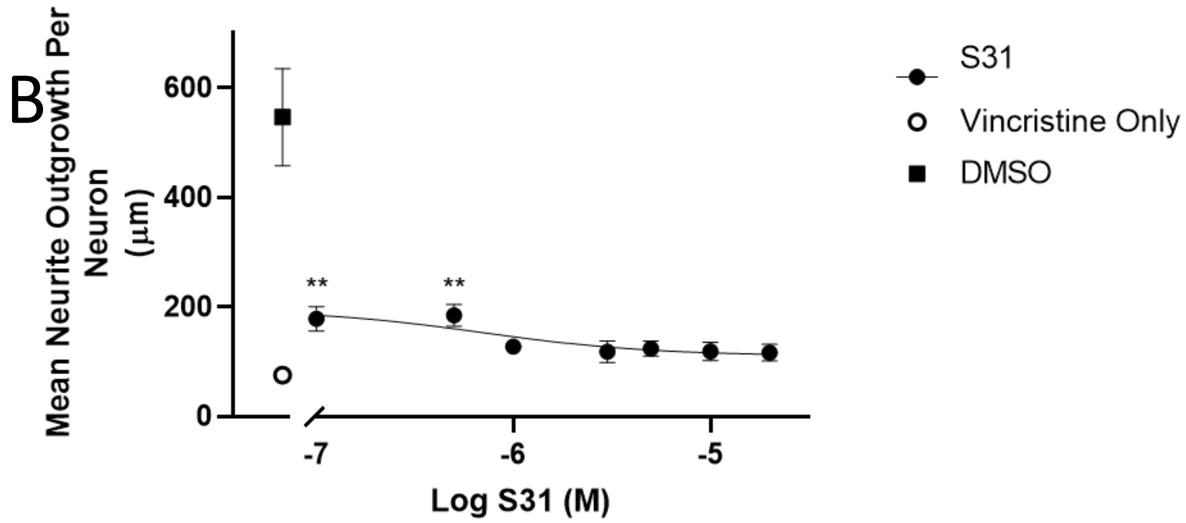

Figure 5.3.3.2 The effect of SPHINX31/Vincristine co-treatment on neurite outgrowth
Representative images (A) of primary rat DRG neurons treated with 10nM vincristine or co-treated with vincristine and 0.1-20µM SPHINX31. All SPHINX31 treated groups display outgrowth greater than that of vincristine alone, but significantly reduced from vehicle control. Outgrowth in 0.1µM and 0.5µM SPHINX31 treatments was significantly higher than vincristine alone. DRG neurons were stained with mouse anti-βIII tubulin and Hoechst. Scale bar = 100µm. (B) Concentration response curve for S31/vincristine co-treatments displaying significant increases in neurite outgrowth at low SPHINX31 concentrations. N=3, statistical test used: One Way ANOVA with Dunnett's Multiple Comparison to vincristine control. ** p= <0.003. Values without error bars were too small to display.

5.3.4.1 Griffin 6 has no effect on neurite outgrowth independent of chemotherapy

To test whether the CLK1/2 inhibitor Griffin 6 would induce changes in neurite outgrowth independent of chemotherapy primary rat DRG neurons were treated for 72 hours with 0.1-10µM of the novel compound. This treatment period followed the same 72 hour period to accommodate neurite outgrowth post isolation as previously described. Griffin 6 treatment neither significantly reduced nor increased neurite outgrowth following 72 hour incubation at all concentrations (Fig 5.3.4.1a). In a similar fashion to SPHINX31 the highest concentration in Griffin 6 exhibited a mild reduction in outgrowth though this was rendered statistically insignificant. These data demonstrate that Griffin 6 treatment of DRG neurons has no effect on neurite outgrowth independent of chemotherapy. Thus any changes in neurite outgrowth observed within the model can be attributed to the presence of vincristine within the co-treatments and neurite dieback is not being mediated by Griffin 6 in a synergistic fashion along with the chemotherapy.

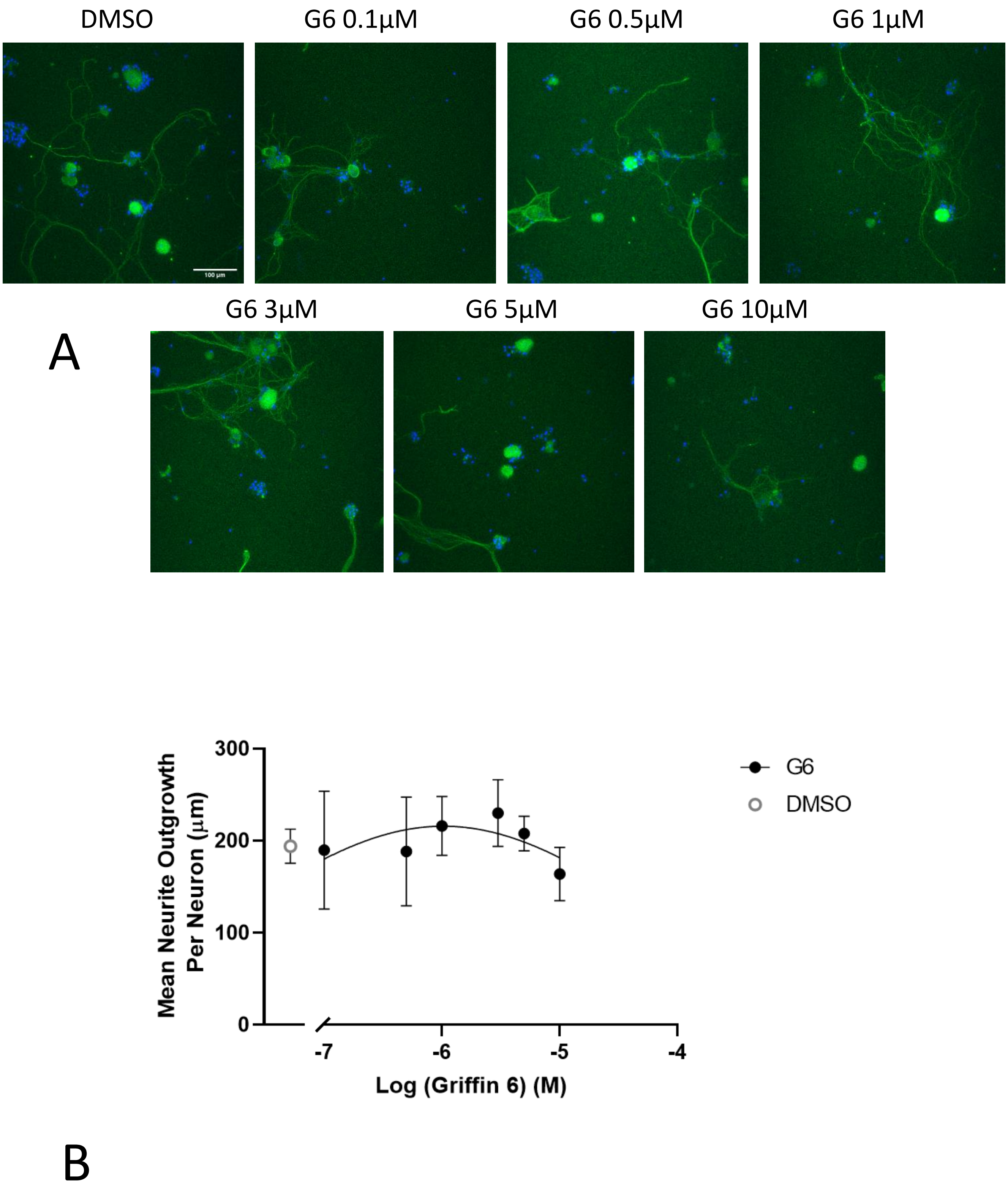

Figure 5.3.4.1 DRG Neurons display robust neurite outgrowth following 72 hour Griffin 6 treatment independent of chemotherapy.

Representative images (A) of primary rat DRG neurons treated with 0.1-10µM of Griffin 6 for 72 hours. All treatment groups display robust neurite outgrowth that is comparative to vehicle control. Neurons are stained with mouse anti βIII tubulin and Hoechst. Scale bar = 100µm. (B) Concentration response curve for Griffin 6 and mean neurite outgrowth per neuron. No statistical difference was detected in any treatment group compared to vehicle. N=3, Statistical test used: One Way ANOVA with Dunnett's multiple comparisons compared to control.

5.3.4.2 Griffin 6 significantly ameliorated vincristine induced neurite dieback in a 72 hour co-treatment

To assess the potential efficacy of Griffin 6 in ameliorating vincristine induced neurite dieback primary rat DRG neurons were treated with 10nM vincristine or a co-treatment of vincristine and 0.1-10µM of Griffin 6 for 72 hours. Following treatment with vincristine all groups exhibited significantly reduced growth compared to that of DMSO vehicle. Vehicle control treated neurons exhibited a mean neurite outgrowth per neuron of 241µm ± 25.99µm SEM. Neurons treated with vincristine alone exhibited a mean neurite outgrowth of 50.13µm ± 6.7µm SEM, approximately 20% of the mean outgrowth in vehicle treated neurons. However, co-treatment of neurons with Griffin 6 revealed some significant increases in neurite outgrowth per neurons compared to vincristine alone. In Griffin 6 co-treatments at 0.1µM and 0.5µM, mean neurite outgrowth per neuron was 108.7µm ± 13.14µm SEM and 117 ± 13.87µm SEM respectively. This represents a significant increase in outgrowth compared to vincristine alone with the groups displaying approximately 45% and 48% of vehicle outgrowth. These data did not however replicate the properties in conferring protection to neurites at all concentrations. At 10µM Griffin 6 co-treatments mean neurite outgrowth per neuron was lower than vincristine treated neurons alone. (41.64µm ± 1.9µm SEM) However, these data confirm that Griffin 6 confers moderate neuroprotection to chemotherapy treated neurons when applied as an adjunct treatment at low concentrations. (Fig 5.3.4.2)

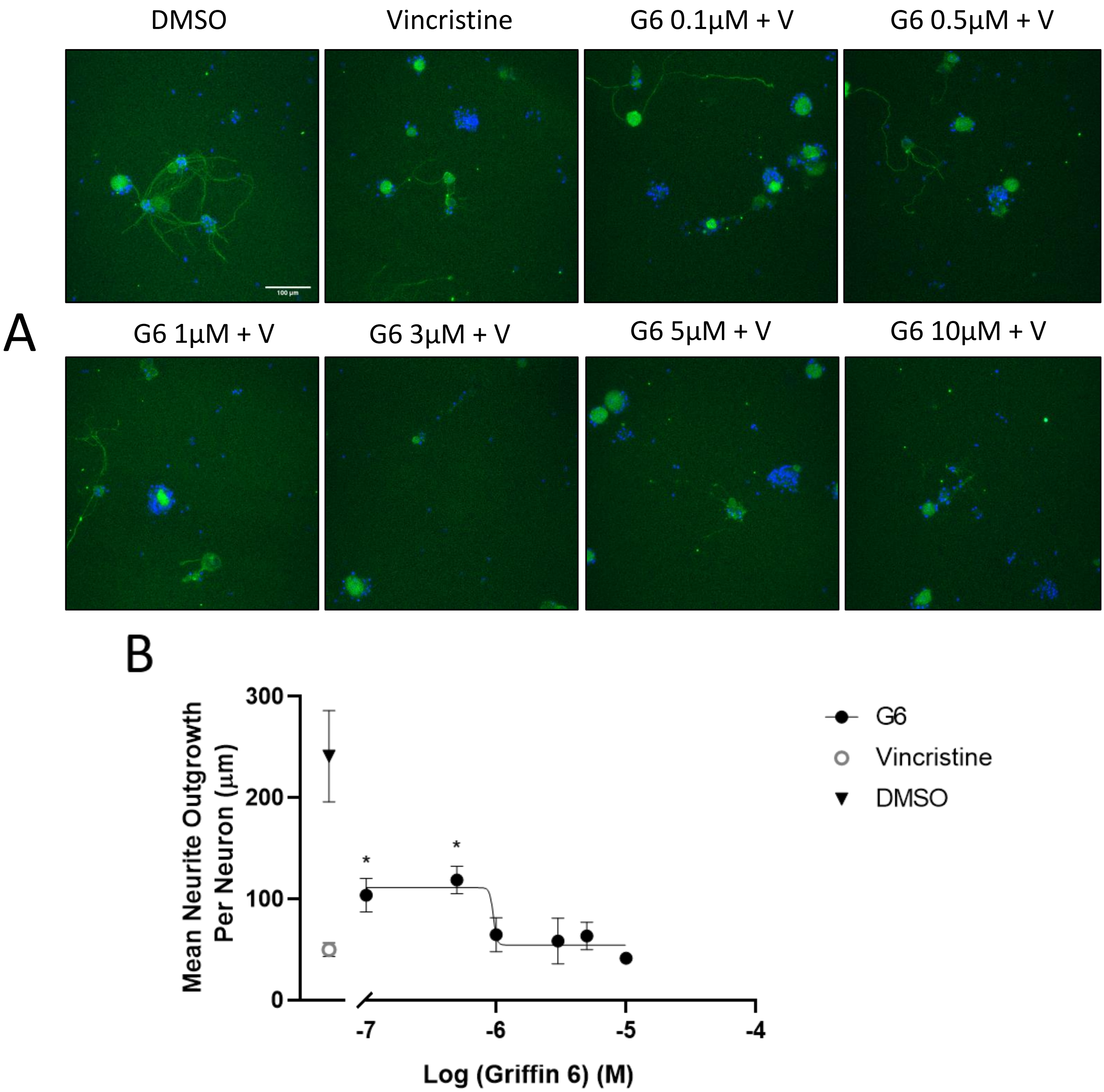

Figure 5.3.4.2 The effect of Griffin 6/Vincristine Co-treatments on neurite outgrowth

Representative images (A) of primary rat DRG neurons treated with vehicle, 10nM vincristine or a co-treatment of 0.1-10µM Griffin 6 and vincristine. Vincristine treatment significantly reduces outgrowth in all co-treatments comparative to vehicle, though 0.1µM and 0.5µM co-treatments do demonstrate robust outgrowth comparative to vincristine only control. Neurons are stained with mouse anti βIII tubulin and Hoechst. Scale bar = 100µm. (B) concentration response curve for Griffin 6 co-treatment effect of mean neurite outgrowth per neuron. Co-treatments with 0.1-0.5µM of Griffin 6 partially reverse vincristine mediated neurite dieback which recapitulates at higher Griffin 6 concentrations. N=3, Statistical Test used: One Way ANOVA with Dunnett's multiple comparisons to vincristine control. * P = <0.05.

5.3.5.1 Hippogriff 1 had no effect on neurite outgrowth at low concentrations but induced moderate reductions in outgrowth at high concentrations

To assess whether the CLK1/DYRK1 inhibitor Hippogriff 1 would induce changes in neurite outgrowth independent of chemotherapy primary rat DRG neurons were treated with 0.1-10µM of the novel compound for 72 hours. This followed the standard 72 hour incubation period post isolation to allow for neurite outgrowth following axotomy previously described. Between 0.1µM and 3µM, outgrowth was comparable to that of DMSO vehicle (220µm ± 15.5µm SEM). However, the robust growth exhibited at these concentrations was not replicated in the higher HG1 concentrations with neurons treated with 5µM and 10µM exhibiting neurite outgrowth of 126.4µm ± 8.3µm SEM and 69.3µm ± 8.4µm SEM respectively. These data therefore differ from those observed following treatment of neurons with SPHINX31 and Griffin 6 independent of chemotherapy which demonstrated robust neurite outgrowth across the low and moderate concentration ranges followed by mild drop off in outgrowth at the highest concentration. These data potentially suggest Hippogriff 1 could engage in some synergistic mediation of neurite dieback when given as an adjunct treatment to chemotherapy. (Fig 5.3.5).

A

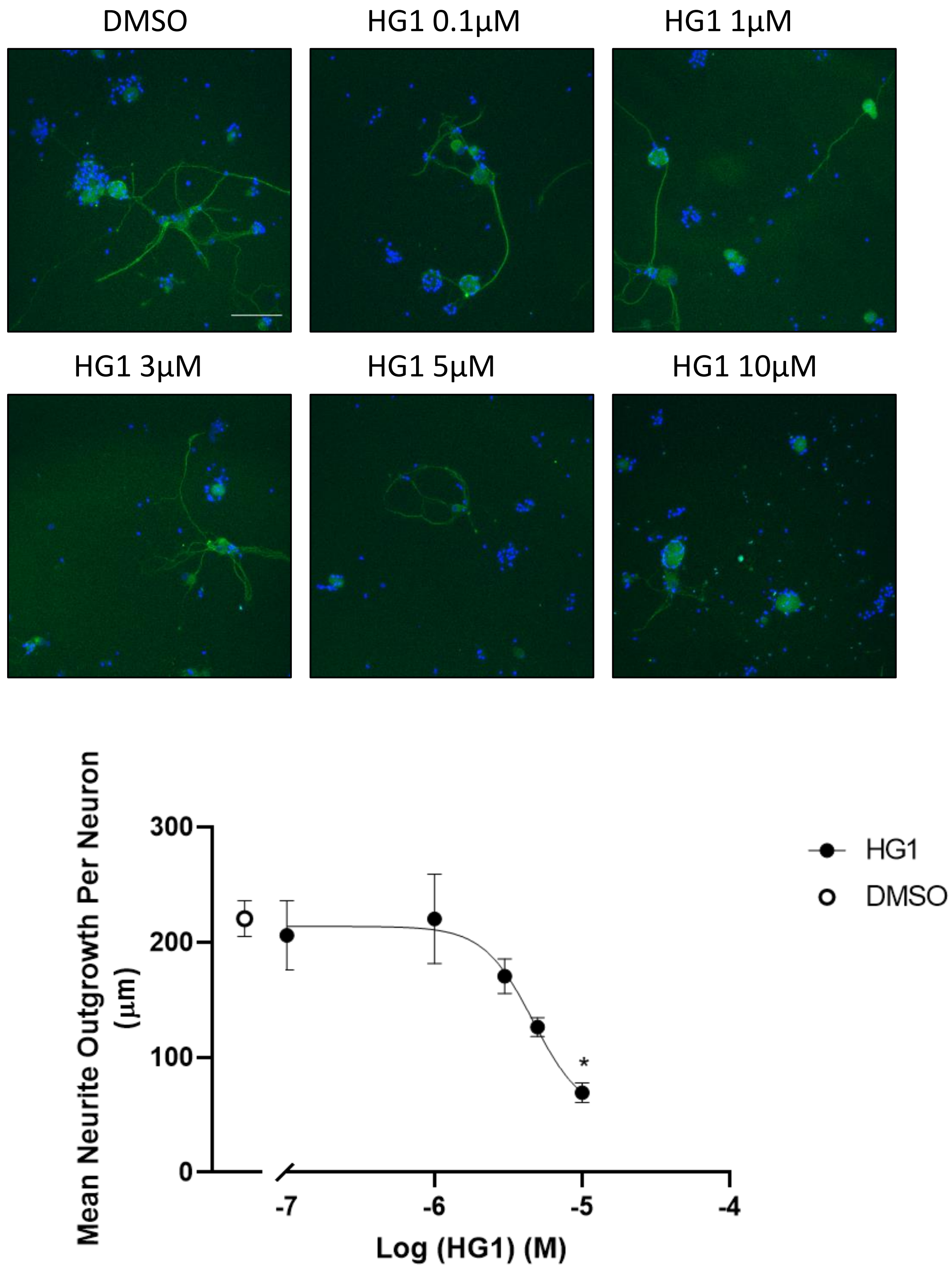

B

Figure 5.3.5 The effect of independent Hippogriff 1 treatment on neurite outgrowth
Representative images (A) of primary rat DRG neurons treated with 0.1-10µM of the novel splicing kinase inhibitor Hippogriff 1 for 72 hours. Treatment with low concentration recapitulate the robust neurite outgrowth demonstrated in vehicle control. This effect is eliminated at higher concentrations which exhibit significantly reduced growth compared to vehicle. Neurons are stained with mouse anti βIII tubulin and Hoechst. Scale bar = 100µm. (B) Concentration response curve for Hippogriff 1 treatment of DRG neurons and associated neurite outgrowth. Hippogriff 1 concentrations above equal to or above 5µM induced dieback of neurites that was significant at 10µM independent of chemotherapy. N=3 Statistical test used: One Way ANOVA with Dunnett's multiple comparisons to DMSO control. * p = <0.02 Data shown are mean ± SEM.

5.3.6 The novel chemotherapy compound jerantinine induced significant neurite dieback following 72 hour treatment, though not as severe as that of vincristine

The novel indole alkaloid jerantinine has been proposed as an alternative chemotherapy agent to traditional microtubule inhibitors such as vincristine and paclitaxel. However, use of any microtubule inhibitor is likely to induce neurite dieback as an adverse effect. Jerantinine is putatively reported to high a higher affinity of tubulin within dividing cells over neuronal tubulin which would manifest as increased neurite outgrowth within this model. Thus I tested the hypothesis that treating DRG neurons with concentrations of jerantinine derived from the IC50 data in metabolic assays would result in reduced neurite dieback compared to vincristine treated neurons. Following 72 hours of incubation post dissection and culturing, primary rat DRG neurons were treated with vehicle, 125nM-500nM of jerantinine or 0.1-10nM of vincristine for a further 72 hours. All treatment groups exhibited in significantly reduced neurite outgrowth compared to vehicle (312.5µm ± 34.91µm SEM). Vincristine induced dieback was concentration-dependent and was reminiscent of the previous data shown in section 5.3.2. Maximal vincristine treatment resulted in a neurite outgrowth of just 76µm ± 14.41µm SEM, an approximate decrease of 75% from vehicle control. By contrast, despite exhibiting significant decreases in neurite outgrowth compared to vehicle, there was no concentration dependent effect observed following jerantinine treatment. The maximal concentration of jerantinine resulted in a mean neurite outgrowth per neuron of 162.6µm ± 39.53µm SEM. This equated to approximately 52% of vehicle outgrowth. These values are comparable to the recovery in neurite outgrowth observed following provision of SPHINX31 and Griffin 6 as adjunct treatments at low concentrations. However, in this experiment the differences between the maximal vincristine concentration and all jerantinine concentrations were not significant. These data therefore imply that there is a disparity in how the two compounds, jerantinine and vincristine manifest their impact on neurite dieback as an adverse effect of chemotherapy.

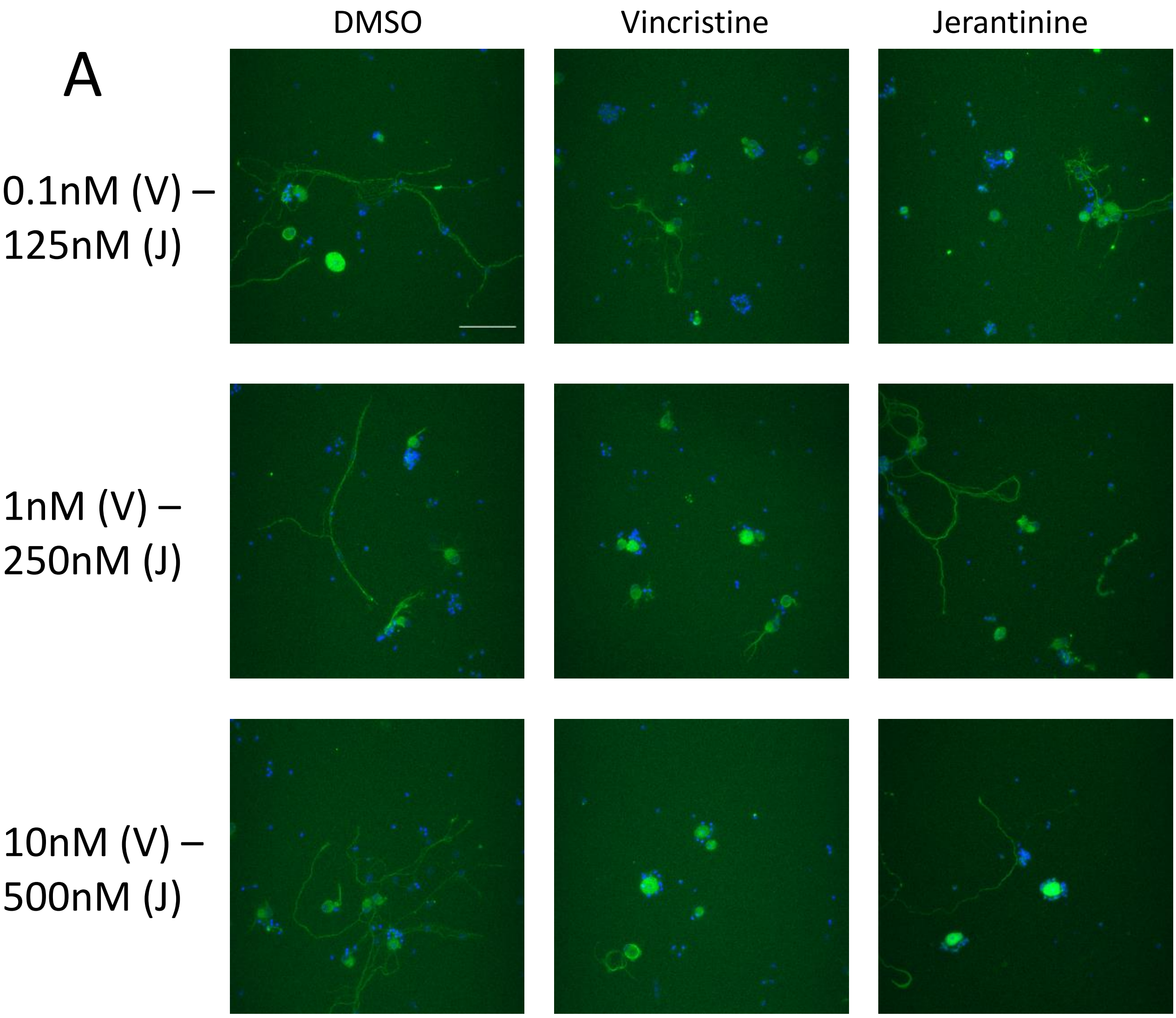

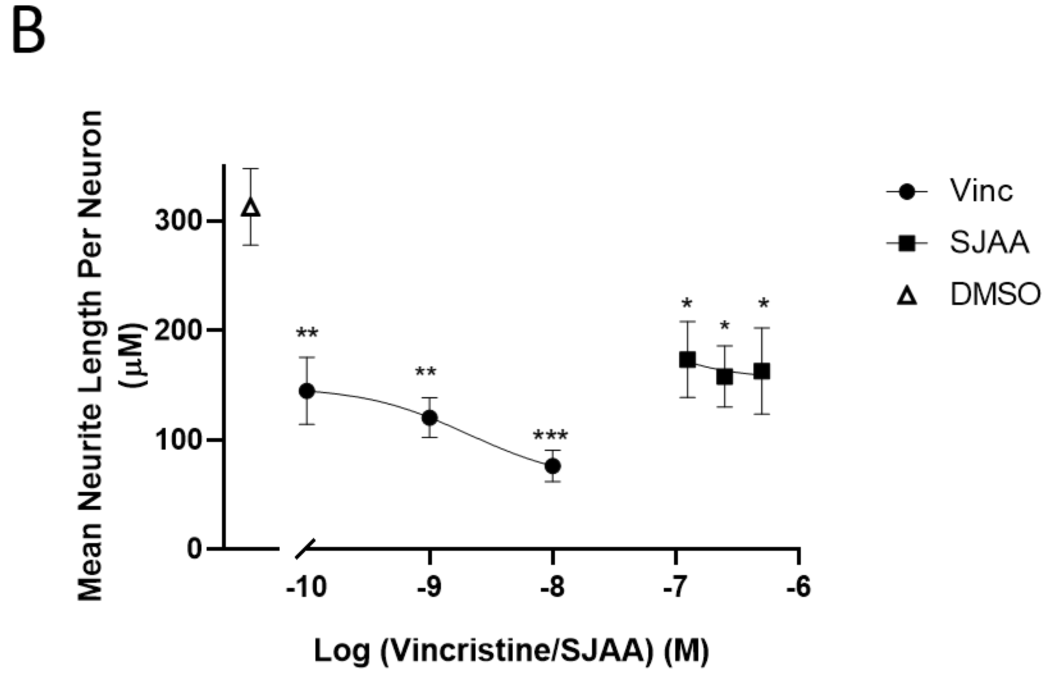

Figure 5.3.5 The effects of vincristine and jerantinine on neurite outgrowth following a 72 hour treatment

Representative images (A) of primary rat DRG neurons treated with either vehicle, 0.1-10nM vincristine or 125-500nM jerantinine. Vincristine treated neurons exhibit a gradual decrease in neurite outgrowth concomitant with concentration, which is not replicated by increasing concentrations of jerantinine. Neurons are stained with mouse anti-βIII tubulin and Hoechst. Scale bar = 100µm. (B) Concentration response curves for vincristine and jerantinine treatments. All concentrations of both drugs induced significant neurite dieback comparative to DMSO vehicle control. No statistical difference was observed between vincristine and jerantinine treatments. Statistical tests used, Neurite outgrowth compared to control = One Way ANOVA with Dunnett's multiple comparisons to DMSO control, n=3 *** p= <0.0005, ** p= <0.007, * p = <0.03. Comparison between jerantinine concentrations and maximal vincristine = One Way ANOVA with Dunnett's multiple comparisons to 10nM vincristine. No statistical significance detected. Data shown are mean ± SEM.

5.4 Discussion

As previously described, chemotherapy induced neurite dieback and disruptions to axonal transport as a result of microtubule inhibition are some of the principle manifestations of CIPN both during the acute treatment phase and possibly many years after the cessation of chemotherapy. Thus, development of physiologically relevant neuronal outgrowth models to screen new adjunct therapeutics and even the adverse neuronal effects of novel chemotherapies is of great importance in countering the growing burden of CIPN. The *in vitro* neurite outgrowth model described in this chapter successfully recapitulated the damage exerted by chemotherapeutic agents in previous *in vitro* studies that reflect some clinical findings in patient studies. Additionally the model provided the capacity with which to test 3 novel splicing kinase inhibitors as adjunct treatments to chemotherapy for the first time. Furthermore, the model examined for the first time the adverse neuronal effects of a novel chemotherapy agent, jerantinine in a pre-clinical model of CIPN. Evidence of some degree of neuroprotection in response to chemotherapeutic challenge was exhibited by 2 compounds, SPHINX31 and Griffin 6. Additionally the novel indole alkaloid jerantinine demonstrated reduced neurotoxicity compared to vincristine, a traditional chemotherapy agent. These data therefore demonstrate the potential impact splicing mechanisms may play in the development and severity of CIPN, and that control of these mechanisms may provide a therapeutic option for treatment of this refractory condition.

5.4.1 Adult Rat Primary DRG Outgrowth is robust enough to establish a viable model

In order to establish a viable model with which to screen novel compounds for their potentially neuroprotective properties a robust model of neurite outgrowth was first needed to be established. Although myriad models of neurite outgrowth have been developed and used in the past, many of these make use of immortalised cell lines or derive neurons from rodents in an early periods of development such as the embryonic or neonatal stage (Clarke *et al.*, 2017; Flatters, Dougherty and Colvin, 2017; Haberberger, Barry and Matusica, 2020). As such neurons contained are fundamentally of a different phenotype to those that are derived from adult populations. DRG neurons derived from adults rats have been found to have reduced neurite outgrowth following isolation and culturing compared to neonatal cultures and thus the latter have often been preferred for investigations into neurite dieback due to their relative regenerative capacity (Shewan, Berry and Cohen, 1995; Zhu and Oxford, 2011). Therefore, it was encouraging to see that adult DRG neurons within cultures demonstrate robust neurite outgrowth following isolation after just 72 hours of incubation (Fig 5.3.1) with a relatively low concentration NGF. Comparatively, previous studies have utilised up to 50ng/mL of NGF to simulate outgrowth following isolation concomitant with increases in GAP-43 protein expression following NGF supplementation. However, even this supplemented rise in GAP-43 a protein associated with growth cone development and neuronal plasticity is smaller than recorded GAP-43 upregulation in developing neurons treated with the same concentration of a neurotrophin after axotomy (Neto *et al.*, 2017). This is likely due to the fact that unlike developing neurons in neonatal stages, adult DRG neuronal populations with terminally differentiated cells retain only a subset of neurons capable of GAP-43 expression and consequently regeneration following isolation is limited. It should also be noted that adult neurons not expressing GAP-43 following axotomy have also been demonstrated to regenerate suggesting that outgrowth is not GAP-43 dependent, but rather faster and more comprehensive in neuron populations with more GAP-43 expression such as neonatal cultures (Andersen and Schreyer, 1999). Evidence for this is also provided in the observation that DMSO controls in drug treatment experiments (*Figures 5.3.2 – 5.3.5*) lasting 144 hours in total; with 72 hours of NGF supplementation and 72 hours without NGF had comparable neurite outgrowth to the NGF supplemented outgrowth across the whole experimental 72 hour period *(Figure 5.3.1)*. This shows a clear reduction in the scale of outgrowth following withdrawal of NGF from the cultures. In future studies, potentially characterising these populations and their variation between isolations could be useful in standardising and assessing the quality of dissection and isolation procedures.

Whilst the neurite outgrowth present at 96 hours and 120 hours incubation was not significantly different than 72 hour incubations there is a positive trend for continued growth (Fig 5.1.1). This suggests that cultures could be maintained with NGF supplementation for a longer period of time if desired and is further evidence that the model developed above is robust enough for a variety of different studies, not just limited to a CIPN context. However, for the purposes of investigations into chemotherapy and based off comparative literature of similar models I deemed the outgrowth at 72 hours to provide a sufficient experimental window with which to test the potency of vincristine in inducing dieback and the potential of novel compounds to ameliorate its effects.

5.4.2 Vincristine is a potent mediator of neurite dieback

The vinca alkaloid vincristine is a common chemotherapy agent that has been implicated as one of the most potent agents associated with the onset of CIPN within patients (Mora *et al.*, 2016). Additionally, vincristine has been demonstrated to induce severe neurite dieback in a number of preclinical models both *in vivo* and *in vitro*. Consequently, for the neurite outgrowth model described above to be considered a viable screening tool for potentially neuroprotective treatments the concentration of vincristine used must recapitulate these previously observed results. Concentrations of vincristine used in this model (Figure 5.3.2) were derived from previous work done by Roper et al. in cancer cell metabolism studies and from plasma concentrations found in patients following provision of chemotherapy (Roper, 2019). The 72 hour treatment time is comparative to the levels of circulating vincristine sulfate in serum following dosing in a patient (D. V. J. Jackson *et al.*, 1981). Vincristine exhibited profound effects on neurite outgrowth with the minimal 0.1nM concentration reducing outgrowth compared to vehicle by approximately 50% with maximal vincristine treatment of 10nM resulting in just ~25% of observed vehicle growth at the terminal end of a concentration dependent decrease in neurite outgrowth. Vincristine was therefore acting as hypothesised and having a significant impact on cultured neurons. This harsh reduction in neurite outgrowth is therefore in concordance with other pre-clinical models assessing the effects of chemotherapeutic agents on dieback. Interestingly, as with other pre-clinical models I observed no evidence of vincristine induced neuronal cell death, though without staining with an apoptotic marker such as caspase this was limited to purely morphological observations. There is reasonable evidence however that this is a common feature with microtubule inhibitors, as many studies have found neurite dieback without accompanying cell death following treatment with paclitaxel or vincristine. Whereas chemotherapy targeting DNA itself such as platinum based treatments and the proteasome inhibitor bortezomib have been found to result in accompanying neuron death (Beijers, Jongen and Vreugdenhil, 2012; Wheeler *et al.*, 2015; Wing *et al.*, 2017). This suggests that vincristine induced neuronal effects are much more likely to be caused by direct effects on neurites rather than as a result of soma pathology. In concordance with this, is the aforementioned body of literature identifying vincristine induced axonal degeneration and nerite dieback to resemble Wallerian degeneration of axons following acute nerve injury or axotomy (Wang *et al.*, 2000; Hilliard, 2009; Berbusse *et al.*, 2016). As previously mentioned, within this degeneration process axons die-back in a retrograde distal to proximal fashion as observed in CIPN models. In a comparative study with bortezomib (BTZ) a chemotherapy that exerts its effects primarily on neuronal soma and thus is purported to induce neuronal damage by activation of apoptotic pathways rather than Wallerian degeneration, the knockout of SARM1 was found to reduce axonal degeneration but not inhibit neuronal cell death induced by apoptosis following BTZ treatment. However, inhibition of the upstream mediators of the apoptosis pathway such as caspase or activation of anti-apoptotic molecules had no effect on vincristine induced Wallerian degeneration phenotypes (Geisler *et al.*, 2019). This suggests clear differences in how chemotherapies manifest their noxious effects and that in terms of the above model it consolidates the decision to prioritise measurement of neurite outgrowth/dieback as a readout rather than direct effects on neuronal cell bodies because of the use of vincristine within the model. Though no direct investigations into SARM1 expression were carried out in the model detailed in the previous sections, for future work it could be useful to characterise SARM1 expression after isolation to assess basal thresholds of the most prominent pro-degenerative factor in recently dissected cultures. This additionally could be extended to further validate and corroborate the proposed SARM1 mediation for vincristine induced dieback to ascertain whether SARM1 expression or activity is increased at higher vincristine concentrations.

5.4.3 Novel Splicing Kinase Inhibitors do not induce neurite dieback independent of chemotherapy

Treatment of primary rat DRG neurons with the novel splicing kinase inhibitors without a co-treatment of vincristine revealed promising data that was similar in 2 of the compounds utilised within the model. I hypothesised that novel splicing kinase inhibition as an independent treatment would not induce reduction in neurite outgrowth. To test this I applied the 3 compounds to the rat DRG outgrowth model for 72 hours. SPHINX31, the only novel compound that has been previously used on neuronal cultures demonstrated no deleterious effect of neurite outgrowth across a concentration range of 0.1-10µM for a 72 hour treatment (Figure 5.3.3.1). Only at the 20µM range was there a non-significant decrease in the neurite outgrowth observed. It should be noted that a concentration of 20µM for SPHINX31 is considered high and likely to trigger multiple off target effects as the selectivity of the compound based on its SRPK1 affinity drops. This is based off previous experiments in other tissue types examining the effects of the compound both on the RPE cells derived from the retina and PC3 cells derived from prostate cancer (Mavrou *et al.*, 2015). Despite this, it was still encouraging to see that even at this high concentration neurite outgrowth was not significantly inhibited to a level observed in the vincristine treatments detailed in figure 5.3.2.

The CLK specific inhibitor Griffin 6 was applied at a concentration range of 0.1-10μM to the neurite outgrowth model. In these experiments the 20μM treatment group was removed as similar to SPHINX31 this concentration is much higher than the proposed recommended concentration for usage and thus would be subject to the same drop off in selectivity of effects on the CLK1/CLK2 kinases as observed for SPHINX31 and SRPK1. Encouragingly as for SPHINX31 between the concentrations of 0.1-10μM Griffin 6 had no deleterious effect on neurite outgrowth compared to vehicle control. Outgrowth was lower in DMSO control in this experiment compared to that of others though this could possibly be explained by the age of the NGF aliquots used in these experiments. For experiments beyond this a fresh batch of NGF was purchased, aliquoted and applied to neurons. The absence of any effect of Griffin 6 across the concentration range suggests that the compound is safe to use on neurons at a wide range and that it would not synergistically contribute to decreases in neurite outgrowth when used in a co-treatment with a chemotherapy agent such as vincristine. This marks is the first time Griffin 6 has been used *in vitro* on primary cells and the absence of any damaging effects of neurons suggests it could now be applied safely to a range of other cell types in order to assess its viability as a CLK inhibitor in targeting a number of diseases driven by erroneous alternative splicing. More specific details discussing the potential mechanisms underpinning these observations for SPHINX31 and Griffin 6 treated neurons can be found in section 5.4.4.

The final compound I analysed in these experiments was the dual kinase inhibitor Hippogriff 1. Hippogriff 1 targets the both CLK1/CLK2 kinases as for Griffin 6 but additionally the DYRK1A kinase. Detailed information of all novel splicing kinase inhibitors can be found in Chapter 1. To test the hypothesis that Hippogriff 1 would not induce reductions in neurite dieback I applied 0.1-10µM of the compound to cells as for SPHINX31 and Griffin 6. However, unlike the previous two compounds there did appear to be a detrimental effect on neurite outgrowth concomitant with increasing concentrations of the compound. This culminated in a significant reduction in neurite outgrowth at the maximal Hippogriff 1 concentration that was just 31% of the outgrowth observed in vehicle control. However even at intermediate concentrations between 3-5µM there was a non-significant decrease in neurite outgrowth compared to vehicle with only low concentrations between 0.1-1µM displaying outgrowth comparable to vehicle control. The absence of this effect in Griffin 6 treated neurons suggests that these effects may be mediated by inhibition of the DYRK1A kinase as part of the dual specificity of Hippogriff 1. As previously mentioned, DYRK1A is a kinase highly associated with neuronal development with mutations and overexpression of the kinase implicated as a potential cause of Down Syndrome and autism spectrum disorder. Loss of function or reduced expression of the kinase is implicated in the development disorder MRD7 (Duchon and Herault, 2016). Indeed in embryonic mouse models DYRK1A expression has been detected in neuroprogenitor cells and implicated as a mediator of expression in a number of downstream developmental and differentiation inducer genes such as Sirt1, Snr1 and Spry2 and Tau proteins (Fernández-Martínez, Zahonero and Sánchez-Gómez, 2015). However with regard to the above experiments, the most important association could be the association between the kinase and the microtubule associated protein 1b (MAP1B). MAP1B is primarily expressed during neuronal development in neonatal and postnatal stages though its expression does rebound in areas of the nervous system associated with high levels of plasticity or indeed regenerating areas of the nervous system post injury (Bodaleo *et al.*, 2016). The neurons contained within the above model were recently axotimised and isolated and therefore fall into the latter category, most likely partially undergoing the aforementioned Wallerian Degeneration. DYRK1A has been found to phosphorylate sites on the MAP1B protein which in turn primes the molecule for binding and phosphorylative behaviour of another kinase heavily associated with developmental neurite outgrowth namely GSK3β . Studies by Scales et al. revealed that pharmacological inhibition of the DYRK1A kinase yielded reduced neurite outgrowth in embryonic cortical neurons and indeed caused a reduction in the number of neurites that subsequently went on to form axons (Scales *et al.*, 2009). Furthermore, microtubule stability has been found to impacted negatively by a lack of priming of kinase binding sites on the MAP1B protein to accommodate the binding and phosphorylative behaviour of GSK3β. As DYRK1A is one of the principle agents within this priming mechanism, inhibition of the kinase would therefore lead to fewer primed sites on the MAP1b protein and thus less binding of GSK3β and reduced microtubule stability. Further evidence of this is provided in the fact that neonatal cortical neurons with developing axons have reduced proportions of detyrosinated tubulin, which is a marker for stable microtubules. Therefore, it is possible to reasonably suggest that neurons within the neurite outgrowth model treated with HG1 were subject to a number of these different mechanisms. Said mechanisms may therefore provide an explanation for the reduction in neurite outgrowth observed following HG1 treatments compared to SPHINX31 and Griffin 6. Further similarities are provided by the fact that both vincristine and DYKR1A inhibition have profound effects on microtubule dynamics and this may be manifesting as interrupted neurite outgrowth at higher concentration of HG1. Studies on DYKR1A function and roles in healthy, non-Down Syndrome/MRD7 affected adult neurons are limited, thus future directions for this study to further corroborate these proposals are required (Ackeifi *et al.*, 2020). However, maximal concentration of HG1 treatment had equivalent effects on neurites as treatment with high vincristine concentrations (section 5.3.2), therefore it is reasonable to speculate that the mechanism behind this may be associated with deleterious activity against microtubule stability and normal function.

5.4.4 SPHINX31 and Griffin 6 Ameliorated Vincristine induced neurite dieback in co-treatment experiments

Following validation of the hypothesis that SPHINX31 and Griffin 6 would not inhibit neurite outgrowth as independent treatments I next hypothesised that they would confer neuroprotection to vincristine treated neurons in co-treatments. In all experiments a 72 hour, 10nM application of vincristine as an independent or co-treatment caused a significant reduction in neurite outgrowth compared to untreated controls. This was concomitant with the data presented in section 5.3.2. However, despite significant reductions in neurite length compared to vehicle control, both compounds encouragingly displayed that at low concentrations of 0.1µM and 0.5µM they were capable of conferring some statistically significant protection to neurons in terms of neurite outgrowth compared to neurons treated with 10nM vincristine alone. This vincristine concentration is comparable to the circulating concentration detected in patients following a continuous infusion with vincristine sulphate in a chemotherapy cycle. Treatments in the aforementioned range for SPHINX31 produced neurite outgrowth that was a third of vehicle control, but 20% greater than cultures treated with vincristine alone. For Griffin 6 these proportional increases in outgrowth were larger still. An explanation for this disparity however is likely to due to differences in the outgrowth in the untreated vehicle control. In SPHINX31 experiments neurite outgrowth in the vehicle control was over 500µm per neuron whereas in Griffin 6 experiments outgrowth in vehicle controls was approximately half of this. This change in experimental window could be caused by natural assay variability, quality of NGF in the 72 hour outgrowth period, quality of dissection and quality of culturing techniques. Therefore, caution must be used if drawing comparisons between the efficacies of the two compounds, future work examining the two compounds in the same experiment would provide a better basis for active comparisons between the two compounds. However, the two compounds do significantly ameliorate the effects of vincristine within their respective experiments and this serves as validation of the initial hypothesis that they would provide a level of neuroprotection to chemotherapy treated neurons.

Interestingly, over the rest of the concentration range beyond the 0.5µM level there were some divergent effects seen between the two compounds. Neurons treated with SPHINX31 in vincristine co-treatments demonstrated growth that was higher than neurons treated with vincristine alone. Whereas neurons treated with Griffin 6 above 0.5µM had neurite growth more comparable to vincristine only treatments. These findings could again be due to inter-assay variability between the experiments involving the two compounds but in the case of Griffin 6 they potentially suggest some synergistic effects between vincristine and high concentrations of the compound, possibly due to the off target effects of Griffin 6 exhibited at said concentrations and as has been observed in other studies assessing kinase inhibition in a variety of contexts. Crucially however, these *in vitro* data suggest that there is potential for splicing kinase inhibition as a means of protecting neurons from high concentrations of vincristine. That said, elucidating the potential mechanisms behind this protection are of equal importance.

Pharmacological inhibition of SRPK1, the principle mechanism of action of SPHINX31 has previously been investigated in the context of the neuroprotective capabilities of alternatively spliced VEGF isoforms (Beazley-Long *et al.*, 2013; Hulse *et al.*, 2014; Vencappa, Donaldson and Hulse, 2015). Additionally, various studies have also mirrored this effect by treating neurons with recombinant forms of VEGF-A_{165}b to assess neuroprotective potential in a variety of different contexts such as diabetic neuropathy and glutamate induced excitotoxicity (Verheyen *et al.*, 2013; Ved *et al.*, 2018). Though no definitive examination of whether the effects seen in the above experiments with SPHINX31 are VEGF dependent were performed, previous work using similar compounds and recombinant VEGF-A_{165}b protein would suggest a potential role for VEGF alternative splicing. Under normal physiological conditions anti-angiogenic and non-nociceptive VEGF-A_{165}b isoforms predominate over the VEGF-A_{165}a isoforms once thought to the canonical form of the growth factor. However, upon insults such as crush injury or full axotomy or hypoxia this expression is reversed and the VEGF-A_{165}a isoform becomes predominant. VEGF-A_{165}a is associated with neurite outgrowth and neurotrophic behaviour within the DRG along with an upregulation of the VEGFR2 receptor, the principle site at which VEGF isoforms exert their effects on tissues. Thus it is likely following the dissection, isolation and subsequent culturing of DRG there is an upregulation of this isoform and receptor within cells and along with NGF supplementation as previously described is concomitant with robust neurite outgrowth described in section 5.3.1. Previous studies have shown this effect can be blocked by inhibiting VEGFR2 receptors further corroborating evidence that neurite outgrowth from neuronal cell bodies following injury and during development is at least in part mediated by VEGF (Hulse *et al.*, 2014).

Vincristine has been found to have anti-angiogenic properties in a wide number of cancers such as glioblastoma cell lines where it was found to reduce VEGF mRNA expression following vincristine treatment, though this was at concentrations up to 1µM and therefore much higher than both the levels circulating within patients and the concentrations used in the neurite outgrowth model (Park *et al.*, 2016). Similar effects were also observed when vincristine was applied various types of leukaemia cell lines (Avramis, Kwock and Avramis, 2001). This is in addition to profound deleterious effects observed when used on endothelial cell lines such as Human Umbilical Vein Endothelial Cells (HUVECs) which have high levels of VEGF-A_{165}a expression (Bota *et al.*, 2019). Therefore, if neurons within the neurite outgrowth model are expressing high levels of pro-angiogenic VEGF isoforms it is possible that vincristine would have profound effects on this expression. Furthermore, SPHINX31 has been found to induce significant changes in VEGF splicing at equivalent concentrations to those used within the neurite outgrowth model, in a study of splicing changes in retinal pigmented epithelial samples (RPE) (Batson *et al.*, 2017). Therefore it is reasonable to suggest that these effects may be occurring in neurons contained within the neurite outgrowth model and this expression of VEGF-A_{165}b isoforms following pharmacological inhibition of SRPK1 is a factor in the neuroprotection conferred in the neurite outgrowth model. Recombinant VEGF-A_{165}b has protected hippocampal, peripheral and retinal neurons both *in vitro* and *in vivo* from a variety of chemical and physical challenges. The absence of any further neurite outgrowth above vehicle in independent SPHINX31 treatments and reduced growth SPHINX31/Vincristine co-treatments further supports the hypothesis that the neuroprotective effects observed could be mediated by altered VEGF-A splicing in favour of VEGF-A_{165}b. As in experiments on the effects of SPHINX31 treatment alone, if modulation of alternative spicing was not being achieved one would expect to see further growth of the neurites even after the withdrawal of NGF supplementation because of the neurotrophic effects of VEGF-A_{165}a predominating. However this was not observed at any concentration of SPHINX31 treatment which concurs with previous data from Batson et al. suggesting efficacy of SRPK1 inhibition in inducing changes in splicing at concentrations as low as 0.1µM of SPHINX31. An argument against this hypothesis however is the fact that both isoforms are neuroprotective, and therefore a shift in splicing may not have a significant effect. This would suggest alternative targets of SRPK1 inhibition producing these ameliorating properties. Future work to assess these hypotheses could include assessment of basal VEGF isoform expression in DRG neurons post dissection and culturing to judge which isoform predominates post injury. Assessment of VEGF expression before and after vincristine treatment would indicate the effects of the vinca alkaloid on these mechanisms. Experiments investigating this expression would likely have to be pooled from multiple plates due to difficulties in collecting sufficient protein from neurons cultured in 96 well plates. Secondly, to judge whether the neuroprotection conferred by SPHINX31 is VEGF-A_{165}b dependent, a VEGF-A_{165}b neutralising antibody could be applied to the model, if neurite outgrowth recovery is abolished in the concentrations where it was previously significant this would greatly increase the likelihood of the observed effects being VEGF-A_{165}b isoform dependent.

In addition to the significant effects observed following use of the SRPK1 specific inhibitor, SPHINX31 there was also a significant neurite protective effect observed when the novel CLK1/2 specific inhibitor Griffin 6 was used in a co-treatment with vincristine. Unlike SPHINX31 this marks the first time that Griffin 6 has been used not only *in vitro* on primary neuronal cells, but also in any functional *in vitro* assays. Therefore comparisons to previous studies are not available to be discussed, however CLK1/2 inhibitors and indeed the role of the CLK1/2 kinases within neuronal and angiogenic contexts have been discussed previously in the literature (Nowak *et al.*, 2008; Harper and Bates, 2009; Gu *et al.*, 2017; Lee *et al.*, 2019b). In the neurite outgrowth model, Griffin 6 only had protective actions at the two lowest concentrations and had no effect alone. This suggests that there may be an effect of CLK1/2 function and neurite outgrowth when neurons are challenged with a chemical insult, as was the case for SPHINX31, though CLK1/2 inhibition does not appear to have neurotrophic actions in itself based on evidence from the literature.

CLKs have been implicated as active in neuronal function in a number of studies, one of the earliest of which demonstrated that CLK1 expression and activity was correlated with neuronal like differentiation of PC12 cells, a pheochromocytoma cell line from the adrenal glands. CLK1 works synergistically with NGF to induce differentiation however CLK1 alone was not able to promote cell survival of this cell line in the absence of NGF (Myers, Murphy and Landreth, 1994). This suggests CLK1 has role in neuronal function and development whilst not necessarily being associated with cell survival pathways within neurons. Additionally, more recent research has linked aberrant CLK2 activity to deficits in SHANK3 expression in cortical neurons, which is linked to many of the phenotypes present in autism spectrum disorders (Bidinosti *et al.*, 2016). This therefore, in a similar fashion to the closely related DYRK1A kinase implies a role of CLK2 in early neuronal development. Inhibition of CLKs using the TG003 inhibitor on primary cortical neurons in the same study restored dendritic spine outgrowth in SHANK3 knockdown conditions, suggesting CLKs play a profound role in neurites and their functional capacity. Dendritic spines are minor protrusions from the dendritic membrane that receive input from an axon and are therefore a major source of synaptic transmission in the central nervous system. Additional evidence for a central nervous system role for CLK1 is provided in the fact erroneous splicing of Tau protein, a microtubule associated protein governed by CLK1, and mutations within this pathway are associated with neurodegenerative conditions such as Parkinson's and Alzheimer's disease (Glatz *et al.*, 2006; Jain *et al.*, 2014). However, information on CLK1/2 function within the peripheral nervous system is limited and therefore further hypotheses generated from these primary observations must be subject to further investigations and scrutiny. The majority of literature regarding CLK kinases is contained within the field of oncology, where CLK inhibition using other novel, non-selective compounds results in reduced phosphorylation of SRSF1. This is to be expected as both CLKs and SRPKs exert strong influence on this splicing factor (Araki *et al.*, 2015; Iwai *et al.*, 2018). However, the activity of SRSF1 is a major upstream mediator of the activity of the S6K kinase, itself an upstream mediator of the S6 ribosomal protein associated with cell size and proliferation governed by mammalian target of rapamycin pathway (mTOR) (Ben-Hur *et al.*, 2013).

The mTOR signalling pathway has a well-established role in the limited neuronal regeneration post injury seen within the CNS and is negatively regulated by

Phosphatase and Tensin Homolog (PTEN). Inhibition of PTEN has increased the regenerative capacity of CNS neurons following injury whereas inhibition of mTOR with rapamycin was found to dramatically decrease axonal regeneration in retinal and cortical neurons, both considered to be part of the CNS (Al-Ali *et al.*, 2017). Indeed, many studies attribute the lack of CNS regeneration post injury to be attributed to the fact mTOR is essential to the process but is chronically inhibited by actions of glial cells within the CNS, cells also key in glial scarring in the CNS (Wei, Luo and Chen, 2019). In the PNS however, mTOR is not considered to be essential for regeneration post injury although a recent study suggests there is an activation of the pathway following injury within peripheral neuronal cell bodies (Chen *et al.*, 2016). Furthermore in a model of sciatic nerve ligation in the PNS neurites were present projecting from injured neurons treated with rapamycin an inhibitor of mTOR, though they were shorter than those not treated with the inhibitor (Abe *et al.*, 2010) This demonstrates that outgrowth is possible in the PNS when mTOR is inhibited, supporting the conclusion that while mTOR may drive PNS regeneration, it is not essential to it. The mTOR pathway has various downstream mediators, one of which is the aforementioned S6K which has been found to have conflicting roles in the literature in the context of neurite regeneration with evidence for both stimulatory and inhibitory roles in this context (Yang *et al.*, 2014; Al-Ali *et al.*, 2017)

This association between S6K activation by mTOR and neurite outgrowth is relevant to the inhibitory activity of Griffin 6 on CLKs splicing kinases and the effects on downstream SRSF1 signalling. CLKs induce strong inhibitory effects on canonical S6K activity and the splicing of S6K itself. Inhibition of CLK results in production of 6 novel S6K kinase transcripts in addition to the canonical form linked to mTOR signalling in breast cancer cell lines (Araki *et al.*, 2015). The presence of these alternatively spliced S6K isoforms is associated with reduced cancer cell growth and reduced S6K activity. It is feasible, due to inhibition of the identical upstream kinase that Griffin 6 could recapitulate these effects in neurons, and produce multiple non-functional S6K transcripts resulting in less phosphorylation of the S6K target, S6. There is conflicting evidence on the effect of S6 on neurite outgrowth with reports of both reduced and enhanced neurite outgrowth that may be a result of different alternative splicing events (Abe *et al.*, 2010; Hubert *et al.*, 2014; Yang *et al.*, 2014; Al-Ali *et al.*, 2017). Alternatively, as the mTOR pathway can be activated by a number of different signalling routes, it is possible that a CLK inhibitor could also stimulate mTOR-dependent neurite outgrowth via the PI3K pathway, which is negatively regulated by the activity of S6K as reported in CNS neurons (Al-Ali *et al.*, 2017). Griffin 6 is a highly selective CLK inhibitor and may be efficacious at preventing neurite dieback at low concentrations where it is likely to be more selective for CLKs, thus exerting inhibitory effects on S6K splicing controls via upstream SRSF1 suppression in the presence of a cytotoxic chemical insult such as vincristine. This may cause activation of the mTOR pathway driving regeneration via another pathways, such as the PI3K, than through S6K which has also been found to regulate mTOR mediated PI3K regeneration in a negative feedback loop. The PI3K pathway avoids inhibition of PTEN, a tumour suppressor linked to tumour cell vincristine resistance and thus might engage a more controlled mTOR activation that results in moderate neurite outgrowth. Given the wide-scale uncertainty in the literature, these hypotheses would need to be tested in further work. As an independent treatment, the hypothetical stimulation of the mTOR pathway by CLK/SRSF1 inhibition and downstream effects on S6K could be limited by the fact that mTOR induced outgrowth is not essential for neurite to outgrowth and activation of other unidentified pathways may be required for further regeneration. In order to determine this, future investigations into Griffin 6 mediated CLK1/2 inhibition and neurite outgrowth could be focused on S6K transcripts following Griffin 6 administration, the expression of mTOR activation markers after dissection, the phosphorylation state of S6, PI3K activation markers and inhibiting mTOR activation via rapamycin supplementation to cultures.

5.4.5 Jerantinine and Vincristine significantly reduce neurite outgrowth, but to a different degree

For the first time, the novel indole alkaloid synthetic jerantinine acetate A (Jerantinine) was used *in vitro* on primary sensory neurons in a direct comparison with a traditional chemotherapy agent, the long established vinca alkaloid vincristine. Though data on jerantinine is scarce, preliminary work identifying the anti-cancer properties of jerantinine have been described by Smedley et al. and Roper et al. (Roper *et al.*, 2018; Smedley *et al.*, 2018). The latter study identified that despite jerantinine demonstrating comparable efficacy to vincristine at sub-micromolar concentrations, the effect of the novel compound on neural stem cell structure and morphology were negligible compared to vincristine treated stem cells. These data suggested that jerantinine could potentially carry fewer severe off-target effects on non-cancerous cells, whilst retaining a potent effect on aberrantly dividing cells. Therefore, I hypothesised that when each compound was applied to adult rat primary dorsal root ganglia neurons, the neurons treated with a physiologically relevant concentration of jerantinine would exhibit reduced neurite dieback compared to neurons treated with the traditional compound vincristine.

The data presented in section 5.3.6 suggest at least partial validation of this hypothesis. Both compounds significantly reduced observed neurite outgrowth compared to vehicle. However, the decrease observed in neurons treated with jerantinine did not recapitulate the concentration-dependent effect observed with increasing vincristine treatments. The effect of the lowest concentration of jerantinine used (125nM) was almost equivalent to the maximal concentration (500nM). When normalised, there was an approximately three percent decrease across the concentration range. Comparatively, vincristine cause a 21% decrease in neurite length across the concentration range (0.1nM to 10nM). Whilst the difference between the compounds was not significant, this might suggest a difference between the mechanisms of the two compounds, possibly in the severity of their non-specific effects on non-cancerous cells. Though both compounds are microtubule inhibitors and function via destabilisation of the microtubules, an immediate difference in their mechanism of action is site at which each compound binds to the microtubule. As previously mentioned, vincristine and the vinca alkaloid class of compounds bind to the vinca domain on the β-tubulin subunit itself, whereas jerantinine binds to the so called colchicine binding site which is located at the β-tubulin interface with α-tubulin (Zhang, Yang and Guo, 2017; Smedley *et al.*, 2018). Colchicine is traditionally a drug used in the treatment of gout. High toxicity severely limited its effectiveness as a potential cancer treatment, but related compounds that bind to the same site are under investigation as chemotherapy agents (Lu *et al.*, 2012). The functional difference in the microtubule inhibition between the two sites is that binding at the vinca site is limited to tubulin molecules at the exposed tip of the microtubules and vinca alkaloids cannot bind to tubulin molecules already polymerised into microtubules. In contrast, microtubule inhibitors binding at the colchicine site are able to copolymerise with tubulin molecules that are already formed and polymerised. The result is the formation of a complex between the colchicine binding molecule and the two tubulin subunit molecules. This in turn leads to the creation of “curved” tubulin dimers which at lower concentrations inhibit microtubule dynamics as lateral contacts with neighbouring dimers is lost. At higher concentrations this effect is exacerbated and colchicine binding compounds actively depolymerise and degrade the microtubules. Jerantinine abolishes tubulin polymerisation as effectively as other colchicine agents such as nocodazole (Raja *et al.*, 2014).

It is feasible given the observed reduction in dieback following jerantinine treatment compared to vincristine that the concentration used was sufficient to interrupt microtubule dynamics in this way, as jerantinine at 500nM is sufficient to initiate G2/M cell cycle arrest in cancer cells which active require microtubules to divide. This concentration may be low enough to limit the potential deleterious effects of actively depolymerisation and loss of microtubule mass, which would manifest as neurite dieback. This is supported by effects in breast cancer cells treated with jerantinine at concentrations above 1µM, where normal microtubule processes such as multipolar spindle formation, misaligned chromosomes and nuclear fragmentation were disrupted indicative of a severe reduction in available microtubule mass. Thus at jerantinine concentrations less than 1µM, such as those used in the neurite dieback model inhibition of microtubule dynamics rather than reduction of microtubule mass could be responsible for the absence any concentration-dependent effect on neurite outgrowth. With vincristine treatment, this window between interruption of microtubule dynamics and reduction in mass is reached at lower concentrations than for jerantinine due to the higher potency and toxicity of vincristine, which results in a concentration-dependent effect (Jordan and Wilson, 2004). It is also important to note that neurites, though they may not be in the process of degeneration while in the presence of splicing kinase inhibitors, could still be functionally affected as evidenced by neuronal sensitisation following acute vincristine or jerantinine treatment. Therefore, these findings and further hypotheses should be considered in conjunction with the sensitisation data found in Chapter 4. Nonetheless, the less severe neurite dieback in jerantinine treated neurons compared to vincristine treated neurons at these concentrations is encouraging given the concentrations used to obtain cytotoxic effects on cancer cells are usually between 125-500nM.

The observed values of normalised outgrowth in jerantinine treated neurons, were comparable to that observed in neuronal co-treatments with vincristine and SPHINX31/Griffin 6. Therefore it would be interesting to assess how efficacious the novel splicing kinase inhibitors would be at further ameliorating the effects of jerantinine induced neuronal dieback. It is reasonable to hypothesise given the neuroprotective effects observed in vincristine treatments that the novel splicing kinase inhibitors might replicate these effects in a compound ostensibly inducing less neurotoxicity. These experiments represent an exciting future direction for both jerantinine and the novel inhibitors as it could further elucidate their potential as a combination therapy for use in cancer patients, for effective anti-cancer effects with mediation of any side effects. It would also be valuable to assess neurite outgrowth at concentrations previously reported as abolishing formation microtubule mass to see whether these effects would be replicated within the model. This would help to corroborate the proposed hypothetical mechanism that at concentrations lower than 1μM jerantinine is acting through inhibition of microtubule dynamics rather than reducing microtubule mass. However, a limitation of these studies is the existing supply of jerantinine. For these experiments the jerantinine used was kindly donated by Dr Tracey Bradshaw of the University of Nottingham, School of Pharmacy. Synthesis of the compound is extremely complicated and difficult and compound stability at temperatures above -80°C is low. Therefore, future experiments are subject to these limiting factors which could result in obstacles to the development of jerantinine. Nonetheless, the compound serves as proof that the neurite outgrowth model can be used for direct comparisons of the adverse effects of a putative and established chemotherapeutic agent.

Chapter 6: Assessment of Novel Splicing Kinase Inhibitors on Chemotherapy Efficacy

6.1.1: Introduction

Whilst the development of adjunct therapies to current chemotherapy regimens is essential in ameliorating the impact of CIPN suffered by patients it is of paramount importance that such therapies do not significantly interfere with the primary function of chemotherapy. (Flatters, Dougherty and Colvin, 2017) Putative pain relief therapies that carry these contraindications could potentially risk patient survival or require the patient to undergo more cycles of chemotherapy in order to achieve the pre-CIPN therapy tumour reduction. (Cavaletti *et al.*, 2019) Thus, it is crucial that any potential adjunct CIPN therapeutics are suitably screened for such effects using relevant *in vitro* models. Traditionally, assays used to assess cytotoxicity caused by novel agents and cell survival such as MTT assays have been carried out using conventional 2D cell culture techniques using cell monolayers. (Ivanov *et al.*, 2016) However, in many cases results generated using these models are then poorly replicated following *in vivo* experiments (Edmondson *et al.*, 2014). Much of this can be attributed to the lack of physiological relevance that 2D cell culture models possess compared to a whole organism (Mehta *et al.*, 2012). As such, there is a pressing need to use more advanced and physiologically relevant models of cytotoxicity within cancer.

Recently, 3D cancer spheroid models have been shown to be much more effective in assessing the effects of anti-cancer drugs *in vitro.* (Präbst *et al.*, 2017) This is largely due to the fact that cancer cells growing in 3D resemble the growth patterns of *in vivo* tumours much more accurately than simple monolayer cultures. Consequently, increasingly well characterised spheroid models can serve as ideal screening assays for assessing the effects of novel splicing kinase inhibitors on the anti-cancer capabilities of vincristine.

The novel splicing kinase inhibitors used in these experiments, Griffin 6, Hippogriff 1 and SPHINX31 all have targets that have been implicated in studies of cancer. For instance SRPK1 and the CLK kinases are key mediators of alternative splicing of *VEGFA,* canonically a potent driver of angiogenesis. Many tumour types rely on dysregulation of VEGF expression and pathological angiogenesis to grow *in situ* and also to provide an opportunity for the cancerous cells to spread via bloodstream metastasis. A recent study by Gao et al. found that the hypoxia linked miRNA-210 was upregulated in primary MB tissues alongside increased expression of VEGF-A. This upregulation was further enhanced in patients with secondary tumours and subarachnoid metastasis in addition to increased levels of both angiogenic components within the cerebrospinal fluid. Therefore, it is possible that novel splicing kinase inhibitors capable of targeting upstream mediators of differential VEGF isoform expression may be able to exert their effects synergistically with traditional chemotherapy agents in treating cancers. This could manifest as a direct effect on the solid tumour *in situ* by cutting off access to the bloodstream resulting in apoptosis, reducing tumour size or by preventing metastasis and subsequent dissemination of spread. However, the role of SRPK1 within medulloblastoma remains relatively obscured compared to other tumour types with CLK and DYRK1A functions in brain tumours explored even less. Therefore, assessing the capability of the novel compounds inhibiting these aforementioned targets will provide a useful "first pass" analysis as to their capabilities as adjunct therapeutics to potentiate paediatric traditional brain tumour therapies such as vincristine. Furthermore it is also proposed that as the novel compound targets are all relevant to a variety tumour types that the novel compounds can potentially serve as discrete and independent treatments. SPHINX, a precursor of SPHINX31 has already been used in this manner in a pre-clinical *in vitro* study of prostate cancer, though none of the compounds presented for screening have been used previously in the context of medulloblastoma (Mavrou *et al.*, 2015).

6.1.2: ONS76 Cells

ONS76 cells are an immortalised cell line derived from a 2 year old female patient with a Sonic Hedgehog (SHH) classification medulloblastoma. SHH medulloblastomas form the second largest subgroup of recorded diagnoses in patients and are regularly treated with the vinca alkaloid vincristine when the patient is considered to be both "standard" and "high" risk. In standard risk patients, vincristine is used at all phases of treatment, initially alongside radiotherapy before being used in conjunction with cisplatin and cyclophosphamide. High risk refers to patients less than 3 years of age, with confirmed metastasis prior to treatment. For SHH hedgehog tumours, the metastasis rate at diagnosis is approximately 20% (Bonfim-Silva *et al.*, 2019). Therefore given the prevalence of SHH tumours, ONS76 cells have been used in traditional 2D drug screens targeting medulloblastoma for approximately 30 years and are well characterised in the literature. More recently they have been used in the development of 3D spheroid models (Ivanov *et al.*, 2016). Importantly, spheroids formed by ONS76 cells can be expediently grown with minimal effort or technical expense other than use of ultra-low attachment plates. As such, ONS-76 cell spheroids were selected as the most practical option with which to assess the potential off-target effects of novel splicing kinase inhibitors on vincristine activity.

6.1.3: Hypotheses & Aims

Hypotheses:

- Application of vincristine to ONS76 spheroids will result in disruption to spheroid morphology, causing fragmentation and reduction in size of tight spheroid conformation.

- The novel splicing kinase inhibitors, SPHINX31, Griffin 6 and Hippogriff 1 will disrupt ONS76 spheroid morphology, causing fragmentation and reduction in size of tight spheroid confirmation as independent treatments.

- Applying vincristine and a novel splicing kinase inhibitor to ONS76 spheroids as co-treatments will not inhibit the ability of vincristine to disrupt tight spheroid conformation and concomitant reduction in spheroid size. Furthermore, vincristine and the novel splicing kinase inhibitor used may synergistically disrupt spheroid size to a greater magnitude than as independent treatments.

Aims:

- Use the 3D ONS76 spheroid model as a preliminary screen for the effects of 3 novel splicing kinase inhibitors as independent cancer treatments, in addition to assessing potential contraindications when used in a co-treatment with vincristine.

6.2: Methods – ONS76 Spheroid Formation

This protocol was initially adapted from Ivanov et al. by S.Roper (Ivano*v et al*, 2016; Roper, 2019). ONS76 cells were grown to ~70% confluence as described in section 2.1.3. Cells were then trypsinised and centrifuged at 100xg for 5 minutes to form a cell pellet. The pellet was then re-suspended in 1mL of RPMI1640 medium and cells were counted using a Neubauer Haemocytometer. Sufficient cells were then removed from the suspension to allow for a cell density of 150 cells/well of an ultra-low attachment 96 well plate. These cells were then pelleted again using centrifugation as previously described above and re-suspended in appropriate volume of Neurosphere medium (DMEM/F12 + 2% B-27 supplement, 1% N2 Supplement, 2µg/mL Heparin, 20ng/mL EGF, 10ng/mL FGF.) to allow for a volume of 200uL per well. If using a maximum of 60 wells this volume was 12mL. Cells were then evenly distributed at the aforementioned density in 200µL in a maximum of 60 wells. HBSS was placed in the surrounding wells to prevent dry out of the central 60 wells. Plates were then incubated at 37°C for 96 hours.

Following the 96 hour incubation period, ONS76 spheroids were imaged using a CMEX-18 Pro microscope camera following calibration using a microscope scale calibration slide (AmScope). Images were taken at 10x magnification. These images were then processed using Image J (Fiji) software. The freehand selection tool was used to trace around the spheroid, calculating area as seen in figure 6.1.

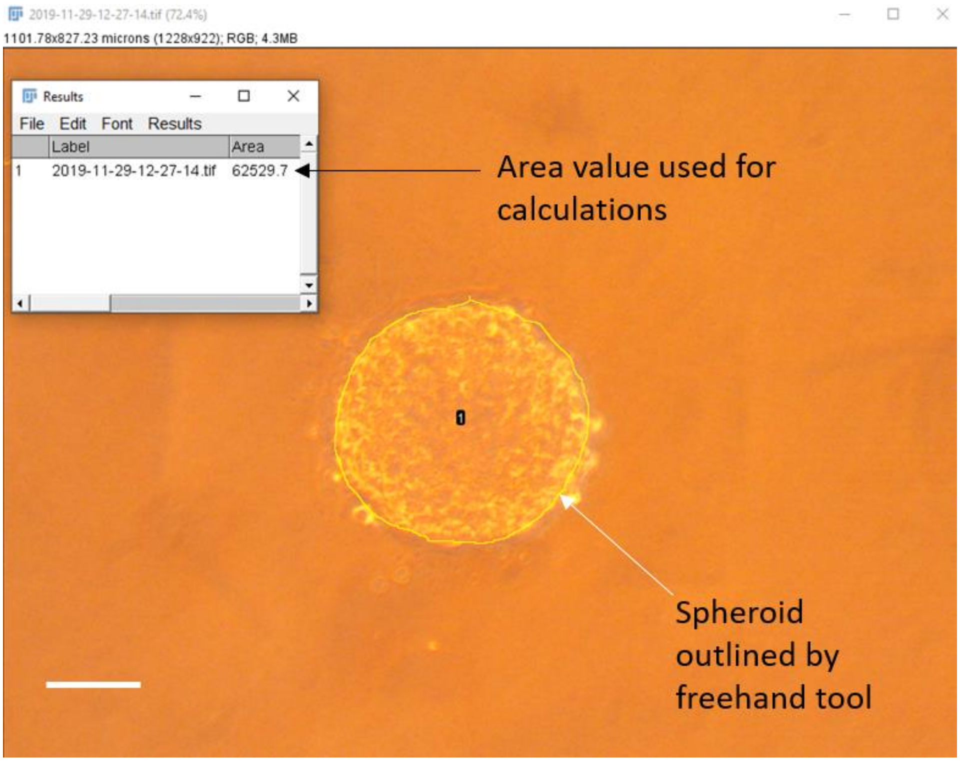

Figure 6.1: Representative Spheroid following 96 hour incubation

Figure denotes a screenshot representative of the spheroid measurement process. Images were opened using Image J software and freehand tool used to trace the circumference of the spheroid (yellow outline). Following this, the area traced was measured by pressing the M key. This created the output window visible in the top left of the figure, which contained the label of the image being quantified and the area of the traced zone. Scale bar = 100µm.

Measured area (A) was then used in the following equations to calculate estimated spheroid radius (r), Diameter (d) and Volume (v).

Radius = $\sqrt{\frac{A}{\pi}}$

Diameter = 2r

Volume = $\frac{4}{3}\pi r^3$

The volume calculated from these equations was then normalised as 100% for each individual spheroid, thus accounting for any heterogeniety in starting spheroid size. Immediately after imaging, cells were treated with vehicle, 10nM vincristine or co-treated with G6, HG1 or S31 (0.1-3µM) for a further 72 hours after which they were imaged and processed using the same basic method previously described above. However, spheroids treated with chemotherapy agents often display a “halo” of cellular debris and apoptotic cells which do not retain the tight conformation of the spheroid seen in figure 6.1. Therefore, for measurements of treated spheroids, only the internal, tight morphological structure was traced. An example of how freehand area selection was applied to disrupted spheroids following treatment can be seen in Figure 6.2.

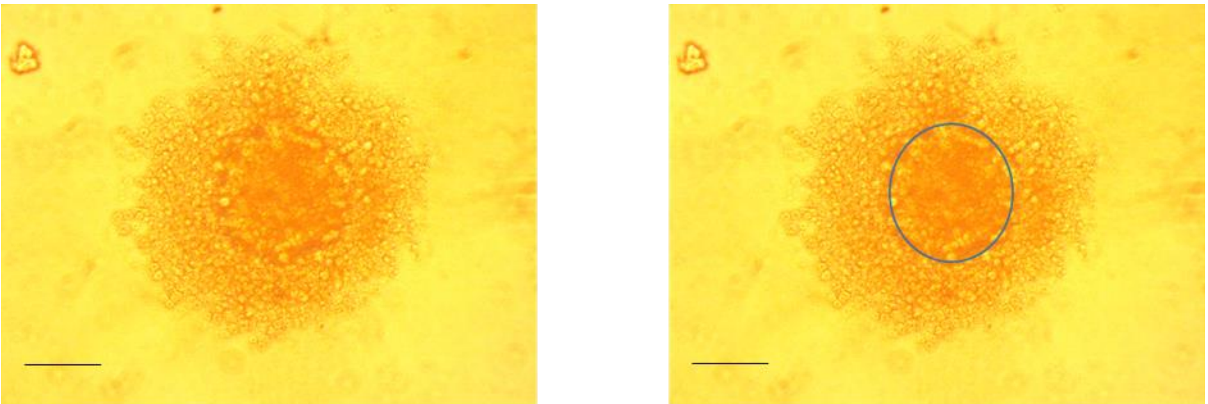

A B

Figure 6.2: Representative image of vincristine treated spheroid

(A) Spheroid retains a clearly defined circumference within the larger “halo” of cellular debris. (B) The same spheroid, with a blue circle denoting the area that was traced for measurement and used in spheroid growth calculations. Traced area measured as in figure 6.1. Scale bar = 100µm.

The radius, diameter and estimated volume of the spheroids calculated after treatment was then expressed as relative to the volume (normalised to 100%) before treatment to assess the effects of kinase inhibitor treatment, and possible effects on vincristine activity. Statistical analysis was then carried out using Graphpad Prism.

6.3.1: Vincristine mediated reduction in ONS76 spheroid growth is not attenuated by co-treatment with SPHINX31. SPHINX31 does not reduce spheroid growth independently.

ONS76 cell spheroids grew uniformly across the initial 96 hour timeframe prior to SPHINX and vincristine treatment (Fig 6.3). ONS76 cell spheroids co-treated with all concentrations of SPHINX31 and vincristine (Fig 6.3) exhibited inhibited growth that was comparable to vincristine treatment alone (F (9, 18 = 22. 42 p = 0.0001) which was significantly reduced compared to vehicle. However there was no evidence of SPHINX31 potentiating vincristine reductions in volumetric growth in a synergistic manner. Additionally, cells treated with SPHINX31 alone did not grow significantly larger than spheroids that were subject to vehicle treatment only, however there was no reduction in spheroid growth as a result of independent SPHINX31 treatment.

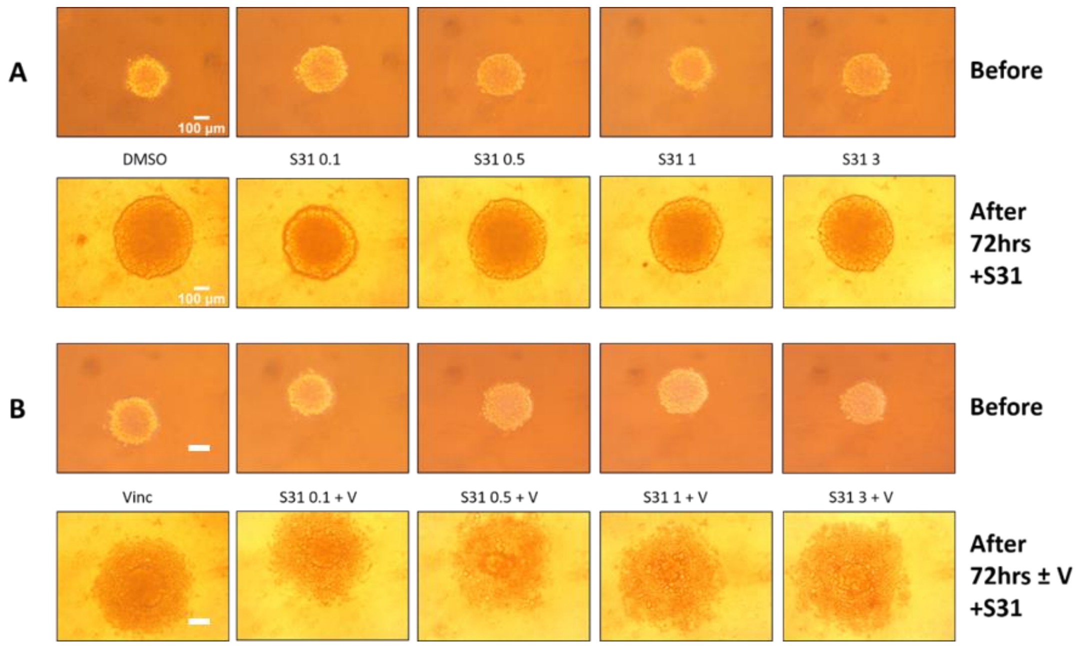

Fig 6.3: ONS76/SPHINX31 Spheroid Images

(A) ONS76 cell spheroids 96 hours post seeding immediately before and 72 hours after the application of SPHINX31 as an independent treatment. Scale bar = 100µm
(B) ONS76 cell spheroids 96 hours post seeding, immediately before and 72 hours after the application of vincristine or vincristine and SPHINX31 as a co-treatment.

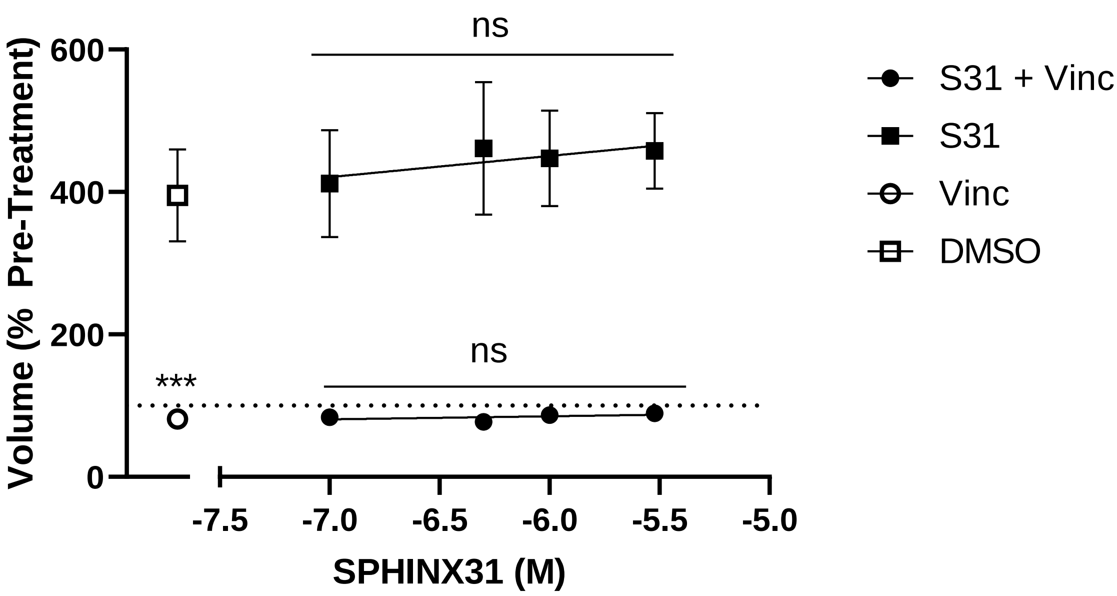

Fig 6.4*: Impact of SPHINX31 treatment on ONS76 volumetric spheroid growth*
ONS76 cell spheroid growth following 72 hour treatments with vehicle, vincristine, SPHINX31 or a co-treatment of both SPHINX31 and vincristine. Spheroid volume following treatment is expressed as a percentage of the estimated volume for the same spheroid calculated from images taken immediately prior to treatment, which was normalised as 100%. This is represented by the dotted line. Data presented is from n=3 plate repeats containing 6 internal replicates per treatment, per plate. All data is mean ± SEM. SEM data for vincristine and vincristine + SPHINX31 is was smaller than the size of symbol. Two way ANOVA with Tukey's Multiple Comparisons *** p = 0.0002 Vinc v DMSO.

6.3.2: Vincristine mediated reduction in ONS76 spheroid growth is not attenuated by co-treatment with Griffin 6. Griffin 6 does not reduce spheroid growth independently.

ONS76 cells grew uniformly across the initial 96 hour timeframe prior to treatment with vincristine and the CLK specific inhibitor Griffin 6 (Fig 6.5). ONS76 spheroids treated with vincristine alone demonstrated significantly reduced volumetric cell growth compared to vehicle. When applied independently, Griffin 6 at all concentrations did not reduce spheroid growth compared to vehicle, though there was no significant increase in spheroid growth in Griffin 6 treated spheroids. Additionally, the inhibition of growth in vincristine and Griffin 6 co-treated spheroids was comparable to independent vincristine treatment, with neither a statistical increase nor decrease in growth observed.

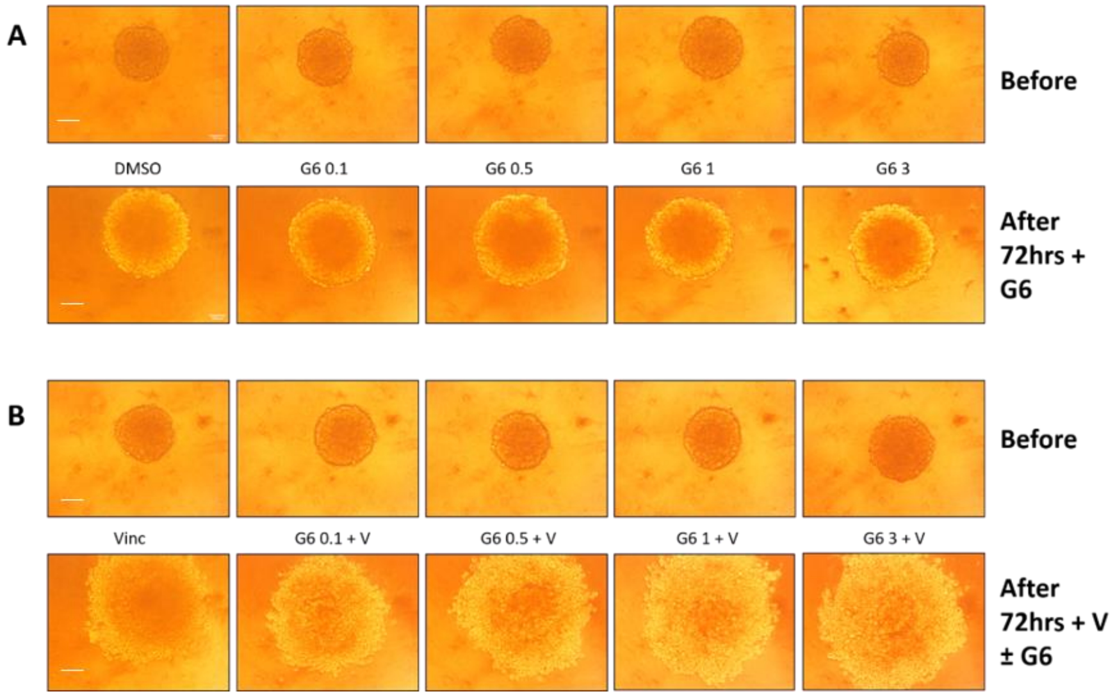

Fig 6.5: ONS76/Griffin 6 Spheroid Images:
(A) ONS76 cell spheroids 96 hours post seeding immediately before and 72 hours after the application of Griffin 6 as an independent treatment. Scale bar = 100µm
(B) ONS76 cell spheroids 96 hours post seeding, immediately before and 72 hours after the application of vincristine or vincristine and Griffin 6 as a co-treatment. Scale bar = 100µm.

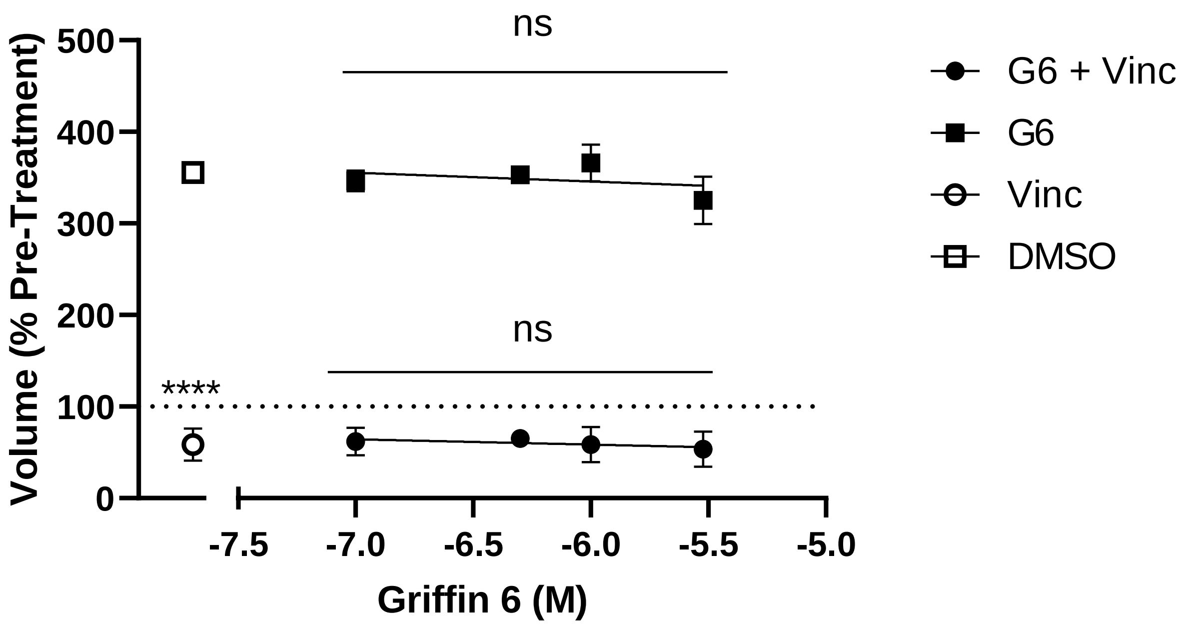

Fig 6.6: Impact of Griffin 6 Treatment on ONS76 Spheroid Growth

ONS76 cell growth following 72 hour treatments with vehicle, vincristine, Griffin 6 or a Griffin 6 and vincristine co-treatment. Spheroid volume following treatment is expressed as a percentage of the estimated spheroid volume for the same spheroid calculated from images taken immediately prior to treatment which was normalised as 100%. This is represented as the dotted line.. Data presented is from n =3 plate repeats with 6 internal replicates per treatment, per plate. All data is mean ± SEM. Where error bars are not visible, this is due to the bars being smaller than the height of the symbol. Two Way ANOVA with Tukey's multiple comparisons, **** p = <0.0001 Vinc v DMSO. Ns = DMSO vs G6 0.1-3µM, Ns = Vinc vs G6 0.1-3µM + Vinc.

6.3.3 Vincristine mediated reduction in ONS76 spheroid growth is not attenuated by co-treatment with Hippogriff 1. Hippogriff 1 does not reduce spheroid growth independently.

ONS76 cell spheroids grew uniformly across the initial 96 hour growth period prior to treatment with vincristine and the multiple splicing kinase inhibitor Hippogriff 1 (Fig 6.7), ONS76 spheroids treated with vincristine alone demonstrated significantly reduced volumetric growth across the 72 hour treatment period than vehicle treated spheroids. When applied as an independent treatment, Hippogriff 1 at all concentrations neither significantly increased nor decreased volumetric cell growth in comparison to vehicle. In spheroids where Hippogriff 1 was used in a co-treatment with vincristine reduction in volumetric spheroid growth was comparable to the independent vincristine treatment control with no significant difference detected at any concentration of Hippogriff 1 co-treatment (Figure 6.8).

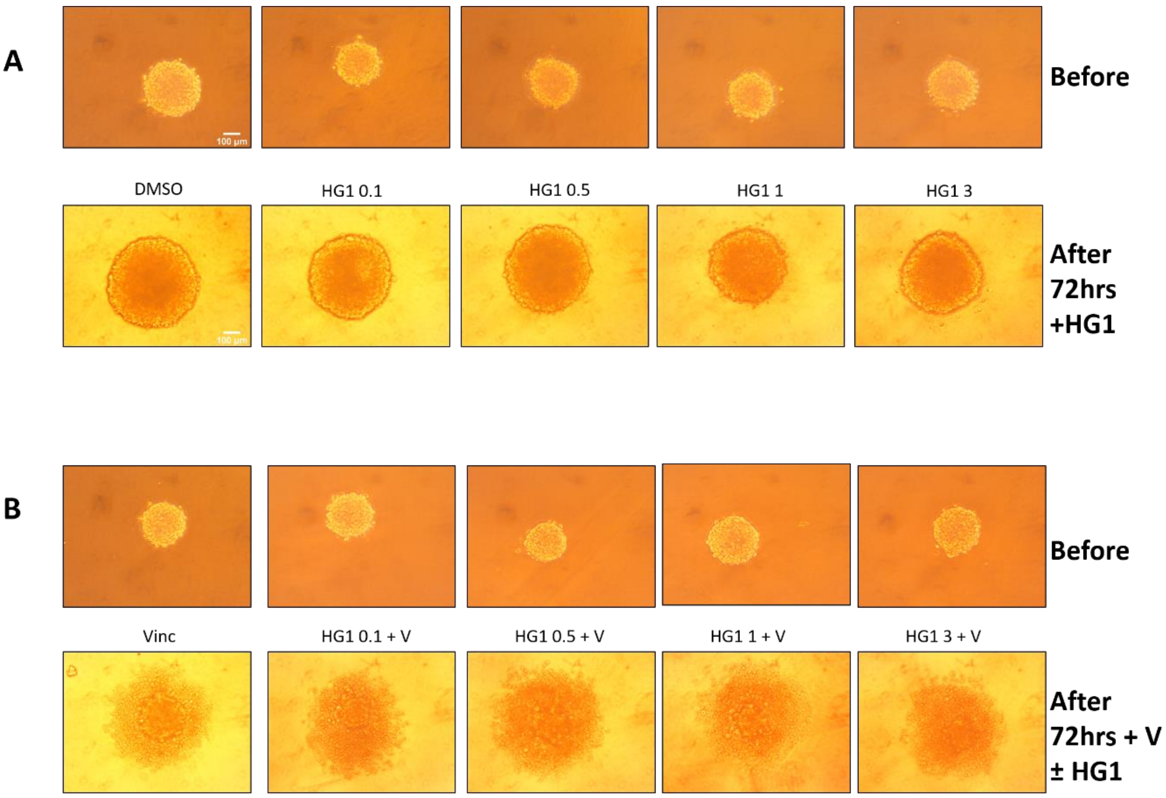

Fig 6.7: ONS76/Hippogriff 1 Spheroid Images
(A) ONS76 cell spheroids 96 hours post seeding and immediately before and 72 hours after the application of Hippogriff 1 as an independent treatment. Scale bar = 100µm.
(B) ONS76 cell spheroids 96 hours post seeding and immediately before and 72 hours after the application of vincristine alone, or vincristine and Hippogriff 1 as a co-treatment.

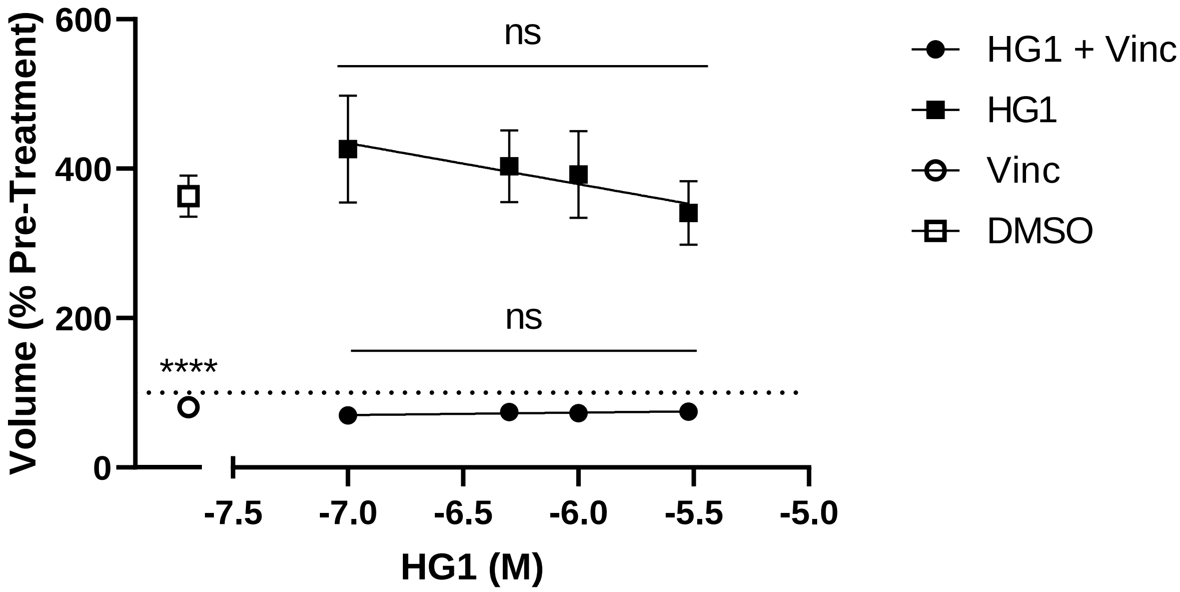

Fig 6.8: Impact of Hippogriff 1 treatment on ONS76 spheroids

ONS76 cell spheroids following 72 hour treatments with vehicle, vincristine alone, Hippogriff 1 or a co-treatment of vincristine and Hippogriff 1. Spheroid volume following treatment is expressed as a percentage of the estimated spheroid volume for the same spheroid calculated from images taken immediately prior to application of treatment which was then normalised to 100%. This is represented by the dotted line. Data presented is from n=3 plate repeats with 6 internal replicates per treatment, per plate. Data shown are mean ± SEM. Error bars for vincristine and vincristine + Hippogriff 1 co-treatments are no visible as they are smaller than the symbol. Two Way ANOVA with Tukey's multiple comparisons: Vinc v DMSO **** p = <0.0001, V+ HG1 (0.1-3µM) = Ns, DMSO v HG1 (0.1-3µM) = Ns

6.4: Discussion

Whilst there remains a deficit in effective treatments for CIPN there has been a myriad of investigations into potential therapeutic agents with which to combat its damaging effects. However, many of these potential treatments are often concomitant with severe side effects themselves or lack efficacy when applied to CIPN caused by a range of antineoplastic agents. (Gadgi*l et al*, 2019) Much of this can be attributed to the lack of clear understanding of CIPN aetiology and how different mechanisms of the condition may be triggered by the differential properties of a variety of antineoplastic agents. It also reflects upon the various pre-clinical models used to assess adverse effects of CIPN treatments, many of which rely on monolayer cultures or relatively outdated techniques (Argyriou *et al.*, 2014). For example, erythropoietin (EPO) was found to moderately restore nerve conduction velocity and provide protection to IENFs in rodent models of taxane and platinum based chemotherapy in addition to reducing the severity of anaemia of both ovarian and oesophageal cancer patients in clinical trials (Beijers, Jongen and Vreugdenhil, 2012). However, there is substantial evidence that EPO supports anti-apoptotic behaviour and even supports tumour growth, leading to concern among clinicians as to its efficacy as a counter-CIPN agent (Wolf *et al.*, 2008).

In order to avoid this conflict, it is essential to identify as many possible contraindications as possible at the pre-clinical stage and utilising the most effective and contemporary models to do so. Utilising a 3D medulloblastoma spheroid model with which to assess the effects of novel splicing kinase inhibitors in relation to both the cancer cells themselves and in relation to the efficacy of the vincristine treatment meets this criteria on multiple levels. Additionally, the flexibility of the model results in a relatively high-throughput assay for testing multiple potential treatments on one plate both in the presence and absence of an anti-neoplastic agent. The latter aspect of this model allows for assessment of the ability of the kinase inhibitors to reduce the volumetric growth of cancerous spheroid although this effect was not demonstrated in the context of medulloblastoma, there is now considerable data within the literature to suggest these effects may be present in other cancer cell types particularly those which have been shown to engage in elevated alternative splicing pathways such as prostate cancer.

6.4.1: SRPK1 Inhibition does not reduce medulloblastoma spheroid growth independently, but does not inhibit the efficacy of vincristine

Using the ONS76 cell spheroid model, I have successfully demonstrated that co-treatments of SPHINX31 and vincristine were able to inhibit the volumetric growth of spheroids whilst independent SPHINX31 treatment did not recapitulate these effects. However, the observed volumetric cell growth was not elevated above vehicle indicating that SRPK1 inhibition in the context of medulloblastoma does not result in elevated neoplastic activity in a manner similar to the aforementioned recombinant EPO. As a result, based on this pre-clinical data I have shown that SPHINX31 and SRPK1 inhibition as a principle has potential to be an adjunct therapy to vincristine in the treatment of medulloblastoma, reducing the adverse effects of chemotherapy whilst not reducing the efficacy of vincristine as an anti-cancer agent. Although the data presented exhibit a negligible effect of SRPK1 inhibition on reducing spheroid growth, the principle should not be discounted out of hand that kinase inhibition as a potential anti-cancer strategy could be used as a treatment independent of traditional chemotherapy. It is also likely that the efficacy of SRPK1 as a novel therapeutic strategy may be greatly influenced by the context of the specific tumour type the inhibitors are used within.

SRPK1 and its influence on alternative splicing have been observed in multiple tumour types and identified as a viable therapeutic target in many pre-clinical studies. Activation of the SRPK1-SRSF1 pathway has been shown in keratinocytes in a pre-clinical model of Human Papillomavirus (HPV) infection. HPV infects epithelial cells and predominantly causes the development of benign warts, however subsets of the virus are responsible for the majority of worldwide cervical cancers. Within infected cells, SRPK1-SRSF1 activity was found to influence the regulation of viral gene expression facilitating viral replication and possible progression to tumour phenotypes. Knockdown and therapeutic inhibition of SRPK1 via another novel splicing kinase inhibitor SRPIN340, was found to reduce SRSF1 levels within the keratinocyte nucleus in spite of putative upregulation of SRPK1 due to HPV infection (Mole *et al.*, 2020). Furthermore in studies of gastric cancer (GC), SRPK1 was found via immunohistochemistry to be upregulated in the majority of paired tissue samples from GC patients. Further investigation into the role of SRPK1 in GC cell lines revealed universally high SRPK1 expression which when knocked down using siRNA significantly reduced colony formation and *in vivo* xenograft tumour size. However there is a lack of comparative literature on SRPK1 demonstrating similar effects within the context of SHH medulloblastoma, to my knowledge, this is the first time that SPHINX31 or even SRPK1 inhibition has been used on SHH group medulloblastoma cells either as a co-treatment or as an independent treatment. The above experiments therefore are one among a paucity of studies investigating the potential role of SRPK1 in brain tumours. The reasons for this could at least in part be due to the myriad attractive targets suggested as major mediators of medulloblastoma taking preference.

Despite the lack of studies centred on SRPK1 within medulloblastoma, SPHINX31 itself has already been used in pre-clinical studies as a putative cancer treatment. For instance a study into acute myeloid leukaemia (AML) demonstrated that SPHINX31 had the capability to reduce cancer cell proliferation in a number of different leukaemia cell lines (Tzelepis *et al*, 2018). This was supported by the fact that SPHINX31 treatment and subsequent SRPK1 inhibition led to alternative splicing in a number of genes responsible for the maintenance and further development of AML. This includes one of the most influential moderators of AML, *BRD4.* Prominently, SPHINX31 was also found to work synergistically with clinical trial stage AML bromodomain inhibitors with minimal toxicity *in vivo*, further corroborating the potential of SPHINX31 as an adjunct treatment as outlined by the data above. Another cancer that has highlighted the potential of SPHINX31 as a standalone treatment is prostate cancer. SRPK1 governed VEGF-A_{165}a expression is elevated in prostate cancer and has been implicated both in late stage disease and metastasis. However, using 2 novel inhibitors of SRPK1, the aforementioned SRPIN340 and SPHINX31 a recent study demonstrated that prophylactic treatment of PC3 cells with SRPIN340 and SPHINX31 significantly reduced EGF induced SRSF1 phosphorylation *in vitro*. (Oltean *et al.*, 2012) Additionally, administration of SPHINX31 to mice with PC3 tumour xenografts was found to significantly reduce tumour growth as a therapeutic agents, rather than prophylaxis. Both of these studies indicate that when applied to cancer with clear SRPK1 related pathogenesis, SPHINX31 and SRPK1 inhibition as a whole has clear pre-clinical benefit in a variety of *in vitro* and *in vivo* models.

Whilst data from these studies is promising, the data I have displayed regarding the use of SPHINX31 as a potential anti-medulloblastoma treatment itself does not replicate these findings. Though as mentioned previously, this is likely not surprising due to the lack of clarity regarding the role of SRPK1 in the development of brain tumours. Indeed the fact that the specific nature of angiogenesis and tumour microvasculature within medulloblastoma sub-types is relatively poorly understood compared to other tumours, even though many studies have clearly demonstrated there is reasonably high VEGF expression in medulloblastoma tissues. Additionally, comparative to other tumours, the links between prognosis of medulloblastoma cases and levels of angiogenesis have proved difficult to establish. However, recent studies have linked increased vascularity of group 3 medulloblastoma tumours in xenograft rodent models to decreased survival. (Thompso*n et al*, 2017) This is logical, as group 3 tumours have a much higher metastasis rate than other sub-types but this does not elucidate on the nature and aetiology of aberrant angiogenesis in sub-types with lower metastasis association such as SHH and cell lines derived from these tumours, such as ONS-76 cells. (Grizzi, Weber and Di Ieva, 2008) Furthermore, anti-VEGF therapies such as bevacizumab have proved to have limited efficacy in treating brain tumours in addition to causing a range of side effects due to the abolition of VEGF mediated cytoprotection and possibly neuroprotection. (Guyot *et al.*, 2016) A study of angiogenesis related growth factors in medulloblastoma revealed the diversity of genes and angiogenic mediators potentially involved in increased tumour vascularity including VEGF-A, VEGF-B, VEGF-C, ANG proteins, TGF and FGF. (Menyhárt, Giangaspero and Gyorffy, 2019) Thus it is prudent to suggest targeting just one of these families, VEGF-A via SRPK1 in the case of SPHINX31 without in-depth knowledge of the key mediators of medulloblastoma growth comparative to AML and prostate cancer may not be sufficient to disrupt the growth of medulloblastoma cells. This hypothesis could in turn possibly explain the lack of impact that SPHINX31 had as an independent treatment on ONS-76 spheroids, particularly as ONS-76 cell characterisation has focused primarily on cell surface proteins, and *in vivo* tumorigenic capacity rather than in-depth analyses of splicing processes related to angiogenesis resulting in the role of splicing inhibition within this context being obscured (Bonfim-Silva *et al.*, 2019).

Another possible factor behind the insensitivity of ONS-76 cells to SRPK1 inhibition via SPHINX31 treatment could be related to the concentration range used within the assay. SPHINX31 in these experiments was used at concentrations where it was effective in other assays involving neurons, conferring neuroprotection and reducing vincristine induced sensitisation as presented in Chapter 4 and Chapter 5. These concentrations may therefore not be appropriate in an assay on a different cell type and measuring a different output. There are also examples in the literature of SPHINX31 IC50 being subject to cell type heterogeneity. For example the aforementioned Tzelepis et al. observed large variations in recorded IC50s for reducing proliferation across a range of different leukaemia cell lines, with the most vulnerable lines having an IC50 that was approximately 70 fold lower than the most resistant cell line. Therefore it is reasonable to hypothesise that the fairly narrow range of concentrations used in the spheroid assays, chosen to match neuronal assays may not cover the range required to induce effects on ONS-76 spheroids that would reduce volumetric growth (Tzelepis *et al*, 2018). Further to this, SRPK1 inhibition influences several components of oncogenesis that are removed from promotion of aberrant angiogenesis. Inhibition of SPRK1 via SPHINX31 in endometrial carcinoma cell lines (EC) and the subset endometrial neoplasm, uterine serous cancer (USC) was found to alter the expression of ~2200 genes including significant downregulation of the prominent oncogenic target MYC (c-MYC) which is highly associated with aggressive ECs and poor prognosis. The role of MYC in medulloblastoma is varied, with Group 3 subsets the most aggressive and readily metastatic tumours demonstrating significantly higher MYC amplification than their SHH counterparts, which are canonically less aggressive and usually present without metastasis. ONS-76 cells, which therefore pertain to the latter subset would be unlikely to be sensitive to any SRPK1 inhibition relating to MYC downregulation that would culminate in apoptosis, due to the already low amplification of the oncogene within this tumour types which may partially explain the absence of effect on spheroids. Effects on MYC could bolster the rationale behind using SPHINX31 against prostate cancer, as in addition to their established vascularity, prostate tumours are found to have elevated MYC expression in both early and developmental stages of the cancer.

Despite these factors limiting SPHINX31 as an independent treatment for SHH medulloblastoma, the clear impact of SPHINX31 as part of a co-treatment with vincristine is highly encouraging. No disruption to the activity of vincristine is observable as a result of SPHINX31 treatment, when this is taken into consideration with the neuroprotection and reduction in sensitisation conferred by provided by

SPHINX31 treatments demonstrated in Chapter 4 and Chapter 5, it suggests viability of SPHINX31 as an adjunct agent to vincristine.

6.4.2 CLK/DYRK1 Inhibition does not reduce medulloblastoma spheroid growth independently, but does not inhibit the efficacy of vincristine

In a similar fashion to SPHINX31, I have shown the specific CLK inhibitor Griffin 6 to be successful in reducing spheroid growth as part of a co-treatment with a traditional chemotherapy agent. Co-treatment with Griffin 6 and vincristine recapitulated the inhibited growth demonstrated by vincristine treatment alone at all Griffin 6 concentrations. This again serves as preliminary confirmation that Griffin 6 is a viable treatment option for use in patients suffering with CIPN, without compromising the efficacy of their chemotherapy regimen. As an independent treatment, Griffin 6 did not induce spheroid growth above that of vehicle providing further evidence of the relative safety of the compound compared to other suggested CIPN treatments. The lack of efficacy of Griffin 6 in reducing spheroid growth within this model is of note, as CLK inhibiting drugs have been effective in many recent studies with some reaching clinical trials (Xu *et al.*, 2016). However, we believe these data represent the first use of a specific CLK inhibitor as a treatment of SHH medulloblastoma cells. As such, although the results shown did not display the viability of Griffin 6 or CLK inhibition as an independent therapy the exact nature as to why this might be the case may yet be revealed in further studies which reveal the extent to which CLKs activity has an influence in the development, maintenance and progression of various cancer types.

The importance of CLK activity and potential as a therapeutic target for cancer has recently been investigated in detail by several studies. As previously mentioned, CLK interactions with SRPK1 and SRSF1 within nuclear speckles are crucial in dictating the process of alternative splicing in both healthy and pathological functions. (Aubol et al., 2018) Recently, a study identified CLKs as major mediators of tumour resistance to therapy, due to their increased expression in hypoxia (Bowler *et al.*, 2018). This effect was identified in prostate, colon and breast cancer cells. Additionally, as a result of this elevated expression, the alternative splicing of 12 genes related to tumour suppression, management of cytoskeleton and cell motility were found to be altered by more than 25% suggesting that CLK may play a major role in how cancer cells adapt to varying conditions. (Arak*i et al*, 2015) Furthermore, CLK inhibition using novel splicing inhibitors other than Griffin 6 has been carried out on Non-Small Cell Lung Carcinoma (NSCLC) A549 cells, a colorectal cancer cells line, HCT116 and a breast cancer cell line, MDA-MB-468. CLK inhibition using 3 novel compounds specific for CLKs was found to significantly reduce the phosphorylation of SR proteins and increased nuclear speckle size within breast cancer cells. (Tam *et al.*, 2020). CLK inhibition was also found to significantly alter the splicing of the S6K kinase, heavily linked canonically to protein synthesis and cell proliferation and observable in a number of breast cancer cell lines. CLK inhibition following use of the 3 novel compounds described in the paper was found to reduce proliferation of the breast cancer cell line (Iwai *et al.*, 2018). The authors further confirmed the role of CLK in modulating the splicing of S6K and a novel interaction between CLK inhibition and potential sensitivity of MYC driven cancers to CLK inhibition, a process that has been suggested often in literature as a therapeutic avenue, due to the fact MYC itself is difficult to target and proposed interventions in MYC based cancers have been hypothesised as having to target the downstream effects of MYC at the mRNA level.

Interestingly, though SHH medulloblastoma expression of n-myc and myc-l is considerably higher than that of other sub-groups and elevated expression of these two genes is heavily associated with poorer prognosis, expression of canonical c-Myc as mentioned previously is lower in SHH tumours. Curiously, despite the prevalence of n-myc expression in SHH tumours, a study of ONS-76 cells also revealed there was an absence of n-myc expression in cell line representing a failure of the cell line to mirror a common aberration present *in situ.* (Roussel and Robinson, 2013). It is therefore logical to suggest that Griffin 6 mediated inhibition of CLK, itself a key component of the splicing process within the cell would have limited anti-cancer properties in a cell line derived from a low metastasis risk sub-group in the form of SHH signalling and with low expression of MYC (Chaturvedi *et al.*, 2019), (Veo *et al.*, 2019). In both the case of SPHINX31 and Griffin 6 it is possible both compounds could have a more profound effect on the Group 3 medulloblastoma subset, which demonstrates considerable MYC overexpression.

To conclude, though not necessarily observed in these experiments, CLK inhibition represents and increasingly intriguing area of investigation in cancer research. Here we have demonstrated that Griffin 6, a CLK specific kinase inhibitor can potentially be used safely as a therapeutic for CIPN in a co-treatment with a traditional chemotherapy agent, vincristine and neither encourages growth of the spheroid nor compromises the effectiveness of vincristine as a chemotherapy agent. Further enhancing the potential of Griffin 6 as an agent to challenge the growing burden of CIPN.

In alignment with the two previously described compounds, treatment of ONS76 cell spheroids with Hippogriff 1 as a co-treatment with vincristine did not reduce the efficacy of the chemotherapy agent in disrupting the spheroid. Neither did the compound reduce or increase spheroid growth as an individual treatment. As such, it can be said that Hippogriff 1 appears to be suitable for use as an anti-CIPN adjunct therapy alongside traditional chemotherapy agents based on the *in vitro* evidence provided. However, as opposed to the other two compounds examined, Hippogriff 1 is unique in that it is an inhibitor of more than one family of splicing kinases, the CLK family as previously discussed and the DRYK1a kinase. Comparatively to the other kinases mentioned, the role of DYRK1 in cancer and indeed, regular biological functions is much more poorly understood with the majority of studies assessing the role of the kinase in neurodegenerative conditions such as Alzheimer's and the development of Down Syndrome due to the locus of the *DYRK1A* gene falling within the Down Syndrome (DS) critical region and the onset of the condition following over expression of the kinase. (Fernández-Martínez, Zahonero and Sánchez-Gómez, 2015) However, DS patients have been found to have a higher prevalence of specific leukaemia cancer subsets such as acute lymphoblastic leukaemia (ALL), sparking speculation that DYRK1A may be a valid therapeutic target for cancer therapy. This was demonstrated within more recent studies which have found strong evidence linking DYRK1A to a controlling role in the cell cycle and overexpression of DYRK1 has been identified in a number of tumours (Li *et al.*, 2019). The prevalence of DRYK1A has been identified as both a tumour suppressor and as a pro-oncogenic mediator in differential brain tumours and thus it is perhaps surprising that no such effects were observed when Hippogriff 1 was applied to a medulloblastoma cell line. For instance, effects of DRYK1A activity have been observed in the Sonic Hedgehog signalling pathway, where the kinase was responsible for retention of GLI1 within the nucleus, GLI1 is a major mediator of the SHH pathway and retention of GLI1 within the nucleus predisposes tumours to proliferation and metastatic activity. However, the exact mechanism by which DYRK1A achieves this and indeed the effects DYRK1 inhibition are yet to be fully elucidated (Jarhad *et al.*, 2018).

DYRK1A has also been found to be active in the caspase-9 apoptotic pathway in which it is responsible for the direct phosphorylation of the threonine 125, a site of caspase-9 inhibition and thus is capable of driving anti-apoptotic behaviour within cells. (Seifert, Allan and Clarke, 2008) Inhibition of the DYRK1A kinase by the β-carboline harmine was found to not only eliminate the phosphorylation of the threonine 125 site within HeLa cells but also prevent maturation of the DYRK1A kinase via reducing autophosphorylation essential for enzyme activity, demonstrating a dual efficacy of Harmine as an inhibitor. These effects were later replicated in further studies into harmine induced DYRK1 inhibition in the context of non-small cell lung carcinoma cell lines, which found harmine not only limited proliferation of cancer cells, but also potentiated the anti-cancer effects of the EGF tyrosine kinase inhibitor (EGF-TKI) AZD9291 in reducing cell growth (Li *et al.*, 2019). It is interesting a similar effect was not observed within the ONS76 spheroids following Hippogriff 1 treatment, though it should be noted the assays carried out in the confirmation of harmine activity on DYRK1 were done by traditional 2d monolayer assays such as propidium iodide staining and colony formation assays and as such they are subject to any and all of the limitations intrinsic to 2d assays that have been previously described. Elucidating the reason behind the absence of similar directly anti-cancer or indeed therapy potentiating responses of Hippogriff 1 within the spheroid model could potentially consist of a number of experiments at both the molecular and protein level to verify the DYRK1A phosphorylation state of threonine 125 following treatment with Hippogriff 1 which could mirror the concentration-dependent effect observed on the impact of a range of harmine concentrations. It would also be of immense value to assess the effects of Hippogriff 1 on DYRK1 related proteins such as the aforementioned GLI1 in SHH related tumours. However, as the main aim of this model was to assess the safety of Hippogriff 1 as a potential adjunct therapy and not primarily as an anti-cancer agent of itself these experiments serve as potentially important considerations for the development of Hippogriff 1 as a multifactorial therapeutic rather than of primary interest as a neuroprotective agent.

6.4.3: Concluding Statement

Application of vincristine to ONS-76 cells significantly disrupted the volumetric growth of the spheroid over a 72 hour period. This reduction in volumetric growth was not stymied or prevented when vincristine was applied in a co-treatment with either SPHINX31, Griffin 6 or Hippogriff 1 at concentrations that were found to be effective at reducing neuronal sensitisation and protecting neurite outgrowth. This therefore provisionally strengthens the possibility of using the compounds as adjunct treatments to limit the adverse effects of vincristine whilst maintaining an adequate level of growth reducing activity against cancerous cells. No novel splicing inhibitor compound effectively reduced ONS-76 volumetric cell growth, though it is likely this was due to a combination of ONS-76 cells being insensitive to kinase inhibition and the compound concentrations used not being in an effective range. Nonetheless, the fact that the kinase inhibitors as independent treatments did not enhance spheroid growth above vehicle is also encouraging and further suggests that the compounds will be safe to use in cancer patients either as adjunct treatments to reverse negative effects or as independent treatments against more sensitive tumour types.

7: Synthesis

Chemotherapy induced peripheral neuropathy is a growing healthcare burden that is exacerbated by a scarcity of adequate treatments to prevent or ameliorate neuropathic symptoms including pain, numbness and co-ordination deficits (Flatters, Dougherty and Colvin, 2017). This is largely due to the fact most existing analgesics do not alleviate symptoms, cannot prevent progressive damage from chemotherapy and that some of the most effective chemotherapy agents such as vinca alkaloids and taxanes are among the most neurotoxic agents in modern clinical use (Vencappa, Donaldson and Hulse, 2015; Luo *et al.*, 2019). Therefore, there is an urgent need to develop novel therapeutics that harness innovative approaches to chemotherapy induced pain which affects a majority of patients and in the case of some drugs, nearly all patients.

One such innovative approach is modulation and inhibition of alternative splicing kinases, which are already being investigated in multiple contexts including oncology and ophthalmology (Oltean *et al.*, 2012; Mavrou *et al.*, 2015; Donaldson and Beazley-Long, 2016). In this thesis I have detailed the design and optimisation of two *in vitro* models with which to assess the potential benefits of novel splicing kinase inhibition in the context of CIPN. Broadly, use of the vincristine sensitisation assay and vincristine induced neurite dieback model has demonstrated that there is a potential role for these novel splicing kinase inhibitors in the amelioration of the CIPN related sequalae. All compounds used displayed the capacity to significantly reduce acutely induced neuronal sensitisation (Section 4.3), though this conclusion potentially oversimplifies some subtle but important differences observed between the compounds and the kinases they inhibit. Firstly, Hippogriff 1 and Griffin 6 are both inhibitors of CLK1 and CLK2. Whilst Griffin 6 is CLK specific, Hippogriff 1 additionally inhibits DYRK1A, despite this there was a remarkable similarity between the two compounds and the response patterns observed (Sections 4.3.3.3 & 4.3.3.4) which suggests a lack of DYRK1A involvement in relation to vincristine induced neuronal sensitisation. This is further supported by evidence that Hippogriff 1 actually induces neurite dieback when applied to neurons as an independent treatment, (Section 5.3.5) the only compound to do so within the dieback model. This suggests that inhibition of the DYRK1A kinase is not appropriate in the treatment of CIPN as it appears to have at best no effect on sensitisation and induces neuronal damage and would likely exacerbate neuropathic symptoms. This is particularly interesting given a recent study found a potential anti-nociceptive and anti-inflammatory role for dual CLK/DYRK1A inhibition in a model of osteoarthritis ((Deshmukh *et al.*, 2019), this however highlights the need for condition specific approaches rather than broad spectrum analgesia across different nociceptive conditions which have largely failed up until this point. This study was also notable as DYRK1A was found to be largely acting on cartilage and inflammation within the arthritis model, rather than neurons themselves.

Inhibition of SRPK1 by SPHINX31 was successful in ameliorating neuronal sensitisation (4.3.3.1) and neurite dieback (Section 5.3.3). In the case of the former this corroborates previous work with the compound which demonstrated similar effects in prevention of neuronal activation via capsaicin (Blackley, 2019). In previous studies, the inhibitory effects of SPHINX31 on neuronal activation were shown to be VEGF-A_{165}b specific. It is reasonable to hypothesise this may also be a key factor in SPHINX31's ameliorating effect on vincristine induced sensitisation, though other factors such MNK2 and MYC could be also be important players in this function (Section 4.4.3.1). Dual inhibition of CLK1, CLK2 and SRPK1 with Griffin 23 (Section 4.3.3.2) also significantly reduced vincristine induced sensitisation, though in a different pattern to that of SPHINX31. The differences in the effects of Griffin 23, Griffin 6 and SPHINX31 potentially suggests that dual inhibition by Griffin 23 of both CLK and SRPK1 kinases at higher concentrations than 10µM could to reduce sensitisation further due to the combined inhibition of both kinases families which does not occur in Griffin 6 or SPHINX31 treatment. Whilst I was unable to test the effects of Griffin 23 in the dieback model, given that inhibition of SRPK1 with SPHINX31 and inhibition of CLK1/CLK2 with Griffin 6 did not induce neurite dieback as independent treatments, I hypothesise that combining this inhibition of these kinases with Griffin 23 would also not result in deleterious effects on neurites independently. I would also hypothesise that Griffin 23 treatment would ameliorate vincristine neurite dieback. Immediate future work would focus upon investigation of these hypotheses. Subsequent work would aim to elucidate the mechanisms behind the effects of CLK1/CLK2 and SRPK1 inhibition and the amelioration of vincristine induced neurite dieback. I discussed the possibility of putative roles for VEGF-A, S6K signalling, mTOR and the PI3K pathway (Section 5.4.3) in contributing towards this inhibitory effect on vincristine-induced neurite dieback, but further investigations involving RNA Seq and analyses of downstream targets of these pathways would help to uncover the specific mechanisms of alternative splicing kinase inhibition beyond the initial upstream targets of SRPK1 and CLK1/2.

Preliminary examination of Griffin 6, SPHINX31 and Hippogriff 1 in a cancer cell spheroid growth model revealed the compounds did not induce spheroid growth as independent treatments nor inhibit the ability of vincristine to halt and reduce spheroid growth. This demonstrates at an early stage the compounds are not likely to exacerbate tumour growth if given as an adjunct to chemotherapy. It was interesting that no compound demonstrated efficacy in reducing tumour growth independently, particularly as SRPK1 inhibition and CLK inhibition have been suggested as a potential oncology targets and demonstrated as effective in the context of prostate cancer and leukaemia (Mavrou *et al.*, 2015; Tzelepis *et al.*, 2018). However, it is important to consider both the concentrations used within the assay and the ONS76 medulloblastoma cell line used. It is reasonable to suggest the compounds may have anti-proliferative effects at higher concentrations, but such investigations were beyond the scope of this thesis. With regard to the ONS-76 cells used, this cell line has low MYC amplification, which has been suggested as an important target for approaches to cancer involving alternative splicing. Most importantly however, the compounds appear to have suitable properties for usage on a first pass experiment.

Another aspect of the work presented was to determine whether it is viable to screen novel chemotherapy agents for the potential to cause CIPN at an early stage of their development. For this, I used a novel chemotherapy agent currently in development, jerantinine. Though jerantinine shares many aspects of traditional vincristine chemotherapy, such as microtubule inhibition in previous studies it has been shown to be less damaging to non-cancerous neural stem cells in culture(Roper *et al.*, 2018; Smedley *et al.*, 2018). Assessment of the capacity of jerantinine to induce neuronal sensitisation (Section 4.3.2) and neurite dieback (Section 5.3.6) showed that the novel compound had reduced effects on neurons with the two assays. These effects could be mediated by the differential microtubule binding site occupied by the respective compounds. Whilst these data look encouraging it is important to consider jerantinine is in an extremely early stage of development at the pre-clinical stage. Therefore, the concentrations of jerantinine used in these assays may be too low or not therapeutically relevant and thus the assays must be repeated at higher concentrations to further examine the off-target neuronal effects of the compound. Further development of jerantinine is also severely hindered by its difficult synthesis process, which makes producing large volumes of the compound difficult. Therefore, whilst the data presented here is of relevance, the main benefit of the investigations is that I have demonstrated that preliminary comparisons can be drawn between novel and existing chemotherapy drugs in two relatively straightforward assays. This does not routinely occur in drug development but given the growing prevalence of CIPN in cancer survivors may become increasingly explored. Models such as those described provide important information for these studies at the earliest stages of development which may expedite treatments and reduce unexpected off-target neuronal symptoms.

To conclude, inhibition of alternative splicing kinases ameliorates vincristine induced sensitisation and neuronal damage. The compounds and the kinases they inhibit warrant future investigations into potential mechanisms underpinning these neuroprotective and anti-nociceptive effects. Translation of these models from *in vitro* assays to *in vivo* studies could additionally bolster these investigations.

7.1 Proposed future work:

Future work and directions for the findings outlined in this thesis include the development of an *in vivo* model of vincristine induced peripheral neuropathy and use of this model to examine the systemic effects of the novel splicing kinase inhibitors. This would also facilitate corroboration of the *in vitro* findings described in Chapter 4 and Chapter 5 in a translational model. Furthermore, use of RNA sequencing techniques on harvested tissue would help to elucidate the downstream targets of splicing kinase inhibition. This is turn would uncover mechanisms of sensitisation and neurite dieback that are ameliorated with adjunct therapy and in turn establish a list of genetic targets which are associated with CIPN sequelae. It would also be preferable in the future for the established vincristine models described to be adapted to investigate the effects of the inhibitors on other classes of chemotherapy such as taxanes and platinum based compounds whilst again adopting RNA sequencing approaches to uncover commonly or differentially implicated genes in the onset and progression of CIPN. Ultimately, the end result of pursuing these future directions would be to potentially create a firm pre-clinical basis and justification with which to trial the novel compounds in human patients for eventual use in the clinic to provide a potential tool with which to ameliorate the damaging and painful effects of CIPN.

References:

Abdel-Wahab, W. M. and Moussa, F. I. (2019) ‘Neuroprotective effect of N-acetylcysteine against cisplatin-induced toxicity in rat brain by modulation of oxidative stress and inflammation’, *Drug design, development and therapy*, 13, pp. 1155–1162. doi: 10.2147/DDDT.S191240.

Abe, N. *et al.* (2010) ‘Mammalian Target of Rapamycin (mTOR) activation increases axonal growth capacity of injured peripheral nerves’, *Journal of Biological Chemistry*, 285(36), pp. 28034–28043. doi: 10.1074/jbc.M110.125336.

Ackeifi, C. *et al.* (2020) ‘Pharmacologic and genetic approaches define human pancreatic β cell mitogenic targets of DYRK1A inhibitors’, *JCI Insight*, 5(1). doi: 10.1172/jci.insight.132594.

Addington, J. and Freimer, M. (2016) ‘Chemotherapy-induced peripheral neuropathy: An update on the current understanding [version 1; referees: 2 approved]’, *F1000Research*, 5, pp. 1–7. doi: 10.12688/f1000research.8053.1.

Ahlquist, M. L. and Frmzta, O. G. (1994) ‘Encoding of the subjective intensity of sharp dental pain’, *Dental Traumatology*, 10(4), pp. 153–166. doi: 10.1111/j.1600-9657.1994.tb00680.x.

Al-Ali, H. *et al.* (2017) ‘The mTOR substrate S6 kinase 1 (S6K1) is a negative regulator of axon regeneration and a potential drug target for central nervous system injury’, *Journal of Neuroscience*, 37(30), pp. 7079–7095. doi:

10.1523/JNEUROSCI.0931-17.2017.

Allen, S. E., Darnell, R. B. and Lipscombe, D. (2010) ‘The neuronal splicing factor Nova controls alternative splicing in N-type and P-type CaV2 calcium channels’, *Channels (Austin, Tex.)*. 2010/11/01, 4(6), pp. 483–489. doi: 10.4161/chan.4.6.12868.

AlQahtani, A. D. *et al.* (2019) ‘Strategies for the production of long-acting therapeutics and efficient drug delivery for cancer treatment’, *Biomedicine and Pharmacotherapy*, 113(January), p. 108750. doi: 10.1016/j.biopha.2019.108750.

Amaya, F. *et al.* (2013) ‘Tissue Injury and Related Mediators of Pain Exacerbation’, *Current Neuropharmacology*, 11(6), pp. 592–597. doi: 10.2174/1570159x11311060003.

Ambrosino, P. *et al.* (2013) ‘Activation and desensitization of TRPV1 channels in sensory neurons by the PPARα agonist palmitoylethanolamide’, *British Journal of Pharmacology*, 168(6), pp. 1430–1444. doi: 10.1111/bph.12029.

Van Amerongen, R. and Berns, A. (2006) ‘TXR1-mediated thrombospondin repression: A novel mechanism of resistance to taxanes?’, *Genes and Development*, 20(15), pp. 1975–1981. doi: 10.1101/gad.1460806.

Amin, E. M. *et al.* (2011) ‘WT1 Mutants Reveal SRPK1 to Be a Downstream Angiogenesis Target by Altering VEGF Splicing’, *Cancer Cell*, 20(6), pp. 768–780. doi: 10.1016/j.ccr.2011.10.016.

Andersen, L. B. and Schreyer, D. J. (1999) ‘Constitutive expression of GAP-43 correlates with rapid, but not slow regrowth of injured dorsal root axons in the adult rat’, *Experimental Neurology*, 155(2), pp. 157–164. doi: 10.1006/exnr.1998.6903.

André, N. and Meille, C. (2006) ‘Taxanes in paediatric oncology: And now?’, *Cancer Treatment Reviews*, 32(2), pp. 65–73. doi: 10.1016/j.ctrv.2005.12.010.

Araki, S. *et al.* (2015) 'Inhibitors of CLK protein kinases suppress cell growth and induce apoptosis by modulating pre-mRNA splicing', *PLoS ONE*, 10(1). doi: 10.1371/journal.pone.0116929.

Argyriou, A. A. *et al.* (2008) 'Peripheral nerve damage associated with administration of taxanes in patients with cancer', *Critical Reviews in Oncology/Hematology*, 66(3), pp. 218–228. doi: 10.1016/j.critrevonc.2008.01.008.

Argyriou, A. A. *et al.* (2014) 'Chemotherapy-induced peripheral neuropathy in adults: A comprehensive update of the literature', *Cancer Management and Research*, 6(1), pp. 135–147. doi: 10.2147/CMAR.S44261.

Arnold, M. *et al.* (2019) 'Progress in cancer survival, mortality, and incidence in seven high-income countries 1995–2014 (ICBP SURVMARK-2): a population-based study', *The Lancet Oncology*, 20(11), pp. 1493–1505. doi: 10.1016/S1470-2045(19)30456-5.

Ataoğlu, E. *et al.* (2013) 'Effects of chronic pain on quality of life and depression in patients with spinal cord injury', *Spinal Cord*, 51(1), pp. 23–26. doi: 10.1038/sc.2012.51.

Aubol, B. E. *et al.* (2013) 'Partitioning RS Domain Phosphorylation in an SR Protein through the CLK and SRPK Protein Kinases', *Journal of Molecular Biology*, 425(16), pp. 2894–2909. doi: https://doi.org/10.1016/j.jmb.2013.05.013.

Aubol, B. E. *et al.* (2016) 'Release of SR Proteins from CLK1 by SRPK1: A Symbiotic Kinase System for Phosphorylation Control of Pre-mRNA Splicing', *Molecular cell*. 2016/07/07, 63(2), pp. 218–228. doi: 10.1016/j.molcel.2016.05.034.

Avramis, I. A., Kwock, R. and Avramis, V. I. (2001) 'Taxotere and vincristine inhibit the secretion of the angiogenesis inducing vascular endothelial growth factor (VEGF) by wild-type and drug-resistant human leukemia T-cell lines.', *Anticancer* *research*, 21(4A), pp. 2281–2286.

Azimi-Nezhad, M. (2014) 'Vascular endothelial growth factor from embryonic status to cardiovascular pathology', *Reports of biochemistry & molecular biology*, 2(2), pp. 59–69. Available at: https://pubmed.ncbi.nlm.nih.gov/26989723.

Bain, P. G. *et al.* (1991) 'Intrathecal vincristine: a fatal chemotherapeutic error with devastating central nervous system effects', *Journal of Neurology*, 238(4), pp. 230–234. doi: 10.1007/BF00314787.

Ballmer-Hofer, K. *et al.* (2011) 'Neuropilin-1 promotes VEGFR-2 trafficking through Rab11 vesicles thereby specifying signal output.', *Blood*, 118(3), pp. 816–826. doi: 10.1182/blood-2011-01-328773.

Basbaum, A. I. *et al.* (2009) 'Cellular and molecular mechanisms of pain', *Cell*, 139(2), pp. 267–284. doi: 10.1016/j.cell.2009.09.028.

Bates, D. and Eastman, A. (2017) 'Microtubule destabilising agents: far more than just antimitotic anticancer drugs', *British Journal of Clinical Pharmacology*, 83(2), pp. 255–268. doi: 10.1111/bcp.13126.

Bates, D. O. *et al.* (2002) 'VEGF165b, an inhibitory splice variant of vascular endothelial growth factor, is down-regulated in renal cell carcinoma.', *Cancer research*, 62(14), pp. 4123–31. doi: 10.1038/35025220.

Batson, J. *et al.* (2017) 'Development of Potent, Selective SRPK1 Inhibitors as Potential Topical Therapeutics for Neovascular Eye Disease', *ACS Chemical Biology*, 12(3), pp. 825–832. doi: 10.1021/acschembio.6b01048.

Baumann, N. and Pham-Dinh, D. (2001) 'Biology of oligodendrocyte and myelin in the mammalian central nervous system', *Physiological Reviews*, 81(2), pp. 871–927. doi: 10.1152/physrev.2001.81.2.871.

Beazley-Long, N., Hua, J., Jehle, T., Hulse, R. P., Dersch, R., Lehrling, C., Bevan, H., Qiu, Y., Lagrèze, W. A., *et al.* (2013) 'VEGF-A165b is an endogenous neuroprotective splice isoform of vascular endothelial growth factor a in vivo and in vitro', *American Journal of Pathology*. doi: 10.1016/j.ajpath.2013.05.031.

Beazley-Long, N., Hua, J., Jehle, T., Hulse, R. P., Dersch, R., Lehrling, C., Bevan, H., Qiu, Y., Lagrèze, W. a., *et al.* (2013) 'VEGF-A165b is an endogenous neuroprotective splice isoform of vascular endothelial growth factor a in vivo and in vitro', *American Journal of Pathology*, 183(3), pp. 918–929. doi: 10.1016/j.ajpath.2013.05.031.

Beazley-Long, N. *et al.* (2018) 'VEGFR2 promotes central endothelial activation and the spread of pain in inflammatory arthritis', *Brain, Behavior, and Immunity*. doi: 10.1016/j.bbi.2018.03.012.

Beijers, A. J. M., Jongen, J. L. M. and Vreugdenhil, G. (2012) 'Chemotherapy-induced neurotoxicity: The value of neuroprotective strategies', *Netherlands Journal of Medicine*, 70(1), pp. 18–25.

Beissner, F. *et al.* (2010) 'Quick discrimination of A(delta) and C fiber mediated pain based on three verbal descriptors', *PloS one*, 5(9), pp. e12944–e12944. doi: 10.1371/journal.pone.0012944.

Belin, S. *et al.* (2015) 'Injury-induced decline of intrinsic regenerative ability revealed by quantitative proteomics', *Neuron*. 2015/04/30, 86(4), pp. 1000–1014. doi: 10.1016/j.neuron.2015.03.060.

Ben-Hur, V. *et al.* (2013) 'S6K1 alternative splicing modulates its oncogenic activity and regulates mTORC1', *Cell reports*. 2012/12/27, 3(1), pp. 103–115. doi: 10.1016/j.celrep.2012.11.020.

Benet, L. Z. *et al.* (2016) 'BDDCS, the Rule of 5 and drugability', *Advanced drug delivery reviews*. 2016/05/13, 101, pp. 89–98. doi: 10.1016/j.addr.2016.05.007.

Benton, R. L. and Whittemore, S. R. (2003) ‘VEGF 165 Therapy Exacerbates Secondary Damage following Spinal Cord Injury *’, 28(11), pp. 1693–1703.

Berbusse, G. W. *et al.* (2016) ‘Mitochondrial dynamics decrease prior to axon degeneration induced by vincristine and are partially rescued by overexpressed cytNmnat1’, *Frontiers in Cellular Neuroscience*, 10(JULY), pp. 1–8. doi: 10.3389/fncel.2016.00179.

Berlin, J. A., Glasser, S. C. and Ellenberg, S. S. (2008) ‘Adverse event detection in drug development: Recommendations and obligations beyond phase 3’, *American Journal of Public Health*, 98(8), pp. 1366–1371. doi: 10.2105/AJPH.2007.124537.

Bestall, S. M. *et al.* (2018) ‘Sensory neuronal sensitisation occurs through HMGB-1–RAGE and TRPV1 in high-glucose conditions’, *Journal of Cell Science*. doi: 10.1242/jcs.215939.

Bhatnagar, B. *et al.* (2014) ‘Chemotherapy dose reduction due to chemotherapy induced peripheral neuropathy in breast cancer patients receiving chemotherapy in the neoadjuvant or adjuvant settings: A single-center experience’, *SpringerPlus*, 3(1), pp. 1–6. doi: 10.1186/2193-1801-3-366.

Bhattacherjee, A., Liao, Z. and Smith, P. G. (2014) ‘Trophic factor and hormonal regulation of neurite outgrowth in sensory neuron-like 50B11 cells’, *Neuroscience Letters*. doi: 10.1016/j.neulet.2013.11.018.

Bidinosti, M. *et al.* (2016) ‘CLK2 inhibition ameliorates autistic features associated with SHANK3 deficiency’, *Science*, 351(6278), pp. 1199 LP – 1203. doi: 10.1126/science.aad5487.

Bjornard, K. L. *et al.* (2018) ‘Peripheral neuropathy in children and adolescents treated for cancer’, *The Lancet. Child & adolescent health*. 2018/09/01, 2(10), pp. 744–754. doi: 10.1016/S2352-4642(18)30236-0.

Blackley, Z. (2019) ‘Novel Mechanisms in Pain Processing : Involvement of Alternative mRNA Splicing’, (September).

Blanco, C. *et al.* (2020) ‘America’s opioid crisis: the need for an integrated public health approach’, *Translational Psychiatry*, 10(1), pp. 1–13. doi: 10.1038/s41398-020-0847-1.

Bodaleo, F. J. *et al.* (2016) ‘Microtubule-associated protein 1B (MAP1B)-deficient neurons show structural presynaptic deficiencies in vitro and altered presynaptic physiology’, *Scientific Reports*, 6(June), pp. 1–15. doi: 10.1038/srep30069.

Boiko, N. *et al.* (2017) ‘TrpA1 activation in peripheral sensory neurons underlies the ionic basis of pain hypersensitivity in response to vinca alkaloids’, *PLoS ONE*. doi: 10.1371/journal.pone.0186888.

Bonfim-Silva, R. *et al.* (2019) ‘Biological characterization of the UW402, UW473, ONS-76 and DAOY pediatric medulloblastoma cell lines’, *Cytotechnology*, 71(5), pp. 893–903. doi: 10.1007/s10616-019-00332-3.

Bonnie, R., Ford, M. and Phillips, J. (2017) *Pain Management and the Opioid Epidemic*, *Pain Management and the Opioid Epidemic*. doi: 10.17226/24781.

Bota, M. *et al.* (2019) ‘Combined effect of propranolol, vincristine and bevacizumab on HUVECs and BJ cells’, *Experimental and Therapeutic Medicine*, 17(1), pp. 307–315. doi: 10.3892/etm.2018.6925.

Bowler, E. *et al.* (2018) ‘Hypoxia leads to significant changes in alternative splicing and elevated expression of CLK splice factor kinases in PC3 prostate cancer cells’, *BMC Cancer*, 18(1), pp. 1–11. doi: 10.1186/s12885-018-4227-7.

van den Broeke, E. N., Lenoir, C. and Mouraux, A. (2016) ‘Secondary hyperalgesia is mediated by heat-insensitive A-fibre nociceptors’, *The Journal of physiology*. 2016/08/02, 594(22), pp. 6767–6776. doi: 10.1113/JP272599.

Bucchia, M. *et al.* (2018) ‘Limitations and challenges in modeling diseases involving spinal motor neuron degeneration in vitro’, *Frontiers in Cellular Neuroscience*, 12(March), pp. 1–8. doi: 10.3389/fncel.2018.00061.

Burbank, K. S. and Mitchison, T. J. (2000) ‘Quick guides Microtubule dynamic instability’, *Curr Biol*, 16(14), pp. 516–517.

Burger, R. A. *et al.* (2007) ‘Phase II trial of bevacizumab in persistent or recurrent epithelial ovarian cancer or primary peritoneal cancer: A Gynecologic Oncology Group study’, *Journal of Clinical Oncology*, 25(33), pp. 5165–5171. doi: 10.1200/JCO.2007.11.5345.

Buttiglione, M. *et al.* (2007) ‘Behaviour of SH-SY5Y neuroblastoma cell line grown in different media and on different chemically modified substrates’, *Biomaterials*, 28(19), pp. 2932–2945. doi: 10.1016/j.biomaterials.2007.02.022.

Calvo, P. M., Pastor, A. M. and de la Cruz, R. R. (2018) ‘Vascular endothelial growth factor: an essential neurotrophic factor for motoneurons?’, *Neural regeneration research*, 13(7), pp. 1181–1182. doi: 10.4103/1673-5374.235024.

Cassidy, P. B. *et al.* (2002) ‘Cyclooxygenase-2 induction by paclitaxel, docetaxel, and taxane analogues in human monocytes and murine macrophages: Structure-activity relationships and their implications’, *Clinical Cancer Research*, 8(3), pp. 846–855.

Caterina, M. J. *et al.* (1997) ‘The capsaicin receptor: A heat-activated ion channel in the pain pathway’, *Nature*, 389(6653), pp. 816–824. doi: 10.1038/39807.

Cavaletti, G. *et al.* (2019) ‘Chemotherapy-induced peripheral neurotoxicity: A multifaceted, still unsolved issue’, *Journal of the Peripheral Nervous System*, 24(S2). doi: 10.1111/jns.12337.

Cavalli, E. *et al.* (2019) ‘The neuropathic pain: An overview of the current treatment

and future therapeutic approaches', *International Journal of Immunopathology and Pharmacology*, 33. doi: 10.1177/2058738419838383.
Cella, D. *et al.* (2003) 'Measuring the side effects of taxane therapy in oncology: The Functional Assessment of Cancer Therapy-Taxane (FACT-Taxane)', *Cancer*, 98(4), pp. 822–831. doi: 10.1002/cncr.11578.
Center for Drug Evaluation and Research (CDER) and U.S. Food and Drug Administration (FDA) (2017) 'The Voice of the Patient: Neuropathic Pain Associated with Peripheral Neuropathy', (February).
Di Cesare Mannelli, L. *et al.* (2018) 'Adipose-derived stem cells decrease pain in a rat model of oxaliplatin-induced neuropathy: Role of VEGF-A modulation', *Neuropharmacology*. doi: 10.1016/j.neuropharm.2017.12.020.
Chambers, S. M. *et al.* (2012) 'Combined small-molecule inhibition accelerates developmental timing and converts human pluripotent stem cells into nociceptors', *Nature Biotechnology*, 30(7), pp. 715–720. doi: 10.1038/nbt.2249.
Chaturvedi, N. K. *et al.* (2019) 'Role of protein arginine methyltransferase 5 in group 3 (MYC-driven) Medulloblastoma', *BMC Cancer*, 19(1), pp. 1–11. doi: 10.1186/s12885-019-6291-z.
Chen, M. and Manley, J. L. (2009) 'Mechanisms of alternative splicing regulation: insights from molecular and genomics approaches', *Nature reviews. Molecular cell biology*. 2009/09/23, 10(11), pp. 741–754. doi: 10.1038/nrm2777.
Chen, S.-C. *et al.* (2007) 'Involvement of Substance P and Neurogenic Inflammation in Arsenic-Induced Early Vascular Dysfunction', *Toxicological Sciences*, 95(1), pp. 82–88. doi: 10.1093/toxsci/kfl136.
Chen, W. *et al.* (2007) 'Immortalization and characterization of a nociceptive dorsal root ganglion sensory neuronal line', *Journal of the Peripheral Nervous System*. doi:

10.1111/j.1529-8027.2007.00131.x.

Chen, W. *et al.* (2016) ‘Rapamycin-resistant mTOR activity is required for sensory axon regeneration induced by a conditioning lesion’, *eNeuro*, 3(6). doi: 10.1523/ENEURO.0358-16.2016.

Chen, Y., Li, G. and Huang, L. Y. M. (2012) ‘P2X7 receptors in satellite glial cells mediate high functional expression of P2X3 receptors in immature dorsal root ganglion neurons’, *Molecular Pain*. doi: 10.1186/1744-8069-8-9.

Chernov-Rogan, T. *et al.* (2018) ‘Mechanism-specific assay design facilitates the discovery of Nav1.7-selective inhibitors’, *Proceedings of the National Academy of Sciences*. doi: 10.1073/pnas.1713701115.

Chiang, H.-L., Wu, J.-Y. and Chen, Y.-T. (2017) ‘Identification of functional single nucleotide polymorphisms in the branchpoint site’, *Human genomics*, 11(1), p. 27. doi: 10.1186/s40246-017-0122-6.

Chiba, T. *et al.* (2017) ‘Vincristine-induced peripheral neuropathic pain and expression of transient receptor potential vanilloid 1 in rat’, *Journal of Pharmacological Sciences*, 133(4), pp. 254–260. doi: 10.1016/j.jphs.2017.03.004.

Clarke, K. E. *et al.* (2017) ‘A robust and reproducible human pluripotent stem cell derived model of neurite outgrowth in a three-dimensional culture system and its application to study neurite inhibition’, *Neurochemistry international*. 2016/12/21, 106, pp. 74–84. doi: 10.1016/j.neuint.2016.12.009.

Cohen, M. H. *et al.* (2007) ‘FDA Drug Approval Summary: Bevacizumab (Avastin®) Plus Carboplatin and Paclitaxel as First-Line Treatment of Advanced/Metastatic Recurrent Nonsquamous Non-Small Cell Lung Cancer’, *The Oncologist*, 12(6), pp. 713–718. doi: https://doi.org/10.1634/theoncologist.12-6-713.

Cohen, M., Quintner, J. and Buchanan, D. (2013) ‘Is Chronic Pain a Disease?’, *Pain*

Medicine, 14(9), pp. 1284–1288. doi: 10.1111/pme.12025.

Colloca, L. *et al.* (2017) ‘Neuropathic pain’, *Nature reviews. Disease primers*, 3, p. 17002. doi: 10.1038/nrdp.2017.2.

Constantin, C. E. *et al.* (2008) ‘Endogenous tumor necrosis factor alpha (TNFalpha) requires TNF receptor type 2 to generate heat hyperalgesia in a mouse cancer model’, *The Journal of neuroscience : the official journal of the Society for Neuroscience*, 28(19), pp. 5072–5081. doi: 10.1523/JNEUROSCI.4476-07.2008.

Cooke, J. P. (2019) ‘Inflammation and Its Role in Regeneration and Repair’, *Circulation research*, 124(8), pp. 1166–1168. doi: 10.1161/CIRCRESAHA.118.314669.

Coyle, B. *et al.* (2015) ‘ABCB1 in children’s brain tumours.’, *Biochemical Society transactions*, 43(5), pp. 1018–1022. doi: 10.1042/BST20150137.

Crocetti, E. *et al.* (2013) ‘Cancer prevalence in United States, Nordic Countries, Italy, Australia, and France: An analysis of geographic variability’, *British Journal of Cancer*, 109(1), pp. 219–228. doi: 10.1038/bjc.2013.311.

Cruccu, G., Truini, A. and NeuPSIG), on behalf of the N. P. S. I. G. of the I. S. of N. (Italian (2017) ‘Neuropathic Pain: The Scope of the Problem’, *Pain and Therapy*, 6(1), pp. 1–3. doi: 10.1007/s40122-017-0086-1.

Cruciani, R. A. *et al.* (1994) ‘Presence in neuroblastoma cells of a μ3 receptor with selectivity for opiate alkaloids but without affinity for opioid peptides’, *Brain Research*, 667(2), pp. 229–237. doi: 10.1016/0006-8993(94)91500-8.

D’Mello, R. and Dickenson, A. H. (2008) ‘Spinal cord mechanisms of pain’, *British Journal of Anaesthesia*, 101(1), pp. 8–16. doi: 10.1093/bja/aen088.

Dalkara, T. and Alarcon-Martinez, L. (2015) ‘Cerebral microvascular pericytes and neurogliovascular signaling in health and disease’, *Brain Research*. doi:

10.1016/j.brainres.2015.03.047.

Dasari, S. and Tchounwou, P. B. (2014) ‘Cisplatin in cancer therapy: molecular mechanisms of action’, *European journal of pharmacology*. 2014/07/21, 740, pp. 364–378. doi: 10.1016/j.ejphar.2014.07.025.

Datta, P. K. (2013) ‘Neuronal Cell Culture’, *Neuronal Cell Culture: Methods and Protocols*, 1078, pp. 35–44. doi: 10.1007/978-1-62703-640-5.

Daw, N. C. *et al.* (2020) ‘Activity of Vincristine and Irinotecan in Diffuse Anaplastic Wilms Tumor and Therapy Outcomes of Stage II to IV Disease: Results of the Children’s Oncology Group AREN0321 Study’, *Journal of Clinical Oncology*, 38(14), pp. 1558–1568. doi: 10.1200/JCO.19.01265.

Derry, W. B. *et al.* (1997) ‘Taxol Differentially Modulates the Dynamics of Microtubules Assembled from Unfractionated and Purified β-Tubulin Isotypes’, *Biochemistry*, 36(12), pp. 3554–3562. doi: 10.1021/bi962724m.

Deshmukh, V. *et al.* (2019) ‘Modulation of the Wnt pathway through inhibition of CLK2 and DYRK1A by lorecivivint as a novel, potentially disease-modifying approach for knee osteoarthritis treatment’, *Osteoarthritis and Cartilage*, 27(9), pp. 1347–1360. doi: 10.1016/j.joca.2019.05.006.

Dib-Hajj, S. D. *et al.* (1999) ‘Two tetrodotoxin-resistant sodium channels in human dorsal root ganglion neurons’, *FEBS Letters*, 462(1–2), pp. 117–120. doi: 10.1016/S0014-5793(99)01519-7.

Dilley, A. and Bove, G. M. (2008) ‘Disruption of axoplasmic transport induces mechanical sensitivity in intact rat C-fibre nociceptor axons’, *Journal of Physiology*, 586(2), pp. 593–604. doi: 10.1113/jphysiol.2007.144105.

Djouhri, L. *et al.* (2012) ‘Partial nerve injury induces electrophysiological changes in conducting (uninjured) nociceptive and nonnociceptive DRG neurons: Possible relationships to aspects of peripheral neuropathic pain and paresthesias', *Pain*, 153(9), pp. 1824–1836. doi: 10.1016/j.pain.2012.04.019.

Djouhri, L. and Lawson, S. N. (2004) 'Abeta-fiber nociceptive primary afferent neurons: a review of incidence and properties in relation to other afferent A-fiber neurons in mammals.', *Brain research. Brain research reviews*, 46(2), pp. 131–145. doi: 10.1016/j.brainresrev.2004.07.015.

Donaldson, L. F. and Beazley-Long, N. (2016) 'Alternative RNA splicing: contribution to pain and potential therapeutic strategy', *Drug Discovery Today*, 21(11), pp. 1787–1798. doi: 10.1016/j.drudis.2016.06.017.

Doran, C. *et al.* (2015) 'Mouse DRG cell line with properties of nociceptors', *PLoS ONE*. doi: 10.1371/journal.pone.0128670.

Douer, D. (2016) 'Efficacy and Safety of Vincristine Sulfate Liposome Injection in the Treatment of Adult Acute Lymphocytic Leukemia.', *The oncologist*, 21(7), pp. 840–847. doi: 10.1634/theoncologist.2015-0391.

Dougherty, P. M. *et al.* (2007) 'Dysfunction in Multiple Primary Afferent Fiber Subtypes Revealed By Quantitative Sensory Testing in Patients with Chronic Vincristine-Induced Pain', *Journal of Pain and Symptom Management*, 33(2), pp. 166–179. doi: 10.1016/j.jpainsymman.2006.08.006.

Dubin, A. E. and Patapoutian, A. (2010) 'Nociceptors : the sensors of the pain pathway Find the latest version : Review series Nociceptors : the sensors of the pain pathway', *Journal of Clinical Investigation*, 120(11), pp. 3760–3772. doi: 10.1172/JCI42843.3760.

Dubin, Adrienne E. and Patapoutian, A. (2010) 'Nociceptors: The sensors of the pain pathway', *Journal of Clinical Investigation*, 120(11), pp. 3760–3772. doi: 10.1172/JCI42843.

Duchon, A. and Herault, Y. (2016) ‘DYRK1A, a dosage-sensitive gene involved in neurodevelopmental disorders, Is a target for drug development in down syndrome’, *Frontiers in Behavioral Neuroscience*, 10(JUN). doi: 10.3389/fnbeh.2016.00104.

Dunn, P. M. *et al.* (1991) ‘Bradykinin evoked depolarization of a novel neuroblastoma × DRG neurone hybrid cell line (ND 7 23)’, *Brain Research*, 545(1–2), pp. 80–86. doi: 10.1016/0006-8993(91)91272-3.

Dvinge, H. (2018) ‘Regulation of alternative mRNA splicing: old players and new perspectives’, *FEBS Letters*, 592(17), pp. 2987–3006. doi: 10.1002/1873-3468.13119.

Eblen, S. T. (2012) ‘Regulation of chemoresistance via alternative messenger RNA splicing’, *Biochemical pharmacology*. 2012/01/08, 83(8), pp. 1063–1072. doi: 10.1016/j.bcp.2011.12.041.

Edmondson, R. *et al.* (2014) ‘Three-dimensional cell culture systems and their applications in drug discovery and cell-based biosensors’, *Assay and Drug Development Technologies*, 12(4), pp. 207–218. doi: 10.1089/adt.2014.573.

Eijkelkamp, N. *et al.* (no date) ‘Neurological perspectives on voltage-gated sodium channels. Neurological perspectives on voltage-gated sodium channels’. Available at: http://qmro.qmul.ac.uk/xmlui/handle/123456789/18436.

Elias, T. and Korzhenevsky, V. (1992) ‘The Presence of Taxol and Related Compounds in Taxus Baccata Native to the Ukraine (Crimea), Georgia, and Southern Russia’, *Aliso*, 13(3), pp. 463–470. doi: 10.5642/aliso.19921303.05.

Ellis, A. and Bennett, D. L. H. (2013) ‘Neuroinflammation and the generation of neuropathic pain’, *British Journal of Anaesthesia*, 111(1), pp. 26–37. doi: 10.1093/bja/aet128.

Ernsberger, U. (2009) ‘Role of neurotrophin signalling in the differentiation of neurons from dorsal root ganglia and sympathetic ganglia', *Cell and Tissue Research*, 336(3), pp. 349–384. doi: 10.1007/s00441-009-0784-z.

Ewertz, M., Qvortrup, C. and Eckhoff, L. (2015) 'Chemotherapy-induced peripheral neuropathy in patients treated with taxanes and platinum derivatives', *Acta Oncologica*. doi: 10.3109/0284186X.2014.995775.

Fabrizio, P. and Lührmann, R. (2012) 'The Spliceosome in Constitutive Splicing', *Alternative pre-mRNA Splicing*. (Wiley Online Books), pp. 49–64. doi: https://doi.org/10.1002/9783527636778.ch5.

Fan, S. F. *et al.* (1992) 'F11 neuroblastoma × DRG neuron hybrid cells express inhibitory μ- and δ-opioid receptors which increase voltage-dependent K+ currents upon activation', *Brain Research*, 590(1–2), pp. 329–333. doi: 10.1016/0006-8993(92)91116-V.

Fayaz, A. *et al.* (no date) 'Prevalence of chronic pain in the UK: a systematic review and meta-analysis of population studies'.

Feldman, P. *et al.* (2012) 'The persistent release of HMGB1 contributes to tactile hyperalgesia in a rodent model of neuropathic pain', *Journal of Neuroinflammation*, 9(1), p. 1. doi: 10.1186/1742-2094-9-180.

Ferguson, P. J. *et al.* (1984) 'Differential Activity of Vincristine and Vinblastine against Cultured Cells', *Cancer Research*, 44(8), pp. 3307–3312.

Fernandes, E. S., Fernandes, M. A. and Keeble, J. E. (2012) 'The functions of TRPA1 and TRPV1: Moving away from sensory nerves', *British Journal of Pharmacology*, 166(2), pp. 510–521. doi: 10.1111/j.1476-5381.2012.01851.x.

Fernandez-Marcos, P. J. and Auwerx, J. (2011) 'Regulation of PGC-1α, a nodal regulator of mitochondrial biogenesis', *The American journal of clinical nutrition*. 2011/02/02, 93(4), pp. 884S–90. doi: 10.3945/ajcn.110.001917.

Fernández-Martínez, P., Zahonero, C. and Sánchez-Gómez, P. (2015) ‘DYRK1A: the double-edged kinase as a protagonist in cell growth and tumorigenesis’, *Molecular and Cellular Oncology*. Taylor and Francis Ltd. doi: 10.4161/23723548.2014.970048.

Ferrara, N. and Davis-Smyth, T. (1997) ‘The biology of vascular endothelial growth factor’, *Endocrine Reviews*, 18(1), pp. 4–25. doi: 10.1210/er.18.1.4.

Ferrara, N., Gerber, H.-P. and LeCouter, J. (2003) ‘The biology of VEGF and its receptors’, *Nature Medicine*, 9(6), pp. 669–676. doi: 10.1038/nm0603-669.

Ferrara, N. and Henzel, W. J. (1989) ‘Pituitary follicular cells secrete a novel heparin-binding growth factor specific for vascular endothelial cells’, *Biochemical and Biophysical Research Communications*, 161(2), pp. 851–858. doi: 10.1016/0006-291X(89)92678-8.

Flatters, S. J. L., Dougherty, P. M. and Colvin, L. A. (2017) ‘Clinical and preclinical perspectives on Chemotherapy-Induced Peripheral Neuropathy (CIPN): A narrative review’, *British Journal of Anaesthesia*. doi: 10.1093/bja/aex229.

Fornasari, D. (2017) ‘Pharmacotherapy for Neuropathic Pain: A Review’, *Pain and Therapy*, 6(S1), pp. 25–33. doi: 10.1007/s40122-017-0091-4.

Fort, A. *et al.* (2009) ‘New insights in the contribution of voltage-gated Nav channels to rat aorta contraction’, *PLoS ONE*. doi: 10.1371/journal.pone.0007360.

Forth, S. and Kapoor, T. M. (2017) ‘The mechanics of microtubule networks in cell division’, *Journal of Cell Biology*, 216(6), pp. 1525–1531. doi: 10.1083/jcb.201612064.

Fukuda, Y., Li, Y. and Segal, R. A. (2017) ‘A mechanistic understanding of axon degeneration in chemotherapy-induced peripheral neuropathy’, *Frontiers in Neuroscience*, 11(August), pp. 1–12. doi: 10.3389/fnins.2017.00481.

Fukuhara, T. *et al.* (2006) ‘Utilization of host SR protein kinases and RNA-splicing machinery during viral replication’, *Proceedings of the National Academy of Sciences of the United States of America*. 2006/07/13, 103(30), pp. 11329–11333. doi: 10.1073/pnas.0604616103.

Gadgil, S. *et al.* (2019) ‘A systematic summary and comparison of animal models for chemotherapy induced (peripheral) neuropathy (CIPN)’, *PLOS ONE*, 14(8), p. e0221787. doi: 10.1371/journal.pone.0221787.

Gammons, M. V. *et al.* (2013) ‘Topical antiangiogenic SRPK1 inhibitors reduce choroidal neovascularization in rodent models of exudative AMD’, *Investigative Ophthalmology and Visual Science*, 54(9), pp. 6052–6062. doi: 10.1167/iovs.13-12422.

Gammons, M. V. *et al.* (2014) ‘Targeting SRPK1 to control VEGF-mediated tumour angiogenesis in metastatic melanoma’, *British Journal of Cancer*, 111(3), pp. 477–485. doi: 10.1038/bjc.2014.342.

Ganguly, A. and Cabral, F. (2011) ‘New insights into mechanisms of resistance to microtubule inhibitors.’, *Biochimica et biophysica acta*, 1816(2), pp. 164–171. doi: 10.1016/j.bbcan.2011.06.001.

Garrison, J. A. *et al.* (2003) ‘Myalgias and arthralgias associated with paclitaxel.’, *Oncology (Williston Park, N.Y.)*, 17(2), pp. 271-272,286-288.

Gartung, A. *et al.* (2019) ‘Suppression of chemotherapy-induced cytokine/lipid mediator surge and ovarian cancer by a dual COX-2/sEH inhibitor’, *Proceedings of the National Academy of Sciences of the United States of America*, 116(5), pp. 1698–1703. doi: 10.1073/pnas.1803999116.

Gascoigne, K. E. and Taylor, S. S. (2009) ‘How do anti-mitotic drugs kill cancer cells?’, *Journal of Cell Science*, 122(15), pp. 2579–2585. doi: 10.1242/jcs.039719.

Gasser, H. S. and Erlanger, J. (1927) ‘The Differential Action of Pressure on Fibers of Different Sizes in a Mixed Nerve.’, *Proceedings of the Society for Experimental Biology and Medicine*, 24(4), pp. 313–314. doi: 10.3181/00379727-24-3344.

Gavrilă, B. I., Ciofu, C. and Stoica, V. (2016) ‘Biomarkers in Rheumatoid Arthritis, what is new?’, *Journal of Medicine and Life*, 9(2), pp. 144–148. Available at: https://www.ncbi.nlm.nih.gov/pmc/articles/PMC4863504/pdf/JMedLife-09-144.pdf.

Geisler, S. *et al.* (2016) ‘Prevention of vincristine-induced peripheral neuropathy by genetic deletion of SARM1 in mice’, *Brain*, 139(12), pp. 3092–3108. doi: 10.1093/brain/aww251.

Geisler, S. *et al.* (2019) ‘Vincristine and bortezomib use distinct upstream mechanisms to activate a common SARM1-dependent axon degeneration program’, *JCI Insight*, 4(17), pp. 1–17. doi: 10.1172/jci.insight.129920.

Gerdts, J. *et al.* (2016) ‘Axon Self-Destruction: New Links among SARM1, MAPKs, and NAD+ Metabolism’, *Neuron*, 89(3), pp. 449–460. doi: 10.1016/j.neuron.2015.12.023.

Ghosh, G. and Adams, J. A. (2011) ‘Phosphorylation mechanism and structure of serine-arginine protein kinases’, *The FEBS journal*. 2011/01/12, 278(4), pp. 587–597. doi: 10.1111/j.1742-4658.2010.07992.x.

Gingras, J. *et al.* (2014) ‘Global Nav1.7 knockout mice recapitulate the phenotype of human congenital indifference to pain’, *PLoS ONE*. doi: 10.1371/journal.pone.0105895.

Glatz, D. C. *et al.* (2006) ‘The alternative splicing of tau exon 10 and its regulatory proteins CLK2 and TRA2-BETA1 changes in sporadic Alzheimer’s disease’, *Journal of Neurochemistry*, 96(3), pp. 635–644. doi: 10.1111/j.1471-4159.2005.03552.x.

Gnavi, S. *et al.* (2015) ‘The Effect of Electrospun Gelatin Fibers Alignment on

Schwann Cell and Axon Behavior and Organization in the Perspective of Artificial Nerve Design.', *International journal of molecular sciences*, 16(6), pp. 12925–12942. doi: 10.3390/ijms160612925.

Golan-Gerstl, R. *et al.* (2011) 'Splicing factor hnRNP A2/B1 regulates tumor suppressor gene splicing and is an oncogenic driver in glioblastoma', *Cancer Research*, 71(13), pp. 4464–4472. doi: 10.1158/0008-5472.CAN-10-4410.

Goldenberg, M. M. (2012) 'Multiple sclerosis review', *P & T : a peer-reviewed journal for formulary management*, 37(3), pp. 175–184. Available at: https://pubmed.ncbi.nlm.nih.gov/22605909.

Gómez-Ruiz, S. *et al.* (2012) 'On the discovery, biological effects, and use of cisplatin and metallocenes in anticancer chemotherapy', *Bioinorganic Chemistry and Applications*, 2012, pp. 15–17. doi: 10.1155/2012/140284.

Gonçalves, V. *et al.* (2014) 'Phosphorylation of SRSF1 by SRPK1 regulates alternative splicing of tumor-related Rac1b in colorectal cells', *RNA (New York, N.Y.)*. 2014/02/18, 20(4), pp. 474–482. doi: 10.1261/rna.041376.113.

Gordon-Weeks, P. R. (2004) 'Microtubules and growth cone function', *Journal of Neurobiology*, 58(1), pp. 70–83. doi: 10.1002/neu.10266.

Grisold, W., Cavaletti, G. and Windebank, A. J. (2012) 'Peripheral neuropathies from chemotherapeutics and targeted agents: Diagnosis, treatment, and prevention', *Neuro-Oncology*. doi: 10.1093/neuonc/nos203.

Grizzi, F., Weber, C. and Di Ieva, A. (2008) *Antiangiogenic Strategies in Medulloblastoma: Reality or Mystery*.

Growth, E., Vegf-a, F. and Bestall, S. (2017) 'Diabetic neuropathy : A mechanism of TRPV1 sensitisation and the treatment with Vascular', (December).

Gu, R. *et al.* (2017) 'Clk1 deficiency promotes neuroinflammation and subsequent dopaminergic cell death through regulation of microglial metabolic reprogramming', *Brain, Behavior, and Immunity*, 60, pp. 206–219. doi: 10.1016/j.bbi.2016.10.018.

Guo, J., Walss-Bass, C. and Ludueña, R. F. (2010) 'The beta isotypes of tubulin in neuronal differentiation', *Cytoskeleton (Hoboken, N.J.)*, 67(7), pp. 431–441. doi: 10.1002/cm.20455.

Guo, L. *et al.* (2017) 'Multiparametric image analysis of rat dorsal root ganglion cultures to evaluate peripheral neuropathy- inducing chemotherapeutics', *Toxicological Sciences*. doi: 10.1093/toxsci/kfw254.

Guyot, M. *et al.* (2016) 'Targeting the pro-angiogenic forms of VEGF or inhibiting their expression as anti-cancer strategies', *Oncotarget*, 8(6), pp. 9174–9188. doi: 10.18632/oncotarget.13942.

Haberberger, R. V., Barry, C. and Matusica, D. (2020) 'Immortalized Dorsal Root Ganglion Neuron Cell Lines', 14(June). doi: 10.3389/fncel.2020.00184.

Hallin, R. G., Torebjork, H. E. and Wiesenfeld, Z. (1982) 'Nociceptors and warm receptors innervated by C fibres in human skin', *Journal of Neurology Neurosurgery and Psychiatry*, 45(4), pp. 313–319. doi: 10.1136/jnnp.45.4.313.

Hameed, S. (2019) 'Nav1.7 and Nav1.8: Role in the pathophysiology of pain', *Molecular Pain*, 15. doi: 10.1177/1744806919858801.

Han, Y. and Smith, M. T. (2013) 'Pathobiology of cancer chemotherapy-induced peripheral neuropathy (CIPN)', *Frontiers in Pharmacology*, 4 DEC(December), pp. 1–16. doi: 10.3389/fphar.2013.00156.

Hanna, N. and Einhorn, L. H. (2014) 'Testicular Cancer: A Reflection on 50 Years of Discovery', *Journal of Clinical Oncology*, 32(28), pp. 3085–3092. doi: 10.1200/JCO.2014.56.0896.

Harper, S. J. and Bates, D. O. (2009) 'UKPMC Funders Group VEGF-A splicing ':, *Microvascular Research*, 8(11), pp. 880–887. doi: 10.1038/nrc2505.VEGF-A.

He, X. *et al.* (2004) 'Alternative splicing of the multidrug resistance protein 1/ATP binding cassette transporter subfamily gene in ovarian cancer creates functional spice variants and is associated with increased expression of the spiking factors PTB and SRp20', *Clinical Cancer Research*, 10(14), pp. 4652–4660. doi: 10.1158/1078-0432.CCR-03-0439.

van Hecke, O. *et al.* (2014) 'Neuropathic pain in the general population: a systematic review of epidemiological studies.', *Pain*, 155(4), pp. 654–662. doi: 10.1016/j.pain.2013.11.013.

Heinig, U., Scholz, S. and Jennewein, S. (2013) 'Getting to the bottom of Taxol biosynthesis by fungi', *Fungal Diversity*, 60(1), pp. 161–170. doi: 10.1007/s13225-013-0228-7.

Hilliard, M. A. (2009) 'Axonal degeneration and regeneration: A mechanistic tug-of-war', *Journal of Neurochemistry*, 108(1), pp. 23–32. doi: 10.1111/j.1471-4159.2008.05754.x.

Hiratsuka, S. *et al.* (2005) 'Vascular endothelial growth factor A (VEGF-A) is involved in guidance of VEGF receptor-positive cells to the anterior portion of early embryos', *Molecular and cellular biology*, 25(1), pp. 355–363. doi: 10.1128/MCB.25.1.355-363.2005.

Hoffmann, T. *et al.* (2008) 'Sensory Transduction in Peripheral Nerve Axons Elicits Ectopic Action Potentials', *Journal of Neuroscience*. doi: 10.1523/JNEUROSCI.1627-08.2008.

Huang, C. Y. *et al.* (2017) 'A review on the effects of current chemotherapy drugs and natural agents in treating non-small cell lung cancer', *BioMedicine (France)*, 7(4), pp. 12–23. doi: 10.1051/bmdcn/2017070423.

Hubert, T. *et al.* (2014) 'S6 kinase inhibits intrinsic axon regeneration capacity via AMP kinase in Caenorhabditis elegans', *Journal of Neuroscience*, 34(3), pp. 758–763. doi: 10.1523/JNEUROSCI.2886-13.2014.

Hulse, R. P. *et al.* (2014) 'Regulation of alternative VEGF-A mRNA splicing is a therapeutic target for analgesia', *Neurobiology of Disease*, 71, pp. 245–259. doi: 10.1016/j.nbd.2014.08.012.

Hulse, R. P. *et al.* (2015) 'Vascular endothelial growth factor-A165b prevents diabetic neuropathic pain and sensory neuronal degeneration.', *Clinical science (London, England : 1979)*, 129(8), pp. 741–56. doi: 10.1042/CS20150124.

Hulse, R. P. *et al.* (2016) 'The control of alternative splicing by SRSF1 in myelinated afferents contributes to the development of neuropathic pain', *Neurobiology of Disease*, 96, pp. 186–200. doi: 10.1016/j.nbd.2016.09.009.

Hutt, M. *et al.* (2012) 'Plasma half-life extension of small recombinant antibodies by fusion to immunoglobulin-binding domains', *The Journal of biological chemistry*. 2011/12/06, 287(7), pp. 4462–4469. doi: 10.1074/jbc.M111.311522.

Iamshanova, O. *et al.* (2016) 'Comparison of fluorescence probes for intracellular sodium imaging in prostate cancer cell lines', *European Biophysics Journal*, 45(7), pp. 765–777. doi: 10.1007/s00249-016-1173-7.

Imai, S. *et al.* (2017) 'Taxanes and platinum derivatives impair Schwann cells via distinct mechanisms', *Scientific Reports*, 7(1), pp. 1–14. doi: 10.1038/s41598-017-05784-1.

Ishikawa, H. *et al.* (2009) 'Total synthesis of vinblastine, vincristine, related natural products, and key structural analogues', *Journal of the American Chemical Society*, 131(13), pp. 4904–4916. doi: 10.1021/ja809842b.

Ivanov, D. P. *et al.* (2016) 'In vitro models of medulloblastoma: Choosing the right tool for the job', *Journal of Biotechnology*, 236, pp. 10–25. doi: 10.1016/j.jbiotec.2016.07.028.

Iwai, K. *et al.* (2018) 'Anti-tumor efficacy of a novel CLK inhibitor via targeting RNA splicing and MYC-dependent vulnerability', *EMBO Molecular Medicine*, 10(6). doi: 10.15252/emmm.201708289.

Jackson, D. V. *et al.* (1981) 'Pharmacokinetics of Vincristine in the Cerebrospinal Fluid of Humans', *Cancer Research*, 41(4), pp. 1466–1468.

Jackson, D. V. J. *et al.* (1981) 'Pharmacokinetics of vincristine in the cerebrospinal fluid of humans.', *Cancer research*, 41(4), pp. 1466–1468.

Jain, P. *et al.* (2014) 'Human CDC2-like kinase 1 (CLK1): a novel target for Alzheimer's disease.', *Current drug targets*, 15(5), pp. 539–550. doi: 10.2174/1389450115666140226112321.

Jarhad, D. B. *et al.* (2018) 'Dual-Specificity Tyrosine Phosphorylation-Regulated Kinase 1A (DYRK1A) Inhibitors as Potential Therapeutics', *Journal of Medicinal Chemistry*. American Chemical Society, pp. 9791–9810. doi: 10.1021/acs.jmedchem.8b00185.

Johnstone, T. C., Park, G. Y. and Lippard, S. J. (2014) 'Understanding and improving platinum anticancer drugs--phenanthriplatin', *Anticancer research*, 34(1), pp. 471–476. Available at: https://pubmed.ncbi.nlm.nih.gov/24403503.

Jordan, M. A., Himes, R. H. and Wilson, L. (1985) 'Comparison of the Effects of Vinblastine, Vincristine, Vindesine, and Vinepidine on Microtubule Dynamics and Cell Proliferation in Vitro', *Cancer Research*, 45(6), pp. 2741–2747.

Jordan, M. A., Thrower, D. and Wilson, L. (1991) 'Mechanism of Inhibition of Cell Proliferation by Vinca Alkaloids', *Cancer Research*, 51(8), pp. 2212–2222.

Jordan, M. A. and Wilson, L. (2004) 'Microtubules As a Target for', 4(April). doi:

10.1038/nr1317.

Joseph, E. K. and Levine, J. D. (2009) ‘Comparison of oxaliplatin- and cisplatin-induced painful peripheral neuropathy in the rat’, *The journal of pain : official journal of the American Pain Society*. 2009/02/23, 10(5), pp. 534–541. doi: 10.1016/j.jpain.2008.12.003.

June, T. G. (2019) ‘Chemotherapy - induced Peripheral Neuropathy Treatment Guidelines June 2019’, (June).

Kanat, O., Ertas, H. and Caner, B. (2017) ‘Platinum-induced neurotoxicity: A review of possible mechanisms’, *World journal of clinical oncology*, 8(4), pp. 329–335. doi: 10.5306/wjco.v8.i4.329.

Kapitein, L. C. and Hoogenraad, C. C. (2015) ‘Building the Neuronal Microtubule Cytoskeleton’, *Neuron*, 87(3), pp. 492–506. doi: 10.1016/j.neuron.2015.05.046.

Kapoor, S., Srivastava, S. and Panda, D. (2018) ‘Indibulin dampens microtubule dynamics and produces synergistic antiproliferative effect with vinblastine in MCF-7 cells: Implications in cancer chemotherapy’, *Scientific Reports*, 8(1), pp. 2–13. doi: 10.1038/s41598-018-30376-y.

Karashima, Y. *et al.* (2007) ‘Bimodal action of menthol on the transient receptor potential channel TRPA1’, *Journal of Neuroscience*, 27(37), pp. 9874–9884. doi: 10.1523/JNEUROSCI.2221-07.2007.

Katsetos, C. D. *et al.* (2002) ‘Localization of the Neuronal Class III β-Tubulin in Oligodendrogliomas: Comparison with Ki-67 Proliferative Index and 1p/19q Status’, *Journal of Neuropathology & Experimental Neurology*, 61(4), pp. 307–320. doi: 10.1093/jnen/61.4.307.

Katz, N. (2002) ‘The impact of pain management on quality of life’, *Journal of Pain and Symptom Management*, 24(1 SUPPL. 1), pp. 38–47. doi: 10.1016/S0885-

3924(02)00411-6.

Kaur, G. and Dufour, J. M. (2012) ‘Cell lines: Valuable tools or useless artifacts.’, *Spermatogenesis*, 2(1), pp. 1–5. doi: 10.4161/spmg.19885.

Ke, S. and Chasin, L. A. (2011) ‘Context-dependent splicing regulation’, *RNA Biology*, 8(3), pp. 384–388. doi: 10.4161/rna.8.3.14458.

Keglevich, P. *et al.* (2012) ‘Modifications on the basic skeletons of vinblastine and vincristine’, *Molecules*, 17(5), pp. 5893–5914. doi: 10.3390/molecules17055893.

Kelley, M. R. and Fehrenbacher, J. C. (2017) ‘Challenges and opportunities identifying therapeutic targets for chemotherapy-induced peripheral neuropathy resulting from oxidative DNA damage’, *Neural regeneration research*, 12(1), pp. 72–74. doi: 10.4103/1673-5374.198986.

Kerckhove, N. *et al.* (2017) ‘Long-term effects, pathophysiological mechanisms, and risk factors of chemotherapy-induced peripheral neuropathies: A comprehensive literature review’, *Frontiers in Pharmacology*, 8(FEB), pp. 1–17. doi: 10.3389/fphar.2017.00086.

Kidd, B. L. and Urban, L. A. (2001) ‘Mechanisms of inflammatory pain’, *BJA: British Journal of Anaesthesia*, 87(1), pp. 3–11. doi: 10.1093/bja/87.1.3.

Kisko, K. *et al.* (2011) ‘Structural analysis of vascular endothelial growth factor receptor-2/ligand complexes by small-angle X-ray solution scattering’, *The FASEB Journal*, 25(9), pp. 2980–2986. doi: https://doi.org/10.1096/fj.11-185397.

Knoerl, R. *et al.* (2019) ‘Characterizing patient-clinician chemotherapy-induced peripheral neuropathy assessment and management communication approaches’, *Patient education and counseling*. 2019/04/09, 102(9), pp. 1636–1643. doi: 10.1016/j.pec.2019.04.012.

Kuenzi, F. M. and Dale, N. (1996) ‘Effect of capsaicin and analogues on potassium and calcium currents and vanilloid receptors in Xenopus embryo spinal neurones', *British Journal of Pharmacology*, 119(1), pp. 81–90. doi: 10.1111/j.1476-5381.1996.tb15680.x.

Kwan, K. Y. *et al.* (2006) 'TRPA1 Contributes to Cold, Mechanical, and Chemical Nociception but Is Not Essential for Hair-Cell Transduction', *Neuron*, 50(2), pp. 277–289. doi: 10.1016/j.neuron.2006.03.042.

Ladomery, M. (2013) 'Aberrant alternative splicing is another hallmark of cancer', *International journal of cell biology*. 2013/09/11, 2013, p. 463786. doi: 10.1155/2013/463786.

Ladomery, M. R., Harper, S. J. and Bates, D. O. (2007) 'Alternative splicing in angiogenesis: the vascular endothelial growth factor paradigm.', *Cancer letters*, 249(2), pp. 133–142. doi: 10.1016/j.canlet.2006.08.015.

Langjahr, M. *et al.* (2018) 'Increased pro-inflammatory cytokine gene expression in peripheral blood mononuclear cells of patients with polyneuropathies', *Journal of Neurology*, (0123456789). doi: 10.1007/s00415-018-8748-4.

Latremoliere, A. and Woolf, C. J. (2009) 'Central sensitization: a generator of pain hypersensitivity by central neural plasticity', *The journal of pain : official journal of the American Pain Society*, 10(9), pp. 895–926. doi: 10.1016/j.jpain.2009.06.012.

Lawson, S. N., Crepps, B. A. and Perl, E. R. (1997) 'Relationship of substance P to afferent characteristics of dorsal root ganglion neurones in guinea-pig', *Journal of Physiology*, 505(1), pp. 177–191. doi: 10.1111/j.1469-7793.1997.00177.x.

Lee, J. Y. *et al.* (2019a) 'Structural Basis for the Selective Inhibition of Cdc2-Like Kinases by CX-4945', *BioMed Research International*, 2019. doi: 10.1155/2019/6125068.

Lee, J. Y. *et al.* (2019b) 'Structural Basis for the Selective Inhibition of Cdc2-Like

Kinases by CX-4945', *BioMed Research International*, 2019. doi: 10.1155/2019/6125068.

Lee, K. M., Choi, K. H. and Ouellette, M. M. (2004) 'Use of exogenous hTERT to immortalize primary human cells', *Cytotechnology*, 45(1–2), pp. 33–38. doi: 10.1007/10.1007/s10616-004-5123-3.

Lee, Y. C., Nassikas, N. J. and Clauw, D. J. (2011) 'The role of the central nervous system in the generation and maintenance of chronic pain in rheumatoid arthritis, osteoarthritis and fibromyalgia', *Arthritis Research & Therapy*, 13(2), p. 211. doi: 10.1186/ar3306.

Lee, Y. and Rio, D. C. (2015) 'Mechanisms and Regulation of Alternative Pre-mRNA Splicing', *Annual Review of Biochemistry*, 84(1), pp. 291–323. doi: 10.1146/annurev-biochem-060614-034316.

Leo, M. *et al.* (2017) 'Cisplatin alters the function and expression of N-type voltage-gated calcium channels in the absence of morphological damage of sensory neurons', *Molecular Pain*, 13, pp. 1–12. doi: 10.1177/1744806917746565.

Lewin, G. R. and McMahon, S. B. (1991) 'Physiological properties of primary sensory neurons appropriately and inappropriately innervating skin in the adult rat.', *Journal of neurophysiology*, 66(4), pp. 1205–1217. doi: 10.1152/jn.1991.66.4.1205.

Li, Y. ling *et al.* (2019) 'DYRK1A inhibition suppresses STAT3/EGFR/Met signalling and sensitizes EGFR wild-type NSCLC cells to AZD9291', *Journal of Cellular and Molecular Medicine*, 23(11), pp. 7427–7437. doi: 10.1111/jcmm.14609.

Liem, L. *et al.* (2016) 'The Dorsal Root Ganglion as a Therapeutic Target for Chronic Pain.', *Regional anesthesia and pain medicine*, 41(4), pp. 511–519. doi: 10.1097/AAP.0000000000000408.

Lin, J. *et al.* (2020) 'Satisfaction with pain management and impact of pain on quality of life in cancer patients', *Asia-Pacific Journal of Clinical Oncology*, 16(2), pp. e91–e98. doi: https://doi.org/10.1111/ajco.13095.

Ling, W., Mooney, L. and Hillhouse, M. (2011) 'Prescription opioid abuse, pain and addiction: Clinical issues and implications', *Drug and Alcohol Review*, 30(3), pp. 300–305. doi: 10.1111/j.1465-3362.2010.00271.x.

Liston, D. R. and Davis, M. (2017) 'Clinically relevant concentrations of anticancer drugs: A guide for nonclinical studies', *Clinical Cancer Research*, 23(14), pp. 3489–3498. doi: 10.1158/1078-0432.CCR-16-3083.

Loring, H. S. and Thompson, P. R. (2020) 'Emergence of SARM1 as a Potential Therapeutic Target for Wallerian-type Diseases', *Cell Chemical Biology*, 27(1), pp. 1–13. doi: 10.1016/j.chembiol.2019.11.002.

Lu, Y. *et al.* (2012) 'An overview of tubulin inhibitors that interact with the colchicine binding site', *Pharmaceutical research*. 2012/07/20, 29(11), pp. 2943–2971. doi: 10.1007/s11095-012-0828-z.

Luo, X. *et al.* (2019) 'Macrophage Toll-like Receptor 9 Contributes to Chemotherapy-Induced Neuropathic Pain in Male Mice', *The Journal of neuroscience : the official journal of the Society for Neuroscience*, 39(35), pp. 6848–6864. doi: 10.1523/JNEUROSCI.3257-18.2019.

Madsen, M. L. *et al.* (2019) 'Aspects of vincristine-induced neuropathy in hematologic malignancies: a systematic review', *Cancer Chemotherapy and Pharmacology*, 84(3), pp. 471–485. doi: 10.1007/s00280-019-03884-5.

Malin, S. A., Davis, B. M. and Molliver, D. C. (2007) 'Production of dissociated sensory neuron cultures and considerations for their use in studying neuronal function and plasticity', *Nature Protocols*. doi: 10.1038/nprot.2006.461.

Maqsood, M. and Abdul, M. (2017) 'Yeast extract elicitation increases vinblastine and vincristine yield in protoplast derived tissues and plantlets in catharanthus roseus’, *Revista Brasileira de Farmacognosia*, 27(5), pp. 549–556. doi: 10.1016/j.bjp.2017.05.008.

Matei, D. *et al.* (2009) ‘Activity of 2 methoxyestradiol (Panzem® NCD) in advanced, platinum-resistant ovarian cancer and primary peritoneal carcinomatosis: A Hoosier Oncology Group trial’, *Gynecologic Oncology*, 115(1), pp. 90–96. doi: 10.1016/j.ygyno.2009.05.042.

Mavrou, A. *et al.* (2015) ‘Serine-arginine protein kinase 1 (SRPK1) inhibition as a potential novel targeted therapeutic strategy in prostate cancer’, *Oncogene*. 2014/11/10, 34(33), pp. 4311–4319. doi: 10.1038/onc.2014.360.

McCarberg, B. H. *et al.* (2008) ‘The Impact of Pain on Quality of Life and the Unmet Needs of Pain Management: Results From Pain Sufferers and Physicians Participating in an Internet Survey’, *American Journal of Therapeutics*, 15(4). Available at: https://journals.lww.com/americantherapeutics/Fulltext/2008/07000/The_Impact_of_Pain_on_Quality_of_Life_and_the.4.aspx.

McCutcheon, J. E. and Marinelli, M. (2009) ‘Age matters’, *The European journal of neuroscience*, 29(5), pp. 997–1014. doi: 10.1111/j.1460-9568.2009.06648.x.

McDermott, L. A. *et al.* (2019) ‘Defining the Functional Role of Na V 1.7 in Human Nociception’, *Neuron*, 101(5), pp. 905-919.e8. doi: 10.1016/j.neuron.2019.01.047.

Meerwaldt, J. H. *et al.* (1997) ‘Persistent improved results after adding vincristine and bleomycin to a cyclophosphamide/hydroxorubicin/Vm-26/prednisone combination (CHVmP) in stage III-IV intermediate- and high-grade non-Hodgkin’s lymphoma’, *Annals of Oncology*, 8(SUPPL. 1), pp. S67–S70. doi: 10.1093/annonc/8.suppl_1.S67.

Mehta, G. *et al.* (2012) ‘Opportunities and challenges for use of tumor spheroids as models to test drug delivery and efficacy’, *Journal of Controlled Release*, 164(2), pp. 192–204. doi: 10.1016/j.jconrel.2012.04.045.

Menezes, J. R. L. and Luskin, M. B. (1994) ‘Expression of neuron-specific tubulin defines a novel population in the proliferative layers of the developing telencephalon’, *Journal of Neuroscience*, 14(9), pp. 5399–5416. doi: 10.1523/jneurosci.14-09-05399.1994.

Menyhárt, O., Giangaspero, F. and Gyorffy, B. (2019) ‘Molecular markers and potential therapeutic targets in non-WNT/non-SHH (group 3 and group 4) medulloblastomas’, *Journal of Hematology and Oncology*. BioMed Central Ltd. doi: 10.1186/s13045-019-0712-y.

Merianda, T. T. *et al.* (2015) ‘Axonal amphoterin mRNA is regulated by translational control and enhances axon outgrowth’, *Journal of Neuroscience*, 35(14), pp. 5693–5706. doi: 10.1523/JNEUROSCI.3397-14.2015.

Meunier, S. and Vernos, I. (2012) ‘Microtubule assembly during mitosis - from distinct origins to distinct functions?’, *Journal of Cell Science*, 125(12), pp. 2805–2814. doi: 10.1242/jcs.092429.

Micheli, A. *et al.* (2002) ‘Cancer prevalence in European registry areas’, *Annals of Oncology*, 13(6), pp. 840–865. doi: 10.1093/annonc/mdf127.

Mohammed, Zainab A *et al.* (2017) ‘Veratridine produces distinct calcium response profiles in mouse Dorsal Root Ganglia neurons’. doi: 10.1038/srep45221.

Mohammed, Zainab A. *et al.* (2017) ‘Veratridine produces distinct calcium response profiles in mouse Dorsal Root Ganglia neurons’, *Scientific Reports*, 7, pp. 1–13. doi: 10.1038/srep45221.

Mohammed, Z. A., Kaloyanova, K. and Nassar, M. A. (2020) ‘An unbiased and efficient assessment of excitability of sensory neurons for analgesic drug discovery', *PAIN*, 161(5). Available at: https://journals.lww.com/pain/Fulltext/2020/05000/An_unbiased_and_efficient_assessment_of.25.aspx.

Mohiuddin, M. S. *et al.* (2019) 'Glucagon-Like Peptide-1 Receptor Agonist Protects Dorsal Root Ganglion Neurons against Oxidative Insult.', *Journal of diabetes research*, 2019, p. 9426014. doi: 10.1155/2019/9426014.

Molassiotis, A. *et al.* (2019) 'Risk factors for chemotherapy-induced peripheral neuropathy in patients receiving taxane- and platinum-based chemotherapy', *Brain and Behavior*, 9(6), pp. 1–10. doi: 10.1002/brb3.1312.

Mole, S. *et al.* (2020) 'Human papillomavirus type 16 infection activates the host serine arginine protein kinase 1 (SRPK1) - splicing factor axis', *Journal of General Virology*, 101(5), pp. 523–532. doi: 10.1099/jgv.0.001402.

Mora, E. *et al.* (2016) 'Vincristine-induced peripheral neuropathy in pediatric cancer patients', *American Journal of Cancer Research*.

Morrison, V. A. (2014) 'Immunosuppression associated with novel chemotherapy agents and monoclonal antibodies', *Clinical Infectious Diseases*, 59(Suppl 5), pp. S360–S364. doi: 10.1093/cid/ciu592.

Moudi, M. *et al.* (2013) 'Vinca alkaloids', *International journal of preventive medicine*, 4(11), pp. 1231–1235. Available at: https://pubmed.ncbi.nlm.nih.gov/24404355.

Mummery, C. (2016) 'Harnessing the power of cardiac stem cells', *Cell and Gene Therapy Insights*, 2(3), pp. 391–396. doi: 10.18609/cgti.2016.041.

Muratori, L. *et al.* (no date) 'Evaluation of Vascular Endothelial Growth Factor (VEGF) and Its Family Member Expression After Peripheral Nerve Regeneration and Denervation'. doi: 10.1002/ar.23842.

Myers, M. P., Murphy, M. B. and Landreth, G. (1994) ‘The dual-specificity CLK kinase induces neuronal differentiation of PC12 cells.’, *Molecular and Cellular Biology*, 14(10), pp. 6954–6961. doi: 10.1128/mcb.14.10.6954.

Naaz, F. *et al.* (2019) ‘Anti-tubulin agents of natural origin: Targeting taxol, vinca, and colchicine binding domains’, *European Journal of Medicinal Chemistry*, 171, pp. 310–331. doi: 10.1016/j.ejmech.2019.03.025.

Nagai, H. and Kim, Y. H. (2017) ‘Cancer prevention from the perspective of global cancer burden patterns’, *Journal of thoracic disease*, 9(3), pp. 448–451. doi: 10.21037/jtd.2017.02.75.

Naim, M. *et al.* (1997) ‘Cells in laminae III and IV of the rat spinal cord that possess the neurokinin-1 receptor and have dorsally directed dendrites receive a major synaptic input from tachykinin-containing primary afferents’, *Journal of Neuroscience*, 17(14), pp. 5536–5548. doi: 10.1523/jneurosci.17-14-05536.1997.

Neto, E. *et al.* (2017) ‘Axonal outgrowth, neuropeptides expression and receptors tyrosine kinase phosphorylation in 3D organotypic cultures of adult dorsal root ganglia’, *PloS one*, 12(7), pp. e0181612–e0181612. doi: 10.1371/journal.pone.0181612.

Nguyen, T.-L. *et al.* (2010) ‘Effects of capsazepine, a transient receptor potential vanilloid type 1 antagonist, on morphine-induced antinociception, tolerance, and dependence in mice.’, *British journal of anaesthesia*, 105(5), pp. 668–674. doi: 10.1093/bja/aeq212.

Nirschl, J. J., Ghiretti, A. E. and Holzbaur, E. L. F. (2017) ‘The impact of cytoskeletal organization on the local regulation of neuronal transport’, *Nature reviews. Neuroscience*. 2017/08/31, 18(10), pp. 585–597. doi: 10.1038/nrn.2017.100.

Nishida, T. *et al.* (2016) ‘Involvement of high mobility group box 1 in the development and maintenance of chemotherapy-induced peripheral neuropathy in rats', *Toxicology*. doi: 10.1016/j.tox.2016.07.016.

Noble, R. L. (1990) 'The discovery of the vinca alkaloids—chemotherapeutic agents against cancer', *Biochemistry and Cell Biology*, 68(12), pp. 1344–1351. doi: 10.1139/o90-197.

Nordin, M. (1990) 'Low-threshold mechanoreceptive and nociceptive units with unmyelinated (C) fibres in the human supraorbital nerve.', *The Journal of physiology*, 426, pp. 229–240. doi: 10.1113/jphysiol.1990.sp018135.

Nowak, D. G. *et al.* (2008) 'Expression of pro- and anti-angiogenic isoforms of VEGF is differentially regulated by splicing and growth factors.', *Journal of cell science*, 121(Pt 20), pp. 3487–95. doi: 10.1242/jcs.016410.

Nowak, D. G. *et al.* (2010) 'Regulation of Vascular Endothelial Growth Factor (VEGF) splicing from pro-angiogenic to anti-angiogenic isoforms: A novel therapeutic strategy for angiogenesis', *Journal of Biological Chemistry*, 285(8), pp. 5532–5540. doi: 10.1074/jbc.M109.074930.

Obinata, M. (2007) 'The immortalized cell lines with differentiation potentials: Their establishment and possible application', *Cancer Science*, 98(3), pp. 275–283. doi: 10.1111/j.1349-7006.2007.00399.x.

Oltean, S. *et al.* (2012) 'SRPK1 inhibition in vivo: modulation of VEGF splicing and potential treatment for multiple diseases.', *Biochemical Society transactions*, 40(4), pp. 831–835. doi: 10.1042/BST20120051.

Onakpoya, I. J. *et al.* (2019) 'Benefits and harms of pregabalin in the management of neuropathic pain: a rapid review and meta-analysis of randomised clinical trials', *BMJ Open*, 9(1), p. e023600. doi: 10.1136/bmjopen-2018-023600.

Van Opdenbosch, N. *et al.* (2012) 'The IE180 protein of pseudorabies virus suppresses phosphorylation of translation initiation factor eIF2α.', *Journal of virology*, 86(13), pp. 7235–7240. doi: 10.1128/JVI.06929-11.

Ordovas-Montanes, J. *et al.* (2015) 'The Regulation of Immunological Processes by Peripheral Neurons in Homeostasis and Disease', *Trends in immunology*, 36(10), pp. 578–604. doi: 10.1016/j.it.2015.08.007.

Orr, G. A. *et al.* (2003) 'Mechanisms of Taxol resistance related to microtubules', *Oncogene*, 22(47), pp. 7280–7295. doi: 10.1038/sj.onc.1206934.

Ortega, M. A. *et al.* (2019) 'Upregulation of VEGF and PEDF in Placentas of Women with Lower Extremity Venous Insufficiency during Pregnancy and Its Implication in Villous Calcification', *BioMed Research International*, 2019(Vi). doi: 10.1155/2019/5320902.

Owellen, R. J. *et al.* (1976) 'Inhibition of Tubulin-Microtubule Polymerization by Drugs of the Vinca Alkaloid Class', *Cancer Research*, 36(4), pp. 1499–1502.

Park, K. J. *et al.* (2016) 'Role of vincristine in the inhibition of angiogenesis in glioblastoma', *Neurological Research*. doi: 10.1080/01616412.2016.1211231.

Peach, C. J., Mignone, V. W., *et al.* (2018) 'Molecular pharmacology of VEGF-A isoforms: Binding and signalling at VEGFR2', *International Journal of Molecular Sciences*. doi: 10.3390/ijms19041264.

Peach, C. J., Kilpatrick, L. E., *et al.* (2018) 'Real-Time Ligand Binding of Fluorescent VEGF-A Isoforms that Discriminate between VEGFR2 and NRP1 in Living Cells', *Cell Chemical Biology*. doi: 10.1016/j.chembiol.2018.06.012.

Pearson, S. E. *et al.* (2019) 'Cancer survivors treated with platinum-based chemotherapy affected by ototoxicity and the impact on quality of life: a narrative synthesis systematic review', *International Journal of Audiology*, 58(11), pp. 685–695. doi: 10.1080/14992027.2019.1660918.

Pedersen, S. F., Owsianik, G. and Nilius, B. (2005) ‘TRP channels: An overview’, *Cell Calcium*, 38(3), pp. 233–252. doi: https://doi.org/10.1016/j.ceca.2005.06.028.

Peirs, C. and Seal, R. P. (2016) ‘Neural circuits for pain: Recent advances and current views’, *Science*, 354(6312), pp. 578 LP – 584. doi: 10.1126/science.aaf8933.

Pennanen, S. and Huhtikangas, A. (1990) ‘PHOTOCHEMICAL ONE-POT SYNTHESIS OF VINBLASTINE and VINCRISTINE’, *Photochemistry and Photobiology*, 51(5), pp. 515–518. doi: https://doi.org/10.1111/j.1751-1097.1990.tb01959.x.

Piccart, M. J., Lamb, H. and Vermorken, J. B. (2001) ‘Current and future potential roles of the platinum drugs in the treatment of ovarian cancer’, *Annals of Oncology*, 12(9), pp. 1195–1203. doi: https://doi.org/10.1023/A:1012259625746.

Ponomarenko, E. A. *et al.* (2016) ‘The Size of the Human Proteome: The Width and Depth’, *International journal of analytical chemistry*. 2016/05/19, 2016, p. 7436849. doi: 10.1155/2016/7436849.

Por, E. D. *et al.* (2013) ‘Phosphorylation regulates TRPV1 association with β-arrestin-2’, *Biochemical Journal*, 451(1), pp. 101–109. doi: 10.1042/BJ20121637.

Präbst, K. *et al.* (2017) ‘Colorimetric Proliferation Assays’, *Basic Colorimetric Proliferation Assays: MTT, WST, and Resazurin*, 1601, pp. 1–17. doi: 10.1007/978-1-4939-6960-9.

Prato, V. *et al.* (2017) ‘Functional and Molecular Characterization of Mechanoinsensitive “Silent” Nociceptors’, *Cell reports*, 21(11), pp. 3102–3115. doi: 10.1016/j.celrep.2017.11.066.

Premkumar, L. and Sikand, P. (2008) ‘TRPV1: A Target for Next Generation Analgesics’, *Current Neuropharmacology*, 6(2), pp. 151–163. doi: 10.2174/157015908784533888.

Pritchard-Jones, R. O. *et al.* (2007) ‘Expression of VEGF(xxx)b, the inhibitory isoforms of VEGF, in malignant melanoma.’, *British journal of cancer*, 97(2), pp. 223–230. doi: 10.1038/sj.bjc.6603839.

Qin, J. *et al.* (2018) ‘Transcription factor networks involved in cell death in the dorsal root ganglia following peripheral nerve injury’, *Neural regeneration research*, 13(9), pp. 1622–1627. doi: 10.4103/1673-5374.237183.

Racca, C. *et al.* (2010) ‘The neuronal splicing factor Nova co-localizes with target RNAs in the dendrite ’, *Frontiers in Neural Circuits* , p. 5. Available at: https://www.frontiersin.org/article/10.3389/neuro.04.005.2010.

Raghavan, D. (2003) ‘Testicular cancer: maintaining the high cure rate.’, *Oncology (Williston Park, N.Y.)*, 17(2), pp. 218–28; discussion 228-9, 234–5, passim.

Raja, V. J. *et al.* (2014) ‘Novel antitumour indole alkaloid, Jerantinine A, evokes potent G2/M cell cycle arrest targeting microtubules’, *Investigational New Drugs*. doi: 10.1007/s10637-014-0126-1.

Raymon, H. K. *et al.* (1999) ‘Immortalized human dorsal root ganglion cells differentiate into neurons with nociceptive properties’, *Journal of Neuroscience*, 19(13), pp. 5420–5428. doi: 10.1523/jneurosci.19-13-05420.1999.

Ren, A.-J. *et al.* (2014) ‘ZBTB20 regulates nociception and pain sensation by modulating TRP channel expression in nociceptive sensory neurons’, *Nature Communications*, 5(1), p. 4984. doi: 10.1038/ncomms5984.

Rodriguez, J. M. *et al.* (2020) ‘An analysis of tissue-specific alternative splicing at the protein level’, *PLOS Computational Biology*, 16(10), p. e1008287. Available at: https://doi.org/10.1371/journal.pcbi.1008287.

Roper, S. J. *et al.* (2018) ‘MBRS-46. JERANTININE: A NOVEL TUMOUR-SPECIFIC ALKALOID FOR THE TREATMENT OF PAEDIATRIC MEDULLOBLASTOMA’, *Neuro-Oncology*, 20(suppl_2), pp. i138–i138. doi: 10.1093/neuonc/noy059.491.

Roper, S. J. (2019) *Development of three-dimensional spheroid models for the analysis of medulloblastoma drug response and metastatic dissemination*.

Roussel, M. F. and Robinson, G. W. (2013) 'Role of MYC in medulloblastoma', *Cold Spring Harbor Perspectives in Medicine*, 3(11). doi: 10.1101/cshperspect.a014308.

Rowinsky Eric K., M. D. (1997) 'THE DEVELOPMENT AND CLINICAL UTILITY OF THE TAXANE CLASS OF ANTIMICROTUBULE CHEMOTHERAPY AGENTS', *Annual Review of Medicine*, 48(1), pp. 353–374. doi: 10.1146/annurev.med.48.1.353.

Rowlinson, J. *et al.* (2015) 'Novel SRPK1 inhibitors specifically target alternative splicing in human primary retinal epithelial cells', *Acta Ophthalmologica*, 93(S255). doi: https://doi.org/10.1111/j.1755-3768.2015.0625.

Ruggiero, A. *et al.* (2013) 'Platinum compounds in children with cancer: toxicity and clinical management.', *Anti-cancer drugs*, 24(10), pp. 1007–1019. doi: 10.1097/CAD.0b013e3283650bda.

Sabarre, C. L., Rassekh, S. R. and Zwicker, J. G. (2014) 'Vincristine and fine motor function of children with acute lymphoblastic leukemia', *Canadian Journal of Occupational Therapy*, 81(4), pp. 256–264. doi: 10.1177/0008417414539926.

Sahenk, Z. *et al.* (1994) 'Taxol neuropathy. Electrodiagnostic and sural nerve biopsy findings.', *Archives of neurology*, 51(7), pp. 726–729. doi: 10.1001/archneur.1994.00540190110024.

Salzer, J. L. (2015) 'Schwann cell myelination', *Cold Spring Harbor perspectives in biology*, 7(8), pp. a020529–a020529. doi: 10.1101/cshperspect.a020529.

Sandkühler, J. (2009) 'Models and mechanisms of hyperalgesia and allodynia', *Physiological Reviews*, 89(2), pp. 707–758. doi: 10.1152/physrev.00025.2008.

Sawaguchi, Y. *et al.* (2015) 'Establishment of a novel in vitro model for predicting incidence and severity of microtubule-targeting agent-induced peripheral neuropathy', *Anticancer Research*, 35(12), pp. 6431–6438.

Scales, T. M. E. *et al.* (2009) 'Nonprimed and DYRK1A-primed GSK3β-phosphorylation sites on MAP1B regulate microtubule dynamics in growing axons', *Journal of Cell Science*, 122(14), pp. 2424–2435. doi: 10.1242/jcs.040162.

Schaible, H. G., Ebersberger, A. and Natura, G. (2011) 'Update on peripheral mechanisms of pain: Beyond prostaglandins and cytokines', *Arthritis Research and Therapy*, 13(2), pp. 1–8. doi: 10.1186/ar3305.

Seifert, A., Allan, L. A. and Clarke, P. R. (2008) 'DYRK1A phosphorylates caspase 9 at an inhibitory site and is potently inhibited in human cells by harmine', *FEBS Journal*, 275(24), pp. 6268–6280. doi: 10.1111/j.1742-4658.2008.06751.x.

Senger, R. *et al.* (1983) 'Tumor cells secrete a vascular permeability factor that promotes accumulation of ascites fluid', *Science*, 219(Table 2), pp. 983–986. doi: 10.1126/science.6823562.

Seretny, M. *et al.* (2014) 'Incidence, prevalence, and predictors of chemotherapy-induced peripheral neuropathy: A systematic review and meta-analysis', *Pain*, 155(12), pp. 2461–2470. doi: 10.1016/j.pain.2014.09.020.

Shahid, W. *et al.* (2019) 'Comparison of the Efficacy of Duloxetine and Pregabalin in Pain Relief Associated with Diabetic Neuropathy', *Cureus*, 11(7). doi: 10.7759/cureus.5293.

Sharma, S. *et al.* (2015) 'Assessment of chemotherapy-induced peripheral neuropathy using the LDIFLARE technique: a novel technique to detect neural small fiber dysfunction', *Brain and behavior*. 2015/05/26, 5(7), pp. e00354–e00354. doi: 10.1002/brb3.354.

Shen, H. and Green, M. R. (2006) ‘RS domains contact splicing signals and promote splicing by a common mechanism in yeast through humans’, *Genes & development*. 2006/06/09, 20(13), pp. 1755–1765. doi: 10.1101/gad.1422106.

Shewan, D. A., Berry, M. and Cohen, J. (1995) ‘Extensive Immature’, *The Journal of Neuroscience*, 15(March), pp. 2057–2062.

Shibuya, M. (2011) ‘Vascular Endothelial Growth Factor (VEGF) and Its Receptor (VEGFR) Signaling in Angiogenesis: A Crucial Target for Anti- and Pro-Angiogenic Therapies’, *Genes & cancer*, 2(12), pp. 1097–1105. doi: 10.1177/1947601911423031.

Shkreta, L. *et al.* (2008) ‘Anticancer drugs affect the alternative splicing of Bcl-x and other human apoptotic genes’, *Molecular Cancer Therapeutics*, 7(6), pp. 1398–1409. doi: 10.1158/1535-7163.MCT-08-0192.

Shu, X. and Mendell, L. M. (1999) ‘Nerve growth factor acutely sensitizes the response of adult rat sensory neurons to capsaicin.’, *Neuroscience letters*, 274(3), pp. 159–162. doi: 10.1016/s0304-3940(99)00701-6.

Silav, G. *et al.* (2016) ‘Relationship of dorsal root ganglion to intervertebral foramen in lumbar region: an anatomical study and review of literature.’, *Journal of neurosurgical sciences*, 60(3), pp. 339–344.

Silva, A. *et al.* (2006) ‘Evidence for direct axonal toxicity in vincristine neuropathy’, *Journal of the Peripheral Nervous System*, 11(3), pp. 211–216. doi: 10.1111/j.1529-8027.2006.0090.x.

Singh, R. (2002) ‘RNA-protein interactions that regulate pre-mRNA splicing’, *Gene expression*, 10(1–2), pp. 79–92. Available at: https://pubmed.ncbi.nlm.nih.gov/11868989.

Sirachainan, N. *et al.* (2018) ‘Outcome of newly diagnosed high risk medulloblastoma treated with carboplatin, vincristine, cyclophosphamide and etoposide', *Journal of Clinical Neuroscience*, 56, pp. 139–142. doi: https://doi.org/10.1016/j.jocn.2018.06.028.

Smedley, C. J. *et al.* (2018) 'Sustainable Syntheses of (-)-Jerantinines A & e and Structural Characterisation of the Jerantinine-Tubulin Complex at the Colchicine Binding Site', *Scientific Reports*, 8(1). doi: 10.1038/s41598-018-28880-2.

Smutzer, G. and Devassy, R. K. (2016) 'Integrating TRPV1 Receptor Function with Capsaicin Psychophysics', *Advances in Pharmacological Sciences*, 2016. doi: 10.1155/2016/1512457.

Sondell, M., Sundler, F. and Kanje, M. (2000) 'Vascular endothelial growth factor is a neurotrophic factor which stimulates axonal outgrowth through the flk-1 receptor.', *The European journal of neuroscience*, 12(12), pp. 4243–4254. doi: 10.1046/j.0953-816x.2000.01326.x.

Spector, D. L. and Lamond, A. I. (2011) 'Nuclear speckles', *Cold Spring Harbor Perspectives in Biology*, 3(2), pp. 1–12. doi: 10.1101/cshperspect.a000646.

Sprowl, J. A. *et al.* (2012) 'Alterations in tumor necrosis factor signaling pathways are associated with cytotoxicity and resistance to taxanes: a study in isogenic resistant tumor cells', *Breast cancer research : BCR*, 14(1), pp. R2–R2. doi: 10.1186/bcr3083.

Staff, N. P. *et al.* (2017) 'Chemotherapy-induced peripheral neuropathy: A current review.', *Annals of neurology*, 81(6), pp. 772–781. doi: 10.1002/ana.24951.

Starobova, H. and Vetter, I. (2017) 'Pathophysiology of Chemotherapy-Induced Peripheral Neuropathy', *Frontiers in Molecular Neuroscience*. doi: 10.3389/fnmol.2017.00174.

Stone, J. B. and DeAngelis, L. M. (2016) 'Cancer-treatment-induced neurotoxicity--focus on newer treatments', *Nature reviews. Clinical oncology*. 2015/09/22, 13(2), pp. 92–105. doi: 10.1038/nrclinonc.2015.152.

Stucky, C. L. and Lewin, G. R. (1999) ‘Isolectin B4-positive and -negative nociceptors are functionally distinct’, *Journal of Neuroscience*, 19(15), pp. 6497–6505. doi: 10.1523/jneurosci.19-15-06497.1999.

Ta, L. E. *et al.* (2006) ‘Neurotoxicity of oxaliplatin and cisplatin for dorsal root ganglion neurons correlates with platinum-DNA binding’, *NeuroToxicology*, 27(6), pp. 992–1002. doi: 10.1016/j.neuro.2006.04.010.

Tabata, M. *et al.* (2014) ‘Cdc2-like kinase 2 suppresses hepatic fatty acid oxidation and ketogenesis through disruption of the PGC-1α and MED1 complex.’, *Diabetes*, 63(5), pp. 1519–1532. doi: 10.2337/db13-1304.

Tahtouh, T. *et al.* (2012) ‘Selectivity, cocrystal structures, and neuroprotective properties of leucettines, a family of protein kinase inhibitors derived from the marine sponge alkaloid leucettamine B’, *Journal of Medicinal Chemistry*, 55(21), pp. 9312–9330. doi: 10.1021/jm301034u.

Takahashi, K. and Ninomiya, T. (1987) ‘Morphological changes of dorsal root ganglion cells in the process-forming period’, *Progress in neurobiology*, 29(4), p. 393—410. doi: 10.1016/0301-0082(87)90020-7.

Tam, B. Y. *et al.* (2020) ‘The CLK inhibitor SM08502 induces anti-tumor activity and reduces Wnt pathway gene expression in gastrointestinal cancer models’, *Cancer Letters*. doi: 10.1016/j.canlet.2019.09.009.

Tanaka, B. S. *et al.* (2017) ‘Gain-of-function mutation of a voltage-gated sodium channel NaV1.7 associated with peripheral pain and impaired limb development’, *Journal of Biological Chemistry*, 292(22), pp. 9262–9272. doi: 10.1074/jbc.M117.778779.

Tay, B. *et al.* (2019) ‘Development of a high-throughput fluorescent no-wash sodium

influx assay’, *PLoS ONE*, 14(3), pp. 1–14. doi: 10.1371/journal.pone.0213751.
Tesfaye, S., Boulton, A. J. M. and Dickenson, A. H. (2013) ‘Mechanisms and management of diabetic painful distal symmetrical polyneuropathy’, *Diabetes Care*, 36(9), pp. 2456–2465. doi: 10.2337/dc12-1964.
Thichanpiang, P. *et al.* (2014) ‘TNF-α-induced ICAM-1 expression and monocyte adhesion in human RPE cells is mediated in part through autocrine VEGF stimulation’, *Molecular vision*, 20, pp. 781–789. Available at: https://pubmed.ncbi.nlm.nih.gov/24940033.
Thompson, E. M. *et al.* (2017) ‘The role of angiogenesis in Group 3 medulloblastoma pathogenesis and survival’, *Neuro-Oncology*, 19(9), pp. 1217–1227. doi: 10.1093/neuonc/nox033.
Tian, Q. *et al.* (2019) ‘Recovery from tachyphylaxis of TRPV1 coincides with recycling to the surface membrane’, *Proceedings of the National Academy of Sciences of the United States of America*, 116(11), pp. 5170–5175. doi: 10.1073/pnas.1819635116.
Tian, W., Czopka, T. and López-Schier, H. (2020) ‘Systemic loss of Sarm1 protects Schwann cells from chemotoxicity by delaying axon degeneration’, *Communications Biology*, 3(1), pp. 1–14. doi: 10.1038/s42003-020-0776-9.
Timmerman, R., Burm, S. M. and Bajramovic, J. J. (2018) ‘An overview of in vitro methods to study microglia’, *Frontiers in Cellular Neuroscience*, 12(August), pp. 1–12. doi: 10.3389/fncel.2018.00242.
Todd, A. J. (2002) ‘Anatomy of primary afferents and projection neurones in the rat spinal dorsal horn with particular emphasis on substance P and the neurokinin 1 receptor’, *Experimental Physiology*, 87(2), pp. 245–249. doi: 10.1113/eph8702351.
Toth, C., Lander, J. and Wiebe, S. (2009) ‘The prevalence and impact of chronic

pain with neuropathic pain symptoms in the general population', *Pain Medicine*, 10(5), pp. 918–929. doi: 10.1111/j.1526-4637.2009.00655.x.

Touska, F. *et al.* (2011) 'A "cute" desensitization of TRPV1.', *Current pharmaceutical biotechnology*, 12(1), pp. 122–9. doi: 10.2174/138920111793937826.

Treede, R. D. *et al.* (1995) 'Evidence for two different heat transduction mechanisms in nociceptive primary afferents innervating monkey skin.', *The Journal of physiology*, 483 (Pt 3(Pt 3), pp. 747–758. doi: 10.1113/jphysiol.1995.sp020619.

Trevisani, M. and Gatti, R. (2013) 'TRPV1 Antagonists as Analgesic Agents', *Journal of Freshwater Ecology*, 28(1), pp. 79–90. doi: 10.1080/02705060.2012.708673.

Tsubaki, M. *et al.* (2018) 'Tamoxifen suppresses paclitaxel-, vincristine-, and bortezomib-induced neuropathy via inhibition of the protein kinase C/extracellular signal-regulated kinase pathway'. doi: 10.1177/1010428318808670.

Turunen, J. J. *et al.* (2013) 'The significant other: splicing by the minor spliceosome', *Wiley interdisciplinary reviews. RNA*. 2012/10/16, 4(1), pp. 61–76. doi: 10.1002/wrna.1141.

Tzelepis, K. *et al.* (2018) 'SRPK1 maintains acute myeloid leukemia through effects on isoform usage of epigenetic regulators including BRD4', *Nature Communications*, 9(1). doi: 10.1038/s41467-018-07620-0.

Vallbo, A. *et al.* (1993) 'A system of unmyelinated afferents for innocuous mechanoreception in the human skin', *Brain Research*, 628(1), pp. 301–304. doi: https://doi.org/10.1016/0006-8993(93)90968-S.

Varey, A. H. R. *et al.* (2008) 'VEGF165b, an antiangiogenic VEGF-A isoform, binds and inhibits bevacizumab treatment in experimental colorectal carcinoma: Balance of pro- and antiangiogenic VEGF-A isoforms has implications for therapy', *British Journal of Cancer*, 98(8), pp. 1366–1379. doi: 10.1038/sj.bjc.6604308.

Ved, N. *et al.* (2018) 'Diabetes-induced microvascular complications at the level of the spinal cord; a contributing factor in diabetic neuropathic pain', *The Journal of Physiology*. doi: 10.1113/JP275067.

Vencappa, S., Donaldson, L. F. and Hulse, R. P. (2015) 'Cisplatin induced sensory neuropathy is prevented by vascular endothelial growth factor-A', *American Journal of Translational Research*, 7(6), pp. 1032–1044.

Veo, B. *et al.* (2019) 'Combined functional genomic and chemical screens identify SETD8 as a therapeutic target in MYC-driven medulloblastoma', *JCI Insight*, 4(1). doi: 10.1172/jci.insight.122933.

Verheyen, A. *et al.* (2013) 'Therapeutic potential of VEGF and VEGF-derived peptide in peripheral neuropathies', *Neuroscience*, 244, pp. 77–89. doi: 10.1016/j.neuroscience.2013.03.050.

Verma, A. *et al.* (2007) 'A simplified procedure for indole alkaloid extraction from Catharanthus roseus combined with a semi-synthetic production process for vinblastine', *Molecules*, 12(7), pp. 1307–1315. doi: 10.3390/12071307.

Verma, B. *et al.* (2018) 'Minor spliceosome and disease', *Seminars in Cell & Developmental Biology*, 79, pp. 103–112. doi: https://doi.org/10.1016/j.semcdb.2017.09.036.

Vetter, I. and Lewis, R. J. (2010) 'Characterization of endogenous calcium responses in neuronal cell lines', *Biochemical Pharmacology*. doi: 10.1016/j.bcp.2009.10.020.

Wang, M. S. *et al.* (2000) 'Pathogenesis of axonal degeneration: Parallels between Wallerian degeneration and vincristine neuropathy', *Journal of Neuropathology and Experimental Neurology*, 59(7), pp. 599–606. doi: 10.1093/jnen/59.7.599.

Wang, Y. *et al.* (2015) 'Mechanism of alternative splicing and its regulation', *Biomedical reports*. 2014/12/17, 3(2), pp. 152–158. doi: 10.3892/br.2014.407.

Wang, Y. *et al.* (2018) 'Sensitization of TRPV1 receptors by TNF-α orchestrates the development of vincristine-induced pain', *Oncology Letters*, 15(4), pp. 5013–5019. doi: 10.3892/ol.2018.7986.

Wang, Y. *et al.* (2019) 'A prospect of cell immortalization combined with matrix microenvironmental optimization strategy for tissue engineering and regeneration 06 Biological Sciences 0601 Biochemistry and Cell Biology', *Cell and Bioscience*, 9(1), pp. 1–21. doi: 10.1186/s13578-018-0264-9.

Wang, Z. and Burge, C. B. (2008) 'Splicing regulation: from a parts list of regulatory elements to an integrated splicing code', *RNA (New York, N.Y.)*. 2008/03/27, 14(5), pp. 802–813. doi: 10.1261/rna.876308.

Ward, A. J. and Cooper, T. A. (2010) 'The pathobiology of splicing', *The Journal of Pathology*, 220(2), pp. 152–163. doi: https://doi.org/10.1002/path.2649.

Watson, J. C. and Dyck, P. J. B. (2015) 'Peripheral Neuropathy: A Practical Approach to Diagnosis and Symptom Management.', *Mayo Clinic proceedings*, 90(7), pp. 940–951. doi: 10.1016/j.mayocp.2015.05.004.

Wei, X., Luo, L. and Chen, J. (2019) 'Roles of mTOR Signaling in Tissue Regeneration', *Cells*, 8(9). doi: 10.3390/cells8091075.

Wheeler, H. E. *et al.* (2015) 'Modeling chemotherapeutic neurotoxicity with human induced pluripotent stem cell-derived neuronal cells', *PLoS ONE*. doi: 10.1371/journal.pone.0118020.

Wickramasinghe, V. O. *et al.* (2015) 'Regulation of constitutive and alternative mRNA splicing across the human transcriptome by PRPF8 is determined by 5′ splice site strength', *Genome Biology*, 16(1), p. 201. doi: 10.1186/s13059-015-0749-3.

Wiffen, P. J. (2013) 'Amitriptyline for neuropathic pain and fibromyalgia in adults', *Journal of Pain and Palliative Care Pharmacotherapy*, 27(2), pp. 179–180. doi:

10.3109/15360288.2013.810895.

Wilkinson, M. E., Charenton, C. and Nagai, K. (2020) 'RNA Splicing by the Spliceosome', *Annual Review of Biochemistry*, 89(1), pp. 359–388. doi: 10.1146/annurev-biochem-091719-064225.

Williamson, J. M. and Lyons, D. A. (2018) 'Myelin dynamics throughout life: An ever-changing landscape?', *Frontiers in Cellular Neuroscience*, 12(November), pp. 1–8. doi: 10.3389/fncel.2018.00424.

Wing, C. *et al.* (2017) 'Application of stem cell derived neuronal cells to evaluate neurotoxic chemotherapy', *Stem cell research*. 2017/06/15, 22, pp. 79–88. doi: 10.1016/j.scr.2017.06.006.

Wolf, S. *et al.* (2008) 'Chemotherapy-induced peripheral neuropathy: Prevention and treatment strategies', *European Journal of Cancer*, 44(11), pp. 1507–1515. doi: 10.1016/j.ejca.2008.04.018.

Woolf, C. J. and Ma, Q. (2007) 'Nociceptors-Noxious Stimulus Detectors', *Neuron*, 55(3), pp. 353–364. doi: 10.1016/j.neuron.2007.07.016.

Wooten, M. *et al.* (2014) 'Three functionally distinct classes of C-fibre nociceptors in primates', *Nature Communications*, 5(1), p. 4122. doi: 10.1038/ncomms5122.

Wozniak, K. M. *et al.* (2016) 'Sustained Accumulation of Microtubule-Binding Chemotherapy Drugs in the Peripheral Nervous System: Correlations with Time Course and Neurotoxic Severity', *Cancer research*. 2016/04/13, 76(11), pp. 3332–3339. doi: 10.1158/0008-5472.CAN-15-2525.

Xicoy, H., Wieringa, B. and Martens, G. J. M. (2017) 'The SH-SY5Y cell line in Parkinson's disease research: a systematic review', *Molecular Neurodegeneration*, 12(1), pp. 1–11. doi: 10.1186/s13024-017-0149-0.

Xu, J. *et al.* (2016) 'Comparison of FDA Approved Kinase Targets to Clinical Trial

Ones: Insights from Their System Profiles and Drug-Target Interaction Networks', *BioMed Research International*, 2016. doi: 10.1155/2016/2509385.

Yamazaki, Y. *et al.* (2009) 'Snake venom Vascular Endothelial Growth Factors (VEGF-Fs) exclusively vary their structures and functions among species', *The Journal of biological chemistry*. 2009/02/10, 284(15), pp. 9885–9891. doi: 10.1074/jbc.M809071200.

Yang, L. *et al.* (2014) 'The mTORC1 effectors S6K1 and 4E-BP play different roles in CNS axon regeneration', *Nature Communications*, 5, pp. 1–7. doi: 10.1038/ncomms6416.

Yang, M. H. *et al.* (2019) 'Pleiotropic pharmacological actions of capsazepine, a synthetic analogue of capsaicin, against various cancers and inflammatory diseases', *Molecules*, 24(5), pp. 1–14. doi: 10.3390/molecules24050995.

Yin, K., Baillie, G. J. and Vetter, I. (2016) 'Neuronal cell lines as model dorsal root ganglion neurons: A transcriptomic comparison', *Molecular Pain*, 12, pp. 1–17. doi: 10.1177/1744806916646111.

Zajaczkowską, R. *et al.* (2019) 'Mechanisms of chemotherapy-induced peripheral neuropathy', *International Journal of Molecular Sciences*, 20(6). doi: 10.3390/ijms20061451.

Zhang, Y., Yang, S. H. and Guo, X. L. (2017) 'New insights into Vinca alkaloids resistance mechanism and circumvention in lung cancer', *Biomedicine and Pharmacotherapy*. doi: 10.1016/j.biopha.2017.10.041.

Zhao, F. *et al.* (2016) 'Development of a rapid throughput assay for identification of hNav1.7 antagonist using unique efficacious sodium channel agonist, antillatoxin', *Marine Drugs*. doi: 10.3390/md14020036.

Zheng, Y., Fu, X. and Ou, J.-H. J. (2005) 'Suppression of hepatitis B virus replication by SRPK1 and SRPK2 via a pathway independent of the phosphorylation of the viral core protein.', *Virology*, 342(1), pp. 150–158. doi: 10.1016/j.virol.2005.07.030.

Zhou, Z. and Fu, X.-D. (2013) 'Regulation of splicing by SR proteins and SR protein-specific kinases', *Chromosoma*. 2013/03/24, 122(3), pp. 191–207. doi: 10.1007/s00412-013-0407-z.

Zhu, W. and Oxford, G. S. (2011) 'Differential gene expression of neonatal and adult DRG neurons correlates with the differential sensitization of TRPV1 responses to nerve growth factor', *Neuroscience letters*. 2011/06/29, 500(3), pp. 192–196. doi: 10.1016/j.neulet.2011.06.034.